NTNU
Norwegian University of
Science and Technology

Offshore Wind Power in the North Sea

Grid Integration of 1000 MW Offshore Wind Power into the Norwegian Power System

Knut Magnus Sommerfelt

Master of Science in Energy and Environment

Submission date: June 2008
Supervisor: Terje Gjengedal, ELKRAFT
Co-supervisor: Espen Hagstrøm, Statkraft

Norwegian University of Science and Technology
Department of Electrical Power Engineering

Problem Description

The last decade attention has really been drawn towards CO2 emissions and climate changes. Norway has an ambitious goal of no net CO2 emission in 2050, and great effort has to be put into reaching this target. Due to the great wind resources along the coast wind power could be an important contribution. In order to install large amounts of wind power in the future, the turbines should be built offshore. Statkraft has a vision of 1000 MW offshore wind power within 2012. The distance to areas with depths suitable for today's technology makes AC cable connection difficult, indicating that HVDC should be used.

In this thesis grid integration of a 1000 MW offshore wind farm in the North Sea shall be investigated. Simulations shall be done with HVDC Light in order to investigate the transient stability on the onshore power system. Possible connection points in the grid have to be found. Simulations with HVDC Light should be compared to a solution with AC cable connection in order to investigate the impact of different transmission technologies on the onshore power system.

Assignment given: 15. January 2008
Supervisor: Terje Gjengedal, ELKRAFT

Preface

This thesis has been written at the Department of Electric Power Engineering at the Norwegian University of Science and Technology in cooperation with Statkraft. The work is a continuation of a project written during the autumn 2007, which dealt with transmission system for offshore wind power.

In this thesis I have been introduced to PSS/E for the first time, which has been a valuable experience. Because of problems with compiling of the user models in PSS/E, it took a long time before I could start with the work in the thesis. Additionally, I did not receive the HVDC Light model from ABB until April.

The HVDC Light model from NTNU could only provide a Fortran compiler for the newest PSS/E version 31. The compiler used for this version is an Intel Fortran compiler. The object files for the user models provided from Statnett and ABB were compiled with the Compaq Visual Fortran compiler which is used for earlier versions of PSS/E. In order to establish a dynamic library DLL file for PSS/E with the user models, the Compaq Visual Fortran compiler is needed. Eventually, an earlier version of PSS/E was installed with a Compaq Visual Fortran compiler belonging to Statkraft.

I would like to thank Leif Warland at Sintef Energy Research for help with getting started with PSS/E, and Albert Leirbukt from ABB for help with the HVDC Light model. I would also thank my supervisor at Statkraft Development and NTNU, Terje Gjengedal.

Finally, a large thanks to Charlotte and Kasper for all the support!

Knut Magnus Sommerfelt
Oslo 04.06.2008

Abstract

This master's thesis is written at the Department of Electric Power Engineering at the Norwegian University of Science and Technology. The work has been carried out at Statkraft Development in Oslo. The thesis deals with transmission systems and grid integration of offshore wind power, and is a continuation of the project written during the autumn 2007.

Norway has great potential for offshore wind power, but the depths just outside the coast probably make floating wind turbines necessary. In order to use today's technology for offshore wind turbines with foundations on the seabed, water depths cannot be much larger than 60 meters. It is possible to install the wind turbines at such depths, but the distance to these areas make AC cable transmission difficult because of the reactive power production in the cables. VSC HVDC is a technology well suited for offshore wind power, and HVDC Light is now commercially available for rating up to 1174 MW. Theory for VSC HVDC in systems in general is given first in the thesis. The case for this thesis is grid integration of a 1000 MW offshore wind farm into the Norwegian power system.

PSS/E was used in simulations of grid integration of the offshore wind power. Two possible connection points in the south of Norway were found based on load flow simulations; Feda and Kårstø. Only a load flow situation with peak load and production in the isolated Norwegian power system was provided. Different load flow situations for the two connection points were established in order to investigate the dynamic response at the connection points for situations with lower load and production.

A case with two sets of 100 km AC cables was used for the dynamic simulations as well as a HVDC Light link with a 600 km cable. SVCs were added at the connection point for the case with AC cable connection in order to fulfil the requirement for capacitive and inductive power factor at the connection point to the grid for wind power. No such compensation of reactive power is necessary for HVDC Light, as the converter can adjust the power factor. The voltage at the connection points is 300 kV. Dynamic simulations were done based on the fault ride through requirement from the Norwegian TSO Statnett for power plants connected to voltage level higher than 200 kV.

Different disturbances were done in the power system onshore close to the two connection points. The simulations done with AC cables and SVCs for reactive power compensation showed that the power system was not able to return to a stable operating point in all the simulations. With HVDC Light on the other side, simulations showed that the voltage at the connection points recovered to the pre fault value in all the simulations. The voltage recovery was within the voltage profile defined in the fault ride through requirement, and the wind turbines had to stay connected.

The wind farm was modelled as one equivalent generator offshore, and a standard PSS/E induction generator model was used. For the case with HVDC Light, the voltage offshore was practically unaffected by the disturbances onshore. The energy produced during the fault was stored as rotational kinetic energy in the wind turbine in order to avoid the DC voltage to increase drastically. This is an approximation done in this thesis. Wind projects planned with HVDC Light will have a DC chopper. A fault onshore will not affect the wind farm, as the power produced during the fault is dissipated in the DC resistance.

Contents

List of Tables

List of Figures

1 Introduction

The last decade attention has really been drawn towards CO_2 emissions and climate changes. Norway has an ambitious goal of no net CO_2 emission in 2050. Emission quotas can be bought in other countries, but a large contribution has to be done nationally. Even though the Norwegian power production mainly consists of hydro power, great effort has to be put into reaching the target. New power production has to be installed in order to be self supplied with power in a year with average precipitation, but the time where large hydro power plants were built in Norway has passed. Due to the great wind resources along the coast, wind power is a promising alternative. In order to install large amounts of wind power, the turbines should be built offshore in the future; the wind resources are even greater offshore, and the wind turbines will not occupy the coastline. With offshore wind power in the North Sea, oil and gas installations can be supplied with offshore wind power instead of using gas turbines with low efficiency.

The technology for offshore wind turbines is available, but only for turbines founded to the seabed for depths up to about 60 meters. Several concepts for floating wind turbines are under development, but they are not yet commercially available. Outside the Norwegian coast depths quickly reach several hundred meters. This implies that floating turbines are necessary for wind farms relatively close to the shore. However, there are areas in the North Sea south of Norway with depths suitable for today's offshore wind turbine technology. The distance is several hundred kilometers, making AC cable connection difficult, or even impossible, because of the large amount of reactive power produced by the cables. As a result of this HVDC probably has to be used. Traditional HVDC based on thyristors is not well suited for offshore wind power applications, among other things because of the need for short-circuit capacity offshore. HVDC Light on the other hand, is a technology well suited for offshore wind power. The technology is based on Voltage Source Converters with IGBT valves, and now has capacity up to 1174 MW.

This thesis is a continuation of a project written during the autumn 2007, which was an introduction to different transmission technologies for offshore wind power. VSC HVDC technology is further described in this thesis. The purpose of this thesis is to study the impact on the dynamic behavior of a 1000 MW offshore wind farm connected to the Norwegian grid with different transmission technologies. Possible connection points in the south of Norway for the offshore wind power shall be selected. PSS/E will be used for all power system simulations. The model for the Norwegian power system is provided by Statnett, and the model for HVDC Light developed by ABB will be used in simulations. Simulations with AC cables will also be done in addition to HVDC Light, in order to compare the results.

With 1000 MW offshore wind power connected to the high voltage grid, the transmission technology will have great influence on the system stability. Transient stability will be investigated for the two different transmission technologies; AC cable and HVDC Light. The wind farm is not modeled in detail, and the focus of the thesis will be power system impact onshore. Some assumptions will have to be made because of limitations regarding the control system for offshore wind power applications in the current HVDC Light model in PSS/E.

2 AC systems

This chapter gives an overview over some aspects of AC power systems that are relevant regarding connection of offshore wind power. The relationship between impedances in transmission lines and cables is given. This can be used to explain the need for HVDC for transmission in long cables. A brief introduction to AC system strength is also presented. The chapter is partly a brief summary of the project written during the autumn 2007.

2.1 Overhead lines

Transmission lines can be described electrically with series impedance and shunt admittance [12]. The series impedance consists of resistance R due to the resistivity in the conductor, and reactance X_L due to the magnetic field around the conductor. The shunt admittance consists of conductance G due to leakage current between the phases and ground, and susceptance B_C due to the electric field between the conductors. The effect from the shunt conductance in transmission lines is small, and usually neglected. Typical parameters for overhead lines are given in Table 2.1 for different voltages.

Nominal voltage	115 kV	230 kV	500 kV
$R\ (\Omega / km)$	0.050	0.037	0.028
$X_L = \omega L\ (\Omega / km)$	0.488	0.367	0.325
$B_C = \omega C\ (\mu s / km)$	3.371	4.518	5.200

Table 2.1: Typical parameters for overhead transmission lines [12]

2.2 Cables

Cables can be described electrically with the same elements as transmission lines. However the series impedance and shunt admittance of power cables have different values from transmission lines due to the construction of the cables. The shunt susceptance in cables is much higher than in transmission lines because the conductors are closer to each other, and the conductors are surrounded by metallic screens. Typical parameters for direct-buried paper-insulated lead-covered cables (PILC) are given in Table 2.2 for different voltages.

Nominal voltage	115 kV	230 kV	500 kV
$R\ (\Omega / km)$	0.0590	0.0277	0.0128
$X_L = \omega L\ (\Omega / km)$	0.3026	0.3388	0.2454
$B_C = \omega C\ (\mu s / km)$	230.4	245.6	96.5

Table 2.2: Typical parameters for cables (PILC) [12]

For cables with high voltage, the three conductors are in separate cables. Hence, the susceptance will decrease compared to a three-core cable because of increased distance between the conductors.

2.3 Surge Impedance Loading

Transmission lines and cables can be described by their characteristic impedance Z_C according to Equation (2.1) [12].

$$Z_C = \sqrt{\frac{R + j\omega L}{j\omega C}} = \sqrt{\frac{L}{C}}\left(1 - j\frac{R}{2\omega L}\right) \tag{2.1}$$

R is the series resistance, L is the series inductance and C is the shunt capacitance. The shunt conductance G is normally ignored for transmission lines and cables. From the characteristic impedance, surge impedance load SIL can be expressed according to Equation (2.2).

$$SIL = \frac{V_0^2}{Z_C} \tag{2.2}$$

V_0 is the rated voltage of the line or cable and Z_C is the characteristic impedance of the line or cable. If a line is loaded at a level below SIL, the line will produce reactive power. The effect from the shunt capacitance is bigger than the effect from the series inductance. On the other side, if a line is loaded at a level above SIL, the line will consume reactive power due to the increased current in the line. The effect from the shunt capacitance is dependent of the voltage, and hence approximately constant.

The SIL of a cable is much higher than for a transmission line for the same voltage [12]. This is due to the high capacitance, as can be seen by comparing Table 2.1 and Table 2.2. A typical power cable will not be able to transfer power equal to SIL, because of the thermal limit.

In the case with an offshore wind farm connected to the grid with AC cables, the reactive power produced by the cable will be highest when the cable is connected, but the active power transfer from the wind farm is small. The higher the active power, the more reactive power is consumed in the series inductance. However, at full power AC cables will still produce large amounts of reactive power.

2.4 Strength of AC systems

A normal parameter for measuring the strength at a busbar in an AC network is short-circuit power $SC\ MVA$ [9]. The definition of short-circuit power is given in Equation (2.3).

$$SC\ MVA = I_{fault} \cdot V_{ac} = \frac{V_{ac}^2}{Z_{th}} \tag{2.3}$$

I_{fault} is the fault current for a three phase fault with zero impedance at the busbar, V_{ac} is the nominal line voltage at the point [kV] and Z_{th} is Thevenin impedance seen from the point [Ω].

Even though the short-circuit impedance is equal to zero, the fault current will be limited by the Thevenin impedance, which corresponds to the diagonal element in the node impedance matrix for the system for the given busbar [7]. Physically, this means that the fault current has to return through impedances from ground other places in the power system.

In fault studies, a generator is represented as Norton equivalent, with a current source in parallel to the generator impedance connected to earth. The closer a generator is located to a busbar, the more will it contribute to reducing the Thevenin impedance seen from the busbar. More lines connected to the busbar will also contribute to reducing the Thevenin impedance; hence also increase the short-circuit power as described in Equation (2.3).

In order to connect a HVDC link based on thyristor technology to an AC system, two requirements have to be fulfilled [9]. The short-circuit power has to be large enough compared to the power from the HVDC link. This is called short-circuit ratio, and is defined according to Equation (2.4).

$$SCR = \frac{SC\ MVA}{P_{HVDC}} = \frac{V_{ac}^2}{Z_{th} P_{HVDC}} \tag{2.4}$$

SC MVA is the short-circuit power in the connection point [MVA], P_{HVDC} is the rating of the HVDC link [MW], V_{ac} is the nominal line AC voltage in the connection point [kV] and Z_{th} is the Thevenin impedance seen from the connection point [Ω]. A rule of thumb is defined in [9], and recommends a SCR larger than 3 for traditional HVDC.

In addition to a sufficient large SCR, the mechanical inertia of the AC system has to be large enough in order to maintain the required voltage and frequency. An effective inertia constant H_{dc} is defined in [9] is defined according to Equation (2.5).

$$H_{dc} = \frac{\text{total rotational inertia of the AC system [MW} \cdot \text{s]}}{\text{MW rating of the AC link}} \tag{2.5}$$

The inertia constant is recommended to be at least 2 - 3 s in order to have satisfactory operation of the HVDC link.

For offshore wind power, grid connection with AC cables will also need a certain level of short-circuit power at the connection point compared to the power from the wind farm [23]. This will be shown in the dynamic simulations presented in chapter 7.

3 Background for HVDC

This chapter gives a brief introduction to HVDC in general, as a summery of the project written during the autumn 2007.

3.1 HVDC in general

The first commercial HVDC transmission system was built in Sweden in 1954 [12]. The technology was based on mercury arc valves. The development of thyristors made HVDC systems more attractive. In 1972 the first thyristor based HVDC system provided a back-to-back connection between the asynchronous areas of Quebec and New Brunswick. HVDC systems based on converters with thyristors are often referred to as traditional HVDC.

There are three main reasons for using HVDC power transmission systems. For large quantities of power over long distances, AC transmission is not economical due to the need for compensation of reactive power [3]. Connection of two asynchronous areas is impossible with AC. A back-to-back HVDC connection or a HVDC connection with cable or transmission lines makes power transfer between the areas possible. Further on is power transfer with AC underground or subsea cables is difficult due to the high capacitance of cables, as described in 2.2. The distance beyond which it is impractical to use AC cables depends on the transmitted power, voltage level, cable construction and compensation for reactive power. Figure 3.1 illustrates the maximal transmitted power in AC cables for different voltage levels and reactive power compensation strategies for a typical AC cable.

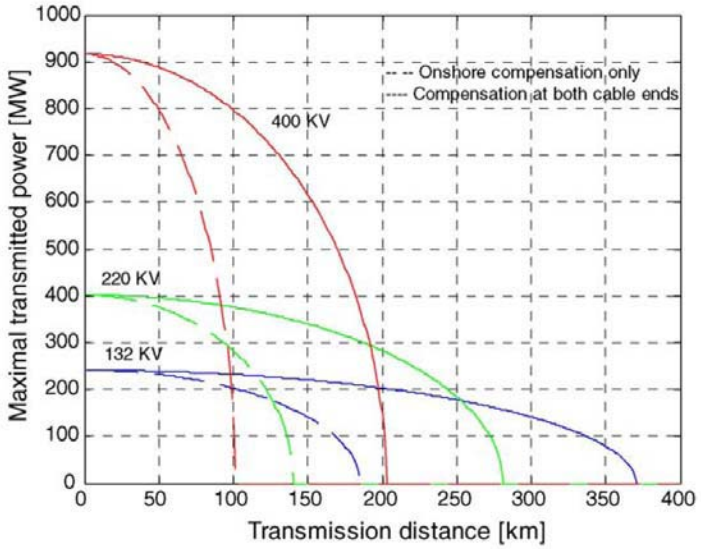

Figure 3.1: Maximal transmitted power through an AC-cable [4]

Traditional HVDC systems are not described in detail in this thesis. However, references to traditional HVDC systems will occur in order to emphasize the difference for Voltage Source Converter (VSC) HVDC systems.

3.2 HVDC Light

Unlike traditional HVDC systems, the converters in VSC HVDC systems are based on IGBT transistors. HVDC Light is the name of ABB's VSC HVDC technology, and has been available since 1997. In this thesis, HVDC Light is used in all dynamic HVDC simulations. The reason for this is that ABB offers a model in PSS/E representing HVDC Light. Siemens has a similar technology to HVDC Light called HVDC PLUS. This technology is still not installed, but commercially available.

Details regarding the VSC HVDC technology will be given in this thesis. In chapter 4, the switching in general Voltage Source Converters is described, as well as power flow and control modes. VSC HVDC systems are referred to in general. This is because the detailed information about the switching of HVDC Light is restricted. However, the basic construction of a HVDC Light system is similar to the technology presented in chapter 4. In this paragraph, practical information relevant for offshore wind power is presented. It has to be emphasized that costs of the technology is not presented, because ABB doesn't give out this information.

The HVDC Light technology is developed for applications both onshore and offshore. For offshore applications, the high-voltage equipment is installed inside a container with ventilation system designed to protect it from the salt and humid air [1]. Costs of installing equipment offshore are higher than onshore. Because of this, the layout for offshore use is made more compact than for onshore use. An example presented in [1] is a 40 MW station. For a land station with this power rating, the dimensions are 40 x 18 x 8,5 meters, and for offshore applications the module is 16 x 10 x 15 meters. An example of a 700 MW land station is also given. The dimensions of the station onshore are 60 x 30 x 20 meters. With the same ratio between onshore and offshore dimensions, the dimensions of the 700 MW offshore module would be 24 x 17 x 35 meters. This is however a very rough assumption, but gives an image of the dimensions.

The HVDC Light submarine cables are insulated with XLPE (Cross-linked polyethylene). ABB is the first cable producer to use this insulation in DC cables. Cables insulated with XLPE are lighter and more mechanically robust [1]. The result is that the cables can be laid on greater depths than paper insulated cables. Repairing of the cables is also easier than for paper insulated cables.

4 VSC HVDC technology

This chapter gives an introduction to the technology used in VSC HVDC systems. The information is mainly based on [17] and [1], and explains the basic theory of switch-mode converters, such as the converters in HVDC Light.

The thyristors in a traditional HVDC converter need a three phase voltage on the AC-side to be able to commutate [17]. A normal terminology for this type of converter is LCC (Line Commutated Converter). The converter in HVDC Light is based on IGBT (Insulated Gate Bipolar Transistors). Unlike thyristors, the transistors in have turn off capability. This results in a better control of the converter output. The input to switch-mode converters is DC-voltage; the terminology for this kind of converters is therefore Voltage Source Converters (VSC).

4.1 Single phase VSC

Figure 4.1 shows a block diagram for a single phase switch-mode inverter. The voltage V_d is the DC-voltage and the voltage v_0 is the AC-voltage. The power flows from the DC-side to the AC-side, and assuming the inverter supplies an inductive AC motor load, the AC-current i_0 will lag the AC-voltage v_0. This is shown in Figure 4.2.

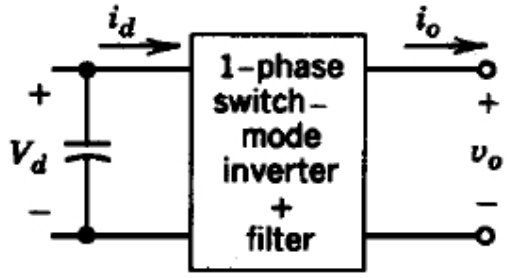

Figure 4.1: Block diagram of a single-phase inverter [17]

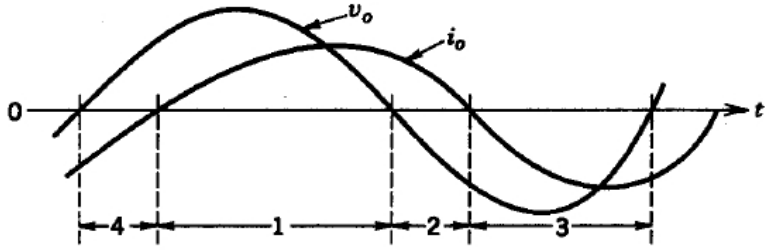

Figure 4.2: Output waveforms of the single-phase switch mode inverter [17]

In period 1, both the current i_0 and the voltage v_0 are positive. The power flows from the DC-side to the AC-side. Due to the lagging of the current, in period 2 the voltage is negative while the current is still positive. The power flows from the AC-side to the DC-side, and the converter is in a rectifier mode of operation. In period 3 both the current and voltage are

negative, but the power again flows from the DC-side to the AC-side. Finally, in period 4 the current is negative and the voltage is positive. The power flows from the AC-side to the DC-side. From this, it can be seen that the converter has to be able to work in all four quadrants of the i_0 - v_0 plane.

4.1.1 Switching

The output AC-voltage in a switch-mode inverter is obtained by switching the transistors in a certain way. First, the switching of the single phase inverter illustrated in Figure 4.1 will be presented. Figure 4.3 shows a half bridge single-phase switch-mode converter. The voltage V_d is assumed to be a constant DC-voltage, v_{AN} is the output AC-voltage and i_0 is the AC-current.

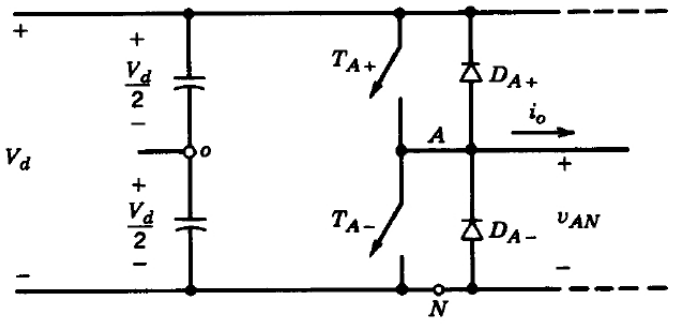

Figure 4.3: One-leg switch mode inverter [17]

In order to control the switching, a signal needs to be given to the transistors. This is achieved by using a Pulse-Width-Modulated (PWM) switching scheme. A control signal $v_{control}$ is compared with a triangular signal v_{tri} in order to decide which of the transistors T_{A+} and T_{A-} that should be conducting. This is shown in Equation (4.1) and (4.2), and in Figure 4.4.

$$v_{control} > v_{tri} \quad \Rightarrow \quad T_{A+} \text{ is on} \quad \Rightarrow \quad v_{A0} = \frac{1}{2} V_d \tag{4.1}$$

$$v_{control} < v_{tri} \quad \Rightarrow \quad T_{A-} \text{ is on} \quad \Rightarrow \quad v_{A0} = -\frac{1}{2} V_d \tag{4.2}$$

The control signal $v_{control}$ is a sinusoidal signal with the frequency f equal to the desired output voltage frequency of the converter. The triangular signal has constant amplitude V_{tri} and frequency f_s. As can be seen from the lower part of Figure 4.4, the voltage v_{A0} is not a sinusoidal wave, and the fundamental component $(v_{a0})_1$ has to be filtered out. Since the voltage is of a very high frequency, the filters can be small. However, it is inevitable that harmonics of a higher order is produced [17].

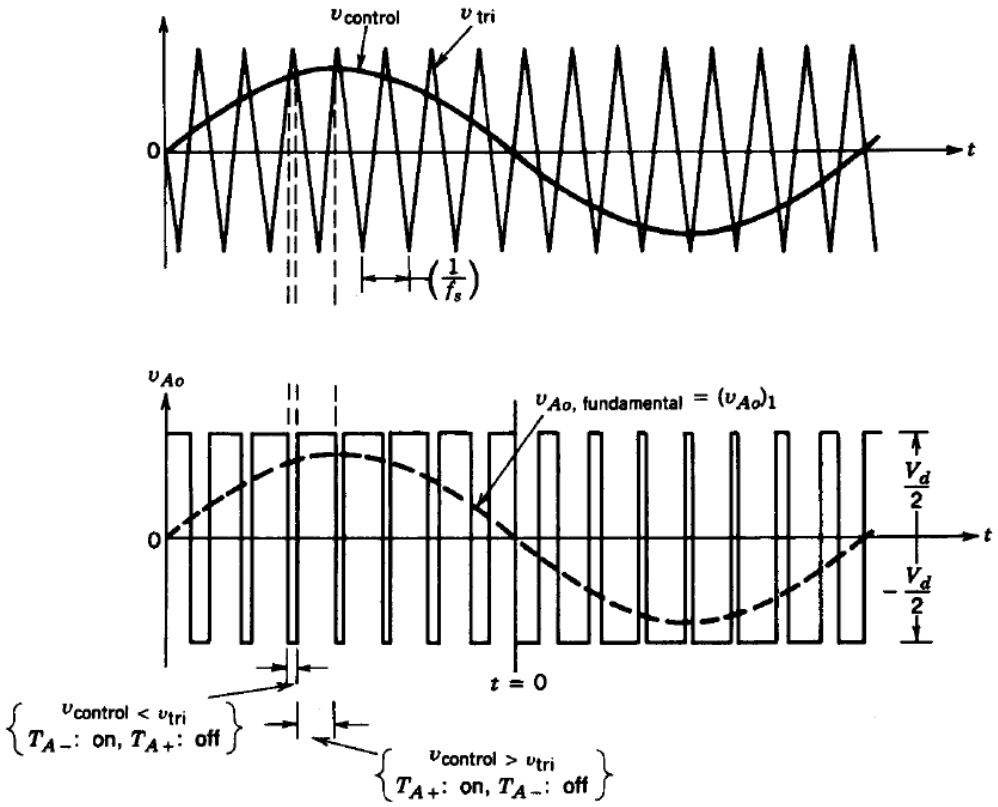

Figure 4.4: Pulse-width modulation of a single-phase converter [17]

As long as the amplitude of $V_{control}$ is smaller then the amplitude of V_{tri}, the amplitude of the fundamental component of the output voltage $(v_{a0})_1$ is proportional with the amplitude of the control signal $v_{control}$. This is called linear modulation. The factor m_a in Equation (4.3) is called modulation ratio.

$$(v_{A0})_{1,peak} = \frac{v_{control,peak}}{v_{tri,peak}} \frac{V_d}{2} = m_a \frac{V_d}{2} \tag{4.3}$$

For m_a larger then 1, the output voltage $(v_{a0})_1$ is no longer proportional with the amplitude of $V_{control}$. This is called overmodulation, and will not be dealt with in this thesis.

4.2 Three-phase VSC

A three-phase VSC converter consists of three legs. Each leg is identical to the leg in the converter in Figure 4.3. Figure 4.5 shows the configuration of a three-phase switch-mode converter.

4.2.1 Switching

There is a separate control signal for each of the three legs in the three-phase converter. The control signals are sinusoidal waves as for the one-leg converter, 120° shifted. This is shown in Figure 4.6.

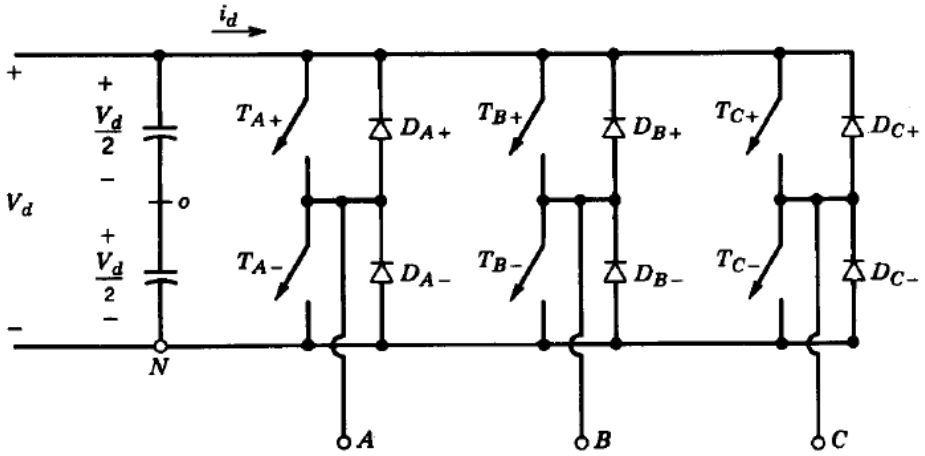

Figure 4.5: Three-phase switch-mode converter [17]

As for the one-leg switch mode converter, the fundamental component of the output AC-voltage is dependent only of the DC-voltage V_d and the switching control signals to the transistors as long as m_a<1. The peak value of the fundamental component of the output AC-voltage for leg A with respect to the point N from Figure 4.5 can be expressed according to Equation (4.4).

$$(v_{AN})_{1,peak} = \frac{v_{control,peak}}{v_{tri,peak}} \frac{V_d}{2} = m_a \frac{V_d}{2} \tag{4.4}$$

The fundamental component of the line-to-line rms voltage can be expressed according to Equation (4.5).

$$(v_{LL})_1 = (v_{AN})_1 - (v_{BN})_1 = \frac{\sqrt{3}}{\sqrt{2}}(v_{AN})_{1,peak} = \frac{\sqrt{3}}{2\sqrt{2}} \frac{v_{control,peak}}{v_{tri,peak}} V_d \approx 0.612 m_a V_d \tag{4.5}$$

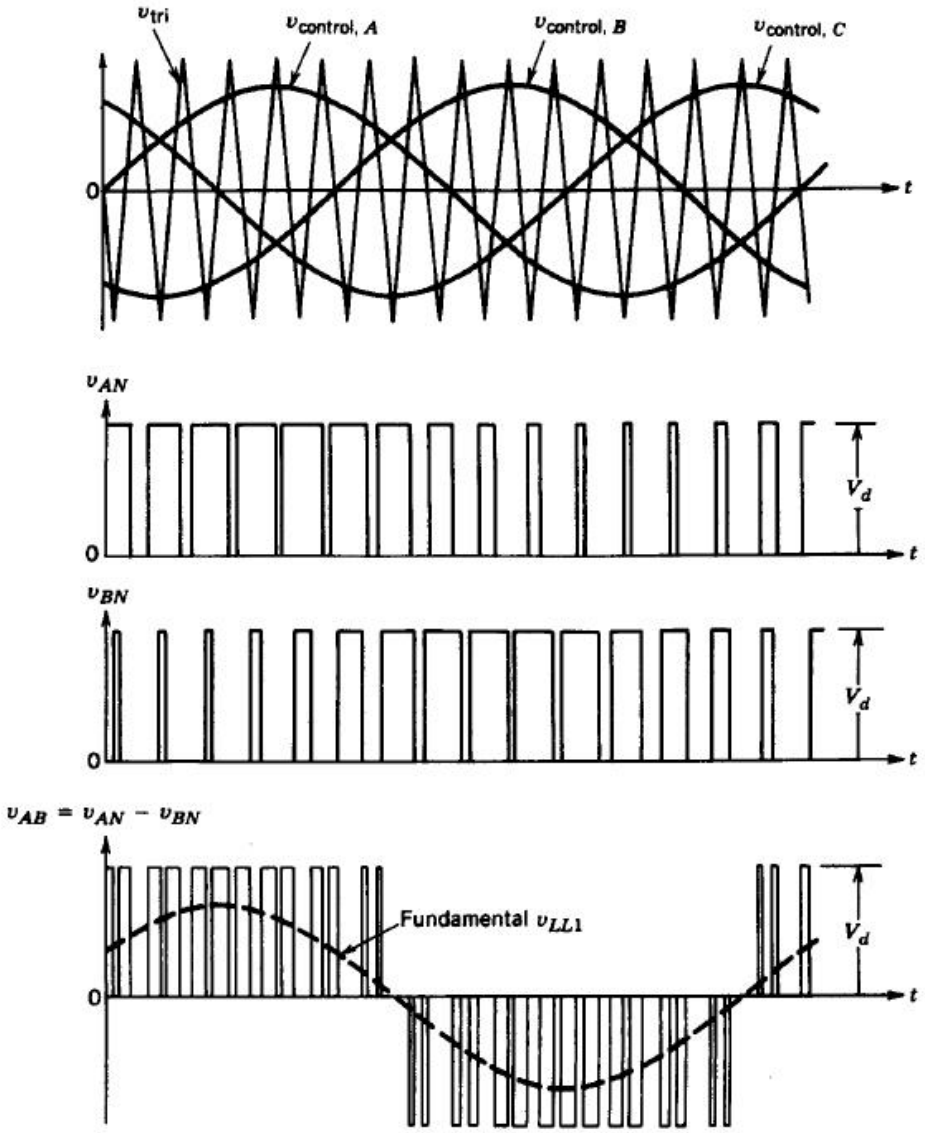

Figure 4.6: Pulse-width modulation of a three-phase converter [17]

4.3 Power flow in Voltage Source Converters

A VSC HVDC system has the advantage compared to a traditional LCC HVDC system that the VSC converter can provide separate control of active and reactive power. This is done by controlling the amplitude and phase angle of the produced AC-voltage, which is obtained by changing the control signal $v_{control}$ in Figure 4.6.

Consider a system topology as shown in Figure 4.7.

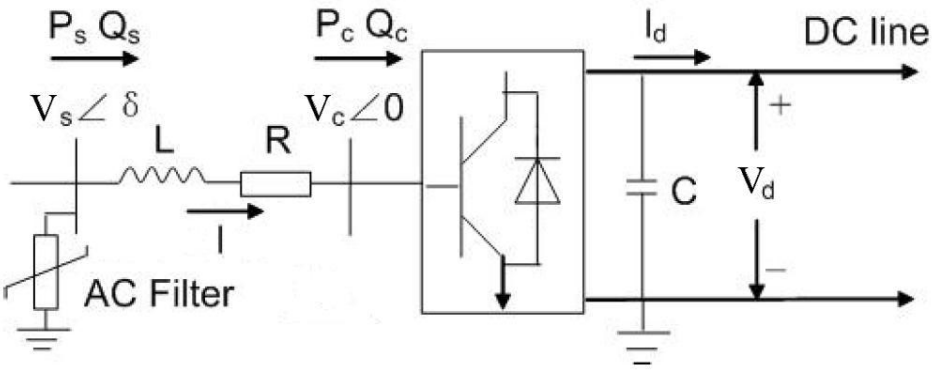

Figure 4.7: System topology of a VSC HVDC system [5]

The VSC converter is connected to an AC-system with voltage V_s. Both sides of the DC-link have the same configuration. The resistance R and inductance L represent the impedance of the commuting reactor, which filters out the fundamental component of the AC-voltage produced by the converter as described in 4.1.1 [5]. The capacitor on the DC-side supports the DC-voltage, as well as reducing harmonics on the DC-side. On the AC-side there is a shunt filter, the purpose of this is to filter out harmonics created by the converter in the AC-system [5].

Assume the power flowing from the AC-system into the converter, corresponding to rectifier mode of operation for the converter. The voltage V_c lags V_s with the angle δ. By neglecting the resistance R, the power transferred to the converter from the AC-system can be derived as in Equation (4.6) [5].

$$\boldsymbol{S_C} = P_C + jQ_C = \boldsymbol{V_C I}^* = \boldsymbol{V_C}\left[\frac{\boldsymbol{V_S} - \boldsymbol{V_C}}{j\omega L}\right]^* = V_C\left[\frac{V_S\cos(\delta) + jV_S\sin(\delta) - V_C}{j\omega L}\right]^* \tag{4.6}$$

With the resistance neglected, the active power from the AC-system equals the received active power at converter. The expression for the active power is found from Equation (4.6) in Equation (4.7) by dividing the imaginary part of the numerator by $j\omega L$, and multiply it with V_C.

$$|P_S| = |P_C| = V_C\left[\frac{V_S\sin(\delta)}{\omega L}\right] = \frac{V_C V_S}{\omega L}\sin(\delta) \tag{4.7}$$

The reactive power Q_C consumed by the converter is found from Equation (4.6) in Equation (4.8), by dividing the real part of the numerator by $j\omega L$, and multiply it with V_C.

$$Q_C = V_C\left[\frac{V_S\cos(\delta) - V_C}{\omega L}\right] = \frac{V_C V_S\cos(\delta) - V_C^2}{\omega L} \tag{4.8}$$

The expression for the power delivered by the AC-system is given in Equation (4.9).

$$\boldsymbol{S_S} = P_S + jQ_S = \boldsymbol{V_S}\boldsymbol{I}^* = \boldsymbol{V_S}\left[\frac{\boldsymbol{V_S} - \boldsymbol{V_C}}{j\omega L}\right]^* = V_S\left[\frac{V_S - V_C\cos(\delta) - jV_C\sin(\delta)}{j\omega L}\right]^* \tag{4.9}$$

The reactive power drawn from the AC-system is expressed in Equation (4.10).

$$Q_S = \frac{V_S^2 - V_S V_C\cos(\delta)}{\omega L} \tag{4.10}$$

In traditional HVDC systems with LCC converters, the direction of the active power flow is changed by changing the firing pulse to the thyristors so that the DC-voltage changes polarity, while the direction of the DC-current remains the same [17]. To change the direction of the active power flow in VSC converters the direction of the DC-current is changed, while the DC-voltage polarity is the same. In this case, the rectifier becomes a inverter, and vice-versa. Considering the system in Figure 4.7 and Equation (4.7), the power flow direction would change if the voltage V_c was made to lead V_s.

In a traditional HVDC system, the converts consume reactive power independently of active power flow direction. In VSC HVDC systems, the reactive power can be controlled at each converter according to (4.8).

As can be seen from the equations in this section, the VSC converter has two controllable variables in order to control the active and reactive power at its terminals. By applying a phase shift δ to the sinusoidal control signal $V_{control}$ from Figure 4.4, the output voltage will get the same phase shift. By increasing the modulation ratio m_a, the amplitude on the output AC-voltage will increase, according to Equation (4.5).

4.4 Control modes

Different control strategies can be used in VSC HVDC. The chosen control strategies are based on which purpose the VSC HVDC system is used for. The control strategy of an offshore wind farm differs from the control strategy of power transfer between two strong AC systems [2].

4.4.1 Normal operation

As described in 4.3, the active and reactive power at both converters can be controlled by changing phase angle of the output AC-voltage δ and AC voltage amplitude modulation ratio m_a. Each converter can either be set to regulate the AC voltage by adjusting the reactive power at the connection busbar, or set to operate at constant reactive power. In addition to the above mentioned parameters, the DC-voltage has to be controlled by one of the converters [11]. The other converter controls the active power, based on an active power set point. In normal operation of a HVDC VSC link, the active power from the rectifier must equal the active power at the inverter plus the losses in the cable. Assume the rectifier has constant DC-voltage control and the inverter has constant active power control. If the inverter increases the voltage angle δ due to a change on the active power set point, the active power from the inverter to the AC-system will increase according to Equation (4.7). With no change in the power transfer at the rectifier, the capacitance on the DC-side will discharge and the DC-voltage will decrease. The rectifier has to increase the voltage angle to transfer more power to

the DC-link in order to charge the capacitances and increase the DC-voltage. Capacitances are associated both with the DC cable and the converters [2]. The general Equation (4.11) explains the mechanism, where v_c is the voltage over the DC side capacitance, C is the total DC capacitance and i is the current flowing through the capacitance due to imbalance of active power between the two converters.

$$v_c = \frac{1}{C}\int_0^t i\ dt \tag{4.11}$$

In a traditional HVDC system, a communication link between the two converter stations is needed in order to control the power flow. The voltage is measured in one end, and the DC-voltage is controlled in the other end so that the voltage difference divided by the DC-line or cable resistance equals the set point of the DC-current [17]. A VSC HVDC system does not require any communication between the two converters. The converters communicate through the measured DC voltage at each end.

4.4.2 Offshore wind power

If a VSC HVDC system is used to connect offshore wind power to the grid onshore, a different control strategy should be used than for normal operation described in 4.4.1 [2], [11]. Consider the system in Figure 4.7 assuming the bus with voltage V_s is the point of common coupling for the offshore wind farm. The power flows into the converter, corresponding to rectifier mode of operation. The power from the wind P_{wind} is a function of the cube of the wind speed, according to Equation (4.12) [16].

$$P_{wind} = \frac{1}{2}\rho A U^3 \tag{4.12}$$

ρ [kg/m^3] is the density of the air, A [m^2] is the swept area of the turbine and U [m/s] is the wind speed. The offshore converter has to absorb all the power produced by the wind turbine generators, instead of transferring power according to an active power set point. For normal induction generator wind turbines, the frequency at the point of common coupling tends to increase for increasing wind speed [11]. The increase in frequency is detected by the rectifier, and the phase angle is increased with respect to the voltage at the point of common coupling in order transfer more power into the DC side. This action will cause the frequency to return to the reference value. Because of the imbalance of active power between the rectifier and the inverter, there will be a current flowing into the capacitor on the DC-side causing an increase in DC-voltage according to the general Equation (4.11). The inverter has to increase the voltage angle δ of the output voltage with respect to the terminal AC-voltage in the connected AC-system. The power out of the inverter will increase, and the capacitor will discharge causing the DC-voltage to return to the reference value.

If there is no wind, or the offshore wind farm is disconnected for some reason, the onshore converter can still function as a STATCOM [10]. Reactive power can be regulated within the PQ diagram in Figure 5.1.

5 PSS/E models

This chapter describes the models used in the simulations. There are several programs available to perform stationary and dynamical analysis of power systems. In this thesis, the options were Simpow and PSS/E. The decision was made to use PSS/E. PSS/E is owned by Siemens [18].

First of all, Statnett, the TSO in Norway, uses PSS/E for analysis on the main grid in Norway. They have developed a detailed model of the Norwegian power system. The model is restricted, but available to companies and universities with confidential agreements. Secondly, companies develop user models for power system equipment in PSS/E. ABB has developed a model for HVDC Light in PSS/E, which is commercial available for companies with confidential agreements.

PSS/E has a large library of models, including a model for VSC HVDC. This model is an early version of the HVDC Light model to ABB. The dynamic response of a VSC HVDC system is highly influenced by the control system of the converters. According to ABB [14], the control system of a HVDC VSC is not realistic represented in this model. The dynamic response is therefore not valid for a HVDC Light system that is on the market today. Based on this, the decision was made to use PSS/E with the user model for HVDC Light provided by ABB.

5.1 The Norwegian model

The PSS/E model provided by Statnett for the power system in Norway consists of 2200 buses, with voltage ranging from 3 to 400 kV. Statnett uses a model that includes the other Nordic countries, as well as user models of the HVDC converters connected to Denmark and the Netherlands. Unfortunately, this complete model is restricted, and could not be given out. The isolated Norwegian model is divided into 17 different geographical areas.

There is only one official model for the Norwegian power system, and this is a peak load situation [6]. The instant load consumption in Norway is 22931 MW, which is very high. During the last five years, the highest hourly average load consumption was 21915 MW [20]. Since there are no connections to other countries in the model, all the power is produced in Norway. Almost all the generators are connected, producing a total of 22640 MW. During the last five years, the highest hourly average production was 24636 MW. The surplus of the power in this situation had to be exported.

Limit checking reports for voltages and branches for voltage level from 130 kV to 400 kV can be found in Appendix A.1 and A.2 for this load flow situation. Some of the voltages are outside the range 0,9 – 1,1 pu, and some of the branches are loaded more than 100 % of the rating. It is assumed that the load flow situation is realistic, and modifications on the system are not done in order to get all branches within the rating and voltages from 130 to 400 kV within the interval of 0,9 – 1,1 pu.

Statnett is not able to give out any other load flow situations than the peak load situation. This implies that the users of the model have to scale down the load and production in the system in order to establish load flow situations with lighter load.

Before dynamic simulations with the model could be done, a modification had to be made. When running a dynamic simulation without any disturbances on the grid, the system was unstable. The initial conditions of several variables for the governor at Svartisen were out of range after initializing the dynamic simulation. Statnett recommended to replace the governor model NORGOV at Svartisen with the standard PSS/E model HYGOV [6]. Without any documentation of the user models, the advices from Statnett were followed. The two models are identical, except that NORGOV reduces the water flow in the regulated turbine if a monitored line is over loaded. In the case of the load flow situation in the model given from Statnett, a line in mid Norway was overloaded, and the governor response led to unstable behavior of the entire system.

5.2 Wind turbine model

In this study a model of conventional induction generator is used to model the wind turbines. The PSS/E model is called CIMTR3. The arguments for this are explained in this section and in 5.3.5. Dynamic data for the wind turbine is taken from the equivalent wind turbine generator at Smøla.

The trend of wind turbines today is utilization of some kind of frequency converter. The rotor in induction generator turbines is often fed with a converter; the wind turbine is then called Double Fed Induction Generator (DFIG). Another normal type of wind turbine used today is full frequency converter and synchronous generator. Both these kinds of wind turbines are more sophisticated than induction generator turbines directly connected to the grid. They are able to operate at variable speed in order to maximize the energy capture from the wind [16]. Additionally, they have capability to regulate the power factor at the connection point.

Induction generator wind turbines operate at rotational speed given by the grid frequency. They also consume reactive power [8].

An interesting aspect regarding offshore wind power connected with HVDC Light is to use as cheap wind turbines as possible. Both the aspects with rotational speed and reactive power can to some extent be solved with conventional induction generators connected with HVDC Light. The offshore converter can adjust the frequency of the entire grid offshore in order to adjust the speed of the wind turbines. Additionally, the converter can supply the reactive power needed for the wind turbines, as long as the converter operates within the PQ diagram in Figure 5.1.

In this study it is assumed that the wind turbines are compensated for reactive power corresponding to $cos(\varphi) = 0{,}99$ at the busbar where the wind turbines are connected offshore. This power factor corresponds to the wind farm at Smøla in the PSS/E model. In the simulations, one equivalent machine is used to model the entire wind farm [21]. This is also done at Smøla, and is a normal simplification for dynamic power system simulations.

5.3 The HVDC Light model

The user model of HVDC Light is developed and provided by ABB. This paragraph will explain the use of the model in PSS/E. A user manual is provided, with sufficient information to set up and use the model [2]. However, the description of the control system is not available, as the user model files were provided as compiled files.

5.3.1 Modules

HVDC Light is a module based technology, with power rating from 98,7 MW to 1174,6 MW [1]. To increase the power of the converters, modules are placed in series and parallel in order to increase the current and voltage. The current and voltage rating of the different modules are shown in Table 5.1.

HVDC Light® modules		Currents		
		580A (2 sub)	1140A (4 sub)	1740A (6 sub)
Voltages	± 80 kV	**M1**	**M2**	**M3**
	± 150 kV	**M4**	**M5**	**M6**
	± 300 kV	**M7**	**M8**	**M9**

Table 5.1: Modules in HVDC Light [1]

5.3.2 Power flow representation

In PSS/E, the HVDC Light system has to be represented in the load flow before dynamical simulations can be done. Standard generator elements from PSS/E are used in order to establish the load flow. The rectifier is modeled as a PU bus connected to a generator and shunt. Because the power is going from the AC to the DC side, the specified power to the generator has to be negative. The generator impedance *Zsource* in PSS/E specifies the commuting reactance L in Figure 4.7. The resistive part R is equal to zero. The shunt AC filter in Figure 4.7 is represented by the reactive power generation of the AC filter capacitors in PSS/E. Additionally, a converter transformer has to be added. One side is connected to the Point of Common Coupling (PCC), and the other side is connected to the PU bus with the generator and AC filter. The voltage at the converter busbar is 408 kV for the largest HVDC Light converter.

The inverter is described in the load flow with the same units as the rectifier, but the power from the generator has to be positive, because the power is going from the DC side into the AC side. The reactive power limits to be specified in the power flow for the generator equivalents depend on the active power. The HVDC Light converter has a capability curve according to Figure 5.1. It is up to the user to select the right reactive power limits for the converter.

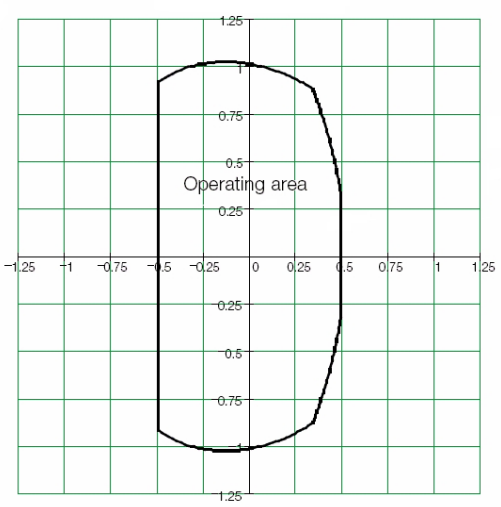

Figure 5.1: PQ diagram of a HVDC Light converter [1]

5.3.3 Losses

The DC cable is not modeled in the load flow. In dynamic simulations, a user model communicates between the two converters, and includes the cable resistance. The power combination has to be defined by the user between the rectifier and inverter so that the power going into the rectifier is larger than the power going out from the inverter. Equation (5.1) describes the power loss in the whole DC system.

$$P_{loss} = -P_{rectifier} - P_{inverter} \tag{5.1}$$

The power loss in the DC system consists of converter loss, and cable loss.

From Table 5.2 the converter losses at full power can be calculated by comparing the sending power with the receiving power when the system is has a back-to-back configuration. In this case, the inverter and the rectifier are at the same location.

Converter	DC voltage	DC current	DC Cable	Sending power	Receiving power (MW)					
types	kV	A	Cu in mm²	MW	Back-to-back	50 km	100 km	200 km	400 km	800 km
M7	300	627	300	382.6	370.0	367.0	364.5	359.0	347.5	
M8	300	1233	1200	752.1	727.3	724.5	722.0	716.5	705.5	683.5
M9	300	1881	2800	1147.9	1110.1	1107.0	1104.5	1099.0	1088.0	1066.0

Table 5.2: Losses in HVDC Light [1]

For the largest converter named M9, the power loss in percentage for each converter at full power can be described according to Equation (5.2).

$$\text{Converter loss, per converter} = \frac{P_{sending} - P_{receiving}}{2 \cdot P_{sending}} = \frac{1147.9 - 1110.1}{2 \cdot 1147.9} \approx 1.65\% \tag{5.2}$$

In percentage, the converter losses for the modules M7 to M9 are identical.

The converter MW losses can be assumed to be independent of the power through the HVDC Light system, since a large part of the losses are caused by the switching of the IGBT's [14]. The cable loss can be calculated by finding the DC current, given a certain cable dimension and length. In [1], an overview of resistance for different cables is presented. In this thesis, data for the largest cable is used, with a copper conductor area of 3000 mm^2. The resistance is 0,0059 Ω per km. With a 600 km distance to the offshore wind farm, the total resistance of the cable will be 7,08 Ω. For 1000 MW produced offshore wind power, the received power is found by using Equation (5.3) to (5.5). The DC current in Equation (5.3) is found by dividing the sending power on DC side $P_{sending,DC}$ for the rectifier by the DC voltage multiplied by 2. Converter loss for one converter is subtracted from the produced wind power in order to find the sending DC power. The DC voltage has to be multiplied by 2 because the given DC voltage is pole to ground.

$$I_{dc} = \frac{P_{sending,DC}}{2 \cdot V_{dc}} = \frac{1000 \cdot 10^6 - \frac{(1147.9 - 1110.1)}{2} \cdot 10^6}{2 \cdot 300 \cdot 10^3} \approx 1635 A \tag{5.3}$$

$$P_{loss,cable} = R_{dc} \cdot I_{dc}^2 = 7.08 \cdot 1635^2 \approx 19 MW \tag{5.4}$$

For 1000 MW offshore wind power, the received power is found in Equation (5.5).

$$P_{received} = P_{wind} - P_{loss,converters} - P_{loss,cable} = 1000 - 37.8 - 19 = 943.2 MW \tag{5.5}$$

$P_{loss,converters}$ are the total converter loss for both the converters. In the simulations received power of 940 MW is assumed.

5.3.4 Dynamic model

In order to represent the dynamics behavior of the HVDC Light system, ABB has developed two user models called CHVDCL and DC_HL2 [2]. The user model CHVDCL represents the dynamics of the converters, and calculates the current injection to be applied by the standard generator models used to model the converters in the load flow.

The model DC_HL2 represents the dynamic behavior of the DC system. Both the cable and the converters have capacitances with corresponding time constants T according to Equation (5.6).

$$T = 2 \cdot \frac{\frac{1}{2} \cdot C \cdot U_{dN}^2}{P_N} = \frac{C \cdot U_{dN}^2}{P_N} \tag{5.6}$$

T is the charging time of the capacitance [s], C is the capacitance pole to ground [F], U_{dN} is the nominal DC voltage, pole to neutral [kV], and P_N is the nominal active power [MW]. The model is based on simple integrator blocks according to Equation (5.7) [2].

$$\text{Integrator block} = \frac{1}{sT} \tag{5.7}$$

In the dynamic description file of the model, a default value of a 100 km cable is given. The user manual doesn't mention that the time constant should be changed for longer cables, but it is assumed that the time constant is 6 times larger for a 600 km cable. According to Equation (5.6), the time constant is proportional with the capacitance of the cable, which is proportional with the length of the cable. The time constant for the converters remains unchanged for increased cable length.

The DC voltage at the converter regulating the DC voltage is calculated as the integration of the net injected current via the integrator. The net current is the difference in active power injection by the converters, minus losses, divided by the DC voltage [2]. For the other converter, the DC voltage is calculated by subtracting or adding the voltage drop due to the resistivity in the system.

Figure 5.2 shows the structure of the load flow and dynamic model of HVDC Light.

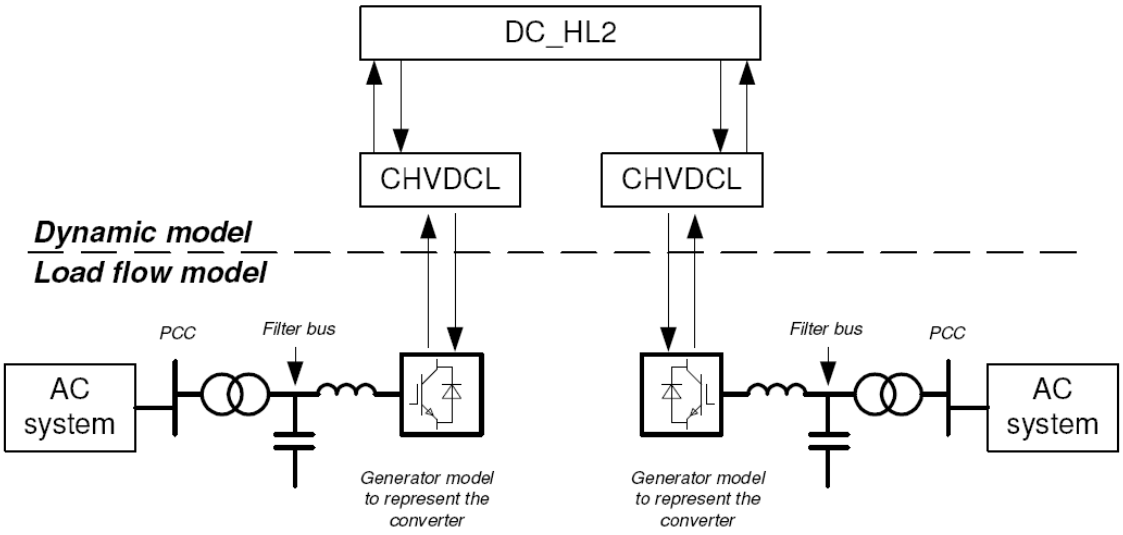

Figure 5.2: HVDC Light model in PSS/E [2]

For each of the modules described in 5.3.1, a default dynamic description file is provided. The control mode for the model as described in 4.4 is given as integer constants in the dynamic description file.

5.3.5 Offshore wind power application

The characteristics of HVDC Light make the technology well suited for transmitting power from offshore wind farms [1]. One main advantage is the controllability of the converters. A HVDC Light system can supply power to a passive network at a desired frequency. There are no requirements regarding short-circuit power at the connected AC system [1]. However, there are some limitations in the control system in the current version of the HVDC Light model in PSS/E regarding offshore wind power applications and transient studies. According to ABB, this will be implemented in the next version of the model [2]. In this paragraph, these limitations are described, and approximations done in the dynamic simulations are explained. It has to be emphasized that the limitations only apply to the current HVDC Light model in PSS/E, and has nothing to do with the actual control system of HVDC Light.

The trend for wind turbines is that they are able to operate at variable speed in order to maximize the power output from the wind speed by keeping the tip speed ratio constant [16]. DFIG turbines or full frequency converter turbines with synchronous generators are the most common types for variable speed wind turbines. The consequence of these technologies is that the local AC system offshore can not be considered having rotating masses that can be used to store power temporarily. The frequency converter on the turbine side defines the frequency on the turbine side; hence also the synchronous speed of the turbine. The frequency converter on the grid side adopts the grid frequency. There is a decoupling between the grid frequency and the rotational speed of the generators. On the other side, with normal induction generators directly connected to the grid, the synchronous speed is directly given from the frequency of the grid. The rotational speed of the turbines is close, but not equal to the synchronous speed, as inductions generators operate with a slip when power is produced. Slip is the difference between the rotational speed and synchronous speed, caused by mechanical torque at the turbine [8]. For normal operation, the slip is in the range of about 1 %. The rotational speed of the wind turbines will be about 1 % larger than the synchronous speed.

If the onshore voltage U_{ac} is reduced due to a fault, the power transmission of the HVDC Light has to be reduced. The maximum power transferred from the onshore converter to the AC system is limited, according to Equation (5.8).

$$S = \sqrt{3} \cdot U_{ac} \cdot I^{*} \tag{5.8}$$

With HVDC Light, the AC voltage offshore is kept almost constant for a fault onshore. This will be shown in the simulations in chapter 7. The wind turbines can continue to produce power as before the fault onshore occurred. However, because of the limitation in the power transfer for the onshore converter during the fault, the wind power fed into the DC system offshore has to be reduced in order to avoid the DC voltage to increase. This can be done in two ways; either increase the wind turbine speed, or burn the excess produced power in a DC chopper during the fault [14]. DC choppers are planned for future offshore wind power applications with HVDC Light. With a DC chopper, the offshore wind farm will not see the fault onshore, and can continue to produce the same amount of power. This is not modeled in the current model of HVDC Light. In the simulations done in this thesis, the rotational speed is increased in order to store the energy offshore during an onshore fault instead of feeding the produced power into the DC system. Because of the decoupling of grid frequency and rotational speed for frequency converter wind turbines, normal induction generator wind turbines are used in the simulations in this study.

If the offshore converter is in passive control mode, it is set to transfer all the power produced offshore; it has the function of a swing bus offshore. This is described in 4.4.2. The AC amplitude and frequency is constant at the defined value. For a fault onshore, the control system for passive mode does not change the amplitude of the AC voltage or the frequency offshore. The wind turbines produce power at the same level as before the fault, causing the DC voltage to increase drastically during the fault onshore.

As an approximation to avoid this, the control system can be changed to normal operation during a fault onshore. This method is used in the simulations. The offshore converter is in U_{dc} control mode, while the onshore converter is in active power control mode. When the fault occurs onshore, the DC voltage will increase immediately because of the power imbalance between the two converters. The power fed into the DC system from the offshore converter is quickly reduced as a response to this in order to reduce the DC voltage. The rotational speed of the wind turbines and frequency offshore and will increase. The energy from the wind is used to accelerate the turbines as long as the fault onshore is too low for the onshore converter to transfer the power produced by the wind farm.

In the simulation done is this study, it is assumed that the wind speed is constant, and hence also the mechanical torque on the wind turbines. Because of this assumption, the control system is set to normal operation during the whole time period in the simulations. If variable wind speed is to be used as input to the wind turbines, the control system has to be changed manually from passive mode to normal control mode at the instant the fault onshore occurs. After the fault onshore is cleared and the voltage has recovered, the control system has to be changed back to passive mode in order for the offshore converter to function as a swing bus. The control system can be changed by changing integer constants for the CHVDCL models for the converters in PSS/E [2].

The wind turbines operate at full power, equal to 1000 MW in total for the offshore wind farm. It is therefore assumed that the wind turbines have some temporary over load capacity, in order to transfer the increased rotational power to the onshore grid after the onshore fault is cleared.

5.3.6 Time step

For the dynamic simulations with HVDC Light, the time step has to be reduced compared to simulations of normal AC systems. A time step of 10 ms is normally used for AC systems in PSS/E, while for simulation with HVDC Light a time step of 5 ms will give a good representation of the dynamic response close to the HVDC Light converters [2]. The reason for this is the small time constants descried in 5.3.4 associated with HVDC systems.

6 Load flow cases

Before dynamic simulations can be done, a load flow case has to be established as a starting point. This chapter describes the different load flow situations established for the simulations done. Two possible connection points of 1000 MW offshore wind power is chosen; Feda and Kårstø. In order to investigate the transient stability in the two connection points for different load flow situations as well as reduced short-circuit power, cases with lower load and production in the system are established.

6.1 Connection point Feda

The case to be studied in this thesis is grid connection of a 1000 MW offshore wind farm in the North Sea. The wind farm is to be connected to the south of Norway. In order to connect large amounts of offshore wind to the grid, the transfer capability from the connection point has to be investigated. One of the connection points for offshore wind power in this thesis is Feda. This is the only busbar in the very south of Norway close to the sea that has enough thermal capacity to transfer 1000 MW offshore wind power to the load centers.

In the south of Norway, the highest voltage is 300 kV. The next voltage level is 132 kV. The 132 kV lines in the Norwegian model typically have thermal limits of a couple of hundred MVA. A 300 kV line can have thermal limit of more than 1000 MW. The voltage at Feda is 300 kV, and there are several lines going out from the busbar. Figure 6.1 shows a section of the 300 kV grid in the south of Norway, with lines going from Stavanger in the west, Arendal in the east, Lista in the south and Lyse in the north. Feda is the connection point of the offshore wind power, marked in red with a circle around. The sum of the capacity of the lines connected to from Feda is 4710 MVA. This does not indicate how much wind power that can be fed into the busbar, but indicates that the point is a strong. By performing a short circuit analysis according to Equation (2.3) in PSS/E on the busbar Feda, the short-circuit capacity is 7147 MVA. As described in 2.4, this is a measure of the strength on the busbar.

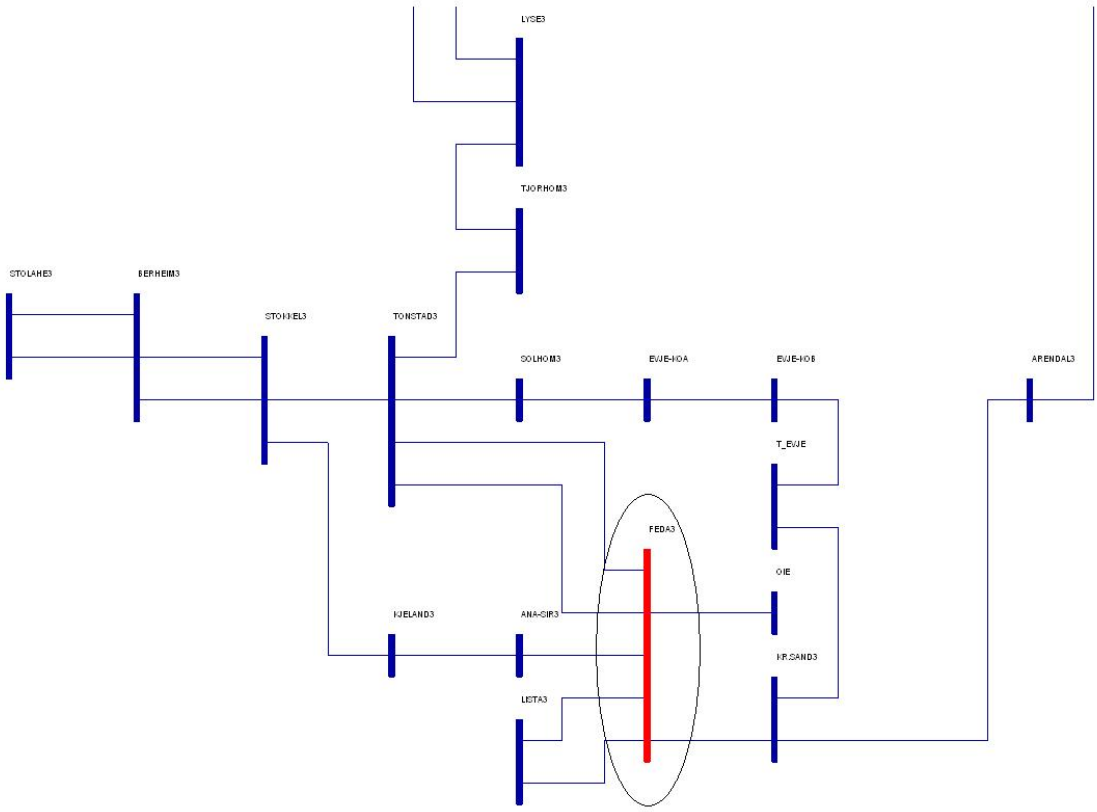

Figure 6.1: Overview of the 300 kV power grid in the south of Norway

A screenshot from the original load flow situation described in 5.1 is presented in Figure 6.2. The number above the line is active power, and the number below the line is reactive power. Power is defined positive out from the busbar. The boxes on the lines indicate the percentage of the maximum current loading in the lines. The voltage is given in pu under the busbars. As described in 5.1, some of the busbar voltages are outside the range of 0,9 – 1,1 pu. Additionally, some branches are over loaded. It is assumed that the load flow situation is realistic with these violations. The limit checking reports for the original load flow case is can be found in Appendix A.1 and A.2.

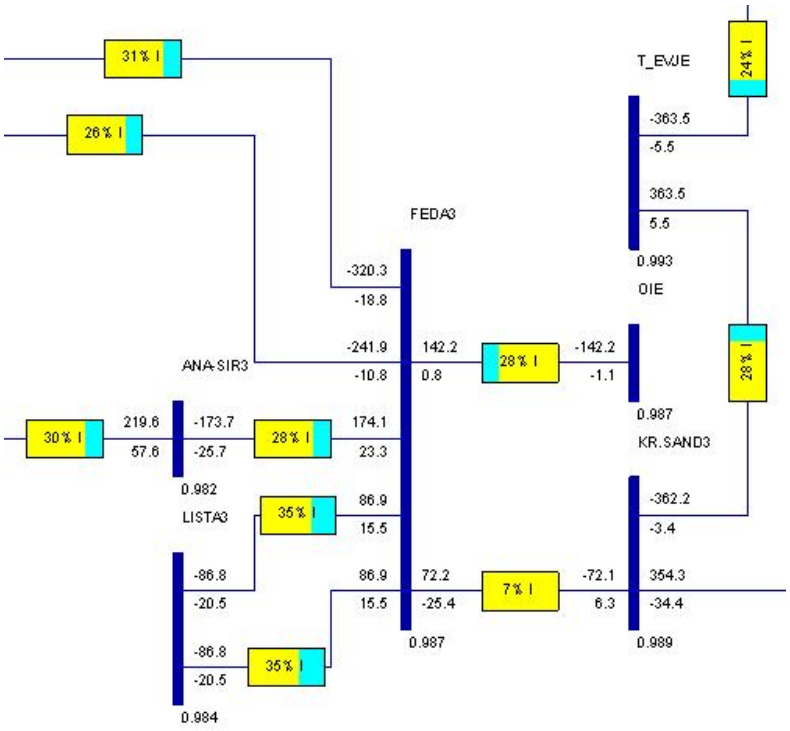

Figure 6.2: Load flow result at Feda, original load flow

In Figure 6.3 a screenshot of the load flow for the same situation is presented, with 1000 MW power added to Feda. The offshore wind power is here simply modeled as a voltage regulating generator connected directly to Feda in order to show the direction of the power in the surrounding transmission lines. For the dynamic simulations, the offshore wind power will be modeled differently.

When additional wind power is added to the system, the swing bus adjusts the production in order to maintain the balance between produced and consumed power in the system. With 1000 MW infeed of offshore wind power, the production at the swing bus becomes negative. One of the main connections out from Norway is the line from Hasle to Borgvik in Sweden. All the power imported from the Netherlands and Denmark is assumed exported out from Norway through this line. A load of 900 MW is added on the 400 kV busbar Hasle. It is assumed that only active power is transferred to Sweden, even though in a real situation some reactive power would flow in the line.

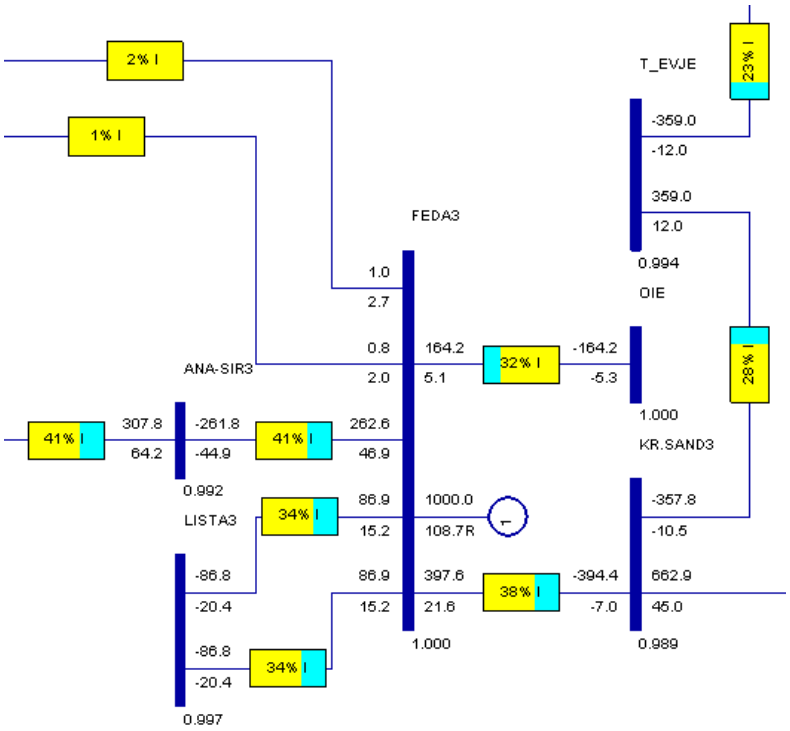

Figure 6.3: Load flow result with 1000 offshore wind, connection point Feda

Limit checking reports for voltages and branches for voltages from 132 kV to 400 kV are made in order to make sure that voltages are within the limits and branches are not over loaded with full power from the wind farm. The limit checking reports can be found in Appendix A.3 and A.4. The limit checking reports for the original load flow case in Appendix A.1 and A.2 are used as references.

6.1.1 Feda with HVDC from the Netherlands and Denmark

Feda is also the connection point for the HVDC cable from the Netherlands, NorNed. This HVDC system is a traditional system based on thyristors, and the rating of the converter is 700 MW. There are also a total of 1000 MW HVDC links to Denmark. These converters are placed in Kristiansand. In order to supply the HVDC converters with reactive power, SVC's are installed in Kristiansand. Additionally, a synchronous condenser is installed at Kristiansand in order to increase the short-circuit power at the connection point.

Since the model for the Norwegian power system provided by Statnett only contains data for Norway isolated, assumptions have to be done in order to estimate the power flow in a real situation. The HVDC converters importing power from the Netherlands and Denmark can be modeled as loads with negative active power. Since the converters consume reactive power corresponding to about 50 % of the active power [17], the complex parts of the loads are modeled as positive loads.

When additional power is added to the system, the swing bus adjusts the production in order to maintain the balance between produced and consumed power in the system. With 1700 MW infeed from the Netherlands and Denmark, the production at the swing bus becomes negative. One of the main connections out from Norway is the line from Hasle to Borgvik in

Sweden. All the power imported from the Netherlands and Denmark is assumed exported out from Norway through this line. A load of 1600 MW is added on the 400 kV busbar Hasle. It is assumed that only active power is transferred to Sweden, even though in a real situation some reactive power would flow in the line.

A screenshot from the original load flow with HVDC added is presented in Figure 6.4.

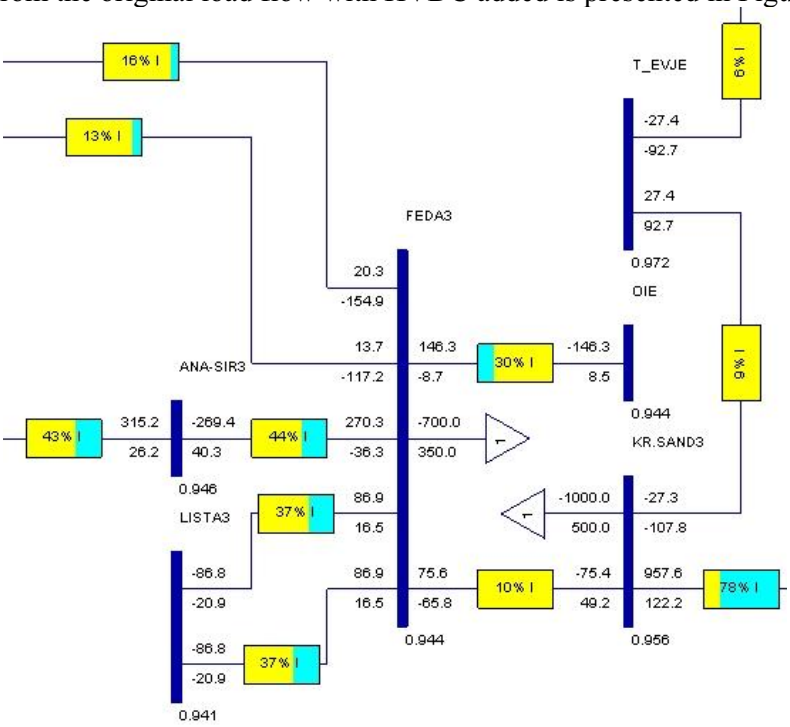

Figure 6.4: Load flow result at Feda with full import of HVDC

The voltages in the screenshot is within the values of 0,9 – 1,1 pu, but voltages on busbars other places in the system are too low compared to the original load flow situation with out any wind power. Additional branches are also slightly over loaded. The 400 kV transmission link from Teige to Bastø, which is one of the main transmission links from the west to the east, is at the limit of being over loaded. The limit checking reports for voltages and branches for voltage from 132 kV to 400 kV can be found in Appendix A.5 and A.6. When adding wind power to Feda, and increasing the load at Hasle, eventually the load flow will not be solved. This is assumed to be an unrealistic load flow situation in the Norwegian system. With this high power production in the system, power will not be imported to Norway from the HVDC links.

6.2 Connection point Kårstø

Kårstø could also be a potential connection point of 1000 MW offshore wind power. Kårstø is a gas processing plant in the south west of Norway, north of Stavanger. The voltage is 300 kV, and the consumption of power from industry in the area is high. The large consumption of power by the industry nearby will lead to less transmission losses for the system.

Figure 6.5 shows a section of the 300 (blue) and 400 kV (orange) grid in the south-west of Norway, with lines going from Karmøy in the west, Vemork and Kvilldal in the east, Blåfall in the north and Saurdal in the south. Kårstø is the connection point of the offshore wind power, marked in red with a circle around. The short-circuit power at Kårstø is 3986 MVA, and the sum of capacity of the connected lines is 1717 MVA. This indicates that Kårstø is a considerable weaker point than Feda.

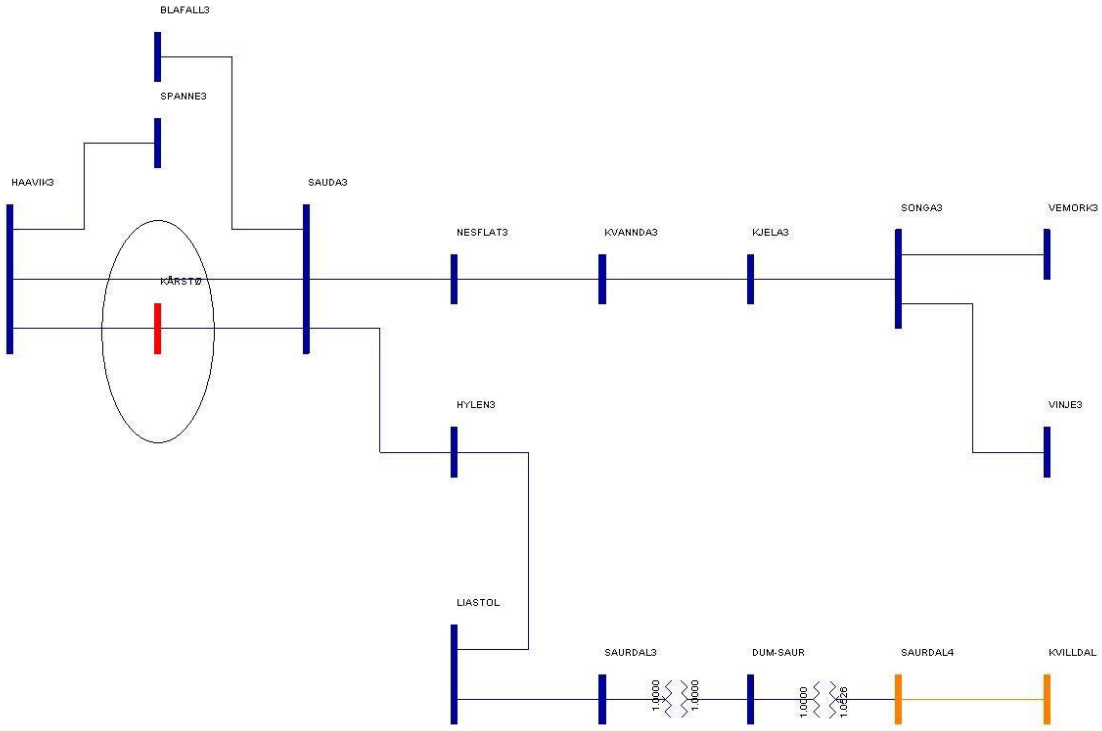

Figure 6.5: Overview of the 300 kV grid in the southwest of Norway

A screenshot from the original load flow for a peak load situation is presented in Figure 6.6.

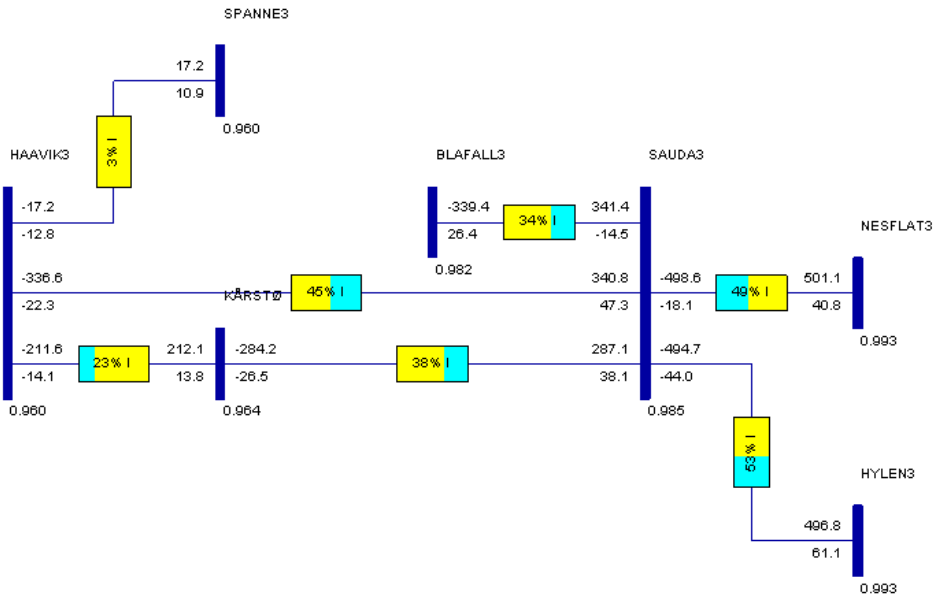

Figure 6.6: Load flow result at Kårstø, original load flow

As can be seen from the load flow screenshot, a large amount of power is flowing to the busbar Haavik. There is a large amount of industry demanding about 500 MW at the neigbour busbar.

In Figure 6.7 a screenshot of the load flow for the same situation is presented, with 1000 MW power added to Kårstø. As in the case for Feda, the offshore wind power is modeled as a voltage regulating generator connected directly to Kårstø in order to investigate the direction of the power in the surrounding transmission lines. A 900 MW load is added at Hasle in order to simulate export of power.

The offshore wind power will be modeled differently in the simulations. As can be seen by comparing Figure 6.6 and Figure 6.7, the direction of the power flow in the transmission line from Kårstø to Sauda is changed. The line from Sauda to Haavik transfer 300 MW less power with the offshore wind power added to Kårstø.

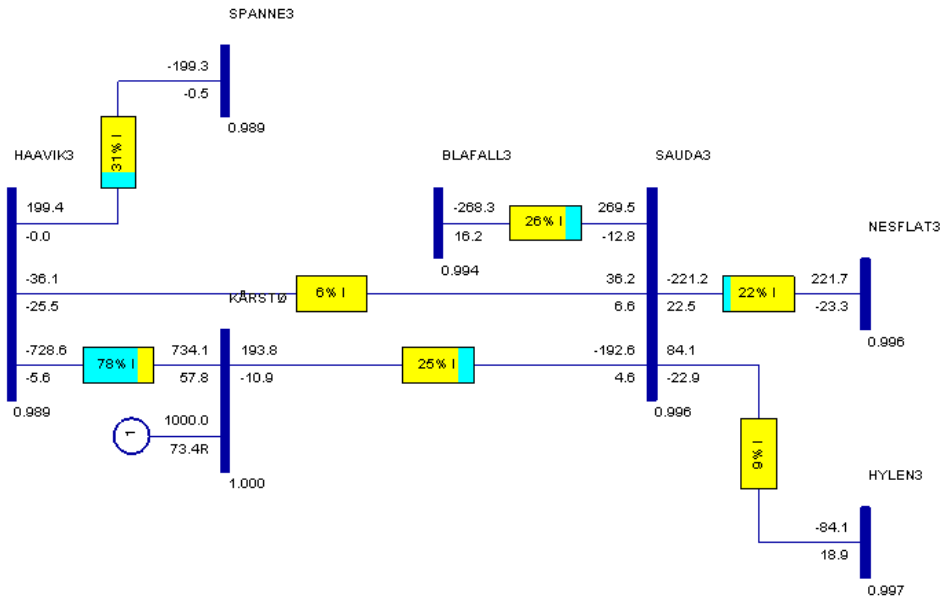

Figure 6.7: Load flow result with 1000 MW offshore wind, connection point Kårstø

Limit checking reports for voltages and branches for voltages from 132 kV to 400 kV are made in order to make sure that voltages are within the limits and branches are not over loaded with full power from the wind farm. The limit checking reports can be found in Appendix A.7 and A.8.

6.3 Background for load flow situations

The load flow limit checking reports made in 6.1.1 indicate that the power system is not able to import wind power in addition to rated power from the HVDC link from the Netherlands and Denmark in a peak load situation in Norway with full production. With additional offshore wind power fed into the same busbar as the HVDC power from the Netherlands, the main transmission lines are even more over loaded, and voltages in the system become too low. The load flow situations are not realistic. With large enough production from the Norwegian power plants to cover the peak load, additional power will not be imported from the HVDC links.

When the production in the system is planned, the cheapest producing unit will be set to produce power first [22]. Even though the water in hydro power plants is free, water values are used as a tool for marginal cost of production. Every hydro reservoir has its own water value, based on the water level in the reservoir, the snow in the mountains, expected precipitation based on weather forecasting, among other things. If the water value for a hydro power plant is higher than the spot price, the power plant will store the water for later in order to maximize the profit for the power producing company. If the water value is lower, the power plant will produce power. When a reservoir is at the maximum level and it is expected that more water will come into the reservoir, the value of saving the water becomes equal to zero. The power plant will then produce as much power as possible. Hydro power plants with small or no reservoirs, typically have low water values. The saved water will not be possible to save for later; hence it is better to produce at maximum power and get a low spot price. Some hydro power plants have large reservoirs that are capable of saving the water from year to year.

The energy cost for wind power is higher than the hydro power in Norway, because of the capital cost of the wind farms. Nevertheless, the marginal cost of producing wind power is practically equal to zero. The wind is free, and the wind farm produce power when the wind blows with no ability to save the wind for later periods with higher spot price. If a wind farm does not produce the maximum power for the given wind speed, the production is lost. Wind power will always be prioritized before hydro power, unless the hydro power plant does not have the capability to store to water in a reservoir.

If the production in Norway is as high as in the original load flow situation, and the offshore wind farm produce additionally 1000 MW, the HVDC links will probably export power to the Netherlands and Denmark or shut down the unit with highest water value in order to maximize profit. The situation with full HVDC import in the original load flow situation is assumed not to be realistic.

During winter time the spot prices can be quite high because of low water levels in the reservoirs, and high power consumption. The HVDC links will import power because the electricity produced in thermal power plants on the continent is cheaper. Even though the offshore wind farm produces full power, this does not necessarily reduce the spot price enough so that the import is stopped. The most realistic case with full import of HVDC and full power from the offshore wind farm is therefore a peak load situation with lower production of hydro power than in the original load flow case.

A realistic case could be full import of the HVDC link from Denmark, and no import from the Netherlands. The Danish power system is dependent of exporting wind power to Norway in periods with high production of wind. If the production of the offshore wind farm in the North Sea is at maximum, it is expected that the wind is blowing in Denmark as well. With wind power fed into Feda instead of HVDC, reactive power is regulated at Feda instead of consumed by the HVDC converter. The regulation of reactive power for wind power will be explained in 6.5. Even though the limit checking report from the case with full HVDC import showed somewhat more over loading of lines in addition to voltages outside the range of 0,9 – 1,1 pu, simulations are done for this load flow situation.

Three different load flow situations for 1000 MW offshore wind production connected to Feda are chosen for dynamic simulations. Additionally, two different load flow situations are chosen for Kårstø as connection point. An overview of the different load flow cases are defined in Table 6.1. Production and load consumption is defined as "original" for the production and load consumption in the original load flow case provided by Statnett. The load flow cases are described in detail in detail in 6.4.

	Point of connection	Production	Load	Import HVDC	Export Sweden	Offshore wind
				[MW]	[MW]	[MW]
Case 1	Feda	Original	Original	0	900	1000
Case 2	Feda	Reduced	Reduced	0	900	1000
Case 3	Feda	Reduced	Original	1000	0	1000
Case 4	Kårstø	Original	Original	0	900	1000
Case 5	Kårstø	Reduced	Original	0	0	1000

Table 6.1: Load flow situations

It has to be emphasized that the power flow situations chosen are supposed to reflect the worst case scenarios in the sense that no power is exported through the HVDC links to the Netherlands and Denmark. With high power production in the Norway, it is likely that the power is exported to the Netherlands and Denmark. For the connection point at Feda, the load flow changes in the rest of the system will be less affected, since a lot of the offshore wind power is exported directly from the same busbar.

6.4 Establishing of the load flow cases

The Norwegian model provided by Statnett was a case with peak load in the system and production corresponding to the load consumption. In order to do dynamic simulations based on different load flow situations, the load flow had to be changed manually.

In the load flow environment, PSS/E has a function that scales the production and load in defined percentage or MW steps. However, in large systems drastic changes in the power production and load consumption become difficult to perform. Even though both the production and load is scaled down in small steps in the system, at a certain point the load flow will not be solved without a very large MVA mismatch. Beyond this point, the mismatch increases drastically for even a small change in the system. All the power plants are set to a specific voltage set point, corresponding to the load flow situation. When the production and load is changed, the set points of the voltage in all the plants and reactive power compensating

units should be changed according to the new load flow. Without any information of what the new set points should be, this becomes a random operation that would not improve the solution of the load flow.

Because of the above mentioned problems, an assumption had to be made in establishing a load flow for situations with low load consumption and low production, and peak load and low production. Only the areas surrounding the area of interest were scaled down in order to be able to solve the load flow. Additionally, assumptions have to be made regarding which power plants should be disconnected during low production in the system. It is assumed that the largest power plants will be disconnected first, as they are assumed to have the highest water values because of storage capacity in the reservoirs. This is an assumption made in this thesis.

Because the production and load was only scaled down in some parts of the south of Norway, the load and production of the entire system is not changed much in percentage. The power flow in the large transmission lines will not be realistic according to the real situation with load and production levels as it would have been in a summer situation with low load in the entire system. In order to do realistic simulation in these cases, load flow situation for the entire system that represents a real situation should be provided. Additional agreements with Statnett would have to be done in order to get access to these files.

In this paragraph, the procedure of establishing the different load flow cases described in Table 6.1 is given. The description names used below for the load flow cases will be used to describe the starting point of the different dynamic simulations performed.

6.4.1 Case 1

The load flow case called Case 1 is the original load flow situation provided from Statnett, with the offshore wind power connected to Feda. The only change in the power flow is adding the wind power, and a 900 MW load at Hasle in order to simulate export of power to Sweden. In Case 1, the short-circuit power at Feda is 7147 MVA. The short-circuit power was found without the offshore wind power connected, and the results from the short-circuit power calculation from PSS/E can be found in Appendix B.

6.4.2 Case 2

The load flow case called Case 2 represents a load flow situation with low load and low production in the system. Feda is the connection point of the offshore wind power. There is export of power to Sweden. As described above, changes are only made in areas surrounding the connection point. The consequence of the disconnection of some generators is that the short-circuit power at Feda is reduced to 5228 MVA, from 7147 MVA in the original configuration. The short-circuit power was found without the offshore wind power connected, and the results from the short-circuit power calculation from PSS/E can be found in Appendix B.

The detailed procedure in establishing the load flow is described in Appendix C. The load is scaled down with a fixed relationship between P and Q on all busbars in the selected subsystem, except the busbars with name starting on KKI and IND. These busbars represent industry, and the power consumption is assumed to be kept constant.

6.4.3 Case 3

The load flow case called Case 3 represents a situation with peak load in the system and import of 1000 MW HVDC from Denmark. The HVDC converter at Kristiansand is modeled as a load equal to -1000 + j500 MVA, corresponding to the approximate consumption of reactive power in the converter. Feda is the connection point of the offshore wind power. There is no export of power to Sweden, so that the production corresponds to the load minus the offshore wind power and imported power from Denmark through the HVDC connection. No generators are disconnected; the production on the largest generators in the south of Norway is scaled down. The short-circuit power at Feda is 6900 MVA. The short-circuit power was found without the offshore wind power connected, and the results from the short-circuit power calculation from PSS/E can be found in Appendix B.

The detailed procedure in establishing the load flow is described in Appendix C.

6.4.4 Case 4

The load flow case called Case 4 is the original load flow situation provided from Statnett, with the offshore wind power connected to Kårstø. The only change in the power flow is adding the wind power, and a 900 MW load at Hasle in order to simulate export of power to Sweden. The short-circuit power at Kårstø is 3986 MVA. The short-circuit power was found without the offshore wind power connected, and the results from the short-circuit power calculation from PSS/E can be found in Appendix B.

6.4.5 Case 5

The load flow case called Case 5 represents a situation with peak load in the system. The offshore wind power is connected to Kårstø. The load is unchanged from the original load flow situation, but the production is scaled down in the surrounding areas, by disconnecting the largest generators. The short-circuit power at Kårstø in this case is reduced to 3556 MVA from 3986 MVA in the original case. The short-circuit power was found without the offshore wind power connected, and the results from the short-circuit power calculation from PSS/E can be found in Appendix B. There is no export of power to Sweden.

The detailed procedure in establishing the load flow is described in Appendix C.

6.5 Adding the offshore wind power

In order to do large changes in the load flow, care has to be taken when solving the case. New busbars added to the system have to be given the same voltage amplitude and angle as the connection busbar. The power has to be ramped up or down in small steps. As described in 5.2, one equivalent machine represents the entire wind farm. The equivalent generator is connected to a 20 kV busbar, and the voltage is transformed up to the transmission voltage in an offshore transformer.

6.5.1 AC cable connection

In all the dynamic simulations performed, a case with AC cable connection is compared to HVDC Light connection. Transmission with traditional HVDC is not modeled. Statnett has requirements regarding the power factor of wind farms connected to the grid. All wind farms larger than 10 MW connected to the regional or central grid, has to be able to operate at a power factor $cos(\varphi) =$ 0,95 capacitive and inductive at rated power [19]. Up until recently, the requirement was even stricter, with $cos(\varphi) = 0{,}91$.

Transmission with AC cable will require large amounts of reactive power compensation in order to fulfill Statnett's requirement of $cos(\varphi) = 0{,}95$ capacitive and inductive. In this thesis a distance of 100 km is assumed with AC cable connection. It has to be emphasized that this distance to the offshore wind farm is not realistic with today's technology, because the depths outside the Norwegian coast would require floating wind turbines at this distance from shore. In order to transfer 1000 MW of power, two sets of AC cables have to be installed. The data used for the cables is provided by Nexans. The per phase series impedance is 0,0604 + j0,1031 Ω/km, and the shunt capacitance is 0,13 μF/km [13]. The copper conductor area is 500 mm^2, and two sets of cables have to be used in order to transfer 1000 MW. Cables of this size are always custom made, so the values for the impedances are typical values [13]. With the given cable data, the two sets of cables produce a total of 520 Mvar at the connection point at voltage equal to 1 pu at rated power from the wind farm. This reactive power could be compensated for with shunt reactors. In the simulations, a shunt reactor at the connection point corresponding to 500 Mvar reactive power consumption at nominal AC voltage is installed. The active power received onshore at 1000 MW produced by the wind farm and 100 km AC cable is about 960 MW. In order to operate at $cos(\varphi) = 0{,}95$, the necessary capacity from SVC can be found according to Equation (6.1).

$$Q_{SVC} = P \cdot \tan(\cos^{-1}(\varphi)) = 960 \cdot \tan(\cos^{-1}(0.95)) \approx 316\text{Mvar} \tag{6.1}$$

Earlier, with $cos(\varphi) = 0{,}91$ the necessary capacity from the SVC would have been 437 Mvar, if all the reactive power produced by the AC cable was compensated for by a shunt reactor.

Two SVCs with a rating of 200 MVA each at the connection point are chosen for simulations with AC cable transmission. In the model for the Norwegian power system, there is a user model for SVC called NORSVC, and the dynamic parameters for this model are used in the simulations. The voltage set point for the SVCs is 1 pu for all the load flow cases.

Figure 6.8 shows the layout of the equivalent offshore wind farm connected to the onshore grid with AC cables. The green busbar is the 20 kV busbar the wind farm equivalent machine is connected to, and the blue busbar to the left is the 300 kV connection point onshore. The two machines onshore represent the SVCs, and the coil is the shunt reactor compensating for the reactive power produced by the two sets of AC cables.

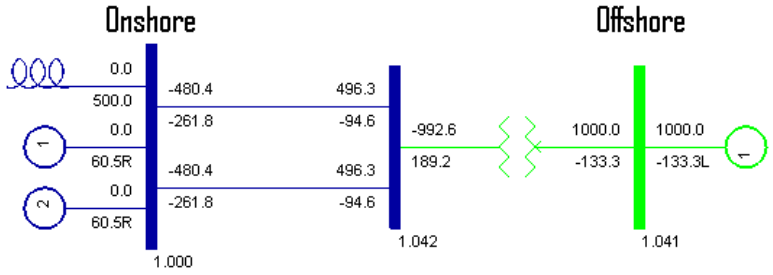

Figure 6.8: Equivalent offshore wind farm connected with AC cables

6.5.2 HVDC Light connection

For transmission with HVDC Light of a 1000 MW wind farm, the requirement from Statnett is fulfilled at the connection point without any auxiliary compensating equipment. This can be verified by inspecting the capability curve of HVDC Light in Figure 5.1. The topology offshore, as well as the length and dimension of the DC cable will influence the losses and hence received power onshore. In this thesis a DC cable length of 600 km is used. As described in 5.3.3, with these assumptions the received power onshore equals about 940 MW, which corresponds to 0.79 pu active power in Figure 5.1. With this active power, the converter onshore can produce about 0,375 pu, or 447 Mvar reactive power, and consume 0,5 pu or 596,5 Mvar. This corresponds to about $cos(\varphi)$ = 0,90 capacitive and $cos(\varphi)$ = 0,84 inductive at the connection point onshore. In order to utilize the HVDC Light system maximal regarding the $cos(\varphi)$ requirement, even more offshore wind power could be installed with the largest HVDC Light converter.

Figure 6.9 shows the layout of the equivalent offshore wind farm connected to the onshore grid with HVDC Light. The green busbar is the 20 kV busbar the wind farm equivalent machine is connected to, and the blue busbar to the left is the 300 kV connection point onshore. The orange busbars are the converter busbars, with a nominal voltage of 408 kV. The shunt capacitors represent the AC filters, and the machines represent the HVDC Light converters.

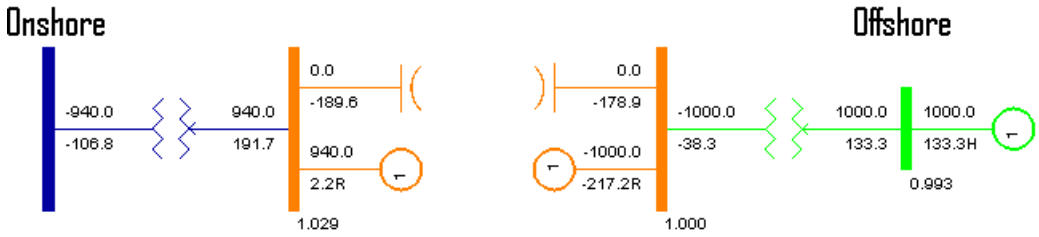

Figure 6.9: Equivalent offshore wind farm connected with AC cables

7 Dynamic simulations

In this chapter dynamic simulations are performed in order to investigate the dynamic behavior of 1000 MW offshore wind power connected to the grid with HVDC Light. As a comparison, an identical case with AC cable transmission is established for each simulation with HVDC Light. In order to fulfill the requirements regarding reactive power control at the connection point, SVCs are added for the cases with AC cable connection.

Simulations with the two different transmission technologies are done for all five load flow cases described in 6.4. Three events are defined in order to investigate the dynamic behavior of the offshore wind farm connected to the grid. All the simulation plots are presented in Appendix D. Some of the plots from the most significant cases are also given in this chapter in order to highlight the most significant characteristics.

7.1 Grid code

All power plants, including wind turbines, connected to the grid have requirements regarding behavior during disturbances in the power system. This is normally referred to as fault ride through [19]. The power plants shall contribute to the short-circuit power during faults, and maintain connected after the fault is cleared. Statnett has requirements for all power plants in Norway connected to directly grounded grid with nominal voltage greater than 200 kV. The power plant has to stay connected and deliver power when the voltage at the connection point is above the voltage profile described as follows:

- Voltage reduction to 0 % for up to 150 ms, followed by voltage increase to 25 %
- Linear voltage increase from 25 % to 90 % for 750 ms
- Constant voltage at 90 %

The requirement is shown graphically in Figure 7.1.

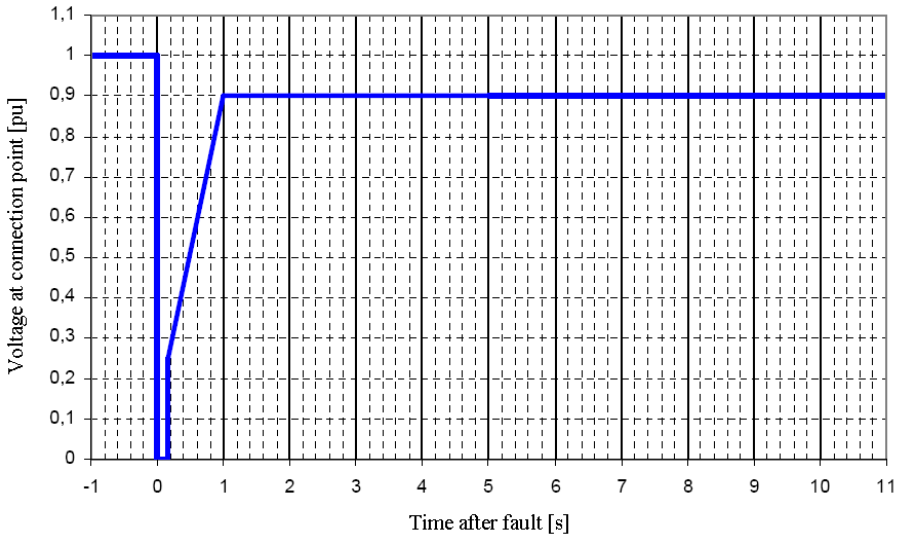

Figure 7.1: Fault ride through requirement for power plants [19]

Power plants connected to busbars with voltage equal or greater to 200 kV generally have a large MVA rating. The dynamic behavior of these power plants will have significant influence on the dynamic behavior of the system. This is the reason why the power plants are required to stay connected even though the voltage at the connection point is zero for 150 ms, as the consequences of tripping of such power plant normally will have undesirable effects on the power system. The fault ride through requirement for power plants connected to voltage level equal or smaller to 132 kV are allowed to trip if the voltage falls below 0,15 pu [19].

For offshore wind power, the transmission technology will have great influence on the dynamic behavior of the system. This will be shown in the dynamic simulations done in this chapter. Protection of the wind turbines is not modeled; it is assumed that the wind turbines will stay connected as long as the voltage at the connection point onshore is within the profile in Figure 7.1. The focus of the simulations will be the impact of the transmission technology on the onshore power system.

7.2 Conversion of loads

Before doing dynamic simulations or fault analyses, the generators and loads have to be converted to Norton equivalents [18]. The loads can be converted as constant current, constant admittance or constant power loads. All the loads in the systems will have slightly different characteristics; hence a few assumptions have to be made in the converting process. Loads in the Norwegian model are assumed divided into two groups; normal loads and industrial loads. Industrial loads are recognized in the model by the connected busbar name starting with IND (industri) or KKI (kraftkrevende industri). The conversion is based on recommendations from Statnett. Table 7.1 describes how the loads are converted.

	Normal load		Industial load	
Load representation	P %	Q %	P %	Q %
Constant power	40	30	0	0
Constant current	40	20	100	0
Constant admittance	20	50	0	100

Table 7.1: Load conversion

7.3 Definition of disturbances

In this study, the focus is on transient stability. In [12], transient stability is defined as follows: "*Transient stability is the ability of the power system to maintain synchronism when subjected to a severe transient disturbance… …The contingencies usually considered are short-circuits of different types."*

The case with voltage equal to zero at the connection point according to the grid code presented in Figure 7.1 is a worst case scenario. Only a perfect three-phase short-circuit at the connection point will result in this. In order to investigate the dynamic behavior of HVDC Light for other situations, simulations are also done with events leading to a smaller voltage reduction at the connection point.

Simulations are done for all the 5 load flow cases described in 6.4; three cases with Feda as connection point and two cases with Kårstø as connection point. The three events are simulated for all the load flow cases, with both AC cable and HVDC Light connection of the offshore wind power. Totally 30 simulations are done, and all the plots can be found in Appendix D. The description names of the events will be used to describe the dynamic simulations performed, along with the names of the load flow cases described in 6.4.

7.3.1 Description of Event 1

In Event 1, a fault at a neigbour busbar of the connection point is applied, with shunt impedance to ground larger than zero. In PSS/E, shunt resistance and reactance are given in the MW and MVA power for the actual voltage at the busbar. In this event, a power of -2E+004 Mvar is added to simulate the fault. For nominal voltage equal to 300 kV at the busbar, the shunt reactance added can be found by Equation (7.1).

$$Q = \frac{U_{ac}^2}{X_{shunt}} \Rightarrow X_{shunt} = \frac{U_{ac}^2}{Q} = \frac{(300 \cdot 10^3)^2}{-2 \cdot 10^{(4+6)}} = -4.5\Omega \tag{7.1}$$

The bus fault is removed after 150 ms. For connection at Feda the fault appears at Øie, while for connection at Kårstø the fault appears at Sauda. The busbars can be recognized by inspection of Figure 6.1 and Figure 6.5.

7.3.2 Description of Event 2

In Event 2, a three-phase short-circuit at a line going from the connection point to a neighbour busbar is applied. The short-circuit is simulated with impedance equal to zero, close to the neigbour busbar. The fault is cleared after 100 ms, and the line is disconnected.

For connection point at Feda, the line with short-circuit is one of the lines going from Tonstad to Feda. For connection point at Kårstø, the faulted line is the line going from Haavik to Kårstø. The lines can be recognized by inspection of Figure 6.1 and Figure 6.5.

The choice of faulted lines are based on which line gives the largest contribution to the short-circuit current at the connection point, and hence short-circuit power. Tripping the line with the largest contribution is a worst case scenario, in terms of short-circuit capacity at the connection point. The short-circuit calculation results can be found in Appendix B.

7.3.3 Description of Event 3

In Event 3, a three-phase short-circuit is applied to the connection busbar. The short-circuit is modeled with impedance equal to zero, so that the voltage at the connection point is zero during the fault. The fault is cleared after 150 ms.

7.4 Simulation results

The wind turbine model used in the simulations is simply a PSS/E model of induction generator called CIMTR3. No protection of the wind farm is modeled. It is assumed that the wind farm will stay connected as long as the system has a stable behavior after a disturbance. This is an approximation, but the main focus of this thesis is to describe the dynamic behavior on the onshore power system with different transmission technologies.

Table 7.2 presents the main results from the simulations.

	Event 1		Event 2		Event 3	
	AC cable	HVDC Light	AC cable	HVDC Light	AC cable	HVDC Light
Case 1	Stable	Stable	Stable	Stable	Unstable	Stable
Case 2	Stable	Stable	Stable	Stable	Stable	Stable
Case 3	Stable	Stable	Stable	Stable	Unstable	Stable
Case 4	Stable	Stable	Unstable	Stable	Unstable	Stable
Case 5	Unstable	Stable	Unstable	Stable	Unstable	Stable

Table 7.2: Simulations results

As can be seen from the table, all simulations with HVDC Light show stable behavior. For all the simulations marked as stable, the onshore voltage recovers in such a manner that the offshore wind farm has to stay connected based on the fault ride through requirement.

For all simulations with AC cable connection the following variables are plotted. System base is equal to 1000 MVA.

- Voltage at the connection point [pu]
- Voltage at the offshore busbar [pu]
- Deviation from synchronous speed of the wind turbine generators [pu]
- Reactive power from one of two 200 Mvar SVC at the connection point [pu on system base]

For all simulations with HVDC Light connection, the following variables are plotted:

- Voltage at the connection point [pu]
- Voltage at the offshore busbar [pu]
- Deviation from synchronous speed of the wind turbine generators [pu]
- DC voltage at the voltage regulating HVDC Light converter [kV]
- Reactive power from the HVDC Light converter at the connection point [pu on system base]

In order to present the main characteristics of the dynamic response both with AC cable and HVDC Light, all the plots described above are given for Case 1 and Event 1 in 7.5 and 7.6.

In the rest of the simulations, only the most significant plots are presented in this chapter. The complete sets of plots are found in Appendix D. For the simulations with unstable behavior, only the voltage at the connection point and reactive power from one SVC are plotted.

7.5 Case 1, AC cable

Simulations with the three events described in 7.3 are done for load flow Case 1, with AC cable connection of the offshore wind farm. Case 1 is the original load flow situation, with 1000 MW offshore wind power added at Feda, and 900 MW load at Hasle to simulate export to Sweden. With AC cable connection, SVCs are added at connection point Feda in order to fulfill the requirements from Statnett regarding *cos(φ)* at the connection point.

7.5.1 Event 1, bus fault at Øie

The fault at Øie lasting for 150 ms reduces the voltage at Feda to about 0,26 pu. The grid code requires that the wind farm should not disconnect as long as the fault is cleared within 150 ms and the voltage recovers according to Figure 7.1. After the fault is cleared, the system has to be stable. The plots for voltage at the onshore connection point Feda, offshore voltage, speed deviation from synchronous speed of the wind turbine generators and reactive power from one SVC at Feda are given in Plot 7.1 to Plot 7.4.

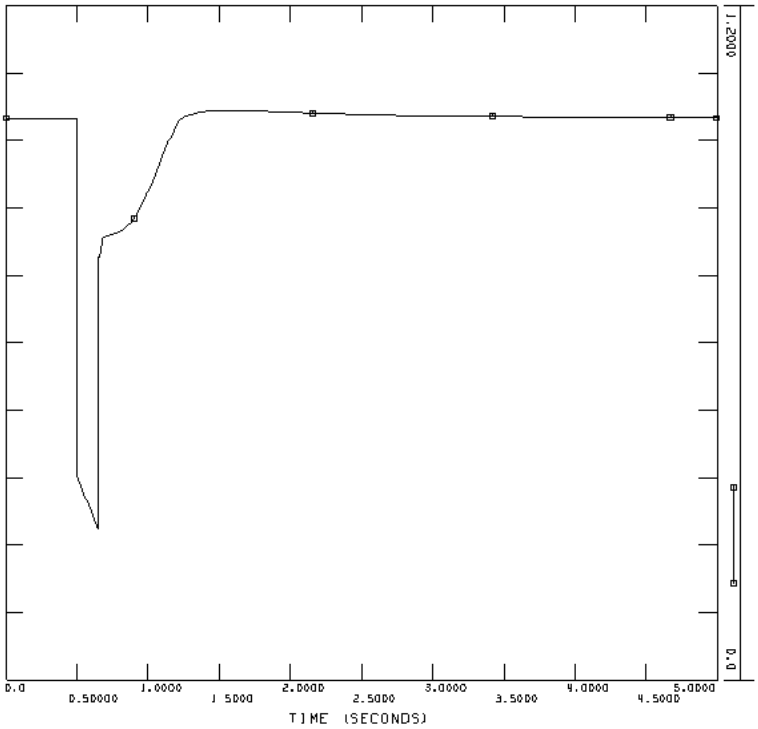

Plot 7.1: Voltage at Feda [pu]

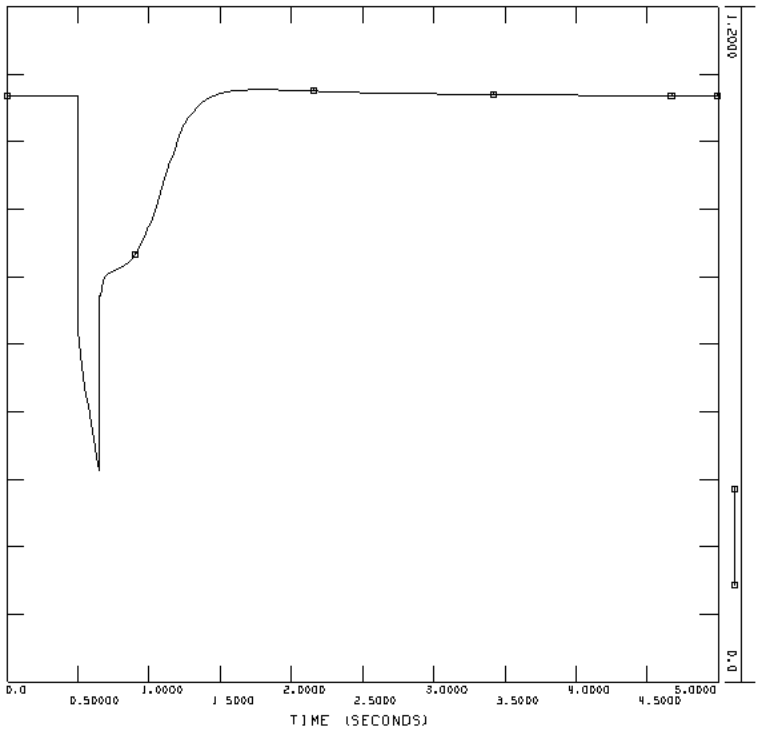

Plot 7.2: Offshore voltage [pu]

As can be seen from the simulation plots in Plot 7.1 and Plot 7.2, the voltage is reduced both onshore and offshore during the fault. The voltage is recovered at the connection point onshore about 0,5 second after the fault is cleared. Based on the fault ride through requirement described in 7.1, this implies that the wind turbines have to stay connected.

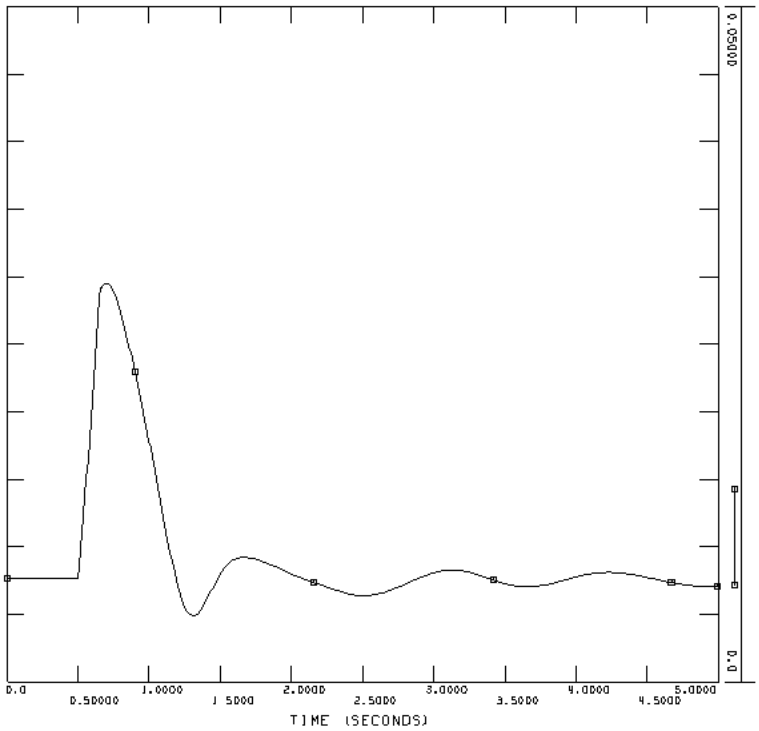

Plot 7.3: Deviation from synchronous speed of the wind turbine generators [pu]

The speed of the equivalent wind turbine increases during the fault because of the reduced electric torque caused by the low voltage onshore. When the fault is cleared, the speed rapidly decreases because of the electric torque, and swings back to the pre fault speed.

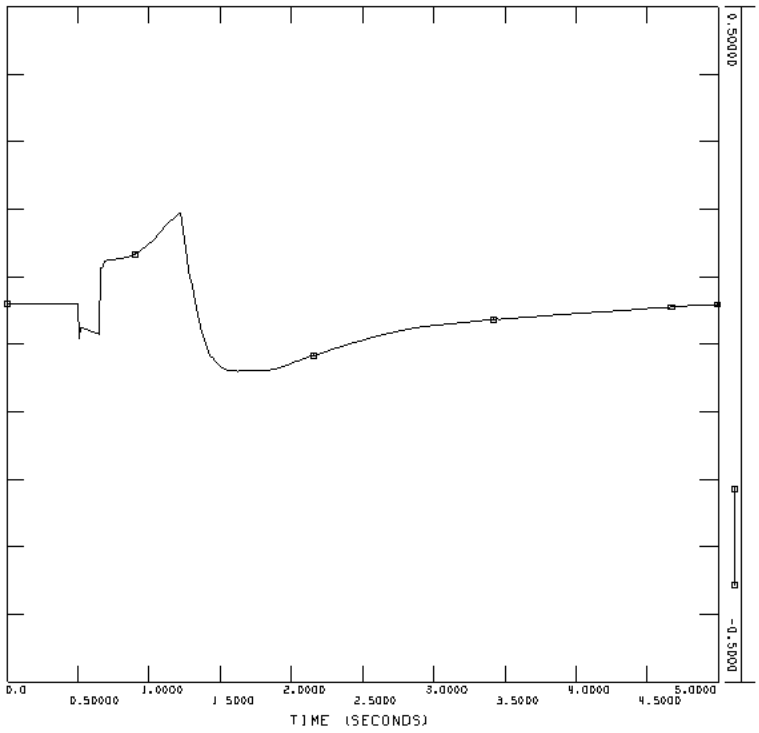

Plot 7.4: Reactive power from one SVC [pu on system base]

The SVCs produce as much reactive power as possible in order to raise the voltage. However, as can be seen in Plot 7.4, one SVC is not able to supply its maximum value of 200 Mvar reactive power until the voltage at the connection point has recovered at approximately t=1,25 s. The reason for this is that the produced reactive power from the SVC is proportional to the voltage squared outside the working range of the SVC, and the voltage is low at the connection point after the fault. After the SVC reaches 200 Mvar at t=1,25 s, the reactive power is quickly regulated down in order to maintain the voltage at approximately 1 pu.

7.5.2 Event 2, line fault and tripping of line

The dynamic behavior after Event 2 (line fault and tripping of line) is similar to those from Event 1 (bus fault at Øie). The voltage onshore and offshore is however reduced more during the fault. Additionally, it can be observed from Plot 7.5 that the speed of the wind turbine generator swings to a speed lower than the pre fault speed.

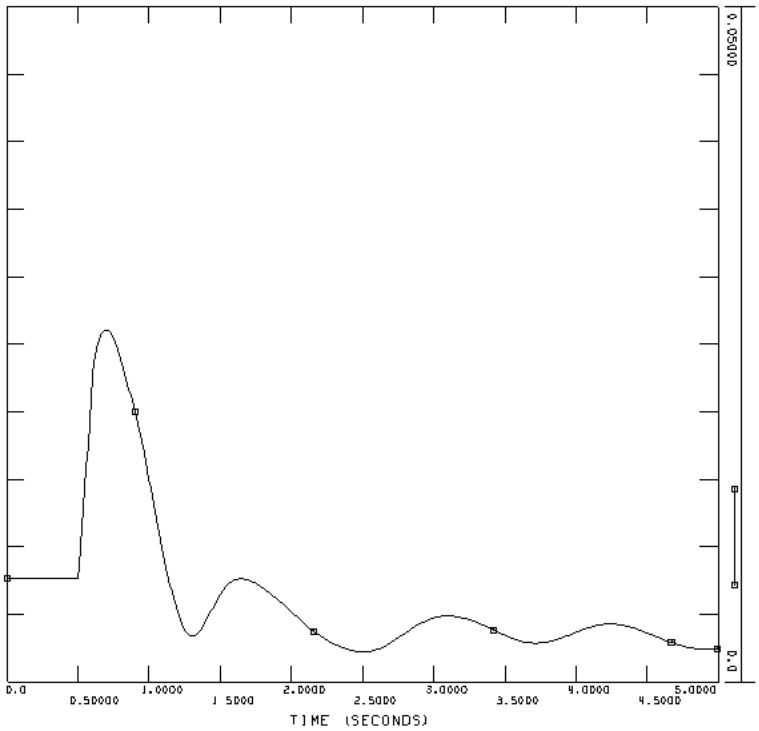

Plot 7.5: Deviation from synchronous speed of the wind turbine generators [pu]

This can be explained from the fact that the frequency in the whole system is reduced for Event 2. The generator speed is dependent on the frequency for induction generators directly connected to the grid. After the line is tripped, the current in the other lines become too large, and some generators trip because of over current protection. With the same load in the system for reduced production, the system frequency will drop according to the speed-droop characteristics of the system [15].

7.5.3 Event 3, three-phase short-circuit at Feda

The voltage onshore never recovers after the three-phase short-circuit at Feda, as can be seen in Plot 7.6. Based on the fault ride through requirement, the wind farm is allowed to trip at approximately t = 0,7 s, just after the fault is cleared. The SVC is not able to supply more than half of the reactive power rating after the fault is cleared, because of the low voltage.

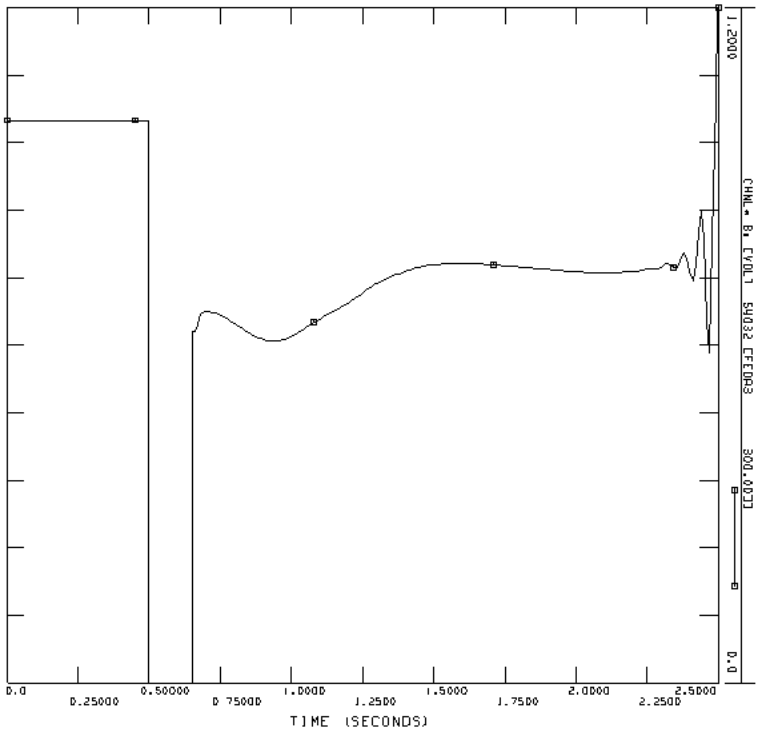

Plot 7.6: Voltage at Feda [pu]

7.6 Case 1, HVDC Light

Simulations for the three events described in 7.3 are done for the load flow situation Case 1 with HVDC Light connection of the offshore wind farm. Case 1 is the original load flow situation, with 1000 MW offshore wind power added at Feda, and 900 MW load at Hasle to simulate export to Sweden.

7.6.1 Event 1, bus fault at Øie

The fault at Øie lasting for 150 ms reduces the voltage at Feda to about 0,26 pu. The grid code requires that the wind farm should not disconnect as log as the fault is cleared within 150 ms. After the fault is cleared, the system should be stable. The plots for voltage at the onshore connection point Feda, offshore voltage, reactive power from the HVDC Light converter at Feda, the DC voltage and the speed of the wind turbines are given in Plot 7.7 to Plot 7.11.

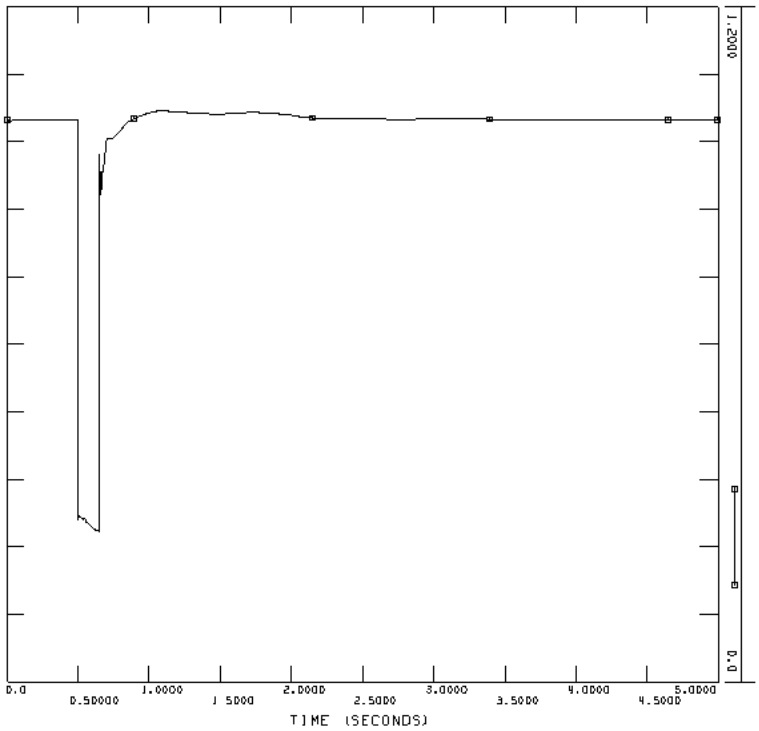

Plot 7.7: Voltage at Feda [pu]

Even though the onshore voltage is reduced approximately to the same value as with AC cable connection, the voltage recovers much faster with HVDC Light. The fault ride through requirement requires the wind turbines to stay connected for the simulated event. A small local peak in the voltage can be observed at the instant the fault is cleared. This corresponds in time to the large peak in reactive power from the onshore converter given in Plot 7.11.

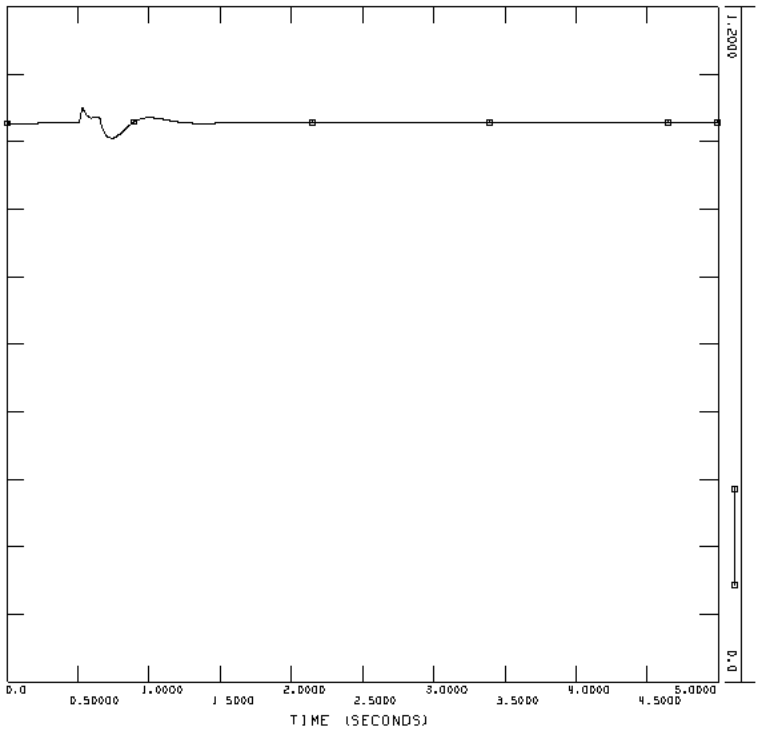

Plot 7.8: Offshore voltage [pu]

The offshore voltage is almost unaffected by the fault onshore. Only a small temporary change is observed in Plot 7.8. The wind turbines can stay online without noticing the fault onshore. However, the problem with this is described in 5.3.5. In order to avoid the DC voltage to increase drastically, power cannot be transferred into the DC side during the fault. The offshore converter is in U_{dc} control mode, and increases the frequency, and hence also the rotational speed of the wind turbines as shown in Plot 7.9. This allows the wind turbines to store the energy produced during the fault as rotational kinetic energy. When the fault is cleared, the rotational speed decreases in order to convert the additional rotational energy to electric energy transferred to the onshore grid through the HVDC Light system. The faster the speed decreases after the fault, the larger the additional power from the wind turbines will be. The HVDC Light converter is loaded relatively close to rated power; hence the decrease in speed can not take place too fast as the IGBTs have limited capacity.

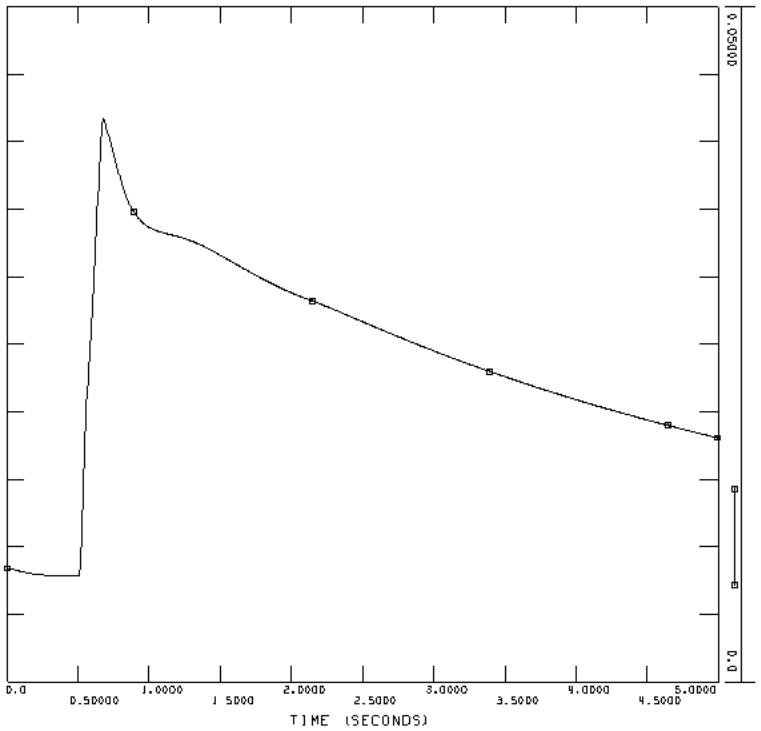

Plot 7.9: Deviation from synchronous speed of the wind turbine generators [pu]

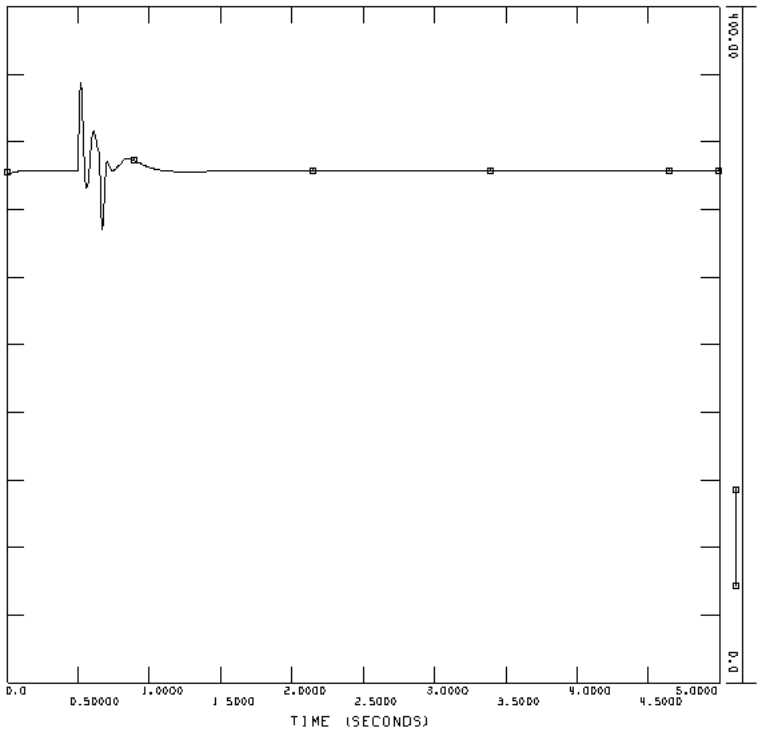

Plot 7.10: DC voltage at the voltage regulating HVDC Light converter [kV]

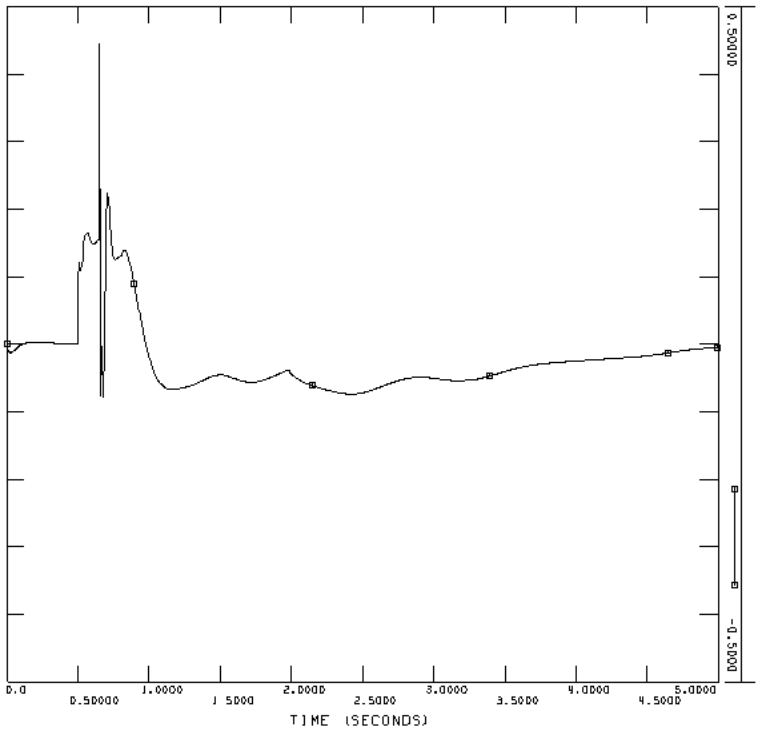

Plot 7.11: Reactive power from the HVDC Light converter at the connection point [pu on system base]

Unlike the situation with SVCs at the connection point, the HVDC Light converter can supply a large amount of reactive power at the instant the fault is disconnected. A high peak of reactive power can be observed from Plot 7.11, causing the voltage to recover almost to the pre fault value. The fact that the HVDC Light converter can supply reactive power during the fault, means that the HVDC Light converter contributes to the short-circuit power [10]. Even so, the converter can only operate inside the PQ diagram in Figure 5.1.

The peak of reactive power supplied from the HVDC Light converter at the instant the fault is cleared should be investigated. Certain aspects of the model could be idealized so that the dynamic behavior is not realistic compared to a physical system. Comparison with measurements from a real HVDC Light system would be useful in order to verify the response shown in the simulation.

7.6.2 Event 2, line fault and tripping of line

The dynamic behavior after Event 2 (line fault and tripping of line) is similar to those from Event 1 (bus fault at Øie). The voltage onshore and offshore is reduced more during the line fault, as was the case with AC cable connection. The system frequency is reduced because of tripping of generators from over-current protection.

7.6.3 Event 3, three-phase short-circuit at Feda

The simulation results are similar as to Event 1 and 2. After the three-phase short-circuit at Feda, the voltage is fully recovered at t = 1 s, as can be seen from Plot 7.12.

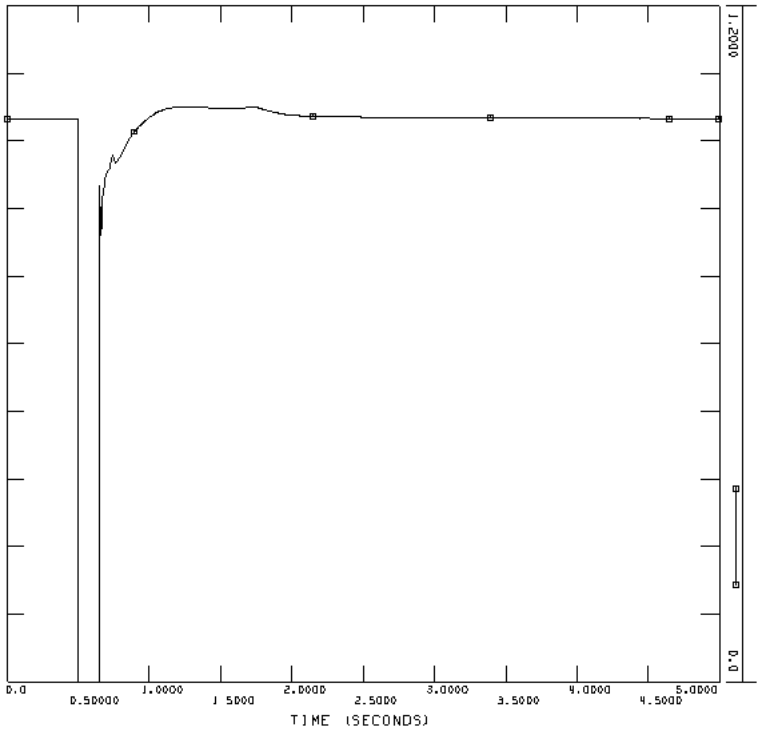

Plot 7.12: Voltage at Feda [pu]

Based on the fault ride through requirement the wind farm must stay connected. The system is stable after the fault is cleared, unlike the same situation with AC cable connection.

7.7 Case 2, AC cable

Simulations for the three events described in 7.3 are done in load flow Case 2 with AC cable connection of the offshore wind farm. In Case 2 both load and production in the areas surrounding Feda is ramped down. Generators are disconnected in order to establish a load flow situation with lower short circuit capacity at the connection point. 1000 MW offshore wind power is assed to Feda, and a 900 MW load is assed at Hasle in order to simulate export of power to Sweden. The short-circuit capacity at Feda is reduced from 7147 MVA in Case 1 to 5228 MVA in Case 2 due to disconnection of generators.

The simulations with AC cable show a stable behavior of all the disturbances. The intention of establishing the load flow situation called Case 2 was to trig unstable dynamic behavior because of reduced short-circuit capacity. The reduction of the loads in the areas however seems to have a bigger influence on the dynamic behavior than the reduction in the short-circuit power.

7.7.1 Event 1, bus fault at Øie

The fault at Øie lasting for 150 ms reduces the voltage at Feda to approximately 0,24 pu. The grid code requires that the wind farm should not disconnect as long as the fault is cleared within 150 ms and the onshore voltage recovers according to Figure 7.1. After the fault is cleared, the system should be stable. The plot for voltage at Feda is given in Plot 7.13.

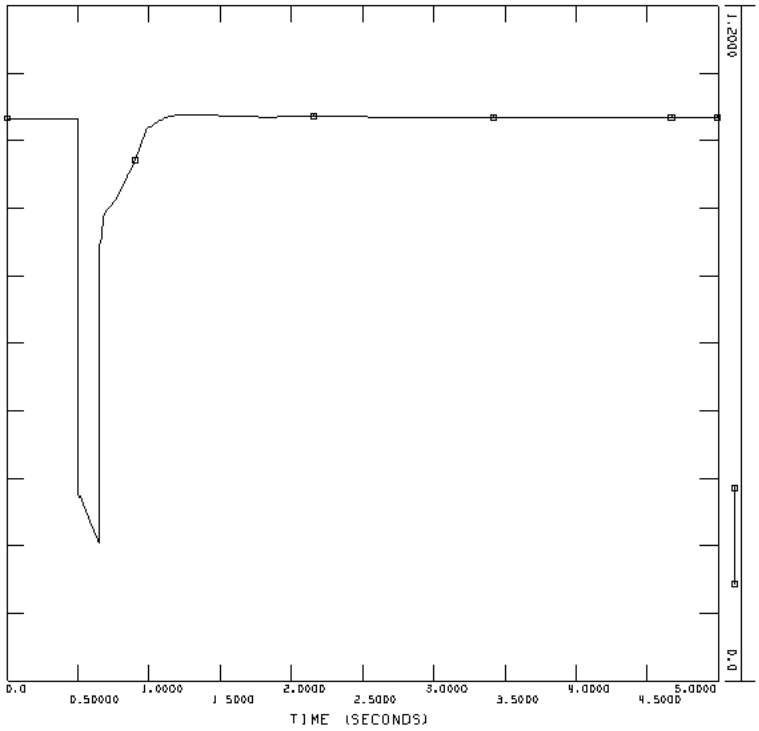

Plot 7.13: Voltage at Feda [pu]

By comparing Plot 7.1 to Plot 7.13, it can be observed that the voltage recovers slightly faster than for the load flow case with all the generators connected.

As short-circuit power at the connection point indicates the strength at the busbar, other factors influence the stability as well. In Case 2, load was scaled down in order to disconnect generators. The active and reactive power load was scaled down at a fixed P/Q ratio. The reduced load in the area surrounding Feda contributes the voltage recovery.

7.7.2 Event 2, line fault and tripping of line

As for Event 1 with bus fault at Øie, the voltage onshore recovers faster than in Case 1. This is despite the reduced short-circuit power at the point, and can be explained by lighter loading in the area from the load flow.

7.7.3 Event 3, three-phase short-circuit at Feda

For the case with a three-phase short-circuit with no impedance at Feda, the voltage recovers after the fault is cleared. This can be observed in Plot 7.14.

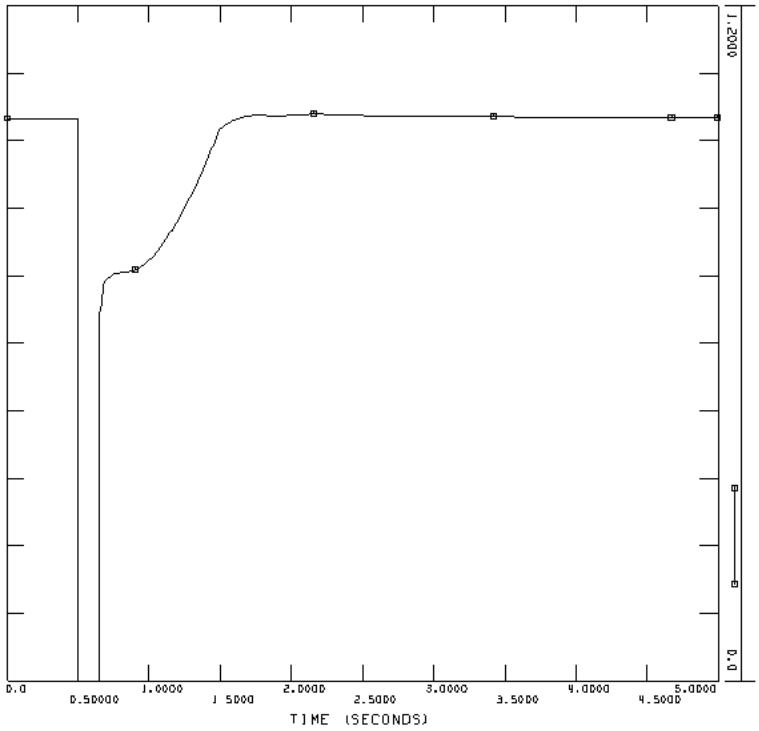

Plot 7.14: Voltage at Feda [pu]

According the fault ride through requirement in Figure 7.1, the voltage recovers fast enough so that the wind farm must stay connected. 750 ms after the fault is cleared, the voltage is higher than 0,9 pu.

7.8 Case 2, HVDC Light

Simulations for the three events described in 7.3 are done in load flow Case 2 with HVDC Light connection of the offshore wind farm. In Case 2 both load and production in the areas surrounding Feda is ramped down. Generators are disconnected in order to establish a load flow situation with lower short circuit capacity at the connection point. 1000 MW offshore wind power is assed to Feda, and a 900 MW load is assed at Hasle in order to simulate export of power to Sweden.

7.8.1 Event 1, bus fault at Øie

The fault at Øie lasting for 150 ms reduces the voltage at Feda to about 0,24 pu. The voltage recovers almost immediately after the fault is cleared, and the dynamic response is similar the one presented for the same event in Case 1.

7.8.2 Event 2, line fault and tripping of line

The dynamic behavior after Event 2 (line fault and tripping of line) is similar to those from Event 1 (bus fault at Øie).

7.8.3 Event 3, three-phase short-circuit at Feda

After the fault is cleared at Feda, the voltage recovers almost immediately. The voltage recovery is slightly faster than in Case 1, as can be seen by comparing Plot 7.12 and Plot 7.15.

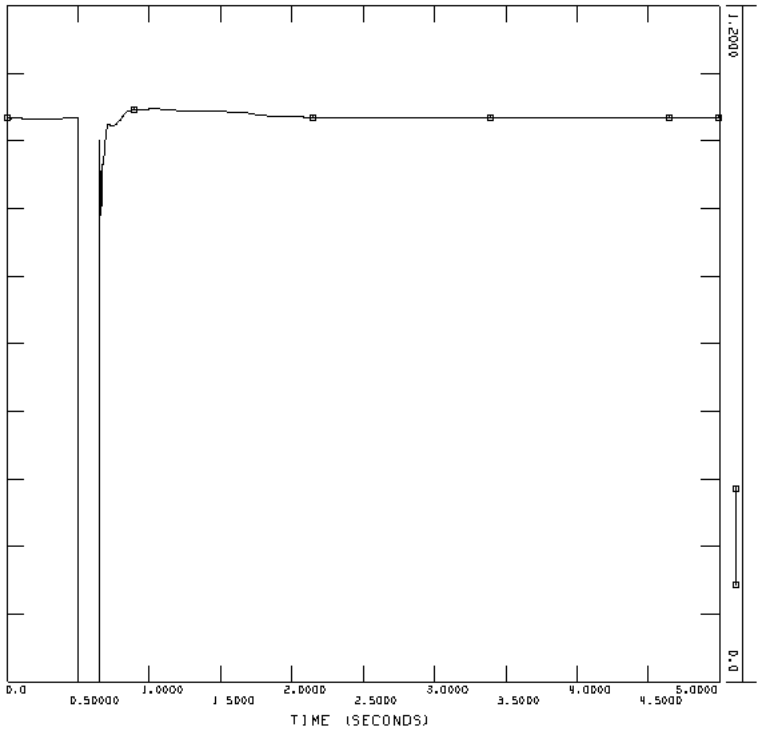

Plot 7.15: Voltage at Feda [pu]

7.9 Case 3, AC cable

Simulations for the three events described in 7.3 are done in load flow Case 3 with AC cable connection of the offshore wind farm. In Case 3 the load is kept at the maximum value corresponding to the original load flow situation, but the production is ramped down, without disconnection any generators. 1000 MW power from Denmark is imported through the HVDC links at Kristiansand, modeled as a load with value -1000 + j 500 MVA. 1000 MW offshore wind power is assed to Feda, and there is no export of power to Sweden.

7.9.1 Event 1, bus fault at Øie

1000 MW HVDC import at Kristiansand in addition to 1000 MW offshore wind power added at Feda result in heavy loading of the transmission lines. After the fault at Øie is cleared, the voltage at Feda recovers. As can be seen from Plot 7.16, the voltage 750 ms after the fault is cleared is just over 0,9 pu. This is the limit for which the wind farm has to stay connected.

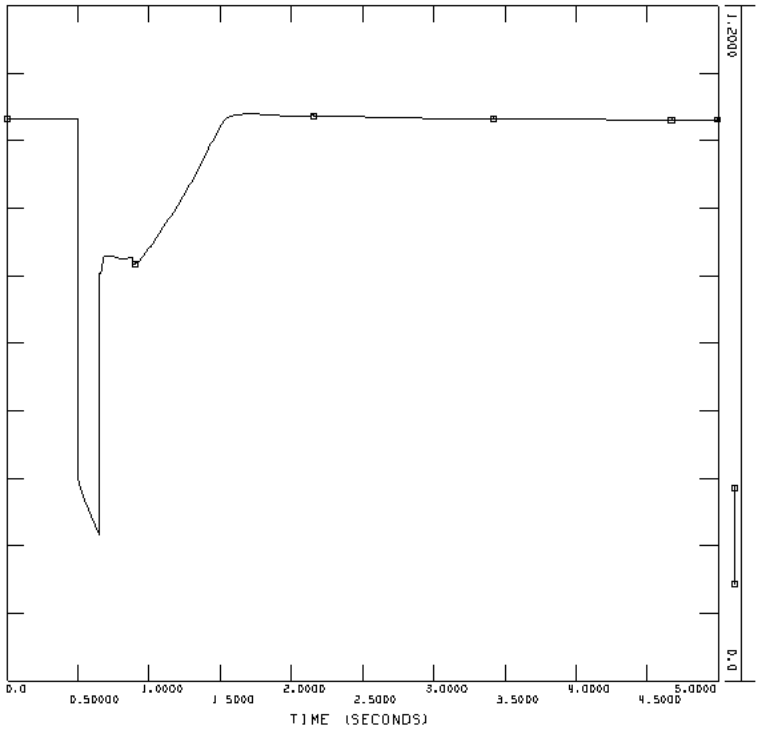

Plot 7.16: Voltage at Feda [pu]

The short-circuit power is larger than in Case 2, but the loading in the lines surrounding Feda is much higher because of the peak load and import of 1000 MW HVDC at Kristiansand. 500 Mvar reactive power is drawn by the HVDC converter at Kristiansand. The system frequency is reduced after the disturbance because of tripping of generators by over current protection.

7.9.2 Event 2, line fault and tripping of line

A similar response as the one observed for Event 1 (line fault at Øie) can be seen from Event 2 (line fault and tripping of line). The voltage recovers in such a manner that the wind farm has to stay connected. A marginally slower recovery of the voltage would allow the wind farm to trip.

7.9.3 Event 3, three-phase short-circuit at Feda

The voltage at Feda never recovers after the three-phase short-circuit at Feda. Based on the fault ride through requirement, the wind farm is allowed to trip just after the fault is cleared.

The SVC is not able to supply more than half of the reactive power rating after the fault is cleared, because of the low voltage.

7.10 Case 3, HVDC Light

Simulations for the three events described in 7.3 are done in load flow Case 3 with HVDC Light connection of the offshore wind farm. In Case 3 the load is kept at the maximum value corresponding to the original load flow situation, but the production is ramped down, without disconnection any generators. 1000 MW power from Denmark is imported through the HVDC links at Kristiansand, modeled as a load with value -1000 + j 500 MVA. 1000 MW offshore wind power is assed to Feda, and there is no export of power to Sweden.

7.10.1 Event 1, bus fault at Øie

After the fault at Øie is cleared, the voltage at Feda recovers almost immediately. The response is similar to the one in Case 1 for the same event. Generators are tripped because of the heavy loading of the lines, and the system frequency decreases.

7.10.2 Event 2, line fault and tripping of line

The response after the line is tripped is very similar the one in Case 1. Generators are tripped because of the heavy loading of the lines, and the system frequency decreases.

7.10.3 Event 3, three-phase short-circuit at Feda

After the fault is cleared at Feda, the dynamic response is very similar to the one in Case 1. As for the other events in Case 3, the system frequency is reduced after the fault is cleared because of tripping of generators.

7.11 Case 4, AC cable

Simulations for the three events described in 7.3 are done in load flow Case 4 with AC cable connection of the offshore wind farm. Case 4 is the original load flow situation, with 1000 MW offshore wind power added at Kårstø, and 900 MW load at Hasle to simulate export to Sweden.

7.11.1 Event 1, bus fault at Sauda

The fault at Sauda lasting for 150 ms reduces the voltage at Kårstø to about 0,44 pu. As long as the voltage is above 0,9 pu 750 ms after the fault is cleared, the wind farm has to stay connected. This correspond to t = 1,4 s in Plot 7.17, and the voltage has recovered to a value higher than 0,9 pu at this time.

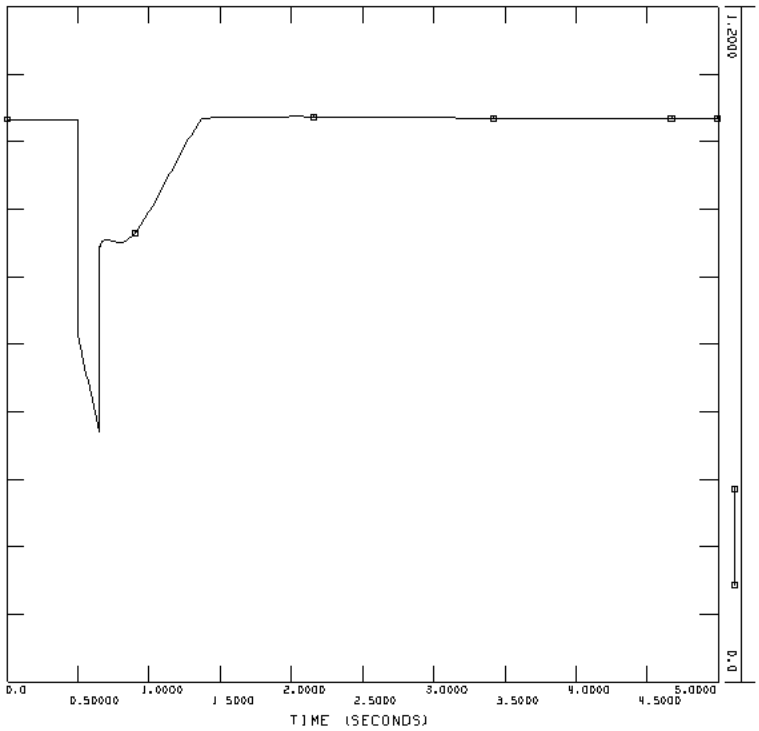

Plot 7.17: Voltage at Kårstø [pu]

The wind farm has to stay connected. However, by inspecting the plots for Case 1, it can be observed that the voltage at Kårstø recovers more slowly in Case 4. This is as expected because of the considerably lower short-circuit power at Kårstø.

Because the voltage offshore does not decrease as much as at Feda, the wind turbine generators do not accelerate as much. The SVCs at Kårstø show the same behavior as the case at Feda, the supplied reactive power does not reach the maximum value of 200 Mvar before the voltage has recovered.

7.11.2 Event 2, line fault and tripping of line

After the fault at Haavik, and then clearing of the line from Haavik to Kårstø, the voltage onshore does not recover. The voltage at Kårstø is shown in Plot 7.18.

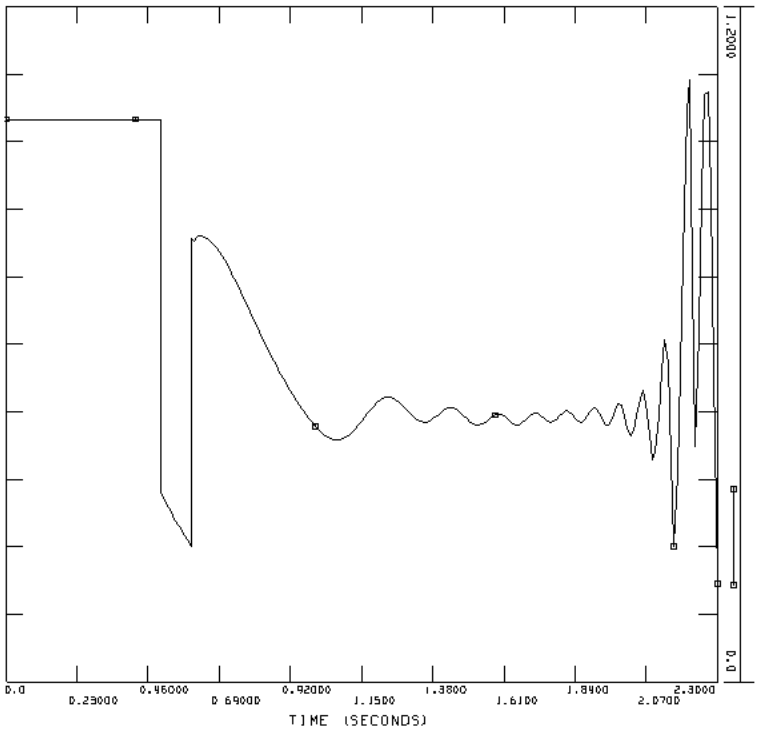

Plot 7.18: Voltage at Kårstø [pu]

The wind farm is allowed to trip shortly after the line is tripped based on the fault ride through requirement described in Figure 7.1.

7.11.3 Event 3, three-phase short-circuit at Kårstø

As for Event 2, the voltage does not recover after the fault at Kårstø is cleared at t = 0,65 s. The voltage at Kårstø is showed in Plot 7.19. The wind farm is allowed to trip.

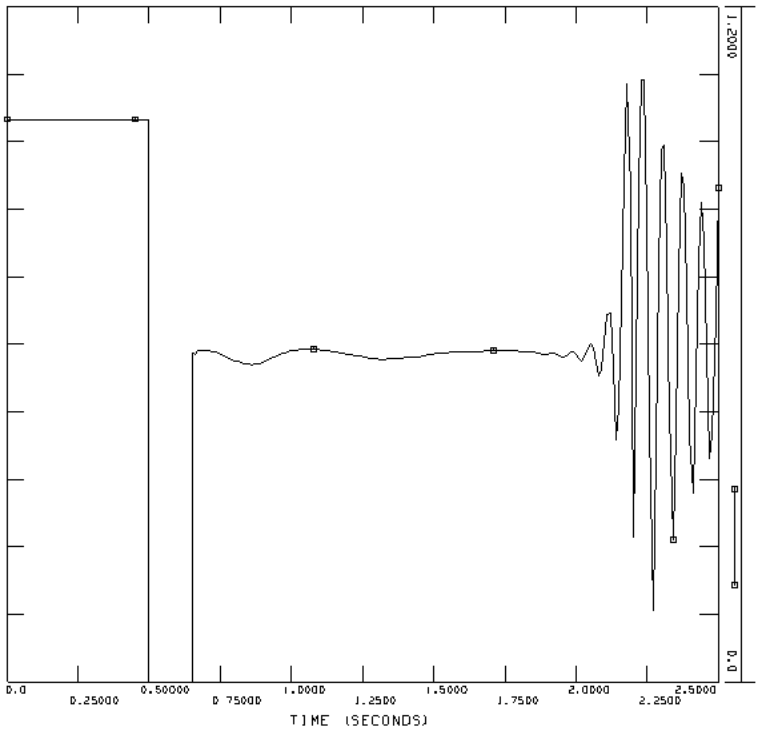

Plot 7.19: Voltage at Kårstø [pu]

7.12 Case 4, HVDC Light

Simulations for the three events described in 7.3 are done in load flow Case 4 with HVDC Light connection of the offshore wind farm. Case 4 is the original load flow situation, with 1000 MW offshore wind power added at Kårstø, and 900 MW load at Hasle to simulate export to Sweden.

7.12.1 Event 1, bus fault at Sauda

With HVDC Light connection, the onshore voltage recovers practically immediately after the fault is cleared. The voltage at Kårstø is showed in Plot 7.20.

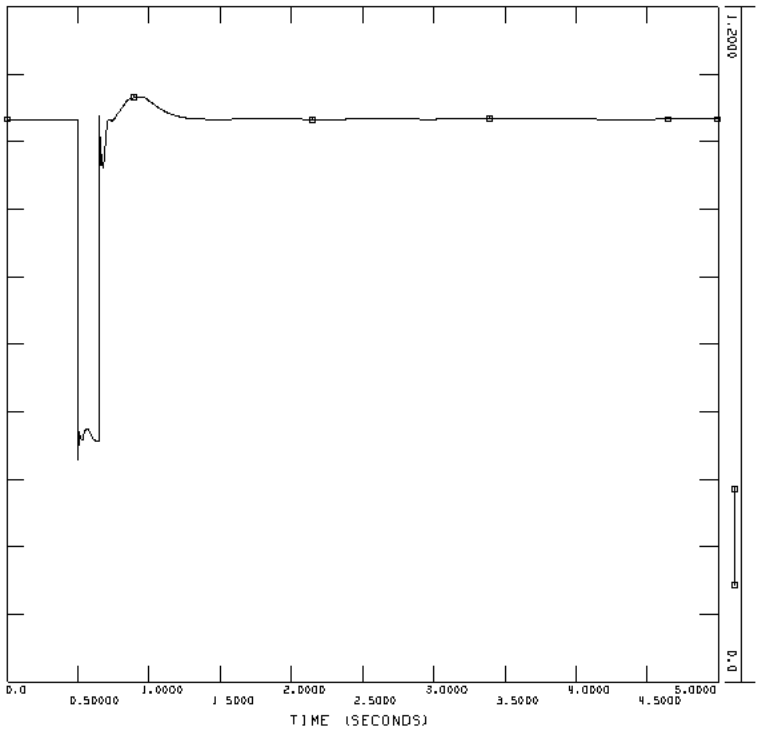

Plot 7.20: Voltage at Kårstø [pu]

The dynamic response is quite similar to the response in Case 1, 2 and 3, even though the connection point in these cases was Feda. A small maximum corresponding to approximately 1,05 pu in the voltage can however be observed at t=1s.

7.12.2 Event 2, line fault and tripping of line

The response after the line is tripped is very similar the one in Case 1.

7.12.3 Event 3, three-phase short-circuit at Kårstø

After the fault is cleared at Feda, the dynamic response is very similar to the one in Case 1.

7.13 Case 5, AC cable

Simulations for the three events described in 7.3 are done in load flow Case 5 with AC cable connection of the offshore wind farm. In Case 5 1000 MW offshore wind power is connected at Kårstø. The load is kept at the maximum value corresponding to the original load flow situation, but the production is reduced by disconnecting large generators close to Kårstø. There is no export of power to Sweden, and no import of power from Denmark through the HVDC links.

7.13.1 Event 1, bus fault at Sauda

The fault at Sauda lasting for 150 ms reduces the voltage at Feda to about 0,35 pu, shown in Plot 7.21. After the fault is cleared, the voltage does not recover. The wind farm is allowed to trip shortly after the fault is cleared based on the fault ride through requirement.

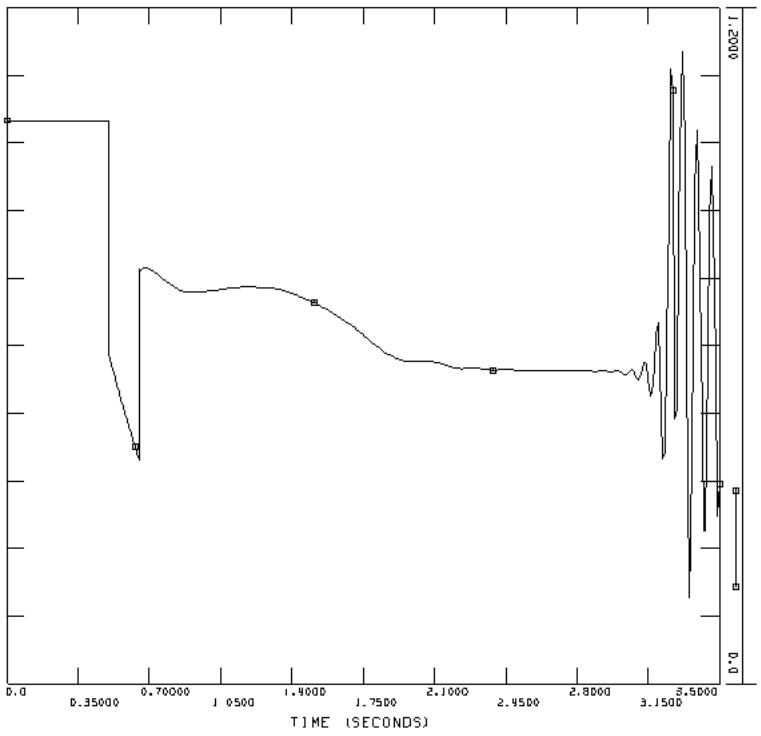

Plot 7.21: Voltage at Kårstø [pu]

Before the disturbance is applied, the SVCs at Kårstø produces rated reactive power. This is shown in Plot 7.22. Because the voltage never recovers, the SVCs are not able to deliver more than half the rated reactive power after the fault is cleared.

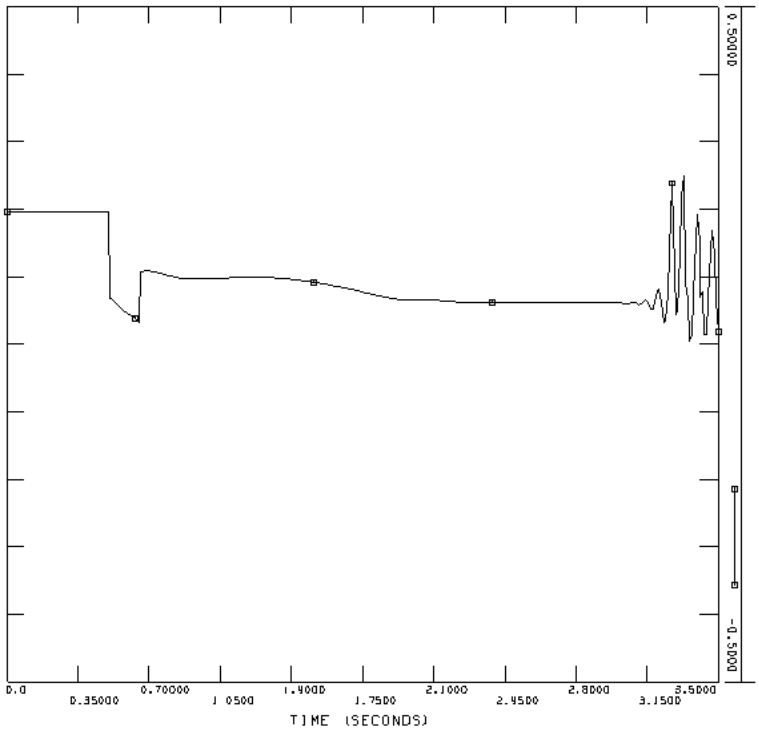

Plot 7.22: Reactive power from one SVC [pu on system base]

7.13.2 Event 2, line fault and tripping of line

As for the case with bus fault at Sauda, the system is not stable after the faulted line is tripped. The wind farm is allowed to trip shortly after the line is tripped.

7.13.3 Event 3, three-phase short-circuit at Kårstø

After the short-circuit at Kårstø, the voltage does not recover. The wind farm is allowed to trip shortly after the short-circuit is cleared.

7.14 Case 5, HVDC Light

Simulations for the three events described in 7.3 are done in load flow Case 5 with HVDC Light connection of the offshore wind farm. In Case 5 1000 MW offshore wind power is connected at Kårstø. The load is kept at the maximum value corresponding to the original load flow situation, but the production is reduced by disconnecting large generators close to Kårstø. There is no export of power to Sweden, and no import of power from Denmark through the HVDC links.

7.14.1 Event 1, bus fault at Sauda

The dynamic response is stable for the case with a bus fault at Sauda. The voltage at Kårstø recovers almost immediately after the fault is cleared, similar the response in Case 1.

7.14.2 Event 2, line fault and tripping of line

The response after the line is tripped is very similar the one in Case 1.

7.14.3 Event 3, three-phase short-circuit at Kårstø

A perfect three-phase short-circuit at Kårstø with reduced short-circuit power is the most critical simulations done in this thesis. Kårstø is the connection point with lowest short-circuit power, and in Case 5 the short-circuit power is reduced additionally. A perfect three-phase short-circuit is the most severe disturbance, as the voltage at the connection point is zero during the fault.

With AC cable connection, all simulations in Case 5 were unstable, and the wind farm had to disconnect. For the case with HVDC Light, the system is stable for all simulations. The voltage at Kårstø recovers almost immediately after the fault is cleared, and the response is similar to the other cases. The voltage at Kårstø is shown in Plot 7.23 for Event 3. The wind farm has to stay connected based on the fault ride through requirement.

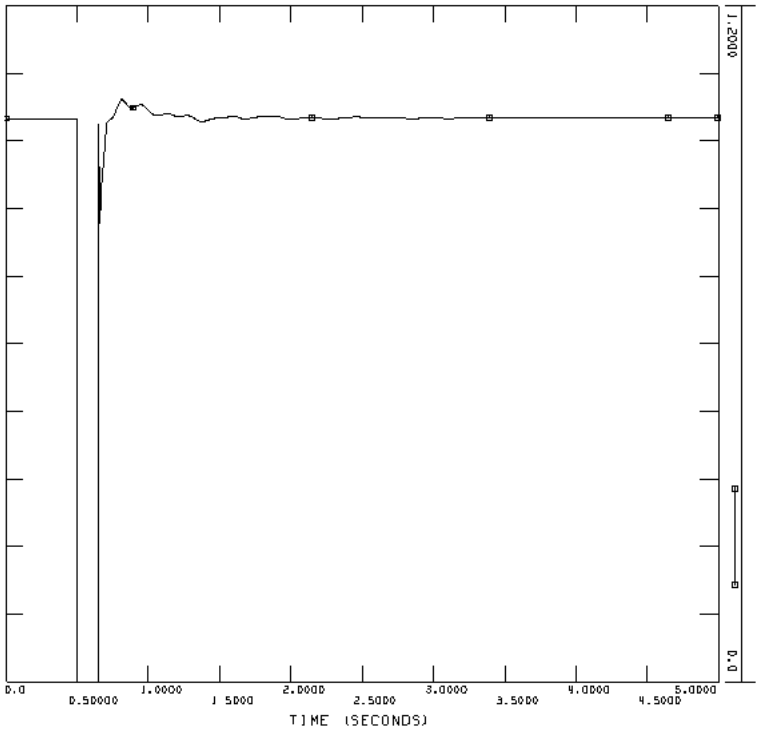

Plot 7.23: Voltage at Kårstø [pu]

8 Improvements of dynamic behavior

In this chapter, suggestions are made to improve the stability of some of the simulations with unstable behavior. Only the simulations with AC cable connection showed unstable behavior. Simulations are done for Case 5 in order to verify the improvement of the dynamic behavior. Case 5 was the load flow case with the offshore wind power connected to Kårstø and reduced short-circuit power at Kårstø.

Two suggestions are made in this chapter in order to improve the stability for the three events described in 7.3 for Case 5 with AC cable connection.

8.1 Changing of the power factor

A 500 Mvar shunt reactor is used for compensation of the reactive power produced by the AC cables in all simulations in 7.4. 500 Mvar is approximately the amount of reactive power produced by the AC cables with voltage equal 1 pu at the connection point. In order to fulfill the requirement regarding $cos(\varphi) = 0{,}95$ capacitive and inductive at the connection point, two SVCs with a total capacity of 400 MVA are installed. ± 400 Mvar from the SVCs correspond to almost $cos(\varphi) = 0{,}91$ inductive and capacitive for rated power from the offshore wind farm. The requirement from Statnett is over fulfilled.

In Case 5, the SVCs produce close to the maximum limit of reactive power in order to keep the voltage at 1 pu before the disturbance. This can be verified by inspection of Plot 7.22 in 7.13.1. The power factor for the connected wind farm at Kårstø is about 0,91 capacitive. The inductance of the shunt reactor could easily be increased, causing the $cos(\varphi)$ capacitive at the connection point to decrease even more. However, the requirement of $cos(\varphi) = 0{,}95$ inductive would not be fulfilled. A switched shunt could be used in order to operate at a lower power factor than $cos(\varphi) = 0{,}91$ capacitive, but still fulfill the power factor requirement of $cos(\varphi) = 0{,}95$ inductive.

In this paragraph, the shunt reactor is adjusted as a suggestion to improve the dynamic behavior in case 5. The shunt reactor is adjusted so that the reactive power from the SVCs in the load flow was equal to zero. The reactive power from the shunt reactor is then 106,2 Mvar, as can be seen from Figure 8.1.

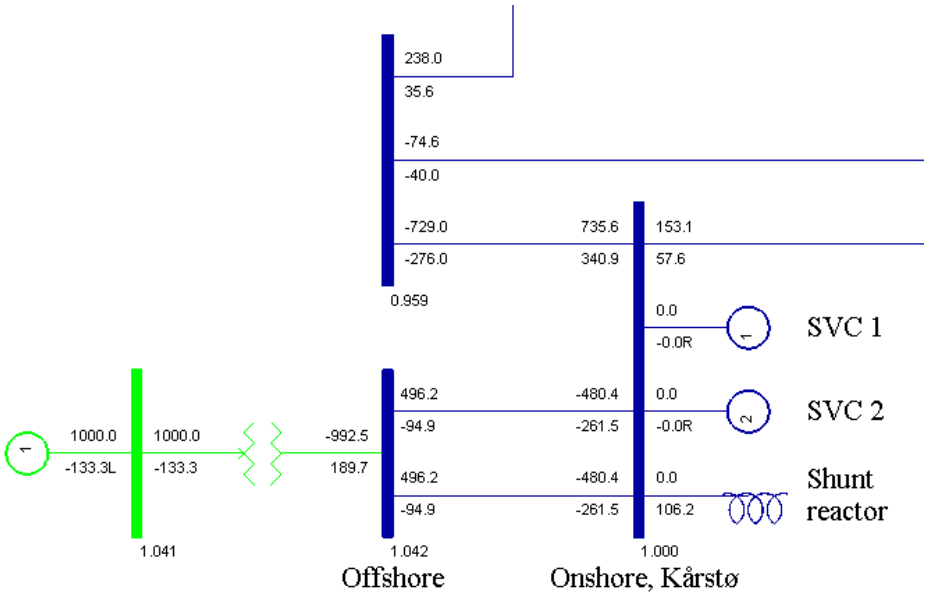

Figure 8.1: Load flow at Kårstø (Case 5), reduced cos(φ)

Plots for the voltage at Kårstø are given for Event 1, 2 and 3 in Plot 8.1, Plot 8.2 and Plot 8.3 respectively.

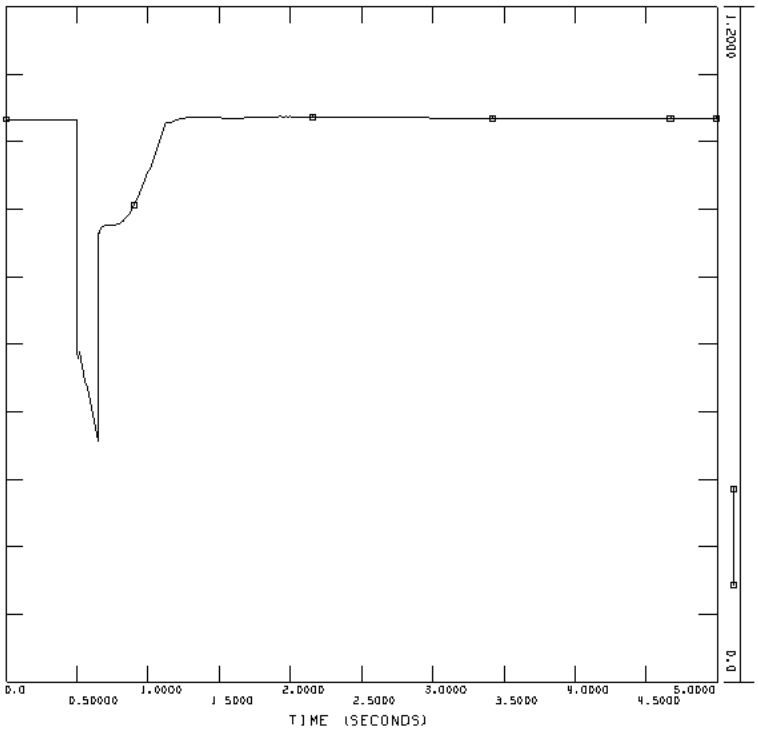

Plot 8.1: Voltage at Kårstø, Case 1 [pu]

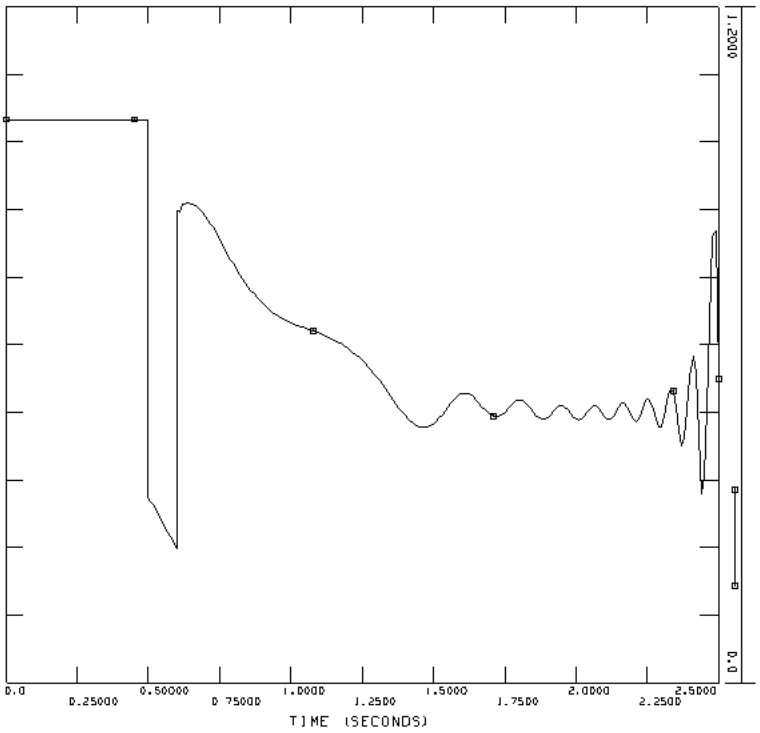

Plot 8.2: Voltage at Kårstø, Case 2 [pu]

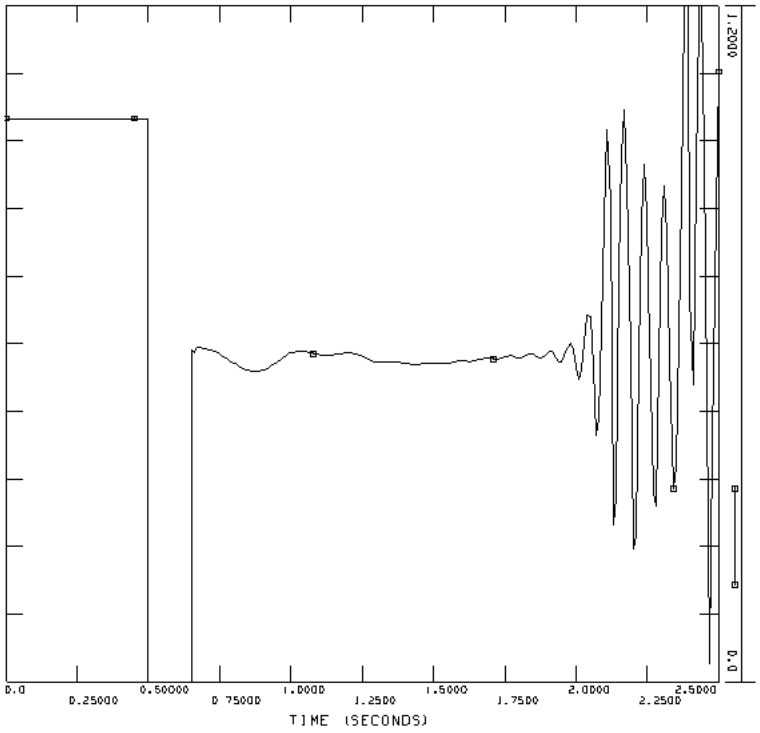

Plot 8.3: Voltage at Kårstø, Case 3 [pu]

As can be observed from the plots, the effect of decreasing the reactive power consumption of the shunt reactor improved the stability for bus fault at Sauda, Event 1. The wind farm has to stay connected. For the other cases, the voltage onshore does not recover, and the wind farm can disconnect.

8.2 Adding synchronous condensers

At Kårstø, the short-circuit power is considerably lower than at Feda. In addition to operate at a lower *cos(φ)* capacitive than required as described in 6.5.1, synchronous condensers were installed at the connection point instead of the SVCs in order to increase the short-circuit power. In Kristiansand, a 140 MVA synchronous condenser is installed in order to increase the short-circuit power at the connection point of the traditional HVDC converters. Data from this machine is used in the simulations. As data from this machine size was the only one available, three machines had to be modeled in order to fulfill the requirement of *cos(φ)* = 0,95, corresponding to ±316 Mvar at rated power. The synchronous condensers are connected to a 17 kV busbar, as shown in Figure 8.2.

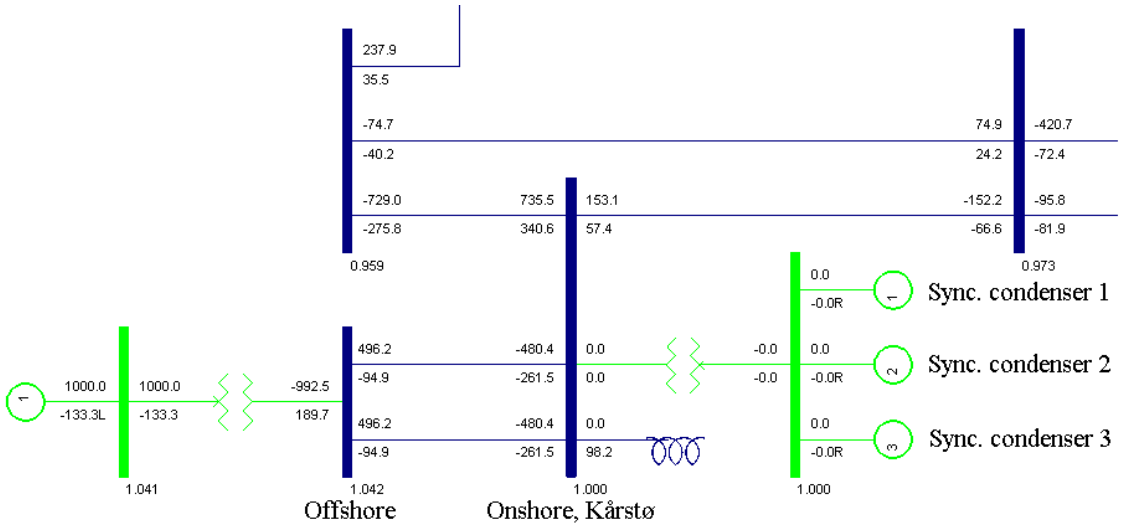

Figure 8.2: Load flow at Kårstø (Case 5), synchronous condensers

Plots for the voltage at Kårstø are given for Event 1, 2 and 3 in Plot 8.4, Plot 8.5 and Plot 8.6, respectively.

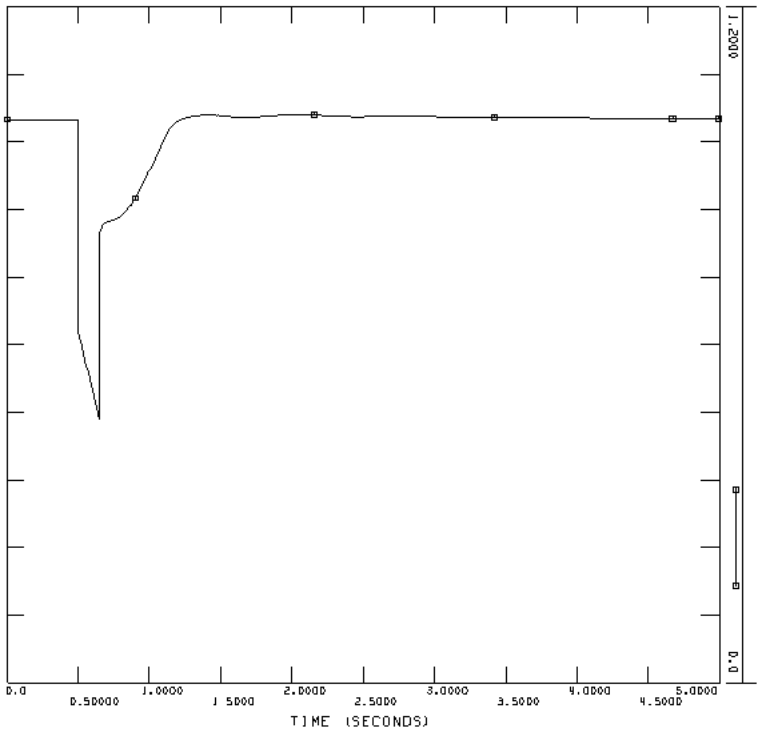

Plot 8.4: Voltage at Kårstø, Case 1 [pu]

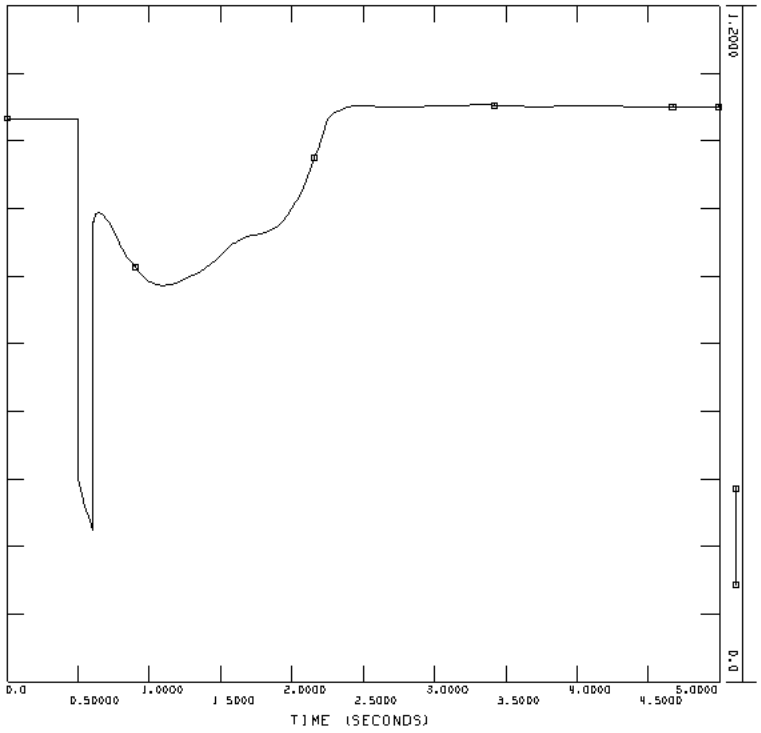

Plot 8.5: Voltage at Kårstø, Case 2 [pu]

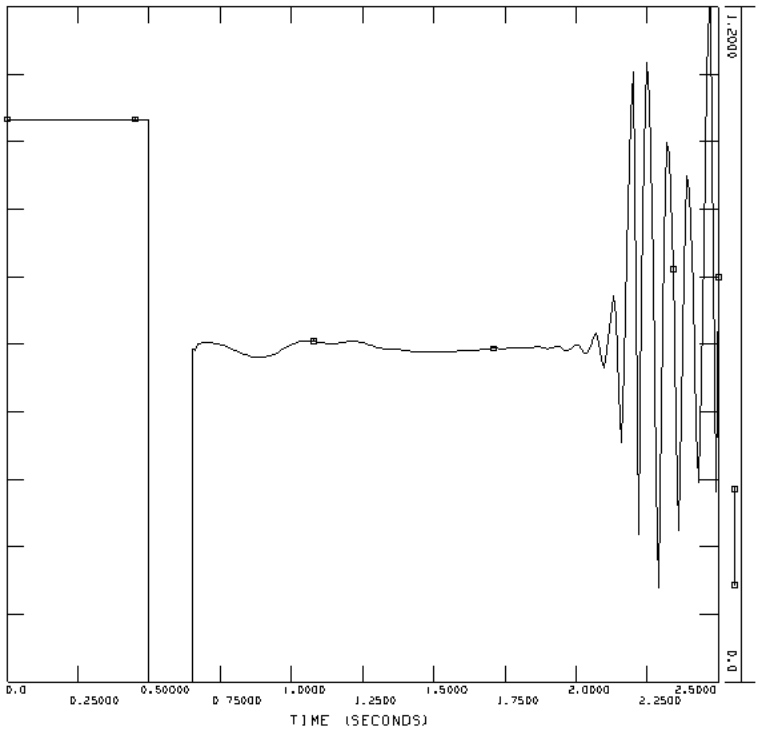

Plot 8.6: Voltage at Kårstø, Case 3 [pu]

As can be seen from the plots, exchanging the SVCs with a total rating of 400 Mvar with three synchronous condensers with a total rating of 420 Mvar, improved the stability further. Event 2, which is the case with line fault and disconnection of the line, is stable. However, the voltage 750 ms after the line is tripped, has not recovered to 0,9 pu. The fault ride through requirement does not require the wind farm to stay connected. For the case with a three-phase short-circuit at Kårstø, the synchronous condenser did not contribute enough to the recovery of the voltage.

It was expected that the contribution from the synchronous condensers would improve the stability more than indicated in the simulations in this paragraph. One possible reason for this is the modeling of the excitation system [14]. The reactive power supplied from one of the three synchronous condensers at the instant the fault is applied is about 160 Mvar. When the fault is cleared, the reactive power supplied is only about 40 Mvar. The plot of the supplied reactive power for Event 3 is given in Plot 8.7.

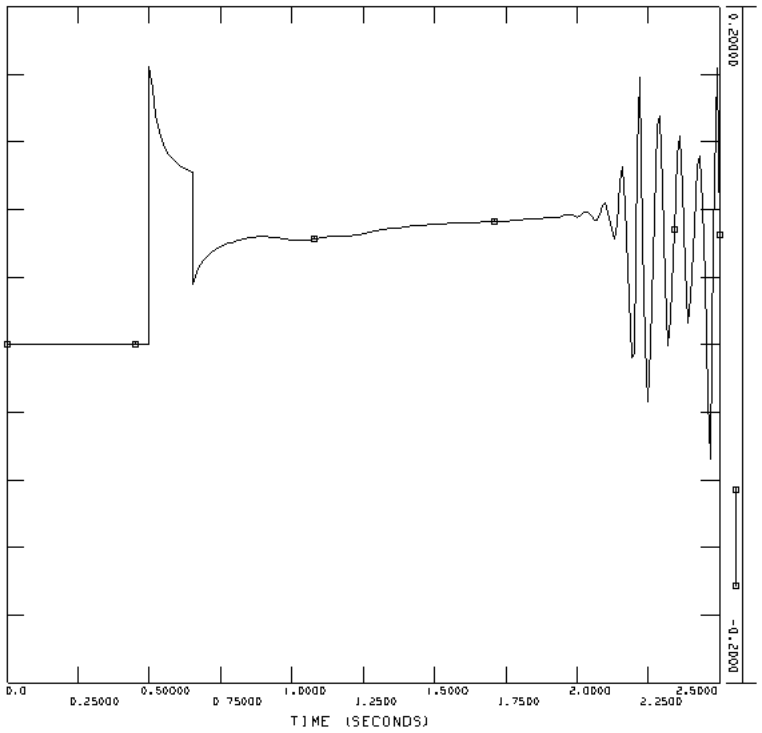

Plot 8.7: Reactive power from one three 140 Mvar synchronous condenser, Event 3 [pu on system base]

Because of the rotating mass involved, the synchronous condenser should be able to contribute with reactive power during the fault and after the fault is cleared, unlike an SVC which is dependent of the voltage squared outside the working area. The rotating field winding induces voltage in the stator of the synchronous machine. By applying a large DC field current the machine will be over magnetized, corresponding to production of reactive power [8]. When the voltage at the connection busbar is low because of the fault, the current from the stator and hence reactive power will be high because of the voltage difference between the stator winding and the connection busbar. This can be seen from Plot 8.7. However, after the fault is cleared the machine only contributes to about 0,3 pu.

A synchronous machine should be able to contribute to the short-circuit power corresponding to 2-3 times in the transient period [14].

The model for the excitation system is a user model called NOREX1. With no user manual for the model, the parameters could not be tuned in the dynamic description file. However, with the description of the dynamic variables for the excitation system, the transient reactances and time constants could be changed in order to provoke a different dynamic behavior. It is expected that a synchronous condenser would contribute with reactive power in such a manner that the voltage recovers. Further work should be done investigating the possibility of using synchronous condensers with AC cable connection of large scale offshore wind power.

9 Discussion

Certain aspects of the models and simulations are discussed consecutively in the previous chapters. An overall discussion is made in this chapter as a summary.

As described in 6.5, the cases with AC cable connection of the offshore wind farm was mainly established in order to have something to compare the response from HVDC Light to. However, if the technology for floating wind turbines became commercial, it is possible to install a large wind farm at a distance from shore that makes AC cable transmission an option. Studies can be made to investigate the possibility of compensating the reactive power produced by the AC cables between the offshore wind farm and the power system onshore. In principal, advanced technology should not be necessary in order to accomplish this.

Case 2 was established in order to provoke unstable behavior caused by reduced short-circuit power at Feda. This was done by reducing the load in the area and disconnection generators. The reduced short-circuit power at Feda was however still higher than the original case at Kårstø. Results from the simulations shows that the stability is not affected in the intended way. In order to disconnect generators, both active and reactive power load was reduced in the areas surrounding Feda. Even though the short-circuit power was reduced, the voltage drop onshore is not as severe as intended because of the lower power consumption by the reduced loads.

For the load flow cases with Feda as connection point for the offshore wind power, only in Case 3 import of HVDC from Denmark is modeled. Import from the Netherlands was not modeled because of the high loading of the lines in the peak load situation. Further work should be done in order to investigate for which load flow situations it is relevant to model full import of HVDC. Since the model of the Norwegian power system provided by Statnett only was an isolated model, the HVDC converters were not modeled. As an assumption, the converters at Kristiansand were modeled as a load equal to -1000 + 500 MVA. The load was converted as 50 % current and 50 % constant power for both active and reactive power. Simulation should be done for the complete model with the HVDC converters both at Feda and Kristiansand in order to get a more realistic dynamic response close to the HVDC converters.

Future plans for upgrades and new production units in the Norwegian power system are not accounted for in any simulations. Such plans should be implemented in a complete model of the power system with the Sweden and the HVDC converters modelled, in order to get a realistic dynamic behavior. The new gas power plant at Kårstø at 420 MW is not modelled. The contribution of the gas power plant will lead to increased short-circuit power at Kårstø, making AC cable connection with SVC more favourable for the kind of events simulated, as the generator can contribute to the short-circuit power during the fault.

The plots for reactive power from the HVDC Light converters should be subject of further investigation. The onshore converter supplies a very fast peak of reactive power at the instant the fault is cleared, contributing to the voltage recovery. In order to verify that the HVDC Light model gives a correct dynamic response of reactive power, simulation results should be compared with real measurements of an existing HVDC Light system.

In the existing plans for offshore wind power application with HVDC Light connection, DC choppers are planned. The excess power produced during the fault onshore will be dissipated in the resistance. In this way, the offshore wind farm will not notice the fault onshore. The focus on fault ride through capability for the wind turbines themselves will not be an issue for faults in the onshore power system. As can be seen from the simulation results with HVDC Light, the voltage offshore is practically unaffected by the fault onshore. Because of the above mentioned reason, the focus in this thesis has therefore been on the impact of the transmission technologies onshore. For simulations with AC cable connection however, the protection of the wind turbines itself should be modeled for different wind turbine technologies.

When synchronous condensers were added at Kårstø, the voltage recovery improved compared to the solution with SVCs. The user model of the excitation system for the synchronous condensers used in the simulations was taken from a synchronous condenser from the Norwegian power system model, without any documentation. It is expected that the dynamic response could improve the voltage recovery even more than showed in the simulations, based on the plot for supplied reactive power after the three-phase short-circuit at Kårstø is cleared.

10 Conclusion

The power production in Norway mainly consists of hydro power, and up until recently there has been a net export of power in years with average precipitation. This situation has now changed, and with the ambitious national goal of no net CO_2 emission in 2050, great effort has to be made. Because of the great wind resources in the sea areas surrounding Norway, offshore wind power seems like a promising alternative.

In this study, grid integration of a 1000 MW offshore wind farm was studied. Two possible connection points in the Norwegian power system were found; Feda and Kårstø. Feda is the point where the HVDC cable to the Netherlands is connected, and the voltage at the busbar is 300 kV. Kårstø is the other connection point, also with a voltage of 300 kV. At Kårstø, and Karmøy west of Kårstø, there is a lot of power consuming industry. The offshore wind power connected to Kårstø will change the direction of the power flow in the lines going to the area.

There are several challenges with offshore wind power. Depths just outside the Norwegian coast reach several hundred meters, indicating that floating turbines should be used. This technology is not yet commercial, but there are several concepts under development. It is however possible to build large offshore wind farms in areas a couple of hundred kilometers south of Norway. Depths are suitable for technology available today, with wind turbines foundations on the seabed. The distance makes AC cable connection difficult because of the reactive power produced by the cables, and HVDC should therefore be used. HVDC Light is a VSC HVDC technology well suited for offshore wind power, and with rating up to 1174 MW connection of large wind farms are possible. The equipment is compact, and there is no requirement for short-circuit capacity either onshore or offshore.

Dynamic simulations have been done for the two connection points both with AC cables of 100 km and HVDC Light of 600 km, for different faults close to the connection points. The HVDC Light converter contributes to the voltage recovery onshore so that the fault ride through requirement requires the wind turbines to stay connected. This counts for all simulations in this thesis. Immediately after the fault is applied, the onshore HVDC Light converter supplies a large amount of reactive power reactive power. The contribution to the fault current during the fault, as well as the reactive power produced after the fault is cleared, supports the voltage at the connection point onshore. The reactive power is regulated so that the onshore voltage is approximately maintained at 1 pu in the time after the fault is cleared. For the cases with AC cable connection, the contribution of reactive power from the SVCs is limited, depending on how low the voltage is during the fault. After the fault is cleared, the SVCs produce as mush reactive power as possible. Because the SVCs are dependent of the voltage squared outside the working area, the amount of reactive power is not large enough in some of the simulations. In these cases, the voltage doesn't recover, and the system becomes unstable. The wind farm is allowed to trip, and the system has to restart in order to return to the pre fault condition.

From the simulations results, the conclusion can be drawn that system stability with AC cable transmission with SVC as reactive power compensation is highly dependent of short-circuit power, load flow situation in the power system and power system topology. With HVDC Light, the system stability is not affected for any of these factors in the simulations done.
Measures can however be done regarding the system stability with AC cable transmission. Synchronous condensers can be added at the connection point in order to contribute to the

short-circuit power. Simulations in this thesis with synchronous condensers did show some improvement compared to the solution with SVCs, but the voltage did not recover after a three-phase short-circuit at Kårstø. The model of the excitation system might need to be tuned in order to give a proper representation of the dynamic response of the synchronous condenser.

The voltage offshore is low during the onshore faults with AC cable connection. The wind turbine protection equipment is not modeled, but they are assumed to stay connected during the fault. With HVDC Light, the voltage offshore remains almost constant during the fault. The energy produced during the fault is stored as rotational kinetic energy in the turbines. A DC chopper will be used in existing plans for wind applications with HVDC Light, so that the wind turbines will be unaffected by a fault onshore.

From the TSO's point of view, the simulations indicate that HVDC Light is the favorable solution compared to AC. The reason for this is the ability of the HVDC Light converter to support the voltage during a fault onshore close to the connection point of the offshore wind farm. For the wind farm owner, the fact that the offshore wind turbines will not notice an onshore fault with a HVDC Light system with DC chopper, HVDC Light seems to be the most favourable transmission technology. Since the focus on fault ride through requirement for wind turbines connected to the onshore grid with HVDC Light is insignificant, the possibility of using less sophisticated wind turbines in terms of electrical properties arises.

11 Further work

This thesis is the end of the work started during the autumn 2007 with the project, and suggestions for further work are presented in this chapter. Statkraft will continue to offer students the possibility to write their master's thesis in cooperation with them, and the suggestions made in this chapter can be used as input for formulating new projects.

There are several challenges with grid integration of large scale offshore wind power. VSC HVDC will probably have to be used, based on the distances to the areas where it is possible to install offshore wind turbines with today's technology. Base on this assumption, power system studies with PSS/E and the user model of HVDC Light from ABB is a good starting point. As the focus in this thesis has been on the onshore grid side, work can be done investigating the offshore power system. The next version of the PSS/E user model for HVDC Light will have implemented a complete control system especially for offshore wind power with an isolated power system.

An interesting case to investigate is the connection of small wind farms to oil platforms. Models of existing platforms should be used in order to investigate how the equipment on the platforms behaves together with the small wind farms, and vice versa. The groups of platforms and wind farms could be could be connected in an offshore grid, with one common HVDC Light converter offshore. The impact of different wind turbine technologies can be investigated for such a case. General models for full frequency turbines and DFIG turbines can be provided by Statkraft, and the models can be tuned in order to correspond to the wind turbines from different manufacturers.

A model of Siemens's VSC HVDC technology HVDC PLUS is also available in PSS/E. Simulations can be done with HVDC Light and HVDC PLUS in order to compare the two technologies.

12 References

[1] ABB, *Its time to connect – technical description of HVDC Light® technology (2007)*

[2] ABB, User manual HVDC Light (2008)

[3] ABB, www.abb.com/hvdc

[4] Barberis N., Todorovic J., Ackermann T. (2005), *Loss evaluation of HVAC and HVDC transmission solutions for large offshore wind farms*, Science Direct

[5] Chengyoug, Z., *A Control Strategy for VSC-HVDC System Based on Analytic Expression*, IEEE

[6] Gustafsson, M. (Statnett), conversations

[7] Holen, A. T., Fosso, O. B., Olsen, K. J. (2006), *TET4115 Power system analysis*, Tapir akademisk forlag

[8] Hubert, C. I. (2002), *ELECTRIC MACHINES Theory, Operation, Applications, Adjustment, and Control*, Prentice Hall

[9] IEEE working group (1997), *IEEE Guide for Planning DC Links Terminating at AC Locations Having Low Short-Circuit Capacities*, IEEE

[10] Jiang-Häfner Y., Hyttinen M., Pääjärvi B., *On the Short Circuit Current Contribution of HVDC Light*, IEEE

[11] Koutiva, X. I., Vrionis, T. D., Vovos, N. A., Giannakopoulos, G. B., *Optimal Integration of an offshore wind farm to a weak grid*, IEEE

[12] Kundur, P. (1994), *Power System Stability and Control*, The McGraw-Hill Companies

[13] Larssen, V. (Nexans), conversations

[14] Leirbukt, A. (ABB), conversations

[15] Machowski, J., Bialek, J. W., Bumby, J. R. (1997), *Power System Dynamics and Stability*, John Wiley & Sons

[16] Manwell J. F., McGowan J. G., Rogers A. L. (2002), *Wind Energy Explained – Theory, Design and Application*, John Wiley & Sons

[17] Mohan, N., Undeland, T. M., Robbins W. P. (2003), *Power electronics – Converters, Applications and Design*, John Wiley & Sons, Inc.

[18] PSS/E user manual

[19] Statnett SF, *FIKS Funksjonskrav i kraftsystemet*

[20] Statnett, www.statnett.no

[21] Wang, C., Wang, L., Shi, L., *A survey on Wind Power Technologies in Power Systems*, IEEE

[22] Wangensteen, I. (2006), *Power System Economics – Nordic Electricity Marked*, Tapir Academic Press

[23] Weimers, L. *New Markets need new Technology*, IEEE

Appendix A: Limit checking reports

A.1 Limit checking report for busbar voltages between 130 and 400 kV

Original load flow case

PTI INTERACTIVE POWER SYSTEM SIMULATOR--PSS/E TUE, MAY 20 2008 10:55
STATNETTS DRIFTDATASETT FOR NORGE

BUSES WITH VOLTAGE GREATER THAN 1.1000:

BUS#	X-- NAME	--X BASKV	AREA	V(PU)	V(KV)	BUS#	X-- NAME	--X BASKV	AREA	V(PU)	V(KV)
50419	DUM-KVA2	130.00	68	1.1121	144.57	50556	DUM-T8-	220.00	67	1.1250	247.51
51168	BERGER	130.00	51	1.1133	144.73	51186	FUSDAL-A	130.00	51	1.1130	144.69
57200	NR-RAZFE	220.00	67	1.1250	247.49	57204	N.ROSS2	220.00	67	1.1250	247.49
57299	SUNDFJ-B	130.00	67	1.1035	143.46	57683	GLOMFJD1	130.00	67	1.1022	143.29
58049	KVAN-NOR	130.00	68	1.1120	144.56	58353	STRAUM1A	130.00	69	1.1075	143.97
58363	INNSET1	130.00	69	1.1119	144.54	58702	VARANGER	220.00	69	1.1169	245.72

BUSES WITH VOLTAGE LESS THAN 0.9000:

BUS#	X-- NAME	--X BASKV	AREA	V(PU)	V(KV)	BUS#	X-- NAME	--X BASKV	AREA	V(PU)	V(KV)
51137	SMESTD1B	130.00	51	0.8906	115.78	51178	PRESTEGA	130.00	51	0.8882	115.47
51179	BRISKEBY	130.00	51	0.8893	115.60	51183	SKOYEN	130.00	51	0.8901	115.72
52403	SAVALEN1	130.00	52	0.8923	116.00	52413	TYNSET1	130.00	52	0.8799	114.38
52433	TRYSIL1	130.00	52	0.8980	116.74	57548	ULSET-B-	130.00	66	0.8942	116.24

A.2 Limit checking report for branches between 130 and 400 kV

Original load flow case

PTI INTERACTIVE POWER SYSTEM SIMULATOR--PSS/E TUE, MAY 20 2008 10:54
STATNETTS DRIFTDATASETT FOR NORGE

BRANCH LOADINGS ABOVE 100.0 % OF RATING SET A:

X--------- FROM BUS ----------				X X---------- TO BUS ----------					CURRENT(MVA)		
BUS#	X-- NAME	--X BASKV	AREA	BUS#	X-- NAME	--X BASKV	AREA	CKT	LOADING	RATING	PERCENT
50029	KKI-THA2	20.000*	66	56573	THAMSHAM	130.00	66	1	37.2	29.1	127.7
50032	KKI-FES1	20.000	67	57623	SVABO-A-	130.00*	67	5	47.2	46.4	101.8
50035	KKI-FINN	20.000	69	58393	FINNFJOR	130.00*	69	1	52.3	52.2	100.2
50280	MF-O.VIN	300.00	52	50539	DUM-VINS	12.000*	52	1	160.8	142.9	112.5
50483	DUM-LUN1	50.000*	56	54463	LUND1	130.00	56	1	77.1	55.0	140.2
50492	DUM-HAVI	66.000*	61	55152	HAAVIK3	300.00	61	1	80.8	79.5	101.6
50495	DUM-T1-	130.00	65	57015	AURA-TEA	17.000*	65	1	77.4	69.6	111.2
50563	DUM-KLE2	66.000	66	57032	KLEBU3	300.00*	66	1	158.1	157.4	100.4
50574	DUM-FAN2	130.00	62	55275	FAN-T2-T	17.000*	62	1	58.9	58.2	101.2
50588	DUM-STOR	66.000	61	55172	STORD3	300.00*	61	1	108.8	99.3	109.6
50605	DUM-FLE1	66.000	55	51203	FLESAK1A	130.00*	55	1	108.1	75.4	143.3
50608	DUM-FLE4	130.00	55	51202	FLESAK3	300.00*	55	1	125.6	116.0	108.2
50608	DUM-FLE4	130.00	55	51203	FLESAK1A	130.00*	55	1	119.3	106.0	112.5
50635	DUM-MYKS	11.000*	53	51393	MYKSTF1A	130.00	53	1	55.4	49.7	111.5
50637	DUM-POR1	130.00	55	51244	PORSGR0	17.000*	55	1	109.3	100.0	109.3
50638	DUM-POR2	130.00	55	51245	PORSGRKA	17.000*	55	1	109.5	100.0	109.5
50654	DUM-T7-	130.00	51	51132	SMESTAD3	300.00*	51	1	268.3	246.2	109.0
50654	DUM-T7-	130.00	51	51137	SMESTD1B	130.00*	51	1	259.8	246.2	105.5
50678	DUM-ULV1	50.000	51	51102	ULVEN3	300.00*	51	1	148.7	138.6	107.3
50679	DUM-ULV2	50.000	51	51102	ULVEN3	300.00*	51	1	149.1	138.6	107.6
50751	DUM-RJUK	130.00	54	51711	RJUKAN	400.00*	54	1	297.4	282.6	105.2
50751	DUM-RJUK	130.00	54	51713	RJUKAN-T	130.00*	54	1	294.1	282.6	104.1
50760	DUM-HAMM	66.000*	69	58543	HAMMERFE	130.00	69	1	56.1	49.2	114.0
51174	PRESTEGA	11.000	51	51178	PRESTEGA	130.00*	51	1	43.5	39.4	110.4
51174	PRESTEGA	11.000	51	51178	PRESTEGA	130.00*	51	2	41.5	39.4	105.3
51175	BRISKEBY	11.000	51	51179	BRISKEBY	130.00*	51	1	44.2	39.4	112.3
51175	BRISKEBY	11.000	51	51179	BRISKEBY	130.00*	51	2	44.5	39.4	112.9
51180	SKOYEN	11.000	51	51183	SKOYEN	130.00*	51	1	44.9	39.4	114.0
51180	SKOYEN	11.000	51	51183	SKOYEN	130.00*	51	2	44.9	39.4	114.0
51196	AKERSBER	130.00*	51	51197	AKERSBER	11.000	51	1	44.3	39.4	112.5
51196	AKERSBER	130.00*	51	51197	AKERSBER	11.000	51	2	44.3	39.4	112.5
51326	SPIKKEST	130.00*	51	51330	SPIKKEST	20.000	51	1	18.3	18.2	100.5
51403	NORE2-A-	130.00	53	51407	NORE2-G2	11.600*	53	1	29.0	28.7	101.1
51483	MAR-A-	130.00	55	51485	MAR-G1-	6.0000*	55	1	37.9	36.1	105.0
51483	MAR-A-	130.00	55	51486	MAR-G2-	6.0000*	55	1	38.8	36.1	107.5
51483	MAR-A-	130.00	55	51487	MAR-G3-	6.0000*	55	1	40.0	36.1	110.8
51484	MAR-B-	130.00	55	51488	MAR-G4-	6.0000*	55	1	39.8	36.1	110.1
51484	MAR-B-	130.00	55	51489	MAR-G5-	6.0000*	55	1	39.8	36.1	110.1
51484	MAR-B-	130.00*	55	51718	RJUKAN-B	130.00	54	1	290.9	218.0	133.4
51593	SUNDLAND	130.00*	55	51595	SUNDLAND	20.000	55	1	34.8	17.4	199.8
51593	SUNDLAND	130.00*	55	51595	SUNDLAND	20.000	55	2	39.8	17.4	228.5
51593	SUNDLAND	130.00	55	51595	SUNDLAND	20.000*	55	3	43.5	17.4	250.0
51713	RJUKAN-T	130.00*	54	51718	RJUKAN-B	130.00	54	1	294.1	184.2	159.7
52323	ABJORA1	130.00	52	52329	AABJ-G4-	11.000*	52	1	100.8	94.3	106.9
53021	DAGALI4	400.00*	53	53025	DAGALI-R	20.000	53	1	112.3	104.4	107.5
53133	UVDAL1-1	130.00	53	53136	UVDA1-G1	8.0000*	53	1	49.1	46.4	105.8
53133	UVDAL1-1	130.00	53	53137	UVDA1-G2	8.0000*	53	1	49.6	46.4	107.0
54022	KR.SAND3	300.00*	56	54025	KR.SAND	110.00	56	3	120.3	110.0	109.4
54152	TJORHOM3	300.00	57	54156	TJORHOM	13.000*	57	1	134.3	131.3	102.3
54193	LYSEBTN1	130.00	57	54197	LYSEB-G4	9.0000*	57	4	48.4	46.4	104.4
54503	AKLAND1	130.00*	56	54543	HOLT1	130.00	56	1	52.2	45.0	115.9
54583	BOYLEFOS	130.00	56	54584	BOYLEFOS	66.000*	56	1	88.7	78.8	112.6
55112	NESFLAT3	300.00	61	55118	SULD2-G1	10.000*	61	1	76.9	76.2	101.0
55513	MIDTBYG1	130.00	62	55519	MIDTBYGD	11.000*	62	1	20.1	20.0	100.5
55825	BJOL-G1	12.000	62	55829	NYEBJOLV	130.00*	62	1	101.4	95.7	105.9
56032	LEIRDOL3	300.00	63	56042	FORTUN3	300.00*	63	1	272.6	259.8	104.9
56403	MOSKOG	130.00*	64	56404	STAK-66A	66.000	64	1	65.2	49.2	132.6
56743	TAF-K4-	130.00	65	56746	TA-K4-G1	11.000*	65	1	55.2	53.1	103.9
57005	SUNNDALS	20.000	65	57013	AURA1	130.00*	65	1	23.9	22.2	107.5
57053	NEA1	130.00*	66	57054	NEA66-	66.000	66	1	29.4	27.8	105.8
57132	TUNSJDAL	300.00	67	57136	TUNN-G12	8.5000*	67	1	88.8	85.7	103.6
57132	TUNSJDAL	300.00	67	57137	TUNN-G34	8.5000*	67	1	89.4	85.7	104.3
57203	N.ROSS1A	130.00	67	57214	NROSS-G1	11.000*	67	1	44.8	44.8	100.0
57203	N.ROSS1A	130.00	67	57215	NROSS-G2	11.000*	67	1	44.8	44.8	100.0
57883	LOMI1	130.00	67	57887	LOMI-G2-	10.500*	67	1	63.9	62.8	101.8
58463	KVALOYA1	130.00	69	58464	KVALOY66	66.000*	69	1	48.7	47.1	103.5
58463	KVALOYA1	130.00	69	58464	KVALOY66	66.000*	69	2	49.0	47.1	104.0

A.3 Limit checking report for busbar voltages between 130 and 400 kV

1000 MW offshore wind connected to Feda, 900 MW load at Hasle

---

PTI INTERACTIVE POWER SYSTEM SIMULATOR--PSS/E FRI, MAY 16 2008 11:58
STATNETTS DRIFTDATASETT FOR NORGE

BUSES WITH VOLTAGE GREATER THAN 1.1000:

BUS#	X-- NAME	--X BASKV	AREA	V(PU)	V(KV)	BUS#	X-- NAME	--X BASKV	AREA	V(PU)	V(KV)
50419	DUM-KVA2	130.00	68	1.1121	144.57	50556	DUM-T8-	220.00	67	1.1250	247.51
57200	NR-RAZFE	220.00	67	1.1250	247.49	57204	N.ROSS2	220.00	67	1.1250	247.49
57299	SUNDFJ-B	130.00	67	1.1035	143.46	57683	GLOMFJD1	130.00	67	1.1022	143.29
58049	KVAN-NOR	130.00	68	1.1120	144.56	58353	STRAUM1A	130.00	69	1.1075	143.97
58363	INNSET1	130.00	69	1.1119	144.54	58702	VARANGER	220.00	69	1.1169	245.72

BUSES WITH VOLTAGE LESS THAN 0.9000:

BUS#	X-- NAME	--X BASKV	AREA	V(PU)	V(KV)	BUS#	X-- NAME	--X BASKV	AREA	V(PU)	V(KV)
51137	SMESTD1B	130.00	51	0.8751	113.77	51178	PRESTEGA	130.00	51	0.8727	113.44
51179	BRISKEBY	130.00	51	0.8738	113.59	51183	SKOYEN	130.00	51	0.8746	113.70
52403	SAVALEN1	130.00	52	0.8908	115.81	52413	TYNSET1	130.00	52	0.8783	114.18
52433	TRYSIL1	130.00	52	0.8963	116.52	57548	ULSET-B-	130.00	66	0.8926	116.04

A.4 Limit checking report for branches between 130 and 400 kV

1000 MW offshore wind connected to Feda, 900 MW load at Hasle

---

PTI INTERACTIVE POWER SYSTEM SIMULATOR--PSS/E FRI, MAY 16 2008 12:00
STATNETTS DRIFTDATASETT FOR NORGE

BRANCH LOADINGS ABOVE 100.0 % OF RATING SET A:

FROM BUS				TO BUS					CURRENT(MVA)		
BUS#	NAME	BASKV	AREA	BUS#	NAME	BASKV	AREA	CKT	LOADING	RATING	PERCENT
50029	KKI-THA2	20.000*	66	56573	THAMSHAM	130.00	66	1	37.1	29.1	127.6
50032	KKI-FES1	20.000	67	57623	SVABO-A-	130.00*	67	5	47.2	46.4	101.8
50035	KKI-FINN	20.000	69	58393	FINNFJOR	130.00*	69	1	52.3	52.2	100.2
50280	MF-O.VIN	300.00	52	50539	DUM-VINS	12.000*	52	1	161.5	142.9	113.0
50483	DUM-LUN1	50.000*	56	54463	LUND1	130.00	56	1	77.0	55.0	140.0
50495	DUM-T1-	130.00	65	57015	AURA-TEA	17.000*	65	1	77.3	69.6	111.1
50563	DUM-KLE2	66.000	66	57032	KLEBU3	300.00*	66	1	158.1	157.4	100.5
50574	DUM-FAN2	130.00	62	55275	FAN-T2-T	17.000*	62	1	59.0	58.2	101.5
50588	DUM-STOR	66.000	61	55172	STORD3	300.00*	61	1	109.6	99.3	110.3
50605	DUM-FLE1	66.000	55	51203	FLESAK1A	130.00*	55	1	104.3	75.4	138.3
50607	DUM-FLE3	130.00	55	51203	FLESAK1A	130.00*	55	1	108.5	106.0	102.3
50608	DUM-FLE4	130.00	55	51202	FLESAK3	300.00*	55	1	125.4	116.0	108.1
50608	DUM-FLE4	130.00	55	51203	FLESAK1A	130.00*	55	1	119.1	106.0	112.4
50635	DUM-MYKS	11.000*	53	51393	MYKSTF1A	130.00	53	1	56.5	49.7	113.6
50637	DUM-POR1	130.00	55	51244	PORSGR0	17.000*	55	1	108.9	100.0	108.9
50638	DUM-POR2	130.00	55	51245	PORSGRKA	17.000*	55	1	109.0	100.0	109.0
50654	DUM-T7-	130.00	51	51132	SMESTAD3	300.00*	51	1	273.8	246.2	111.2
50654	DUM-T7-	130.00	51	51137	SMESTD1B	130.00*	51	1	265.1	246.2	107.7
50678	DUM-ULV1	50.000	51	51102	ULVEN3	300.00*	51	1	150.8	138.6	108.8
50679	DUM-ULV2	50.000	51	51102	ULVEN3	300.00*	51	1	151.2	138.6	109.1
50751	DUM-RJUK	130.00	54	51711	RJUKAN	400.00*	54	1	298.8	282.6	105.7
50751	DUM-RJUK	130.00	54	51713	RJUKAN-T	130.00*	54	1	295.5	282.6	104.6
50760	DUM-HAMM	66.000*	69	58543	HAMMERFE	130.00	69	1	56.1	49.2	114.0
51174	PRESTEGA	11.000	51	51178	PRESTEGA	130.00*	51	1	44.4	39.4	112.7
51174	PRESTEGA	11.000	51	51178	PRESTEGA	130.00*	51	2	42.4	39.4	107.5
51175	BRISKEBY	11.000	51	51179	BRISKEBY	130.00*	51	1	45.0	39.4	114.3
51175	BRISKEBY	11.000	51	51179	BRISKEBY	130.00*	51	2	45.3	39.4	114.9
51180	SKOYEN	11.000	51	51183	SKOYEN	130.00*	51	1	45.9	39.4	116.4
51180	SKOYEN	11.000	51	51183	SKOYEN	130.00*	51	2	45.9	39.4	116.4
51196	AKERSBER	130.00*	51	51197	AKERSBER	11.000	51	1	45.0	39.4	114.3
51196	AKERSBER	130.00*	51	51197	AKERSBER	11.000	51	2	45.0	39.4	114.3
51326	SPIKKEST	130.00*	51	51330	SPIKKEST	20.000	51	1	18.6	18.2	102.0
51403	NORE2-A-	130.00	53	51407	NORE2-G2	11.600*	53	1	29.5	28.7	102.8
51483	MAR-A-	130.00	55	51485	MAR-G1-	6.0000*	55	1	38.4	36.1	106.5
51483	MAR-A-	130.00	55	51486	MAR-G2-	6.0000*	55	1	39.0	36.1	108.0
51483	MAR-A-	130.00	55	51487	MAR-G3-	6.0000*	55	1	40.2	36.1	111.3
51484	MAR-B-	130.00	55	51488	MAR-G4-	6.0000*	55	1	39.6	36.1	109.6
51484	MAR-B-	130.00	55	51489	MAR-G5-	6.0000*	55	1	39.6	36.1	109.6
51484	MAR-B-	130.00	55	51718	RJUKAN-B	130.00*	54	1	292.2	218.0	134.1
51593	SUNDLAND	130.00*	55	51595	SUNDLAND	20.000	55	1	34.7	17.4	199.1
51593	SUNDLAND	130.00*	55	51595	SUNDLAND	20.000	55	2	39.6	17.4	227.8
51593	SUNDLAND	130.00	55	51595	SUNDLAND	20.000*	55	3	43.2	17.4	248.0
51713	RJUKAN-T	130.00*	54	51718	RJUKAN-B	130.00	54	1	295.5	184.2	160.4
52052	FABERG3	300.00*	52	52072	N.VINST3	300.00	52	1	312.2	311.8	100.2
52062	RENDAL3	300.00	52	52066	RENDA-G1	14.000*	52	1	106.7	106.1	100.6
52307	DOKKA-G2	8.0000*	52	52309	DOKK-KRV	130.00	52	2	23.2	23.2	100.1
52323	ABJORA1	130.00	52	52329	AABJ-G4-	11.000*	52	1	100.9	94.3	107.0
53133	UVDAL1-1	130.00	53	53136	UVDA1-G1	8.0000*	53	1	49.2	46.4	106.0
53133	UVDAL1-1	130.00	53	53137	UVDA1-G2	8.0000*	53	1	49.7	46.4	107.1
54022	KR.SAND3	300.00*	56	54025	KR.SAND	110.00	56	3	114.9	110.0	104.5
54152	TJORHOM3	300.00	57	54156	TJORHOM	13.000*	57	1	134.3	131.3	102.3
54193	LYSEBTN1	130.00	57	54197	LYSEB-G4	9.0000*	57	4	48.4	46.4	104.3
54503	AKLAND1	130.00	56	54543	HOLT1	130.00*	56	1	91.5	45.0	203.2
54583	BOYLEFOS	130.00	56	54584	BOYLEFOS	66.000*	56	1	88.5	78.8	112.3
55112	NESFLAT3	300.00	61	55118	SULD2-G1	10.000*	61	1	76.9	76.2	100.9
55513	MIDTBYG1	130.00	62	55519	MIDTBYGD	11.000*	62	1	20.1	20.0	100.3
55825	BJOL-G1	12.000	62	55829	NYEBJOLV	130.00*	62	1	101.6	95.7	106.1
56032	LEIRDOL3	300.00	63	56042	FORTUN3	300.00*	63	1	272.6	259.8	104.9
56403	MOSKOG	130.00*	64	56404	STAK-66A	66.000	64	1	65.2	49.2	132.6
56743	TAF-K4-	130.00	65	56746	TA-K4-G1	11.000*	65	1	55.2	53.1	104.0
57005	SUNNDALS	20.000	65	57013	AURA1	130.00*	65	1	23.9	22.2	107.5
57053	NEA1	130.00*	66	57054	NEA66-	66.000	66	1	29.4	27.8	105.8
57132	TUNSJDAL	300.00	67	57136	TUNN-G12	8.5000*	67	1	88.8	85.7	103.6
57132	TUNSJDAL	300.00	67	57137	TUNN-G34	8.5000*	67	1	89.4	85.7	104.3
57203	N.ROSS1A	130.00	67	57214	NROSS-G1	11.000*	67	1	44.8	44.8	100.0
57203	N.ROSS1A	130.00	67	57215	NROSS-G2	11.000*	67	1	44.8	44.8	100.0
57883	LOMI1	130.00	67	57887	LOMI-G2-	10.500*	67	1	63.9	62.8	101.8
58463	KVALOYA1	130.00	69	58464	KVALOY66	66.000*	69	1	48.7	47.1	103.5
58463	KVALOYA1	130.00	69	58464	KVALOY66	66.000*	69	2	49.0	47.1	104.0
58683	TANA1	130.00*	69	58685	TANA22	20.000	69	1	10.1	8.3	121.3

A.5 Limit checking report for busbar voltages between 130 and 400 kV

1700 MW import of HVDC, 1600 MW load at Hasle

PTI INTERACTIVE POWER SYSTEM SIMULATOR--PSS/E WED, MAY 14 2008 15:01
STATNETTS DRIFTDATASETT FOR NORGE

BUSES WITH VOLTAGE GREATER THAN 1.1000:

BUS#	X-- NAME	--X BASKV	AREA	V(PU)	V(KV)	BUS#	X-- NAME	--X BASKV	AREA	V(PU)	V(KV)
50419	DUM-KVA2	130.00	68	1.1121	144.57	50556	DUM-T8-	220.00	67	1.1250	247.51
57200	NR-RAZFE	220.00	67	1.1250	247.49	57204	N.ROSS2	220.00	67	1.1250	247.49
57299	SUNDFJ-B	130.00	67	1.1035	143.46	57683	GLOMFJD1	130.00	67	1.1022	143.29
58049	KVAN-NOR	130.00	68	1.1120	144.56	58353	STRAUM1A	130.00	69	1.1075	143.97
58363	INNSET1	130.00	69	1.1119	144.54	58702	VARANGER	220.00	69	1.1169	245.72

BUSES WITH VOLTAGE LESS THAN 0.9000:

BUS#	X-- NAME	--X BASKV	AREA	V(PU)	V(KV)	BUS#	X-- NAME	--X BASKV	AREA	V(PU)	V(KV)
51092	ROYKAS3	300.00	51	0.8957	268.72	51102	ULVEN3	300.00	51	0.8892	266.76
51112	FURUSET3	300.00	51	0.8913	267.40	51122	SOGN3	300.00	51	0.8857	265.72
51123	SOGN1	130.00	51	0.8879	115.43	51132	SMESTAD3	300.00	51	0.8838	265.14
51137	SMESTD1B	130.00	51	0.8443	109.76	51140	HAM-REAK	300.00	51	0.8876	266.27
51177	SAGENE	130.00	51	0.8855	115.12	51178	PRESTEGA	130.00	51	0.8416	109.41
51179	BRISKEBY	130.00	51	0.8428	109.56	51182	BERUM3	300.00	51	0.8853	265.60
51183	SKOYEN	130.00	51	0.8437	109.69	51196	AKERSBER	130.00	51	0.8799	114.39
51302	HADELAND	300.00	51	0.8999	269.97	52012	MINNE3	300.00	52	0.8992	269.77
52403	SAVALEN1	130.00	52	0.8859	115.17	52413	TYNSET1	130.00	52	0.8734	113.54
52423	ENGERD1	130.00	52	0.8963	116.52	52433	TRYSIL1	130.00	52	0.8909	115.82
57548	ULSET-B-	130.00	66	0.8877	115.41						

A.6 Limit checking report for branches between 130 and 400 kV

1700 MW import of HVDC, 1600 MW load at Hasle

PTI INTERACTIVE POWER SYSTEM SIMULATOR--PSS/E WED, MAY 14 2008 15:02
STATNETTS DRIFTDATASETT FOR NORGE

BRANCH LOADINGS ABOVE 100.0 % OF RATING SET A:

FROM BUS				TO BUS					CURRENT(MVA)		
BUS#	NAME	BASKV	AREA	BUS#	NAME	BASKV	AREA	CKT	LOADING	RATING	PERCENT
50029	KKI-THA2	20.000*	66	56573	THAMSHAM	130.00	66	1	37.1	29.1	127.5
50032	KKI-FES1	20.000	67	57623	SVABO-A-	130.00*	67	5	47.2	46.4	101.8
50035	KKI-FINN	20.000	69	58393	FINNFJOR	130.00*	69	1	52.3	52.2	100.2
50280	MF-O.VIN	300.00	52	50539	DUM-VINS	12.000*	52	1	163.6	142.9	114.5
50483	DUM-LUN1	50.000*	56	54463	LUND1	130.00	56	1	78.3	55.0	142.4
50492	DUM-HAVI	66.000*	61	55152	HAAVIK3	300.00	61	1	80.1	79.5	100.7
50495	DUM-T1-	130.00	65	57015	AURA-TEA	17.000*	65	1	77.2	69.6	110.9
50563	DUM-KLE2	66.000	66	57032	KLEBU3	300.00*	66	1	158.4	157.4	100.6
50574	DUM-FAN2	130.00	62	55275	FAN-T2-T	17.000*	62	1	59.0	58.2	101.3
50588	DUM-STOR	66.000	61	55172	STORD3	300.00*	61	1	109.1	99.3	109.8
50605	DUM-FLE1	66.000	55	51203	FLESAK1A	130.00*	55	1	91.5	75.4	121.4
50607	DUM-FLE3	130.00*	55	51202	FLESAK3	300.00	55	1	117.4	116.0	101.2
50607	DUM-FLE3	130.00	55	51203	FLESAK1A	130.00*	55	1	117.4	106.0	110.8
50608	DUM-FLE4	130.00	55	51202	FLESAK3	300.00*	55	1	118.1	116.0	101.8
50608	DUM-FLE4	130.00*	55	51203	FLESAK1A	130.00	55	1	112.2	106.0	105.9
50619	DUM-HAM1	50.000	51	51142	HAMANG3	300.00*	51	1	134.7	133.0	101.3
50620	DUM-HAM2	50.000	51	51142	HAMANG3	300.00*	51	1	136.4	133.0	102.6
50635	DUM-MYKS	11.000*	53	51393	MYKSTF1A	130.00	53	1	57.9	49.7	116.6
50637	DUM-POR1	130.00	55	51244	PORSGR0	17.000*	55	1	107.4	100.0	107.4
50638	DUM-POR2	130.00	55	51245	PORSGRKA	17.000*	55	1	107.5	100.0	107.5
50641	DUM-RING	130.00	51	51161	RINGERI4	400.00*	51	1	248.0	246.2	100.7
50652	DUM-T4-	50.000*	51	51132	SMESTAD3	300.00	51	1	156.4	154.4	101.3
50653	DUM-T5-	50.000*	51	51132	SMESTAD3	300.00	51	1	157.1	154.4	101.7
50654	DUM-T7-	130.00	51	51132	SMESTAD3	300.00*	51	1	290.4	246.2	117.9
50654	DUM-T7-	130.00	51	51137	SMESTD1B	130.00*	51	1	277.0	246.2	112.5
50678	DUM-ULV1	50.000	51	51102	ULVEN3	300.00*	51	1	157.1	138.6	113.3
50679	DUM-ULV2	50.000	51	51102	ULVEN3	300.00*	51	1	157.4	138.6	113.5
50751	DUM-RJUK	130.00	54	51711	RJUKAN	400.00*	54	1	303.6	282.6	107.4
50751	DUM-RJUK	130.00*	54	51713	RJUKAN-T	130.00	54	1	300.3	282.6	106.3
50760	DUM-HAMM	66.000*	69	58543	HAMMERFE	130.00	69	1	56.1	49.2	114.0
51081	FROGNER4	400.00	51	51086	FROGN-F1	17.000*	51	1	231.5	220.8	104.8
51174	PRESTEGA	11.000	51	51178	PRESTEGA	130.00*	51	1	46.4	39.4	117.8
51174	PRESTEGA	11.000	51	51178	PRESTEGA	130.00*	51	2	44.3	39.4	112.3
51175	BRISKEBY	11.000	51	51179	BRISKEBY	130.00*	51	1	47.0	39.4	119.2
51175	BRISKEBY	11.000	51	51179	BRISKEBY	130.00*	51	2	47.2	39.4	119.8
51180	SKOYEN	11.000	51	51183	SKOYEN	130.00*	51	1	48.0	39.4	121.7
51180	SKOYEN	11.000	51	51183	SKOYEN	130.00*	51	2	48.0	39.4	121.7
51196	AKERSBER	130.00*	51	51197	AKERSBER	11.000	51	1	46.5	39.4	118.0
51196	AKERSBER	130.00*	51	51197	AKERSBER	11.000	51	2	46.5	39.4	118.0
51276	GOKSTAD	11.000	55	51278	GOKSTAD1	130.00*	55	1	24.3	23.9	101.8
51277	HOLMESTR	20.000	55	51408	HOLMESI1	130.00*	55	1	26.3	26.1	100.8
51326	SPIKKEST	130.00*	51	51330	SPIKKEST	20.000	51	1	19.1	18.2	105.1
51403	NORE2-A-	130.00	53	51407	NORE2-G2	11.600*	53	1	30.2	28.7	105.3
51404	SLAGEN22	20.000	55	51418	SLAGEN1	130.00*	55	1	26.3	26.1	100.8
51483	MAR-A-	130.00	55	51485	MAR-G1-	6.0000*	55	1	39.5	36.1	109.3
51483	MAR-A-	130.00	55	51486	MAR-G2-	6.0000*	55	1	39.4	36.1	109.2
51483	MAR-A-	130.00	55	51487	MAR-G3-	6.0000*	55	1	40.7	36.1	112.6
51484	MAR-B-	130.00	55	51488	MAR-G4-	6.0000*	55	1	39.3	36.1	109.0
51484	MAR-B-	130.00	55	51489	MAR-G5-	6.0000*	55	1	39.3	36.1	109.0
51484	MAR-B-	130.00	55	51718	RJUKAN-B	130.00*	54	1	297.0	218.0	136.2
51593	SUNDLAND	130.00*	55	51595	SUNDLAND	20.000	55	1	35.6	17.4	204.9
51593	SUNDLAND	130.00*	55	51595	SUNDLAND	20.000	55	2	40.8	17.4	234.3
51593	SUNDLAND	130.00	55	51595	SUNDLAND	20.000*	55	3	43.0	17.4	247.2
51693	HOLTANE1	130.00	55	54507	GJERST_T	130.00*	56	1	151.4	112.6	134.5
51713	RJUKAN-T	130.00*	54	51718	RJUKAN-B	130.00	54	1	300.3	184.2	163.0
52052	FABERG3	300.00*	52	52072	N.VINST3	300.00	52	1	325.7	311.8	104.5
52062	RENDAL3	300.00	52	52066	RENDA-G1	14.000*	52	1	111.4	106.1	105.0
52307	DOKKA-G2	8.0000*	52	52309	DOKK-KRV	130.00	52	2	23.9	23.2	103.0
52323	ABJORA1	130.00	52	52329	AABJ-G4-	11.000*	52	1	101.5	94.3	107.7
53133	UVDAL1-1	130.00	53	53136	UVDA1-G1	8.0000*	53	1	49.5	46.4	106.8
53133	UVDAL1-1	130.00	53	53137	UVDA1-G2	8.0000*	53	1	50.1	46.4	107.9
54020	KR.SA-F1	17.000*	56	54022	KR.SAND3	300.00	56	1	125.9	125.8	100.1
54022	KR.SAND3	300.00*	56	54025	KR.SAND	110.00	56	3	118.8	110.0	108.0
54152	TJORHOM3	300.00	57	54156	TJORHOM	13.000*	57	1	138.8	131.3	105.7
54193	LYSEBTN1	130.00	57	54197	LYSEB-G4	9.0000*	57	4	51.3	46.4	110.5
54503	AKLAND1	130.00*	56	54507	GJERST_T	130.00	56	1	160.1	135.1	118.5
54503	AKLAND1	130.00	56	54543	HOLT1	130.00*	56	1	136.6	45.0	303.4
54583	BOYLEFOS	130.00	56	54584	BOYLEFOS	66.000*	56	1	93.9	78.8	119.2
55112	NESFLAT3	300.00	61	55118	SULD2-G1	10.000*	61	1	77.9	76.2	102.3

55513	MIDTBYG1	130.00	62	55519	MIDTBYGD	11.000*	62	1	20.1	20.0	100.5
55825	BJOL-G1	12.000	62	55829	NYEBJOLV	130.00*	62	1	101.4	95.7	105.9
56032	LEIRDOL3	300.00	63	56042	FORTUN3	300.00*	63	1	273.0	259.8	105.1
56356	GRYTT-G1	16.000*	65	56359	GR.KRV	130.00	65	1	143.6	143.5	100.1
56403	MOSKOG	130.00*	64	56404	STAK-66A	66.000	64	1	65.3	49.2	132.7
56743	TAF-K4-	130.00	65	56746	TA-K4-G1	11.000*	65	1	55.3	53.1	104.1
57005	SUNNDALS	20.000	65	57013	AURA1	130.00*	65	1	23.9	22.2	107.8
57053	NEA1	130.00*	66	57054	NEA66-	66.000	66	1	29.4	27.8	105.7
57132	TUNSJDAL	300.00	67	57136	TUNN-G12	8.5000*	67	1	88.8	85.7	103.6
57132	TUNSJDAL	300.00	67	57137	TUNN-G34	8.5000*	67	1	89.4	85.7	104.3
57203	N.ROSS1A	130.00	67	57214	NROSS-G1	11.000*	67	1	44.8	44.8	100.0
57203	N.ROSS1A	130.00	67	57215	NROSS-G2	11.000*	67	1	44.8	44.8	100.0
57883	LOMI1	130.00	67	57887	LOMI-G2-	10.500*	67	1	63.9	62.8	101.8
58463	KVALOYA1	130.00	69	58464	KVALOY66	66.000*	69	1	48.7	47.1	103.5
58463	KVALOYA1	130.00	69	58464	KVALOY66	66.000*	69	2	49.0	47.1	104.0
58683	TANA1	130.00*	69	58685	TANA22	20.000	69	1	10.1	8.3	121.3

A.7 Limit checking report for busbar voltages between 130 and 400 kV

1000 MW offshore wind connected to Kårstø, 900 MW load at Hasle

---

PTI INTERACTIVE POWER SYSTEM SIMULATOR--PSS/E WED, MAY 14 2008 15:08
STATNETTS DRIFTDATASETT FOR NORGE

BUSES WITH VOLTAGE GREATER THAN 1.1000:

BUS#	X-- NAME	--X BASKV	AREA	V(PU)	V(KV)	BUS#	X-- NAME	--X BASKV	AREA	V(PU)	V(KV)
50419	DUM-KVA2	130.00	68	1.1121	144.57	50556	DUM-T8-	220.00	67	1.1250	247.51
57200	NR-RAZFE	220.00	67	1.1250	247.49	57204	N.ROSS2	220.00	67	1.1250	247.49
57299	SUNDFJ-B	130.00	67	1.1035	143.46	57683	GLOMFJD1	130.00	67	1.1022	143.29
58049	KVAN-NOR	130.00	68	1.1120	144.56	58353	STRAUM1A	130.00	69	1.1075	143.97
58363	INNSET1	130.00	69	1.1119	144.54	58702	VARANGER	220.00	69	1.1169	245.72

BUSES WITH VOLTAGE LESS THAN 0.9000:

BUS#	X-- NAME	--X BASKV	AREA	V(PU)	V(KV)	BUS#	X-- NAME	--X BASKV	AREA	V(PU)	V(KV)
51137	SMESTD1B	130.00	51	0.8710	113.23	51178	PRESTEGA	130.00	51	0.8685	112.90
51179	BRISKEBY	130.00	51	0.8696	113.04	51183	SKOYEN	130.00	51	0.8705	113.16
52403	SAVALEN1	130.00	52	0.8905	115.76	52413	TYNSET1	130.00	52	0.8780	114.13
52433	TRYSIL1	130.00	52	0.8960	116.47	57548	ULSET-B-	130.00	66	0.8923	116.00

A.8 Limit checking report for branches between 130 and 400 kV

1000 MW offshore wind connected to Kårstø, 900 MW load at Hasle

---

PTI INTERACTIVE POWER SYSTEM SIMULATOR--PSS/E WED, MAY 14 2008 15:07
STATNETTS DRIFTDATASETT FOR NORGE

BRANCH LOADINGS ABOVE 100.0 % OF RATING SET A:

FROM BUS				TO BUS					CURRENT(MVA)		
BUS#	NAME	BASKV	AREA	BUS#	NAME	BASKV	AREA	CKT	LOADING	RATING	PERCENT
50029	KKI-THA2	20.000*	66	56573	THAMSHAM	130.00	66	1	37.1	29.1	127.6
50032	KKI-FES1	20.000	67	57623	SVABO-A-	130.00*	67	5	47.2	46.4	101.8
50035	KKI-FINN	20.000	69	58393	FINNFJOR	130.00*	69	1	52.3	52.2	100.2
50280	MF-O.VIN	300.00	52	50539	DUM-VINS	12.000*	52	1	161.6	142.9	113.1
50483	DUM-LUN1	50.000*	56	54463	LUND1	130.00	56	1	77.1	55.0	140.2
50495	DUM-T1-	130.00	65	57015	AURA-TEA	17.000*	65	1	77.3	69.6	111.1
50563	DUM-KLE2	66.000	66	57032	KLEBU3	300.00*	66	1	158.1	157.4	100.5
50574	DUM-FAN2	130.00	62	55275	FAN-T2-T	17.000*	62	1	59.2	58.2	101.7
50588	DUM-STOR	66.000	61	55172	STORD3	300.00*	61	1	110.3	99.3	111.1
50605	DUM-FLE1	66.000	55	51203	FLESAK1A	130.00*	55	1	102.8	75.4	136.3
50607	DUM-FLE3	130.00	55	51203	FLESAK1A	130.00*	55	1	109.3	106.0	103.1
50608	DUM-FLE4	130.00	55	51202	FLESAK3	300.00*	55	1	124.1	116.0	107.0
50608	DUM-FLE4	130.00	55	51203	FLESAK1A	130.00*	55	1	117.9	106.0	111.2
50635	DUM-MYKS	11.000*	53	51393	MYKSTF1A	130.00	53	1	56.6	49.7	113.9
50637	DUM-POR1	130.00	55	51244	PORSGR0	17.000*	55	1	109.0	100.0	109.0
50638	DUM-POR2	130.00*	55	51245	PORSGRKA	17.000	55	1	109.1	100.0	109.1
50654	DUM-T7-	130.00	51	51132	SMESTAD3	300.00*	51	1	275.4	246.2	111.8
50654	DUM-T7-	130.00	51	51137	SMESTD1B	130.00*	51	1	266.7	246.2	108.3
50678	DUM-ULV1	50.000	51	51102	ULVEN3	300.00*	51	1	151.4	138.6	109.2
50679	DUM-ULV2	50.000	51	51102	ULVEN3	300.00*	51	1	151.7	138.6	109.5
50751	DUM-RJUK	130.00	54	51711	RJUKAN	400.00*	54	1	298.8	282.6	105.7
50751	DUM-RJUK	130.00	54	51713	RJUKAN-T	130.00*	54	1	295.5	282.6	104.6
50760	DUM-HAMM	66.000*	69	58543	HAMMERFE	130.00	69	1	56.1	49.2	114.0
51174	PRESTEGA	11.000	51	51178	PRESTEGA	130.00*	51	1	44.7	39.4	113.4
51174	PRESTEGA	11.000	51	51178	PRESTEGA	130.00*	51	2	42.6	39.4	108.1
51175	BRISKEBY	11.000	51	51179	BRISKEBY	130.00*	51	1	45.3	39.4	114.9
51175	BRISKEBY	11.000	51	51179	BRISKEBY	130.00*	51	2	45.5	39.4	115.5
51180	SKOYEN	11.000	51	51183	SKOYEN	130.00*	51	1	46.1	39.4	117.1
51180	SKOYEN	11.000	51	51183	SKOYEN	130.00*	51	2	46.1	39.4	117.1
51196	AKERSBER	130.00*	51	51197	AKERSBER	11.000	51	1	45.2	39.4	114.8
51196	AKERSBER	130.00*	51	51197	AKERSBER	11.000	51	2	45.2	39.4	114.8
51326	SPIKKEST	130.00*	51	51330	SPIKKEST	20.000	51	1	18.6	18.2	102.4
51403	NORE2-A-	130.00	53	51407	NORE2-G2	11.600*	53	1	29.5	28.7	102.9
51483	MAR-A-	130.00	55	51485	MAR-G1-	6.0000*	55	1	38.4	36.1	106.5
51483	MAR-A-	130.00	55	51486	MAR-G2-	6.0000*	55	1	39.0	36.1	108.0
51483	MAR-A-	130.00	55	51487	MAR-G3-	6.0000*	55	1	40.2	36.1	111.3
51484	MAR-B-	130.00	55	51488	MAR-G4-	6.0000*	55	1	39.6	36.1	109.6
51484	MAR-B-	130.00	55	51489	MAR-G5-	6.0000*	55	1	39.6	36.1	109.6
51484	MAR-B-	130.00	55	51718	RJUKAN-B	130.00*	54	1	292.3	218.0	134.1
51593	SUNDLAND	130.00*	55	51595	SUNDLAND	20.000	55	1	34.6	17.4	199.1
51593	SUNDLAND	130.00*	55	51595	SUNDLAND	20.000	55	2	39.6	17.4	227.7
51593	SUNDLAND	130.00	55	51595	SUNDLAND	20.000*	55	3	43.1	17.4	247.7
51713	RJUKAN-T	130.00*	54	51718	RJUKAN-B	130.00	54	1	295.5	184.2	160.4
52052	FABERG3	300.00*	52	52072	N.VINST3	300.00	52	1	313.1	311.8	100.4
52062	RENDAL3	300.00	52	52066	RENDA-G1	14.000*	52	1	107.0	106.1	100.8
52307	DOKKA-G2	8.0000*	52	52309	DOKK-KRV	130.00	52	2	23.3	23.2	100.3
52323	ABJORA1	130.00	52	52329	AABJ-G4-	11.000*	52	1	101.0	94.3	107.1
53133	UVDAL1-1	130.00	53	53136	UVDA1-G1	8.0000*	53	1	49.2	46.4	106.1
53133	UVDAL1-1	130.00	53	53137	UVDA1-G2	8.0000*	53	1	49.7	46.4	107.2
54022	KR.SAND3	300.00*	56	54025	KR.SAND	110.00	56	3	120.5	110.0	109.5
54152	TJORHOM3	300.00	57	54156	TJORHOM	13.000*	57	1	134.4	131.3	102.3
54193	LYSEBTN1	130.00	57	54197	LYSEB-G4	9.0000*	57	4	48.5	46.4	104.5
54503	AKLAND1	130.00	56	54543	HOLT1	130.00*	56	1	64.0	45.0	142.2
54583	BOYLEFOS	130.00	56	54584	BOYLEFOS	66.000*	56	1	89.0	78.8	112.9
55112	NESFLAT3	300.00	61	55118	SULD2-G1	10.000*	61	1	76.6	76.2	100.5
55513	MIDTBYG1	130.00	62	55519	MIDTBYGD	11.000*	62	1	20.0	20.0	100.1
55825	BJOL-G1	12.000	62	55829	NYEBJOLV	130.00*	62	1	101.8	95.7	106.4
56032	LEIRDOL3	300.00	63	56042	FORTUN3	300.00*	63	1	272.7	259.8	105.0
56403	MOSKOG	130.00*	64	56404	STAK-66A	66.000	64	1	65.2	49.2	132.6
56743	TAF-K4-	130.00	65	56746	TA-K4-G1	11.000*	65	1	55.2	53.1	104.0
57005	SUNNDALS	20.000	65	57013	AURA1	130.00*	65	1	23.9	22.2	107.6
57053	NEA1	130.00*	66	57054	NEA66-	66.000	66	1	29.4	27.8	105.8
57132	TUNSJDAL	300.00	67	57136	TUNN-G12	8.5000*	67	1	88.8	85.7	103.6
57132	TUNSJDAL	300.00	67	57137	TUNN-G34	8.5000*	67	1	89.4	85.7	104.3
57203	N.ROSS1A	130.00	67	57214	NROSS-G1	11.000*	67	1	44.8	44.8	100.0
57203	N.ROSS1A	130.00	67	57215	NROSS-G2	11.000*	67	1	44.8	44.8	100.0
57883	LOMI1	130.00	67	57887	LOMI-G2-	10.500*	67	1	63.9	62.8	101.8
58463	KVALOYA1	130.00	69	58464	KVALOY66	66.000*	69	1	48.7	47.1	103.5
58463	KVALOYA1	130.00	69	58464	KVALOY66	66.000*	69	2	49.0	47.1	104.0
58683	TANA1	130.00*	69	58685	TANA22	20.000	69	1	10.1	8.3	121.3

Appendix B: Short-circuit power calculations

The short-circuit power can be found in two ways from the bottom line of the print from PSS/E.

FAULT MVA A [MW] B [MVAR] C [A]

1:

$$Fault\ MVA = \sqrt{A^2 + B^2}$$

2:

$$Fault\ MVA = \sqrt{3} \cdot 300 \cdot C \cdot 10^{-3}$$

Case 1

```
                    PTI INTERACTIVE POWER SYSTEM SIMULATOR--PSS/E      TUE, JUN 03 2008  10:21
                        STATNETTS DRIFTDATASETT FOR NORGE


 X------- FROM BUS ------X AREA  VOLT          GEN    LOAD    SHUNT  X---------- TO BUS ----------X                TRANSFORMER
RATING
   BUS# X-- NAME --X BASKV ZONE  PU/KV  ANGLE  MW/MVAR MW/MVAR MW/MVAR   BUS# X-- NAME --X BASKV AREA
CKT   MW    MVAR   RATIO   ANGLE   AMPS  %I  SET A

 54032 FEDA3      300.00   57 0.0000  156.6     0.0      0.0     0.0 ----------------------------------------------------------------------------------------
                  510 0.0011           0.0      0.0     0.0  54022 KR.SAND3    300.00   56  1     0.0    0.0              3604 180  2000A
                                                                  54042 LISTA3      300.00   57  1     0.0    0.0               0   0   500A
                                                                  54042 LISTA3      300.00   57  2     0.0    0.0               0   0   500A
                                                                  54052 ANA-SIR3    300.00   57  1     0.0    0.0            1811 145  1250A
                                                                  54102 TONSTAD3    300.00   57  1     0.0    0.0            3378 186  1815A
                                                                  54102 TONSTAD3    300.00   57  2     0.0    0.0            4474 224  2000A
                                                                  54592 OIE         300.00   57  1     0.0    0.0             585  59  1000A
                                                                       F A U L T   M V A          2839.2 6558.3              13753
```

Case 2

```
                    PTI INTERACTIVE POWER SYSTEM SIMULATOR--PSS/E      TUE, JUN 03 2008  10:25
                        STATNETTS DRIFTDATASETT FOR NORGE


 X------- FROM BUS ------X AREA  VOLT          GEN    LOAD    SHUNT  X---------- TO BUS ----------X                TRANSFORMER
RATING
   BUS# X-- NAME --X BASKV ZONE  PU/KV  ANGLE  MW/MVAR MW/MVAR MW/MVAR   BUS# X-- NAME --X BASKV AREA
CKT   MW    MVAR   RATIO   ANGLE   AMPS  %I  SET A

 54032 FEDA3      300.00   57 0.0000  160.2     0.0      0.0     0.0 ----------------------------------------------------------------------------------------
                  510 0.0008           0.0      0.0     0.0  54022 KR.SAND3    300.00   56  1     0.0    0.0              2974 149  2000A
                                                                  54042 LISTA3      300.00   57  1     0.0    0.0               0   0   500A
                                                                  54042 LISTA3      300.00   57  2     0.0    0.0               0   0   500A
                                                                  54052 ANA-SIR3    300.00   57  1     0.0    0.0            1680 134  1250A
                                                                  54102 TONSTAD3    300.00   57  1     0.0    0.0            2106 116  1815A
                                                                  54102 TONSTAD3    300.00   57  2     0.0    0.0            2789 139  2000A
                                                                  54592 OIE         300.00   57  1     0.0    0.0             538  54  1000A
                                                                       F A U L T   M V A          1774.5 4917.5              10061
```

Case 3

PTI INTERACTIVE POWER SYSTEM SIMULATOR--PSS/E TUE, JUN 03 2008 10:28
STATNETTS DRIFTDATASETT FOR NORGE

X------- FROM BUS ------X AREA VOLT GEN LOAD SHUNT X---------- TO BUS ----------X TRANSFORMER RATING
BUS# X-- NAME --X BASKV ZONE PU/KV ANGLE MW/MVAR MW/MVAR MW/MVAR BUS# X-- NAME --X BASKV AREA CKT MW MVAR RATIO ANGLE AMPS %I SET A

54032 FEDA3 300.00 57 0.0000 166.9 0.0 0.0 0.0 ----------
510 0.0010 0.0 0.0 0.0 54022 KR.SAND3 300.00 56 1 0.0 0.0 3379 169 2000A
54042 LISTA3 300.00 57 1 0.0 0.0 0 0 500A
54042 LISTA3 300.00 57 2 0.0 0.0 0 0 500A
54052 ANA-SIR3 300.00 57 1 0.0 0.0 1746 140 1250A
54102 TONSTAD3 300.00 57 1 0.0 0.0 3276 180 1815A
54102 TONSTAD3 300.00 57 2 0.0 0.0 4338 217 2000A
54592 OIE 300.00 57 1 0.0 0.0 580 58 1000A
F A U L T M V A 1560.3 6721.4 13279

Case 4

PTI INTERACTIVE POWER SYSTEM SIMULATOR--PSS/E TUE, JUN 03 2008 10:30
STATNETTS DRIFTDATASETT FOR NORGE

X------- FROM BUS ------X AREA VOLT GEN LOAD SHUNT X---------- TO BUS ----------X TRANSFORMER RATING
BUS# X-- NAME --X BASKV ZONE PU/KV ANGLE MW/MVAR MW/MVAR MW/MVAR BUS# X-- NAME --X BASKV AREA CKT MW MVAR RATIO ANGLE AMPS %I SET A

55232 KÅRSTØ 300.00 61 0.0000 152.6 0.0 0.0 0.0 ----------
512 0.0006 0.0 0.0 0.0 50070 IND-KARS 20.000 61 1 0.0 0.0 0.935RG 65 87 39M
50070 IND-KARS 20.000 61 2 0.0 0.0 0.935RG 67 89 39M
50070 IND-KARS 20.000 61 3 0.0 0.0 0.945RG 65 74 46M
50070 IND-KARS 20.000 61 4 0.0 0.0 0.947RG 65 74 46M
55102 SAUDA3 300.00 61 1 0.0 0.0 3554 239 1490A
55152 HAAVIK3 300.00 61 1 0.0 0.0 3890 214 1815A
55233 KÅRSTØ 130.00 61 1 0.0 0.0 0.985RG 0 0 172M
F A U L T M V A 1832.1 3539.8 7671

Case 5

PTI INTERACTIVE POWER SYSTEM SIMULATOR--PSS/E TUE, JUN 03 2008 10:32
STATNETTS DRIFTDATASETT FOR NORGE

X------- FROM BUS ------X AREA VOLT GEN LOAD SHUNT X---------- TO BUS ----------X TRANSFORMER RATING
BUS# X-- NAME --X BASKV ZONE PU/KV ANGLE MW/MVAR MW/MVAR MW/MVAR BUS# X-- NAME --X BASKV AREA CKT MW MVAR RATIO ANGLE AMPS %I SET A

55232 KÅRSTØ 300.00 61 0.0000 111.9 0.0 0.0 0.0 ----------
512 0.0005 0.0 0.0 0.0 50070 IND-KARS 20.000 61 1 0.0 0.0 0.815RG 70 93 39M
50070 IND-KARS 20.000 61 2 0.0 0.0 0.815RG 71 95 39M
50070 IND-KARS 20.000 61 3 0.0 0.0 0.827RG 69 79 46M
50070 IND-KARS 20.000 61 4 0.0 0.0 0.909LO 63 72 46M
55102 SAUDA3 300.00 61 1 0.0 0.0 3190 214 1490A
55152 HAAVIK3 300.00 61 1 0.0 0.0 3445 190 1815A
55233 KÅRSTØ 130.00 61 1 0.0 0.0 0.876RG 0 0 172M
F A U L T M V A 3300.4 1323.7 6844

Appendix C: Establishing of load flow cases

Case 2

Connection point of offshore wind power: Feda (54032)

The production and load consumption in the system is scaled down. The load is not scaled down at busbars starting with KKI- or IND-. These busbars represent industrial loads. The load is scaled down with a constant P/Q ratio. Generators are disconnected from the system.

Because of difficulties of doing drastic changes throughout the entire system, only the areas 55, 56, 57, 60 and 61 are chosen for the scaling. The result is not a realistic situation, but the areas surrounding the connection point of the offshore wind power have a low load with generators disconnected. Generators are given by the busbar number of the generator. The short circuit power at the connection point will be reduced as a consequence of the disconnection of generators.

- Load is scaled down: -500 MW
- Generators are disconnected: 51204, 51356, 51507, 54106 - 54108
- Load is scaled down: -500 MW
- Generators are disconnected: 54109, 54116, 54117
- Load is scaled down: -500 MW
- Generators are disconnected: 54126, 54146, 54147, 54156 (id 1 and 2)
- Load is scaled down: -500 MW
- Generators are disconnected: 54186, 54246, 54326 - 54329
- Load is scaled down: -500 MW
- Generators are disconnected: 54406, 54585, 54619, 55026 - 55029
- Load is scaled down: -500 MW
- Load is scaled down: -500 MW
- Generators are disconnected: 55056 - 55058
- Generator is disconnected: 55146
- Load is scaled down: -100 MW

The offshore wind power equals 1000 MW.
No import or export of HVDC.
Export of 900 MW to Sweden through Hasle (51031)

Case 3

Connection point of offshore wind power: Feda (54032)

The production in the system is scaled down. The load consumption in the system is at its maximum. No generators are disconnected.

- Production in all areas is scaled down: -500 MW
- Value of load at Kristiansand (55032): -500 + j 250 MVA
- Production in all areas is scaled down: -100 MW
- New value at (53206 - 53207): 200 MW each
- New value at (53208 - 53209): 200 MW each
- New value at (54109): 150 MW
- New value at (53156 - 53158): 50 MW each
- New value at (56146): 50 MW
- New value at (55146): 50 MW
- New value at (55056 - 55058): 150 MW each
- New value of load at Kristiansand (55032): -1000 + j 500 MVA

The offshore wind power equals 1000 MW.
1000 MW of HVDC from Denmark.
No export of power to Sweden.

Case 5

Connection point of offshore wind power: Kårstø (55232)

The generation in the surrounding area of the connection point is reduced by disconnection generators. Generators are given by the busbar number of the generator. The load is not scaled down.

- Generators are disconnected: 55026 - 55029 (Saurdal)
- Generators are disconnected: 55076 - 55077 (Hylen)
- Generators are disconnected: 55104 (id 1 - 4) (Sauda)
- Generators are disconnected: 55194 (id 1 - 4) (Blåfall)
- Generators are disconnected: 55206 - 55207 (Mauranger)
- Generators are disconnected: 55226 - 55227 (Blåfall)
- Generators is disconnected: 55376 (Stord)

The offshore wind power equal 1000 MW.
No import or export of HVDC.
No export of power to Sweden.

Appendix D: Dynamic simulation results

Summary of load flow cases and events:

	Point of connection	Production	Load	Import HVDC	Export Sweden	Offshore wind
				[MW]	[MW]	[MW]
Case 1	Feda	Original	Original	0	900	1000
Case 2	Feda	Reduced	Reduced	0	900	1000
Case 3	Feda	Reduced	Original	1000	0	1000
Case 4	Kårstø	Original	Original	0	900	1000
Case 5	Kårstø	Reduced	Original	0	0	1000

Summary of disturbances for dynamic simulations:

Event 1	Bus fault at neighbour busbar, -2E+004 MVAR (150 ms)
Event 2	Line fault close to neighbour busbar (100 ms), followed by tripping of the line
Event 3	Perfect three-phase short-circuit at connection busbar (150 ms)

System frequency: 50 Hz
System base: 1000 MVA

Case 1, AC cable

Event 1, bus fault at Øie

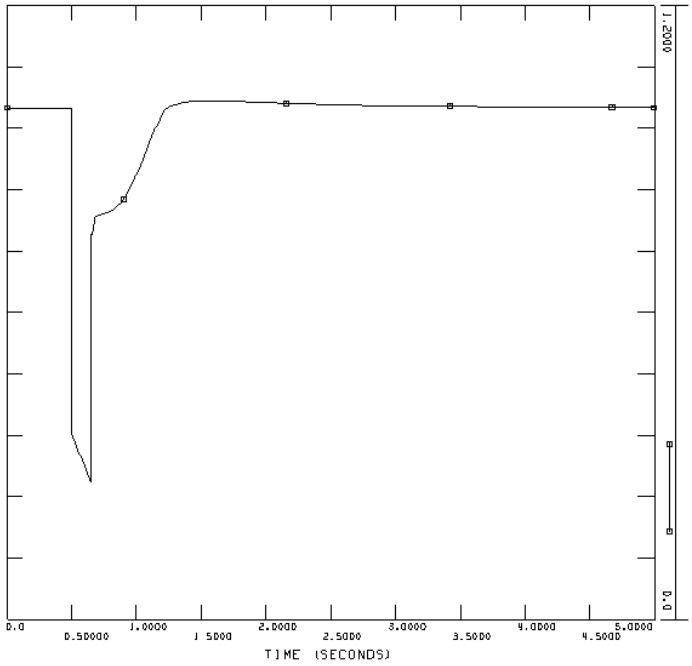

Voltage at Feda [pu]

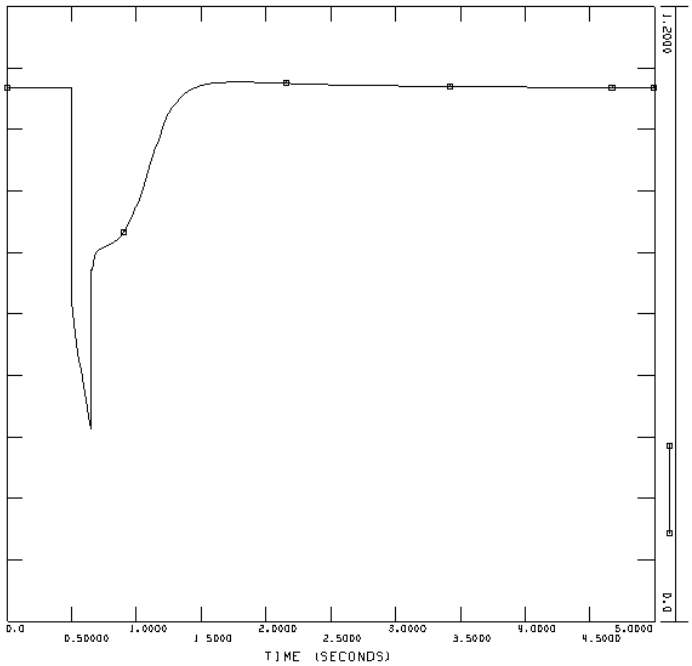

Voltage offshore [pu]

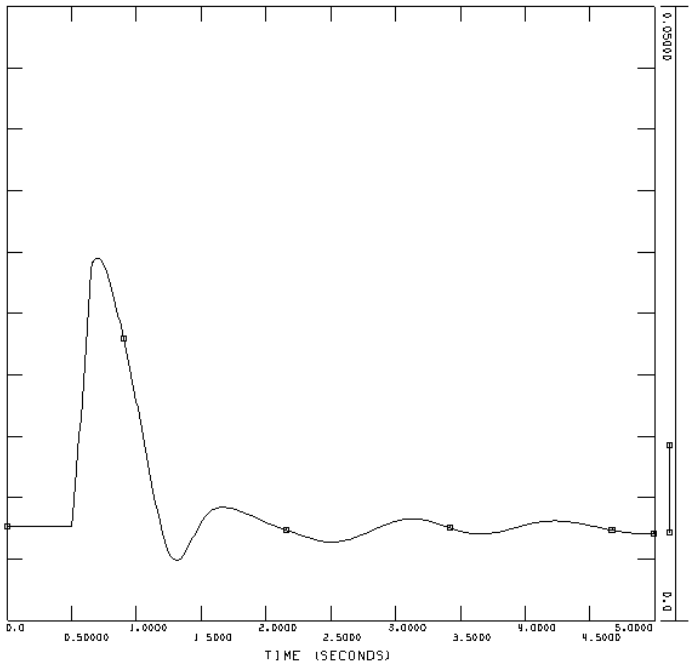

Speed deviation of wind turbine generators [pu]

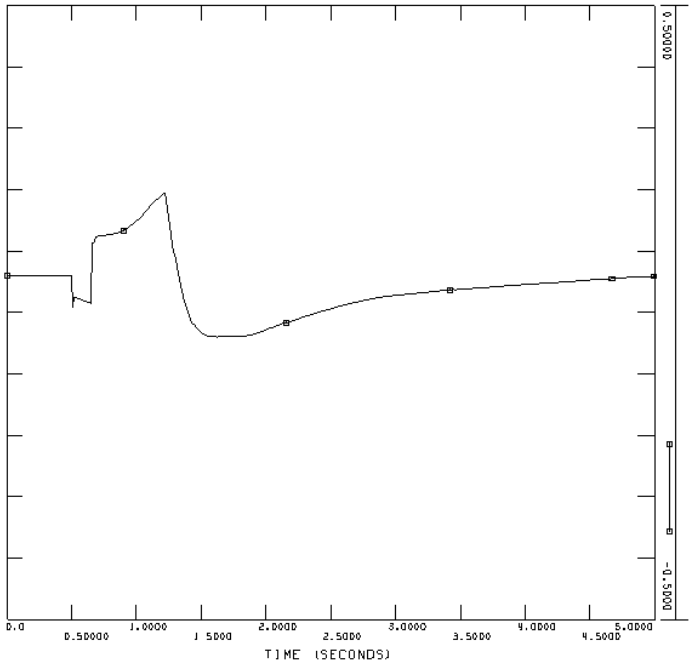

Reactive power from one SVC [pu on system base]

Event 2, line fault and tripping of line

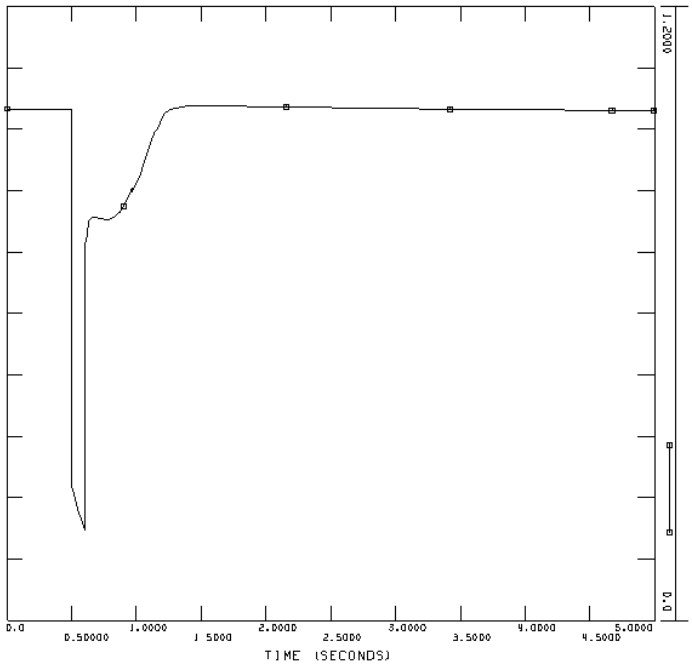

Voltage at Feda [pu]

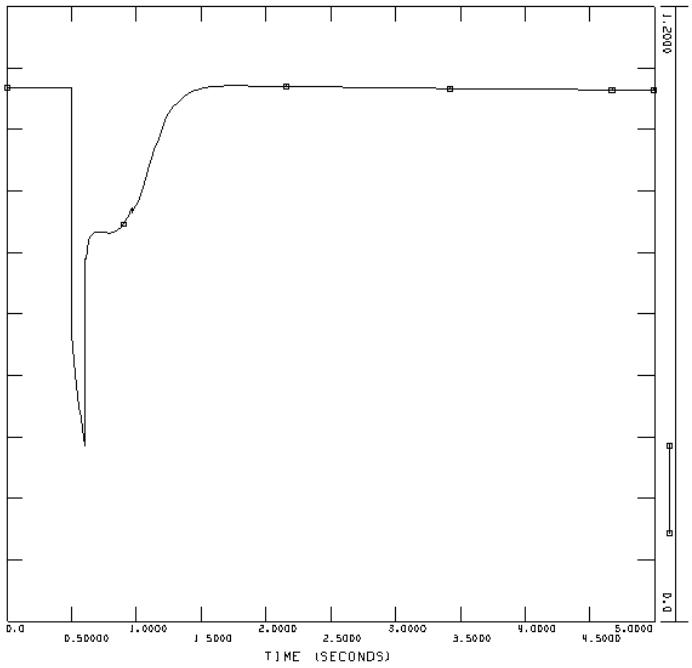

Voltage offshore [pu]

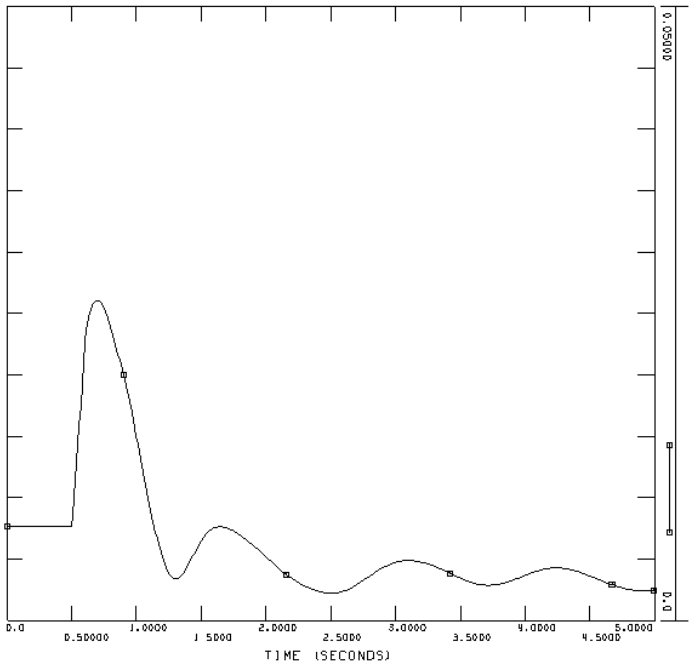

Speed deviation of wind turbine generators [pu]

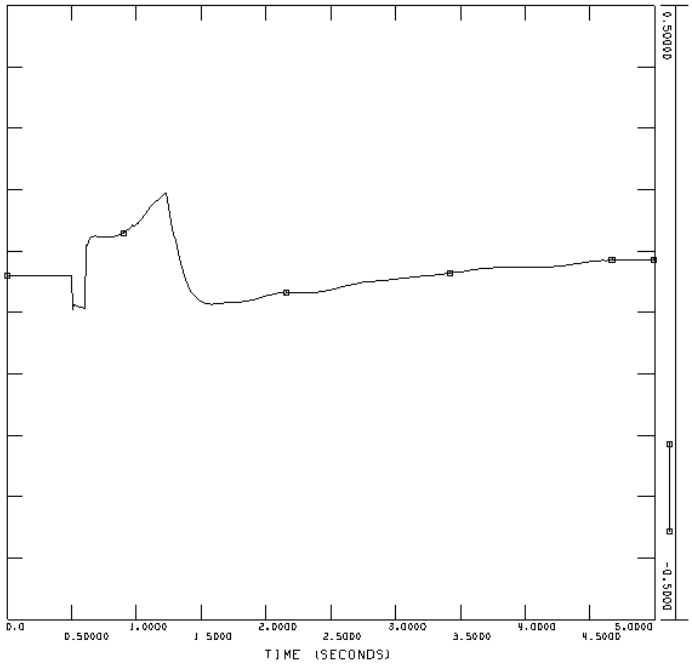

Reactive power from one SVC [pu on system base]

Event 3, three-phase short-circuit at Feda

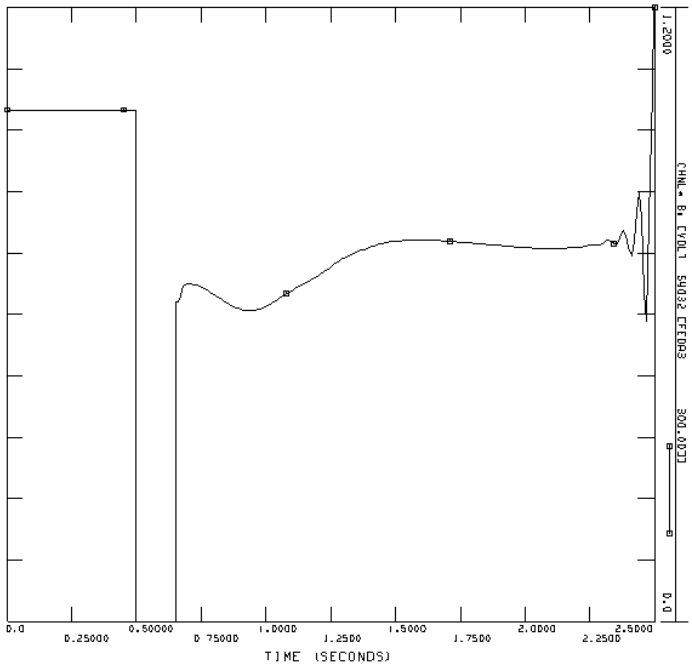

Voltage at Feda [pu]

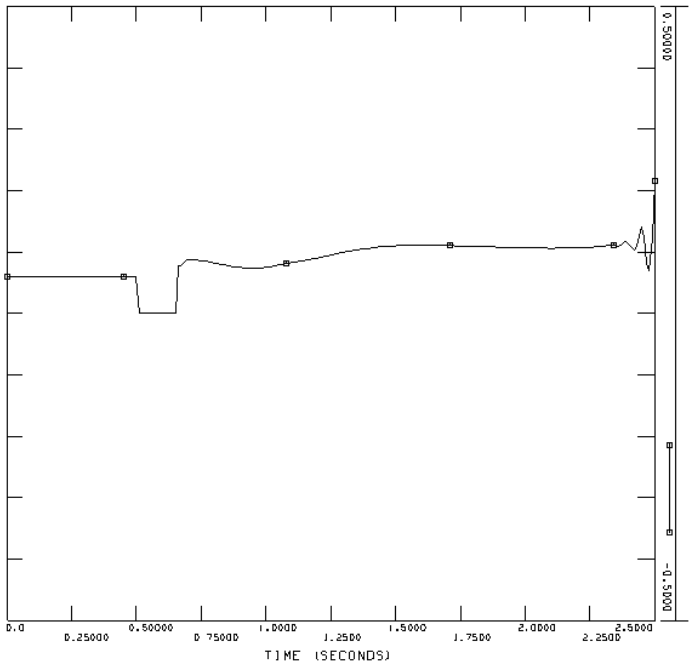

Reactive power from one SVC [pu on system base]

Case 1, HVDC Light

Event 1, bus fault at Øie

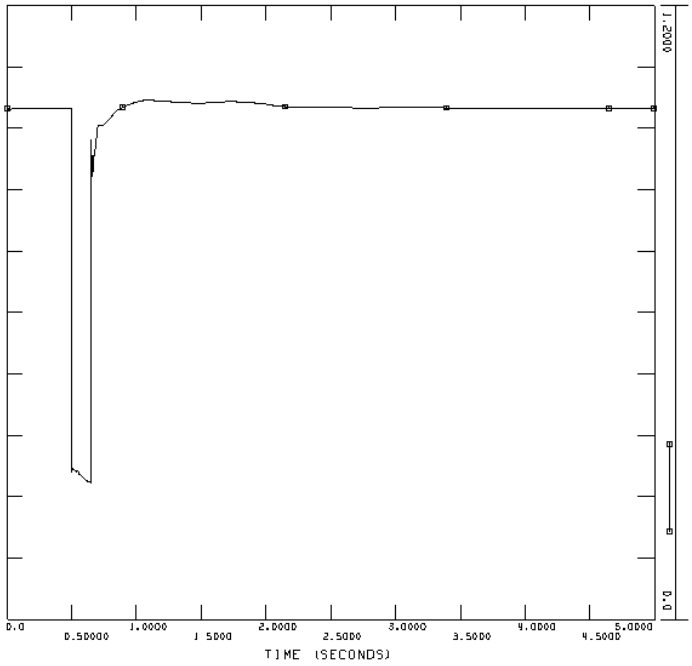

Voltage at Feda [pu]

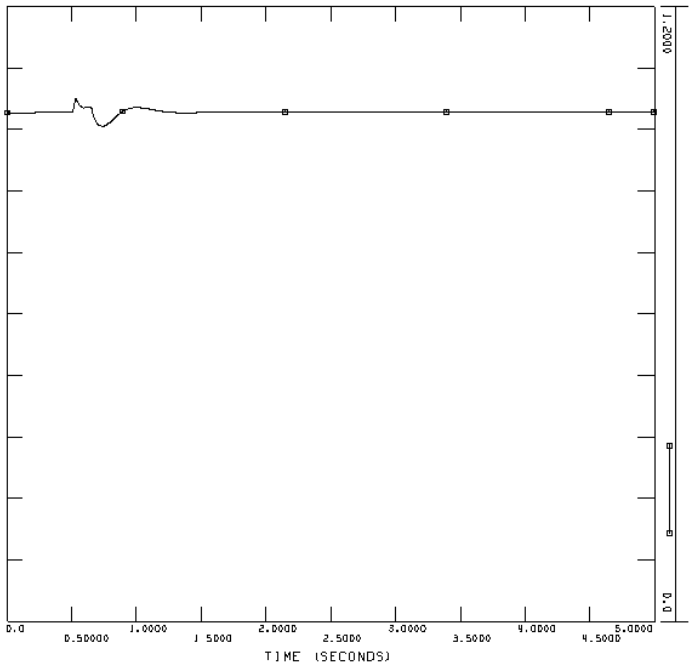

Voltage offshore [pu]

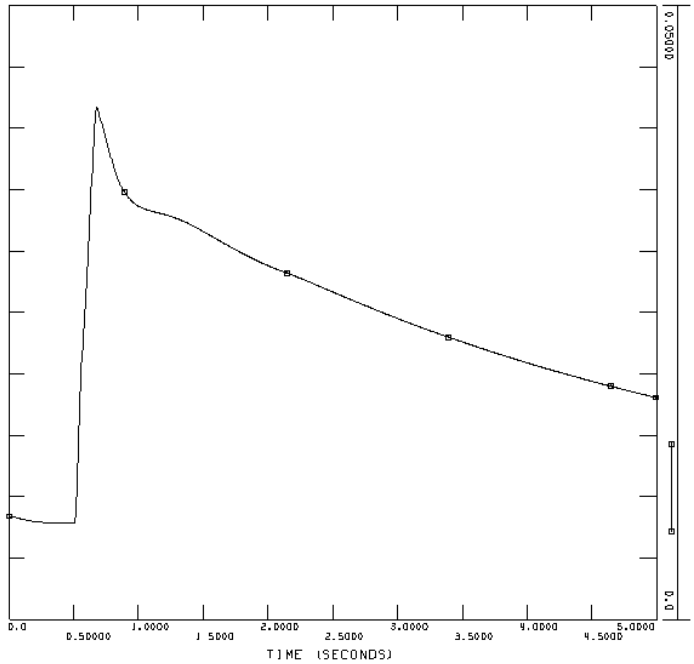

Speed deviation of wind turbine generators [pu]

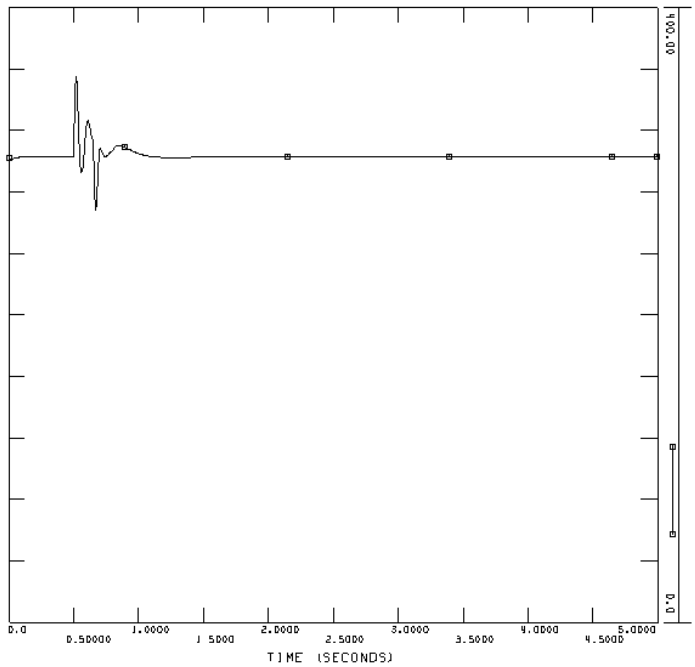

DC voltage at the voltage regulating HVDC Light converter [kV]

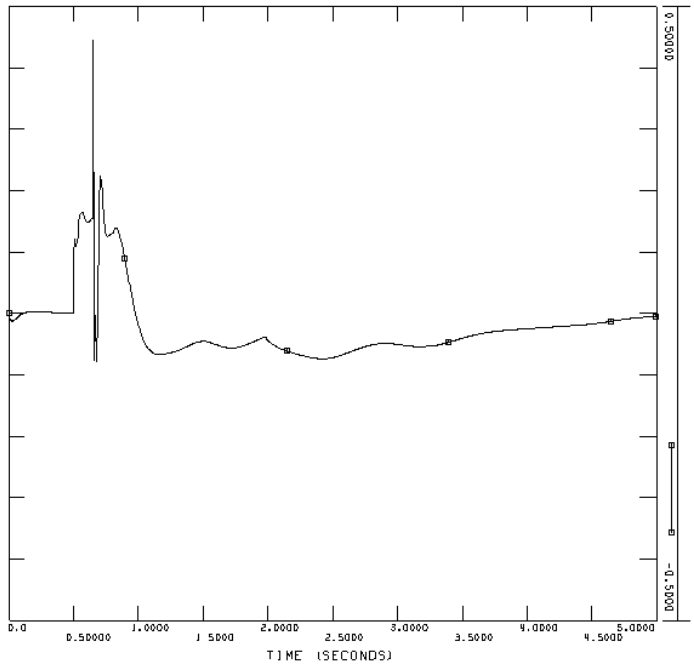

Reactive power from the HVDC Light converter at the connection point [pu on system base]

Event 2, line fault and tripping of line

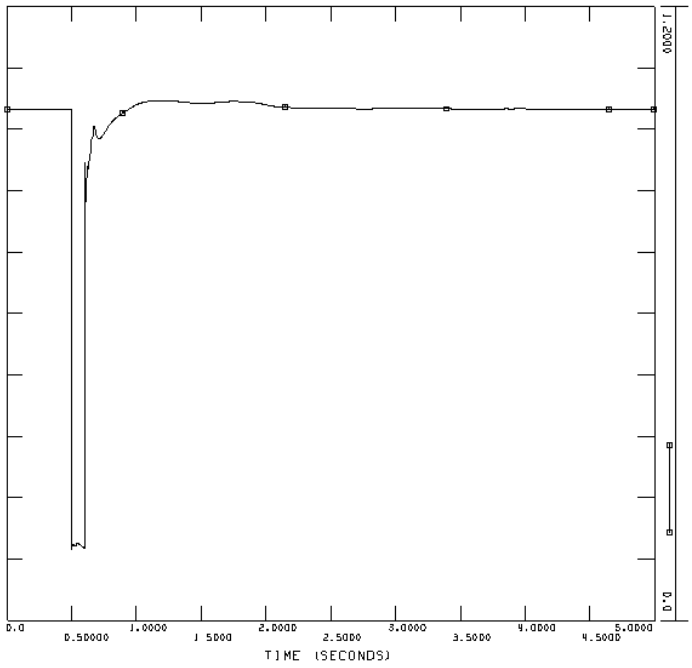

Voltage at Feda [pu]

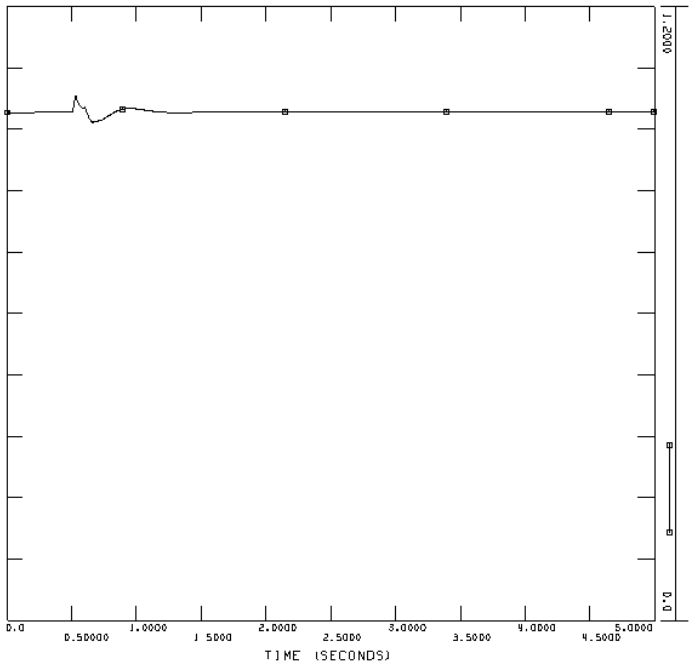

Voltage offshore [pu]

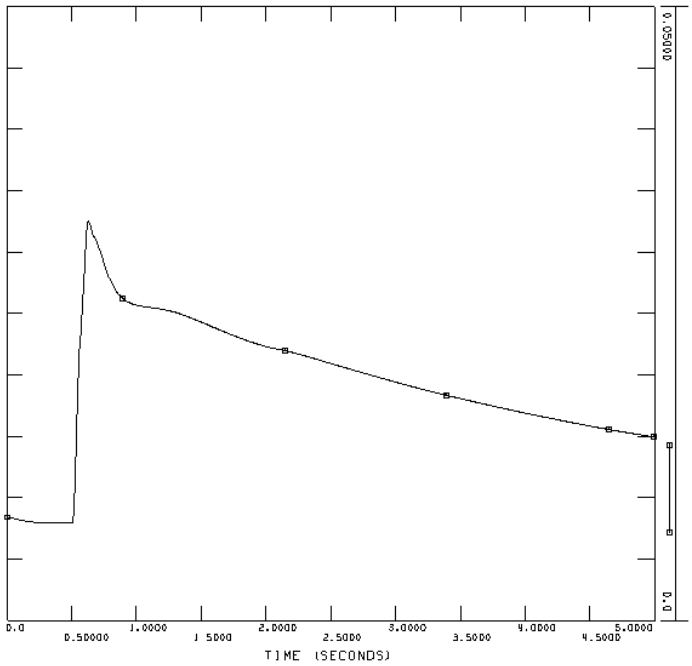

Speed deviation of wind turbine generators [pu]

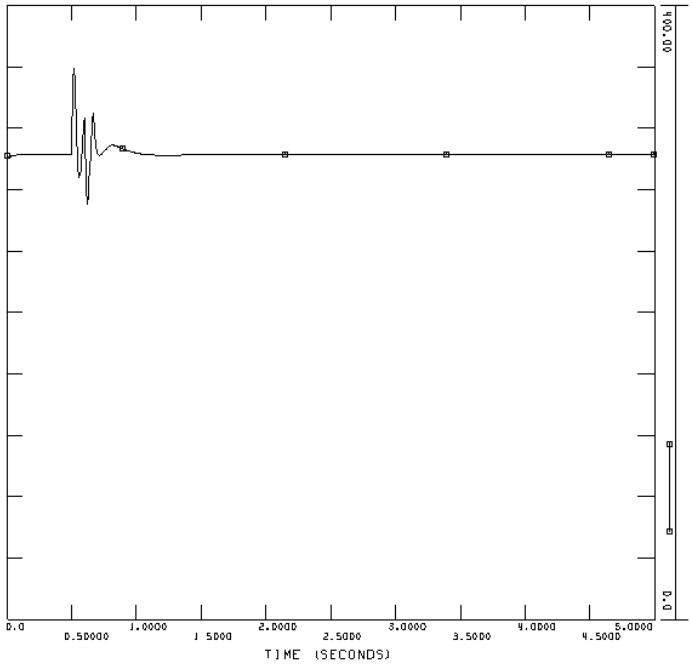

DC voltage at the voltage regulating HVDC Light converter [kV]

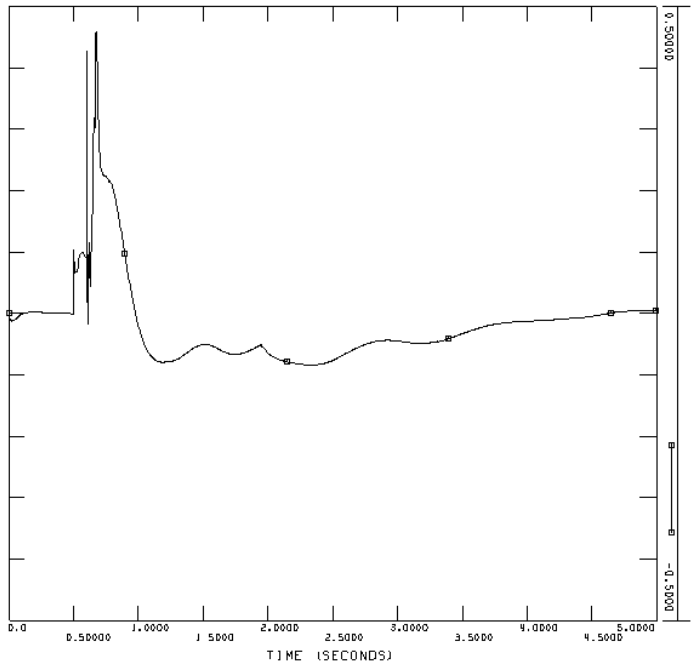

Reactive power from the HVDC Light converter at the connection point [pu on system base]

Event 3, three-phase short-circuit at Feda

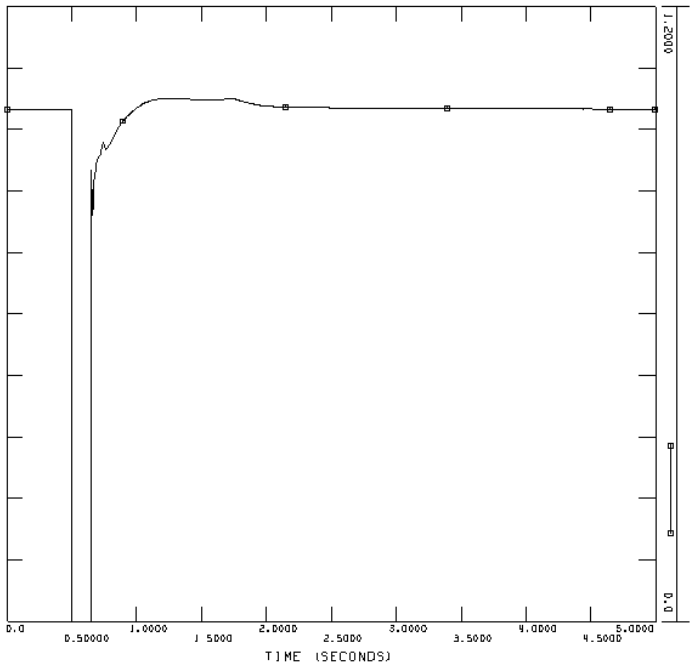

Voltage at Feda [pu]

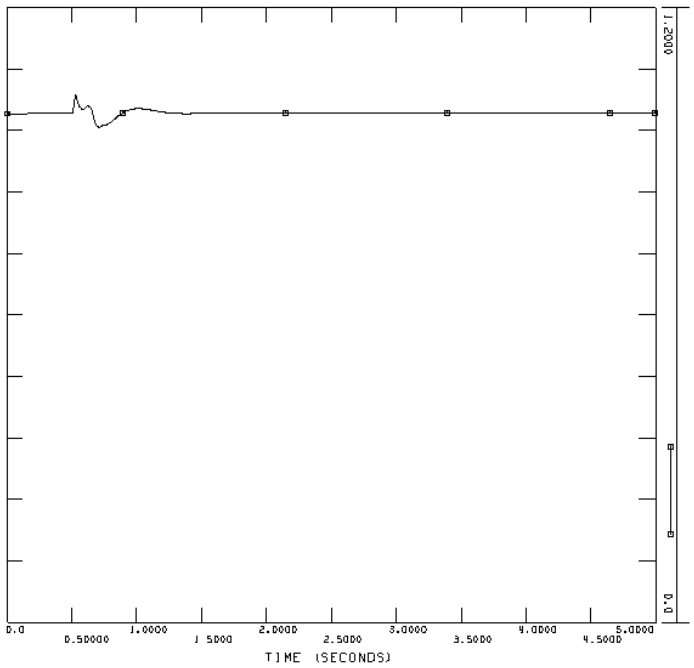

Voltage offshore [pu]

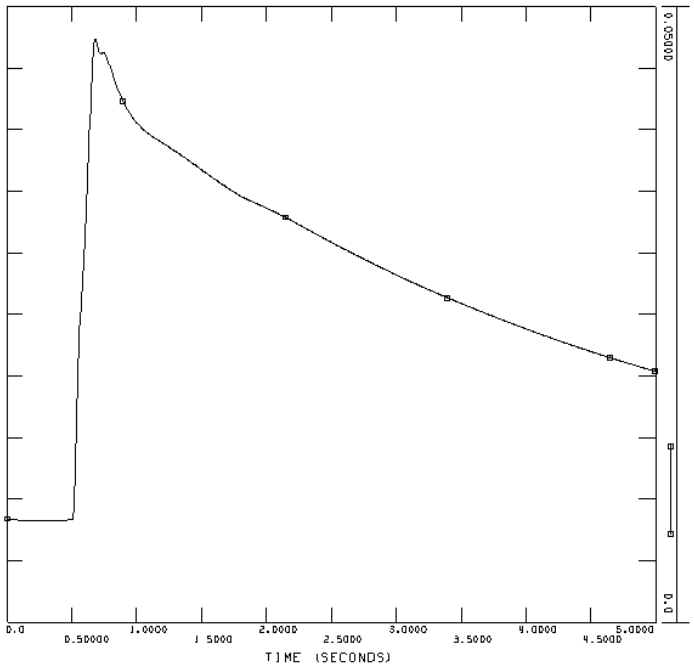

Speed deviation of wind turbine generators [pu]

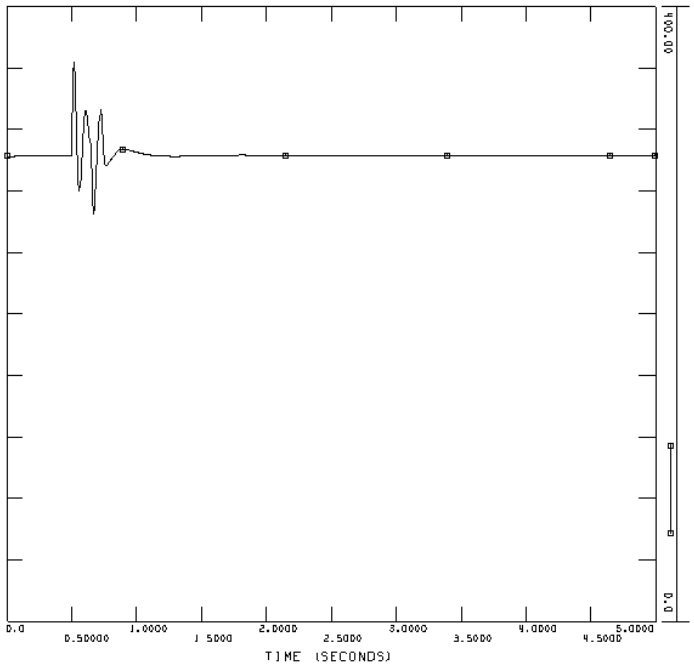

DC voltage at the voltage regulating HVDC Light converter [kV]

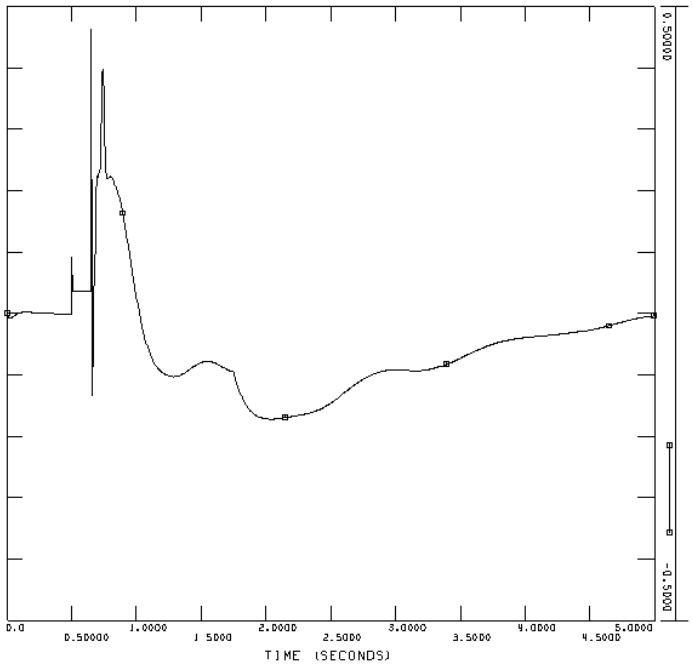

Reactive power from the HVDC Light converter at the connection point [pu on system base]

Case 2, AC cable

Event 1, bus fault at Øie

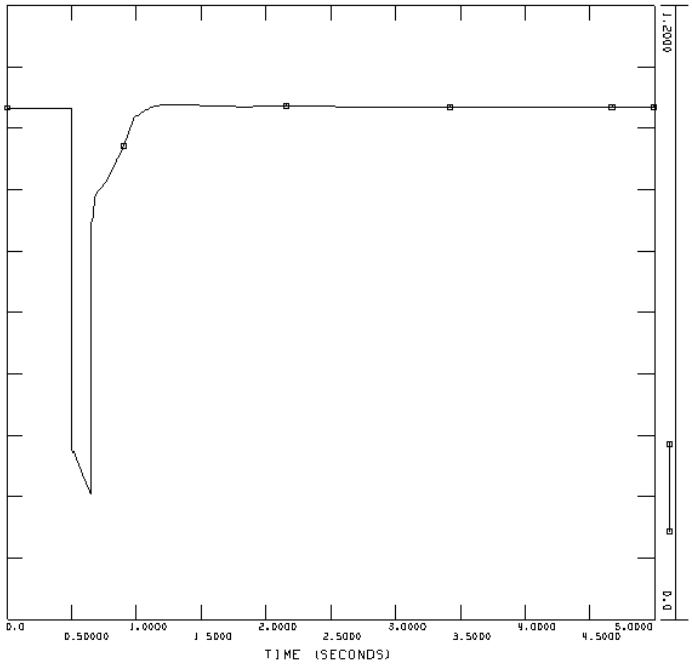

Voltage at Feda [pu]

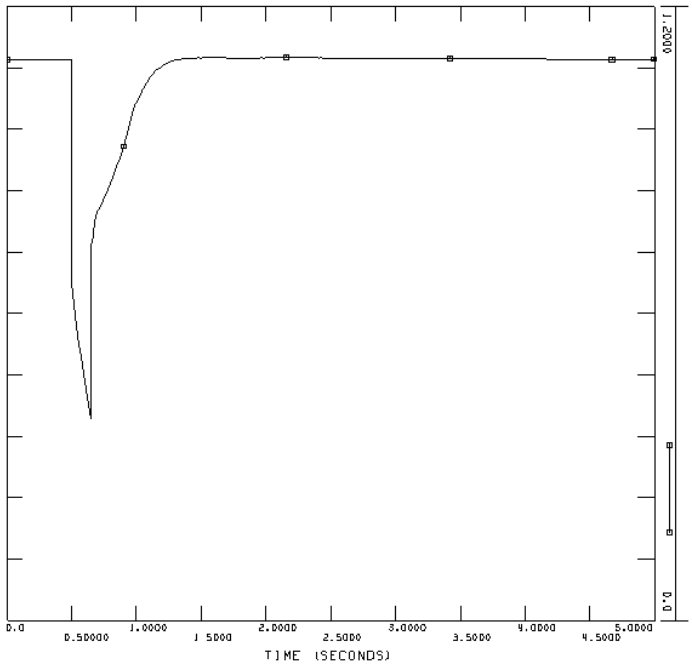

Voltage offshore [pu]

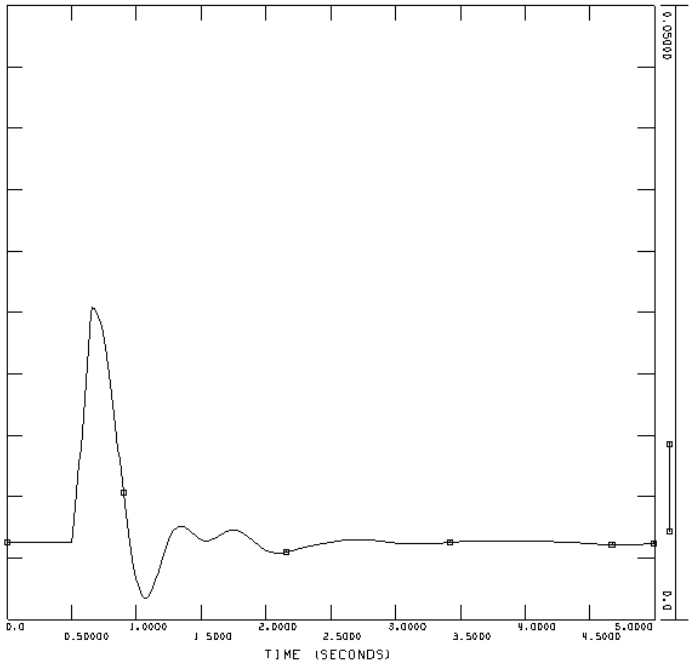

Speed deviation of wind turbine generators [pu]

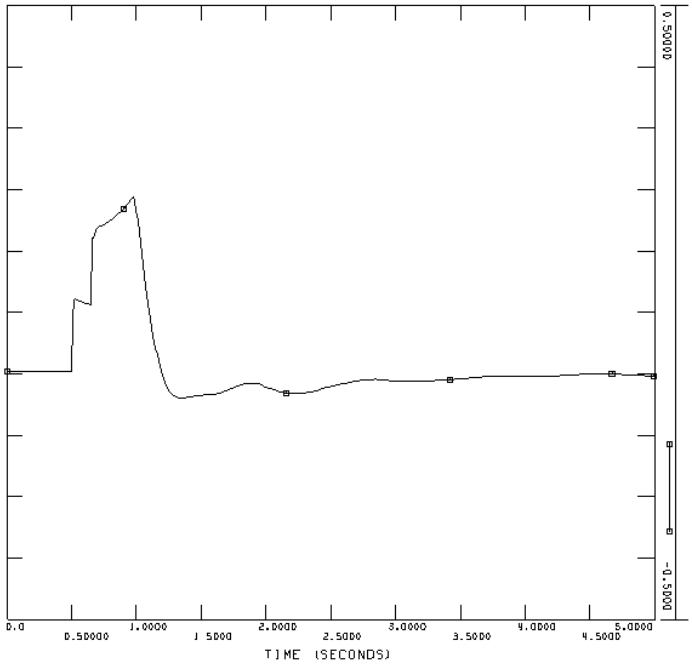

Reactive power from one SVC [pu on system base]

Event 2, line fault and tripping of line

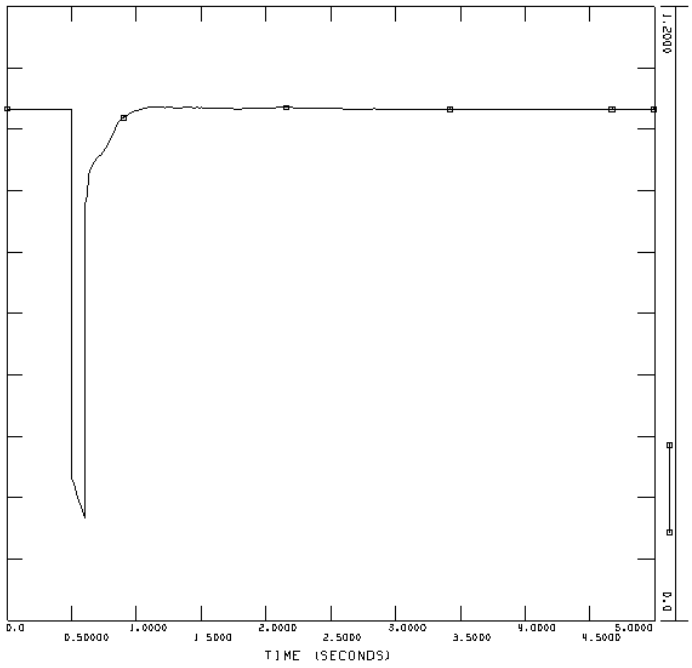

Voltage at Feda [pu]

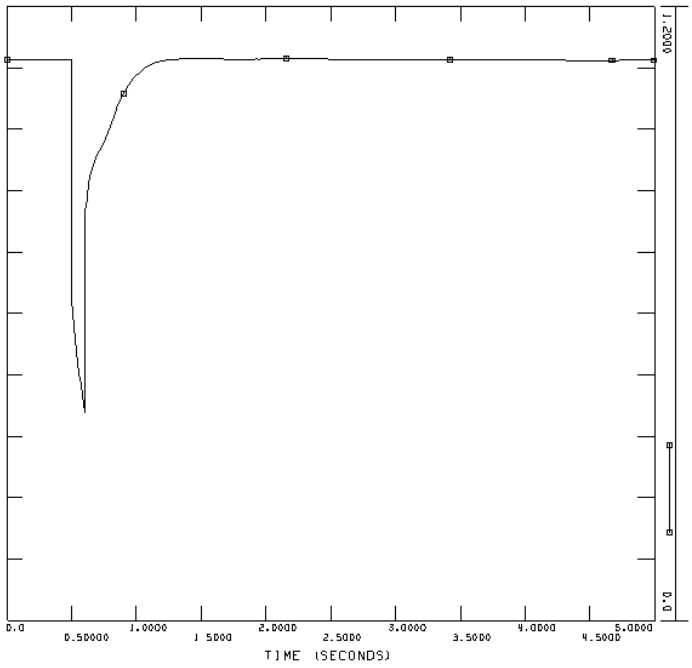

Voltage offshore [pu]

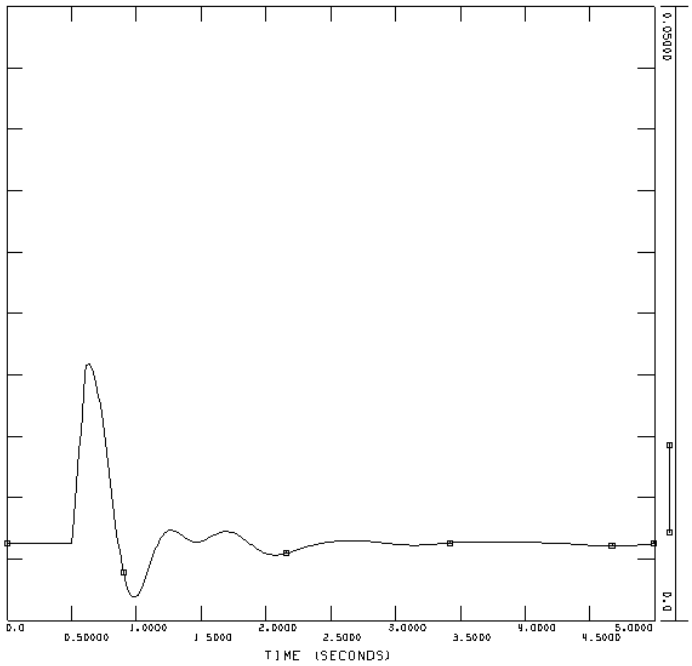

Speed deviation of wind turbine generators [pu]

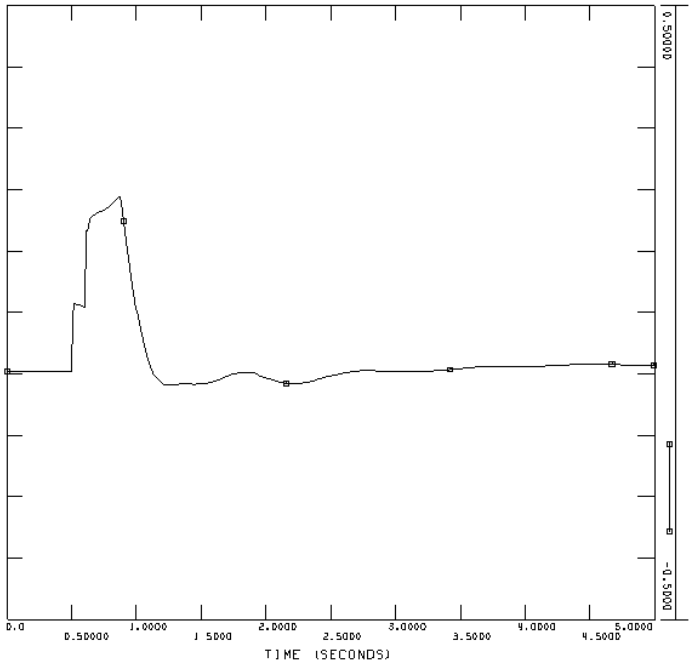

Reactive power from one SVC [pu on system base]

Event 3, three-phase short-circuit at Feda

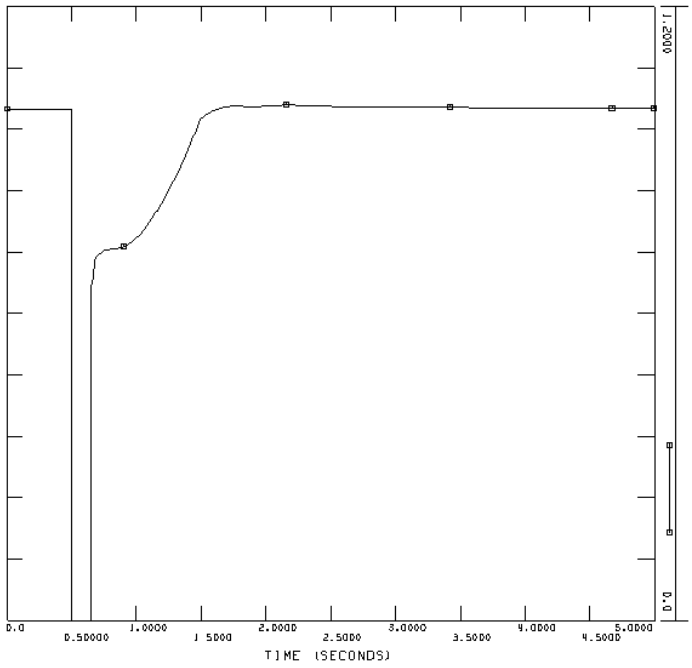

Voltage at Feda [pu]

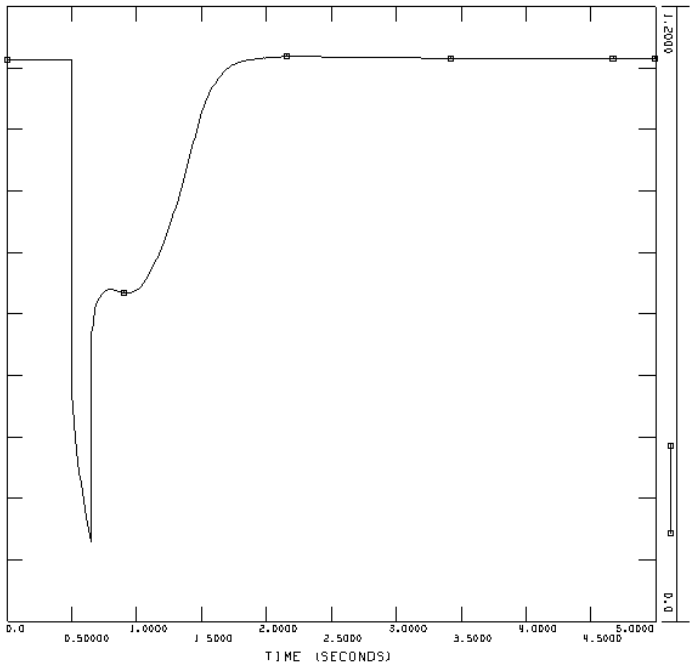

Voltage offshore [pu]

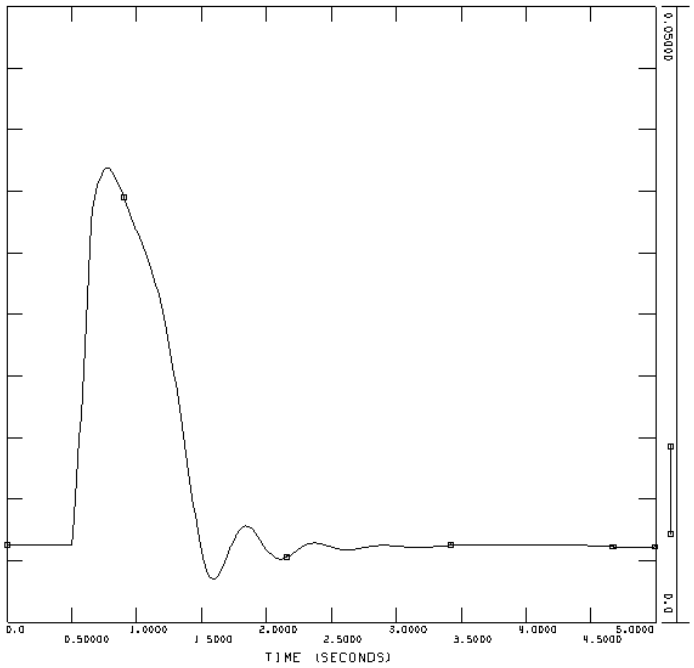

Speed deviation of wind turbine generators [pu]

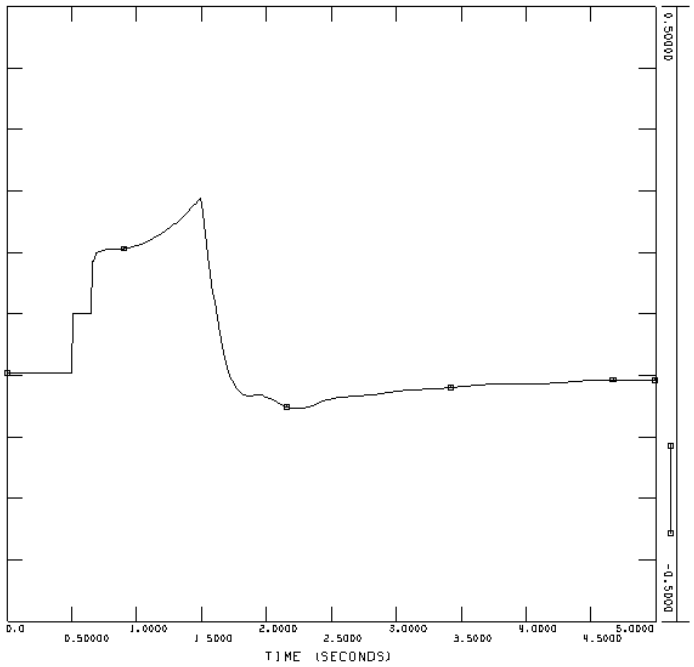

Reactive power from one SVC [pu on system base]

Case 2, HVDC Light

Event 1, bus fault at Øie

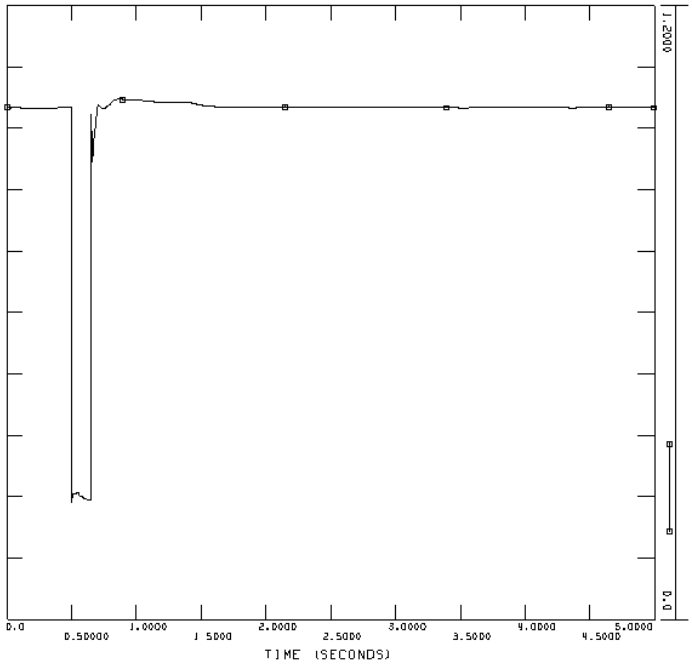

Voltage at Feda [pu]

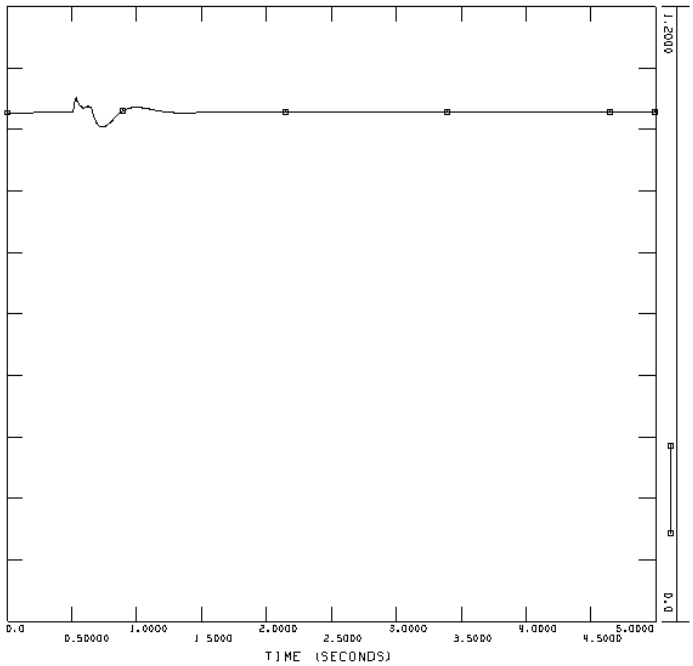

Voltage offshore [pu]

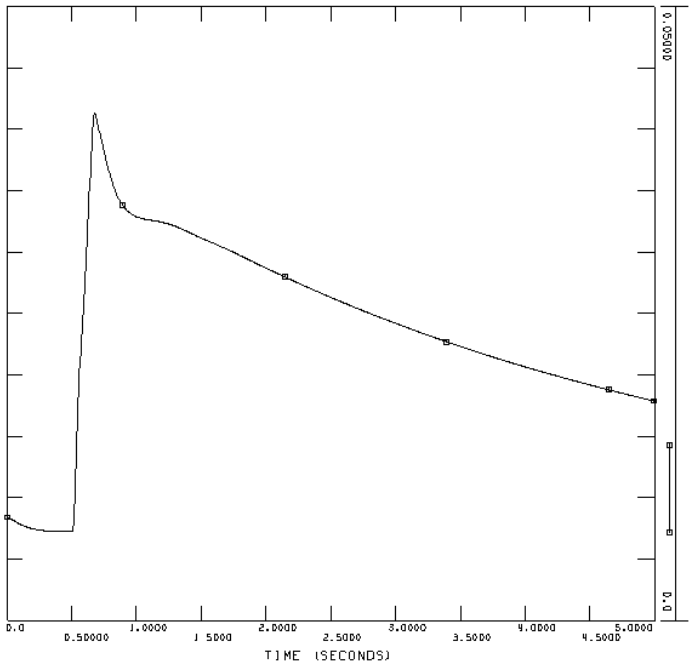

Speed deviation of wind turbine generators [pu]

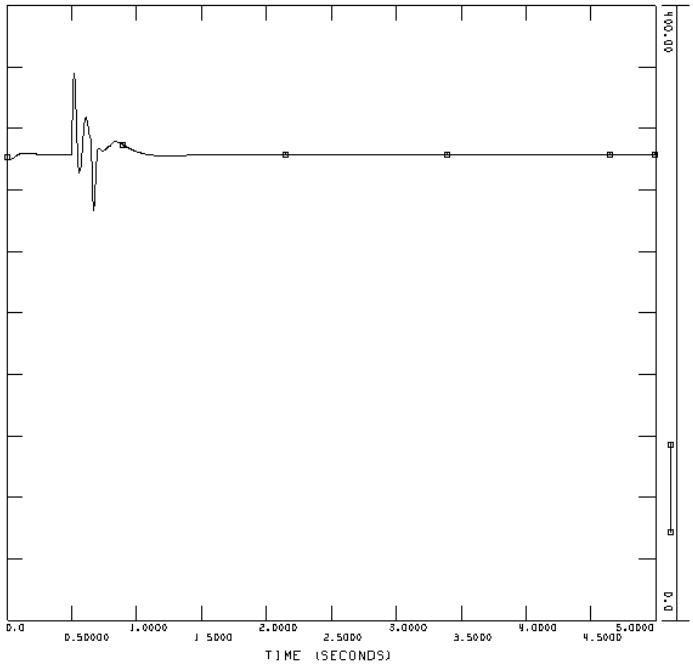

DC voltage at the voltage regulating HVDC Light converter [kV]

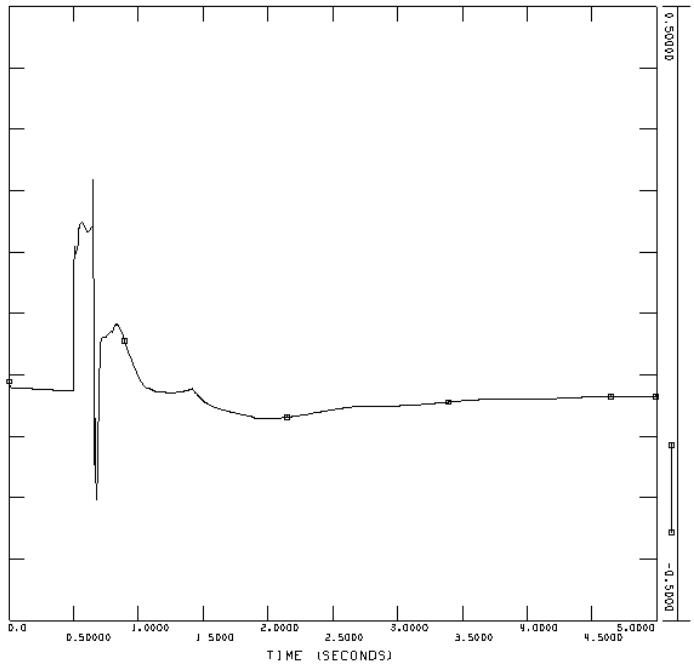

Reactive power from the HVDC Light converter at the connection point [pu on system base]

Event 2, line fault and tripping of line

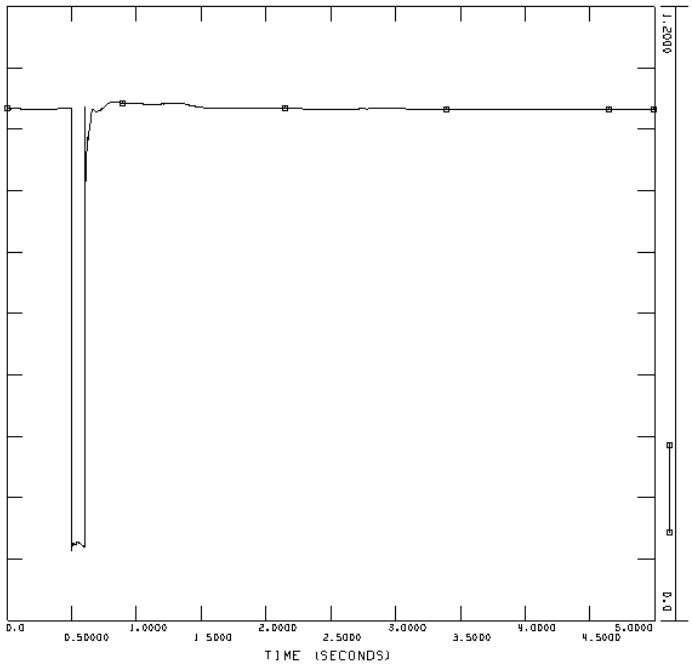

Voltage at Feda [pu]

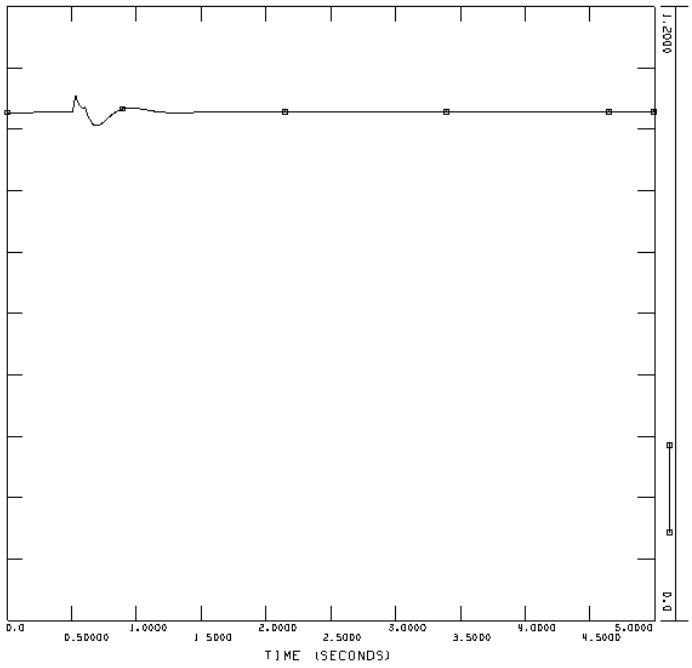

Voltage offshore [pu]

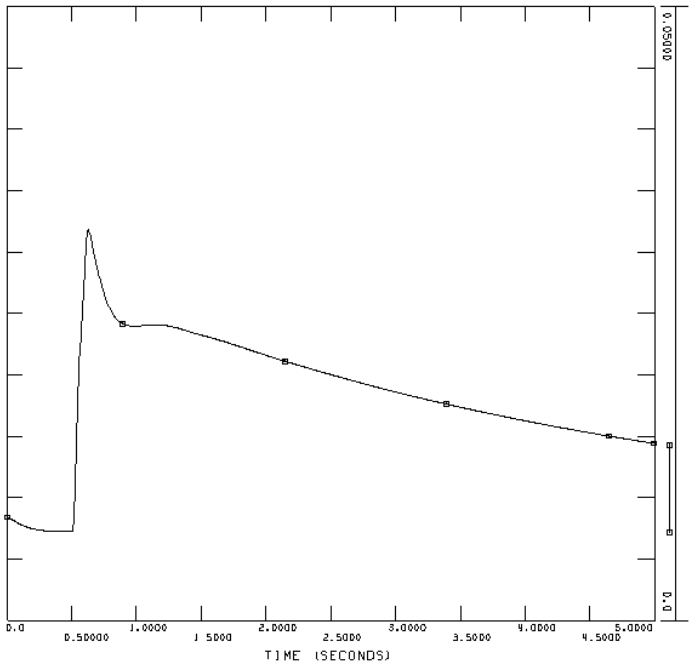

Speed deviation of wind turbine generators [pu]

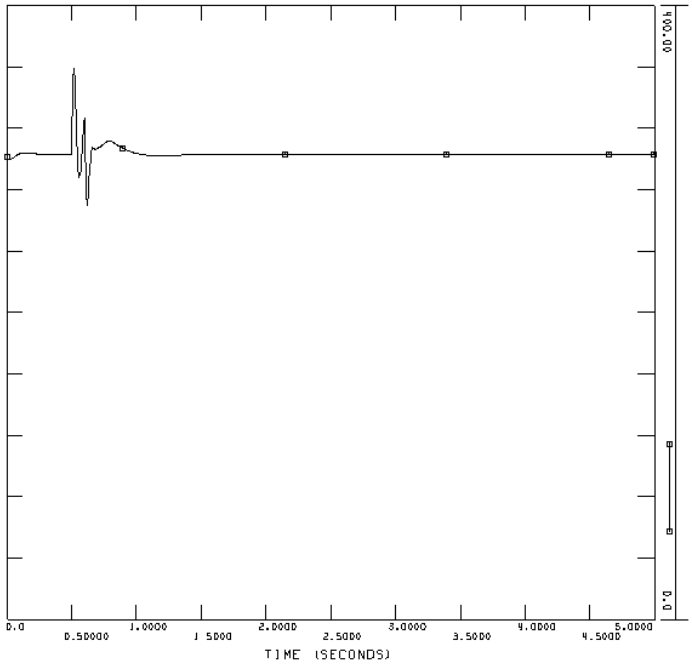

DC voltage at the voltage regulating HVDC Light converter [kV]

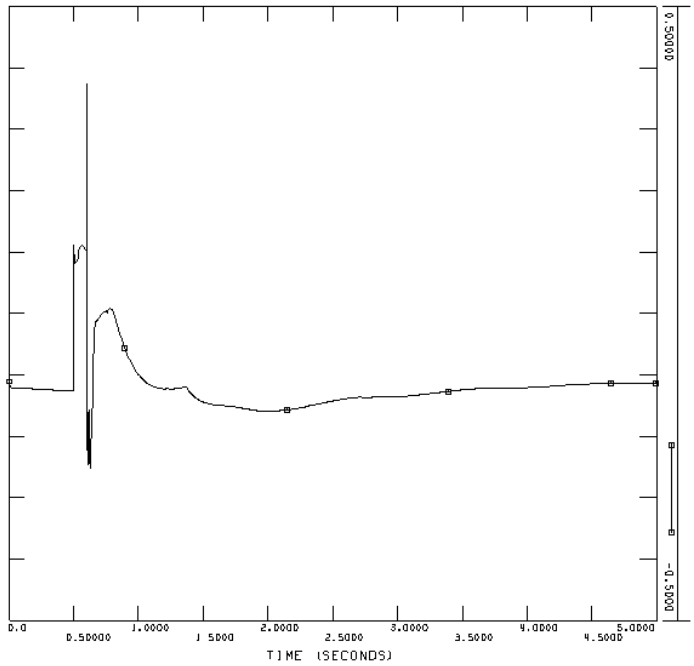

Reactive power from the HVDC Light converter at the connection point [pu on system base]

Event 3, three-phase short-circuit at Feda

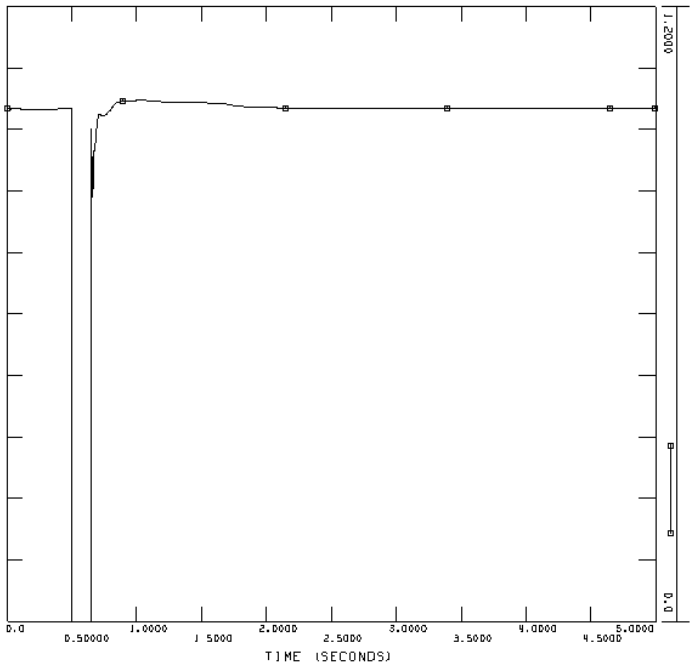

Voltage at Feda [pu]

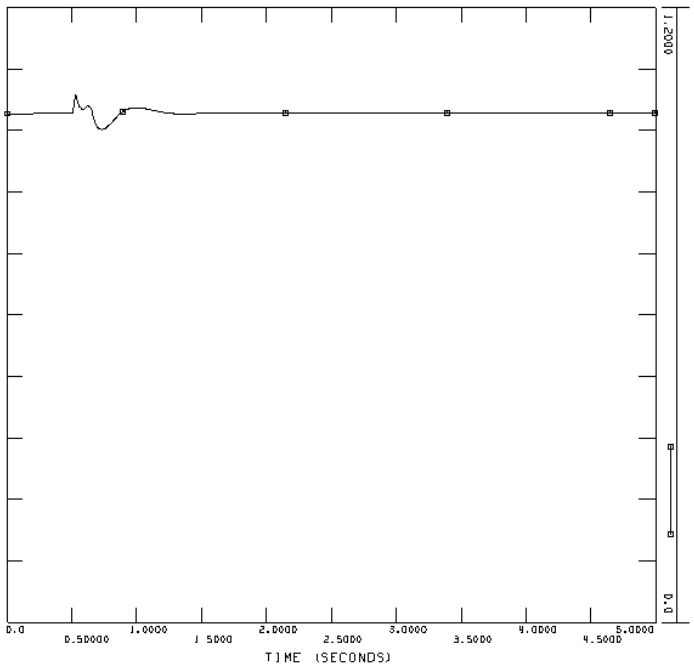

Voltage offshore [pu]

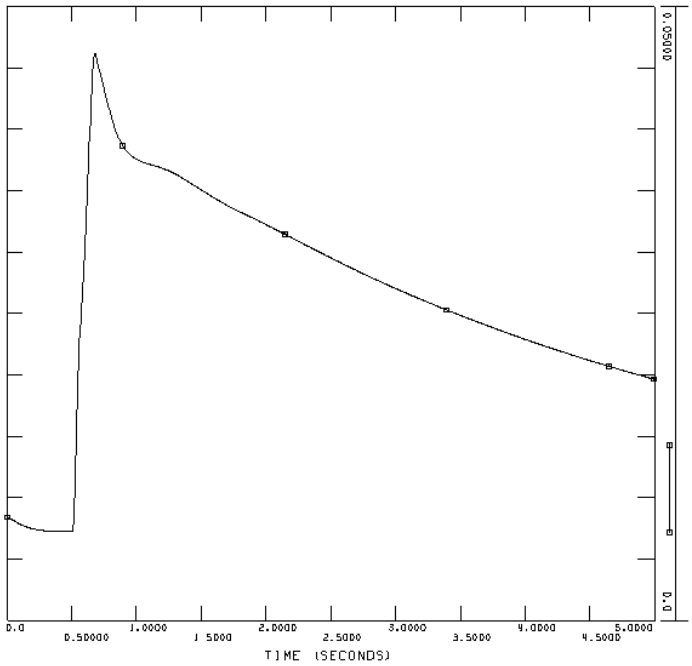

Speed deviation of wind turbine generators [pu]

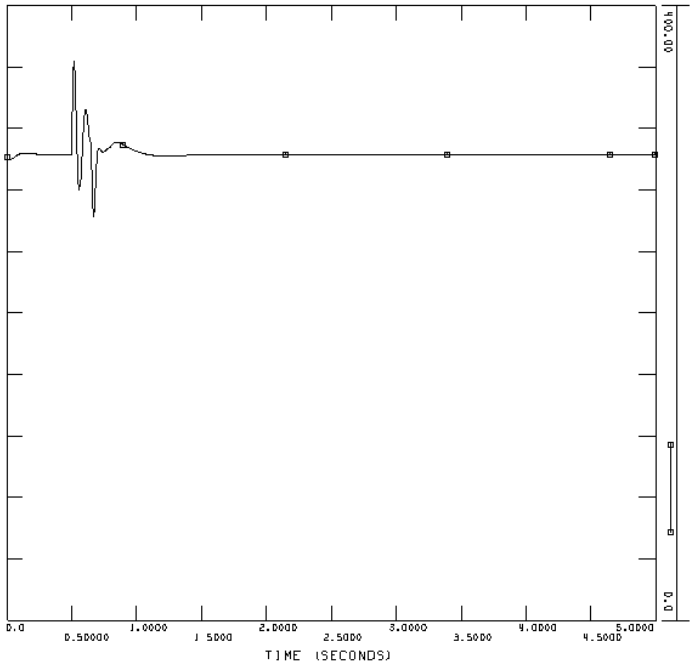

DC voltage at the voltage regulating HVDC Light converter [kV]

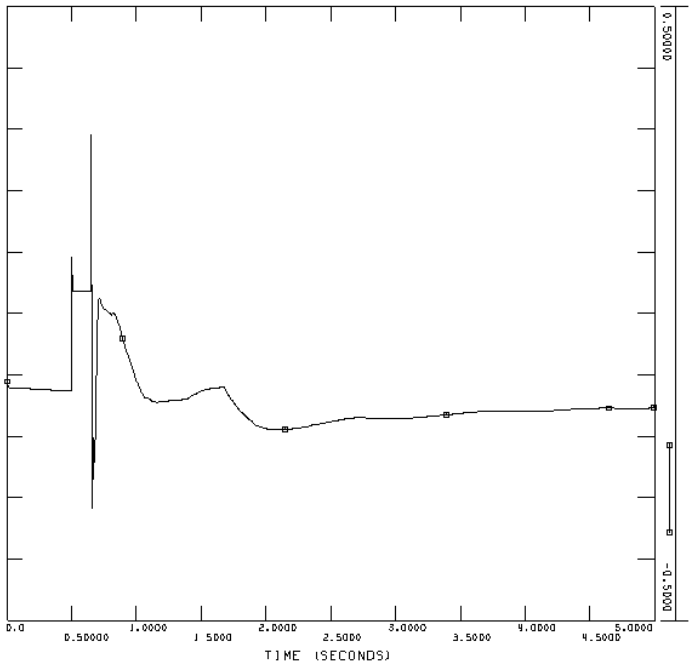

Reactive power from the HVDC Light converter at the connection point [pu on system base]

Case 3, AC cable

Event 1, bus fault at Øie

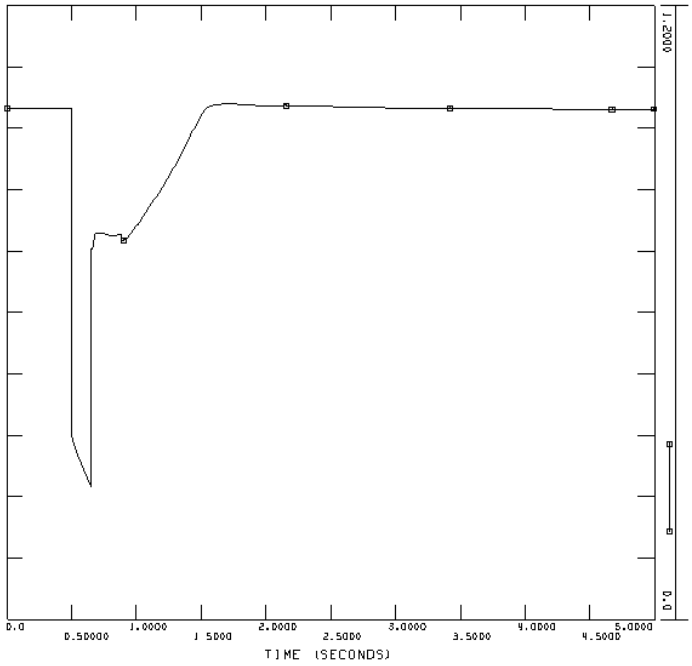

Voltage at Feda [pu]

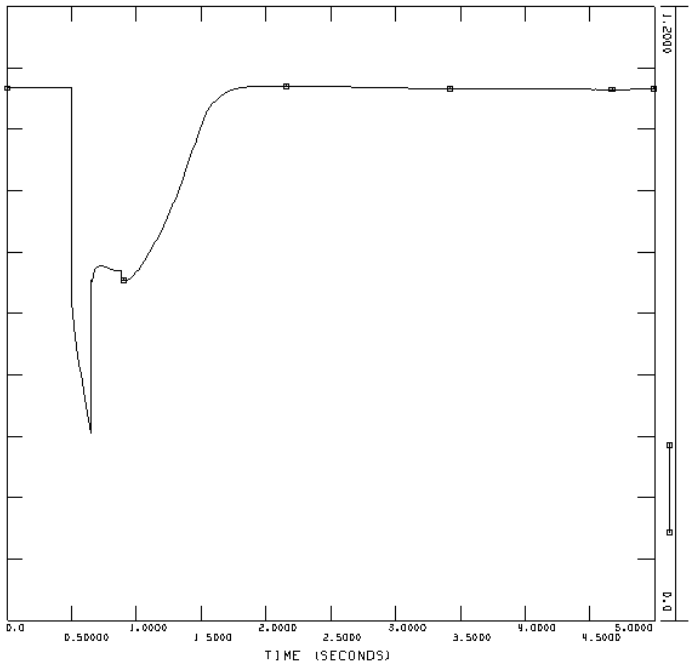

Voltage offshore [pu]

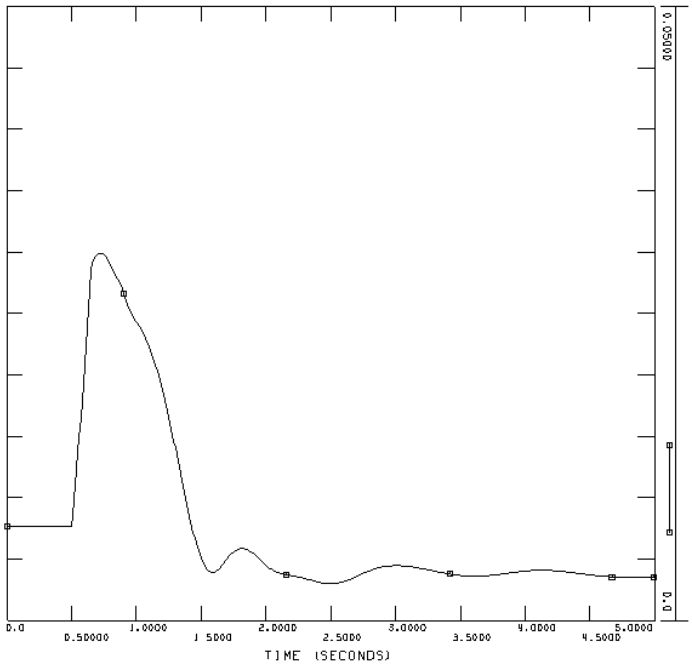

Speed deviation of wind turbine generators [pu]

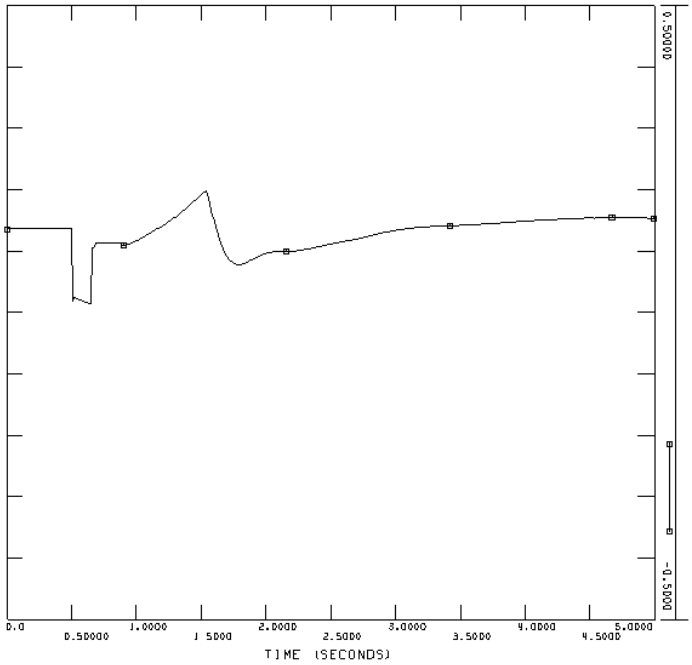

Reactive power from one SVC [pu on system base]

Event 2, line fault and tripping of line

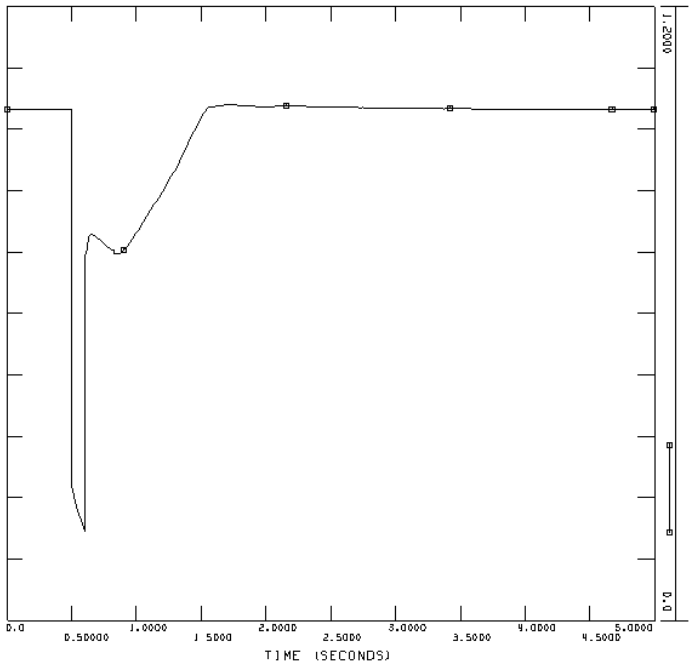

Voltage at Feda [pu]

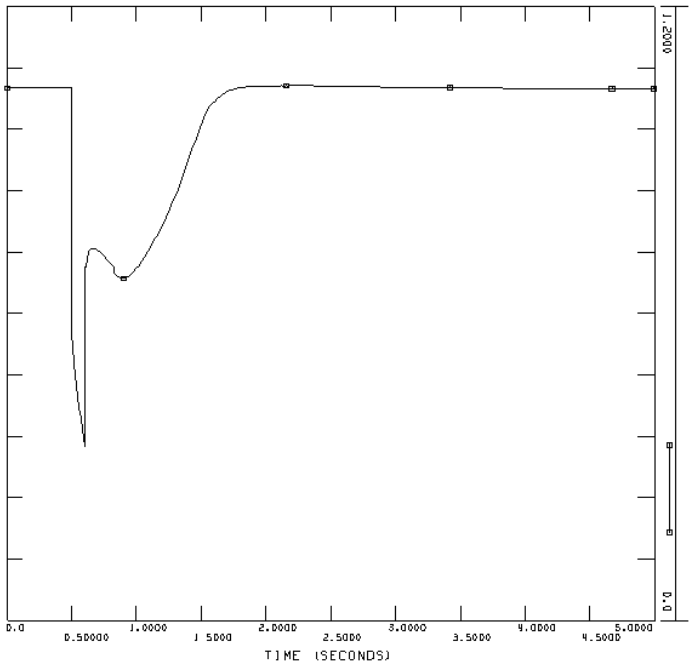

Voltage offshore [pu]

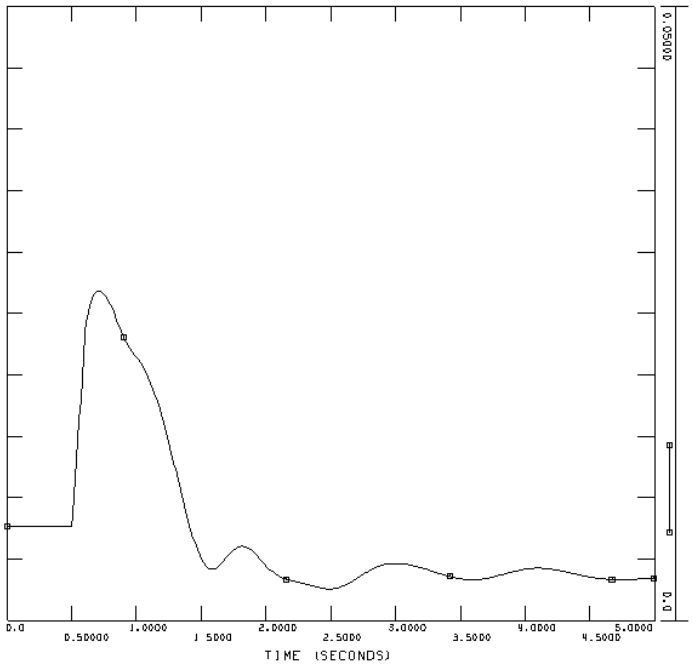

Speed deviation of wind turbine generators [pu]

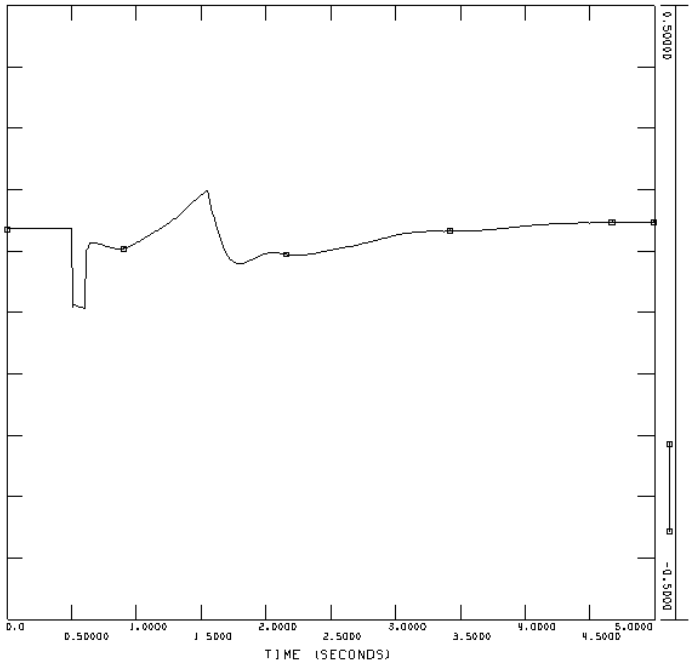

Reactive power from one SVC [pu on system base]

Event 3, three-phase short-circuit at Feda

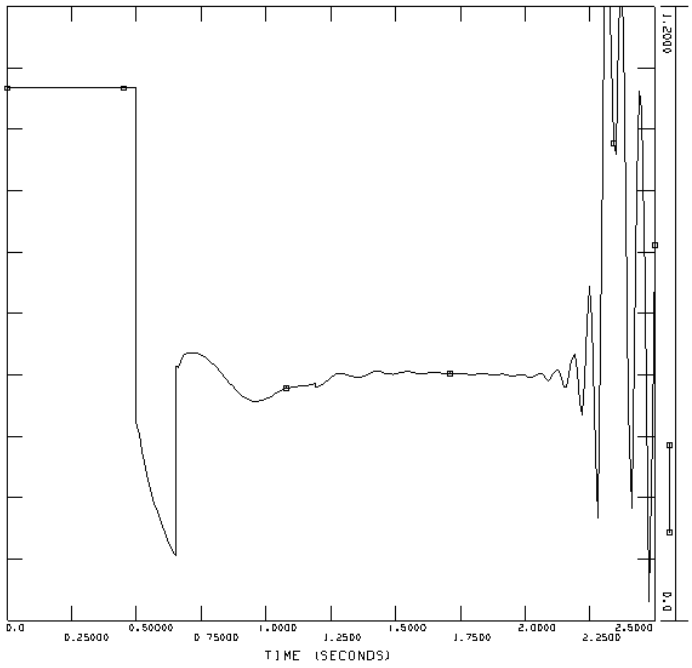

Voltage at Feda [pu]

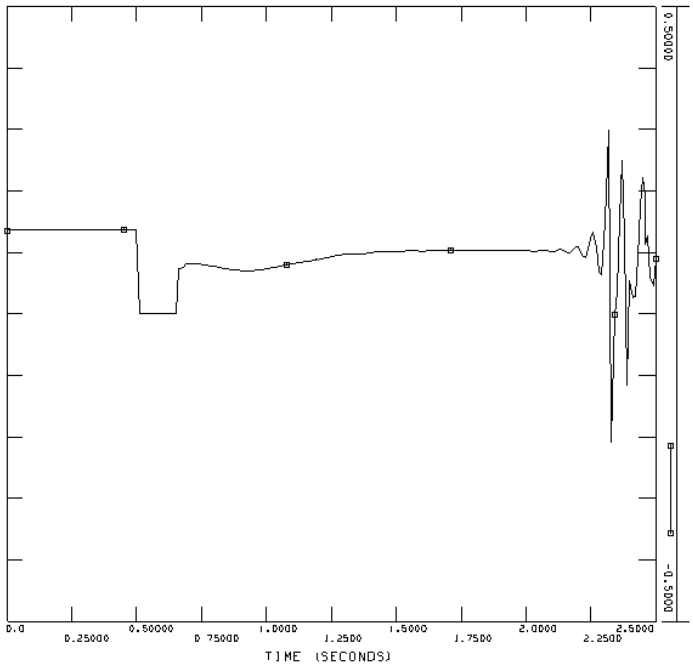

Reactive power from one SVC [pu on system base]

Case 3, HVDC Light

Event 1, bus fault at Øie

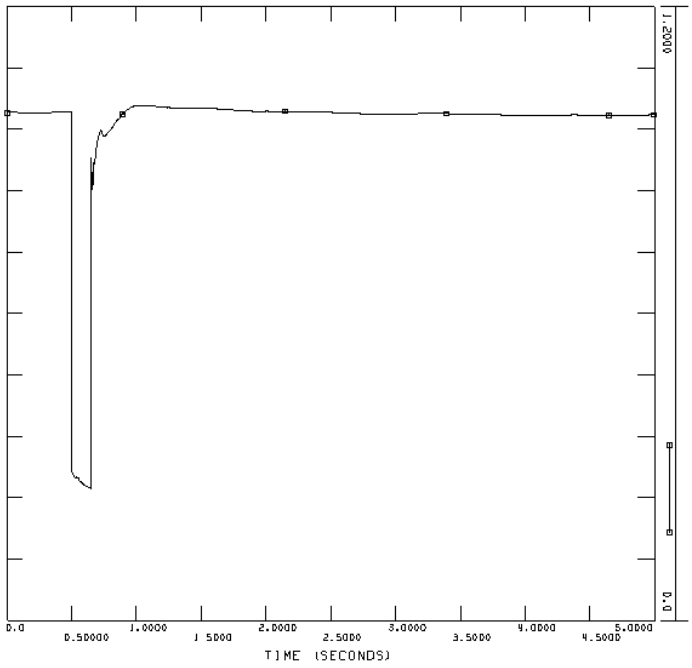

Voltage at Feda [pu]

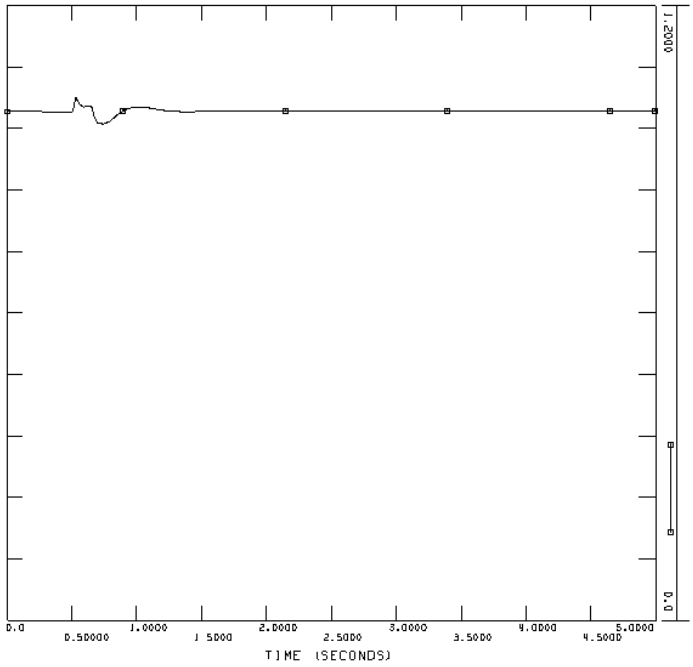

Voltage offshore [pu]

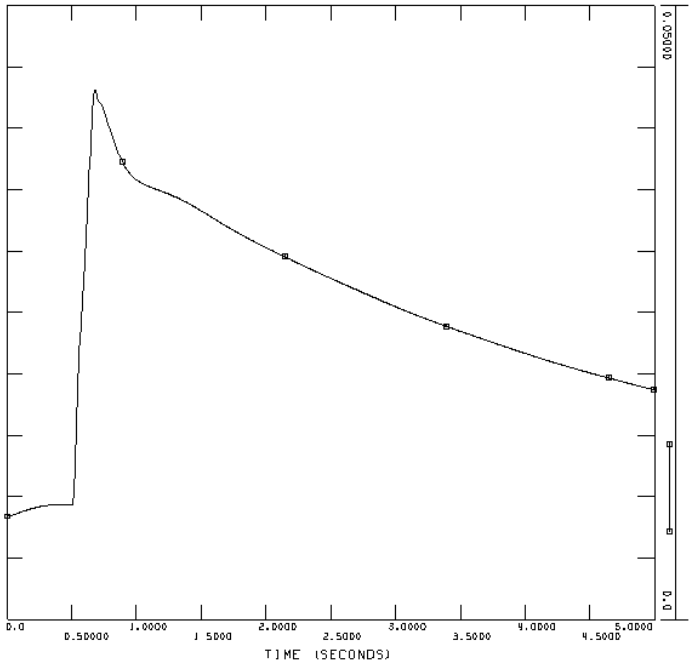

Speed deviation of wind turbine generators [pu]

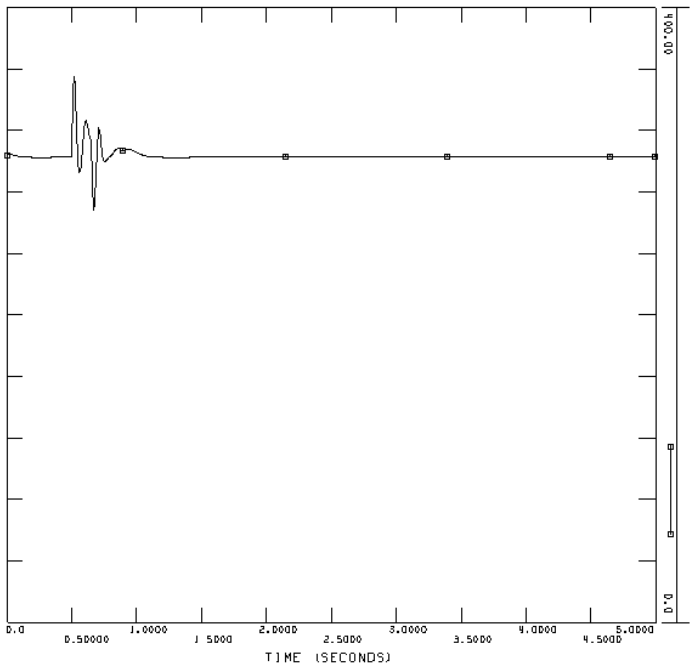

DC voltage at the voltage regulating HVDC Light converter [kV]

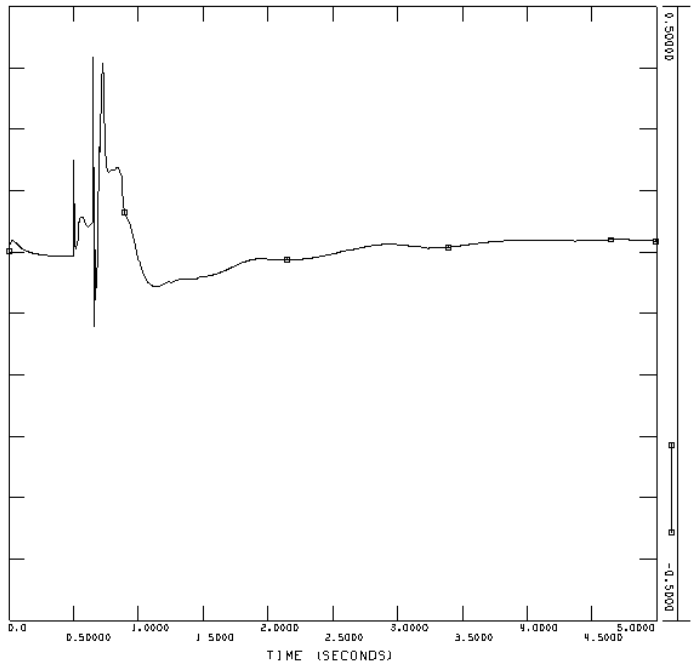

Reactive power from the HVDC Light converter at the connection point [pu on system base]

Event 2, line fault and tripping of line

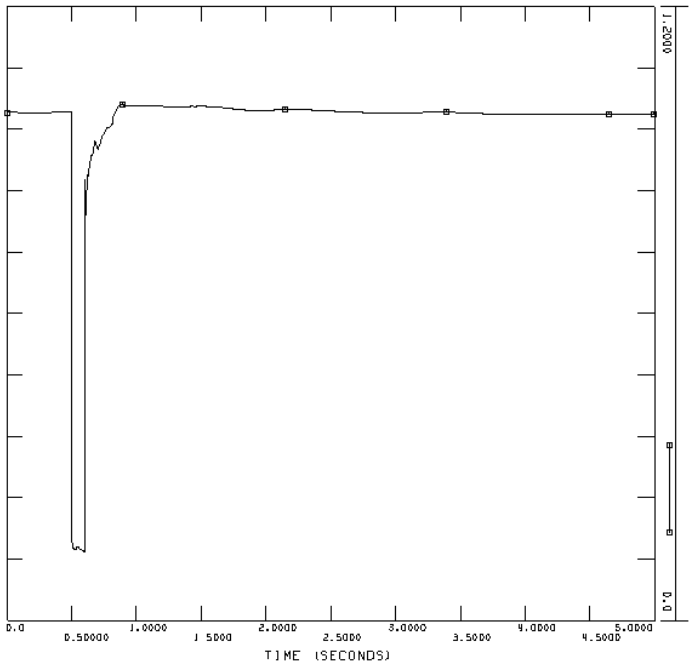

Voltage at Feda [pu]

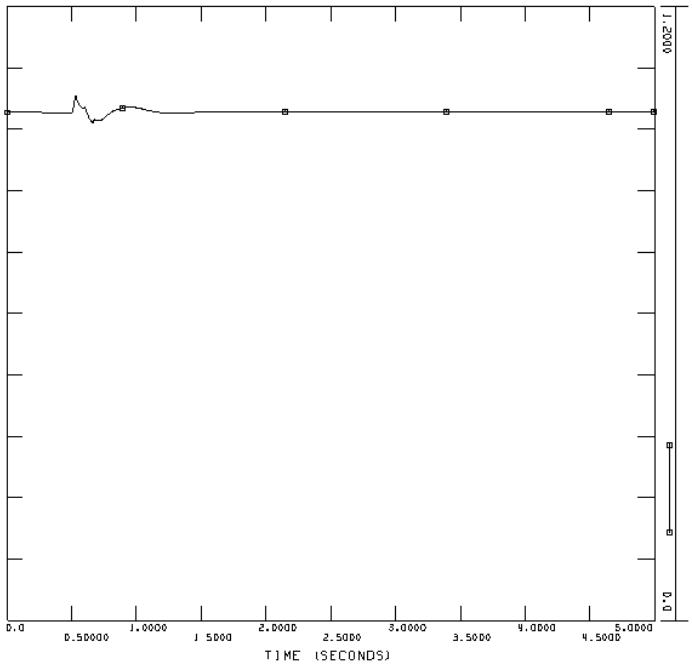

Voltage offshore [pu]

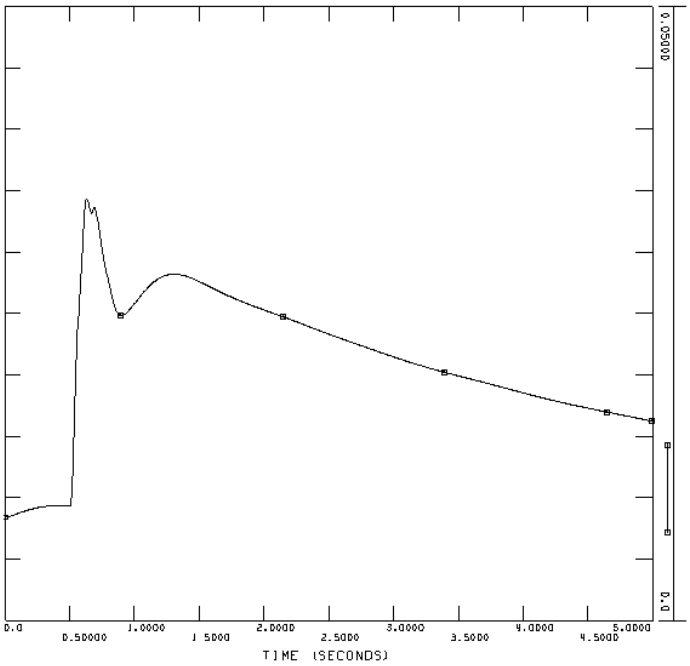

Speed deviation of wind turbine generators [pu]

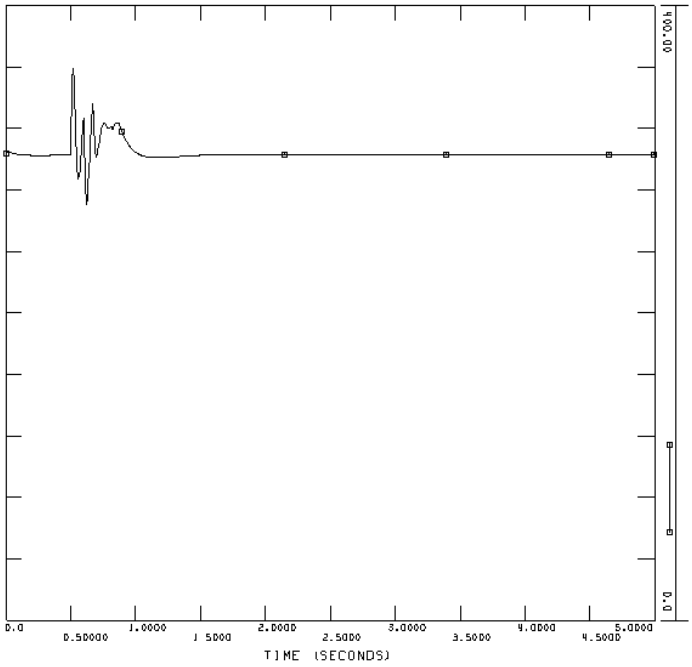

DC voltage at the voltage regulating HVDC Light converter [kV]

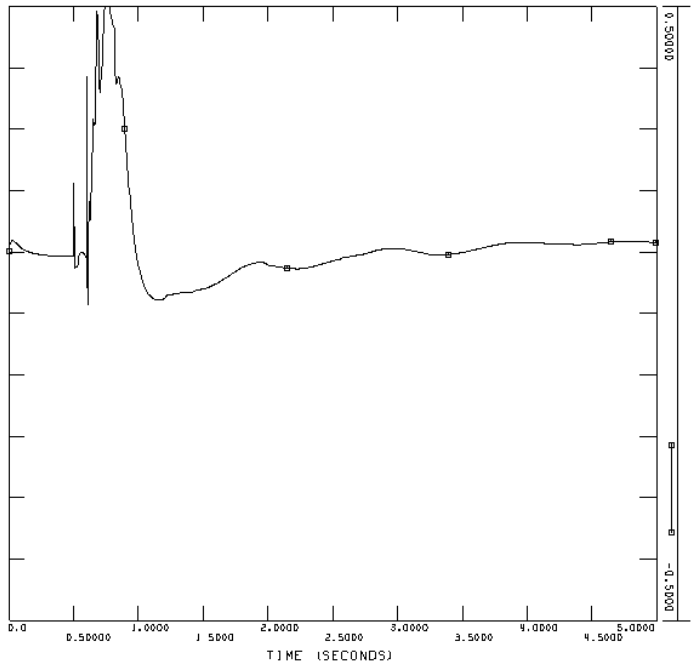

Reactive power from the HVDC Light converter at the connection point [pu on system base]

Event 3, three-phase short-circuit at Feda

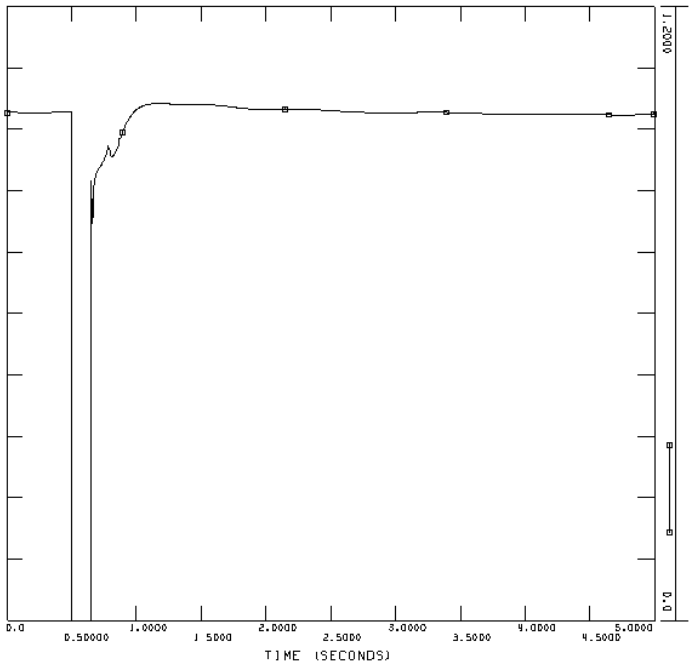

Voltage at Feda [pu]

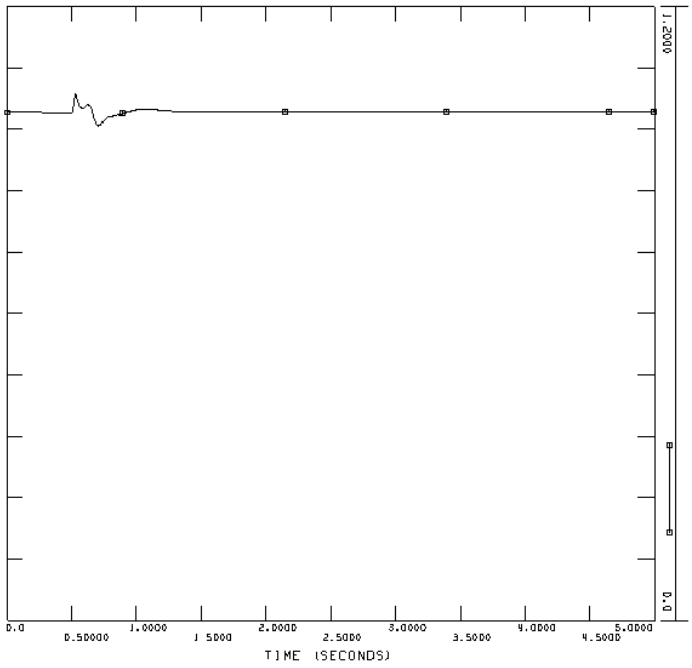

Voltage offshore [pu]

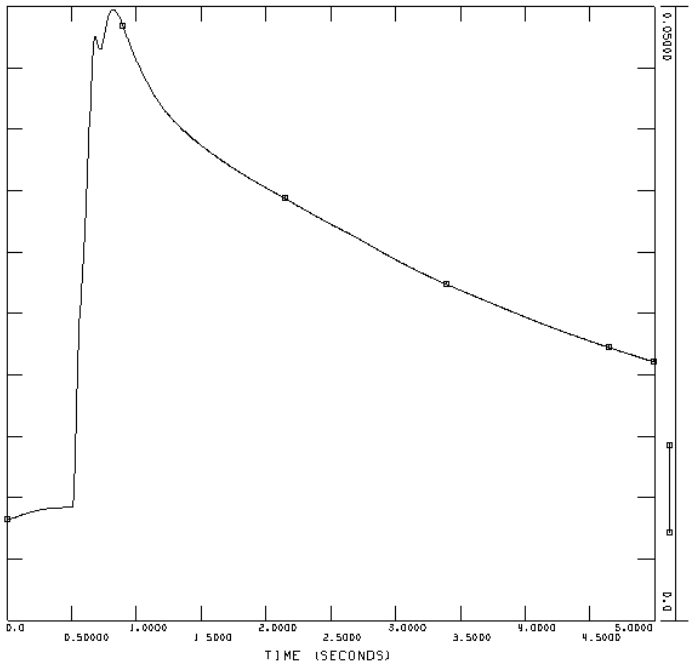

Speed deviation of wind turbine generators [pu]

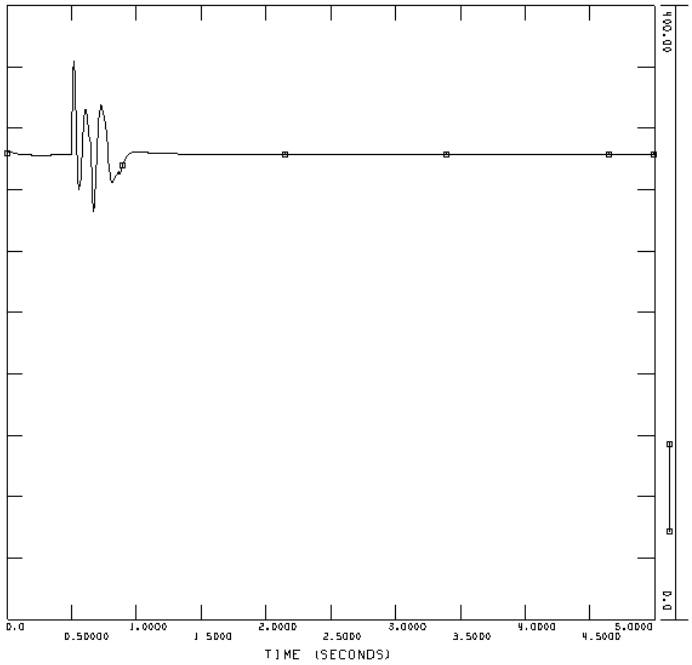

DC voltage at the voltage regulating HVDC Light converter [kV]

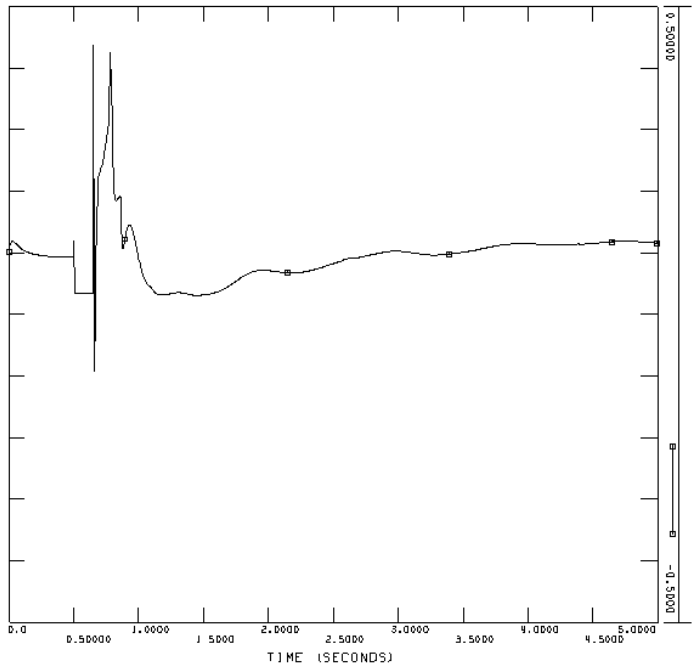

Reactive power from the HVDC Light converter at the connection point [pu on system base]

Case 4, AC cable

Event 1, bus fault at Sauda

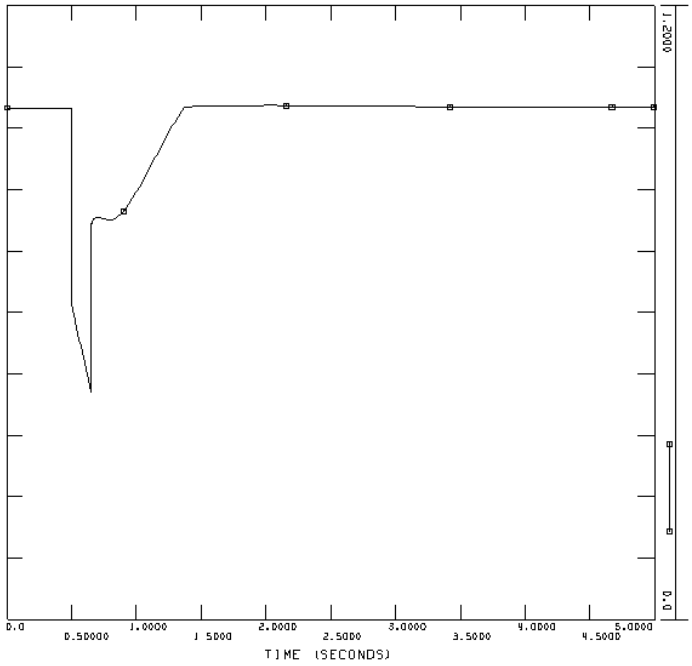

Voltage at Kårstø [pu]

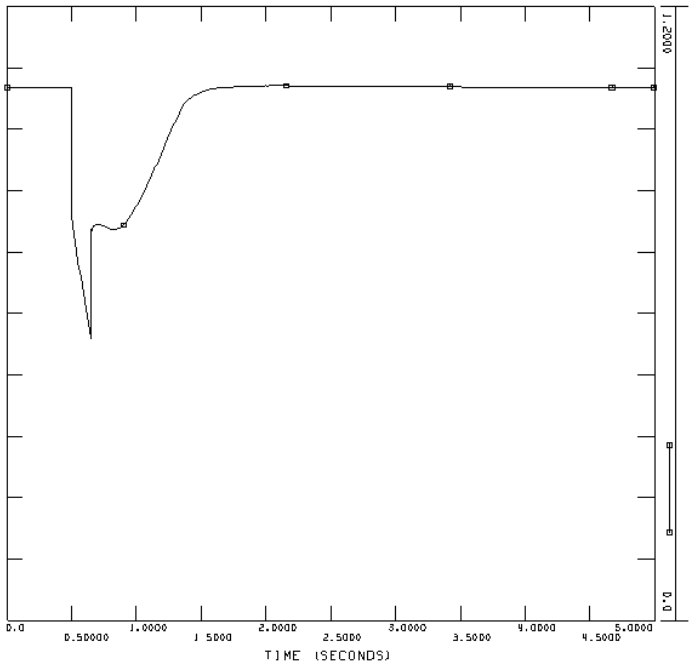

Voltage offshore [pu]

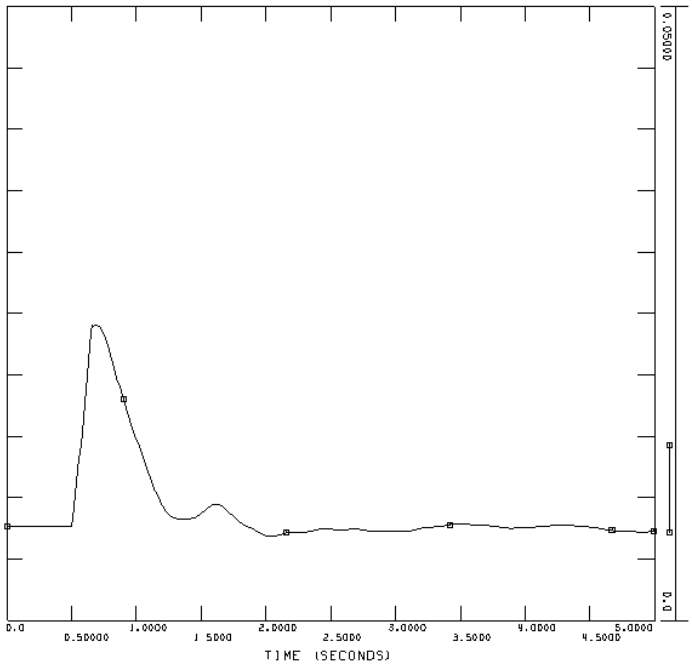

Speed deviation of wind turbine generators [pu]

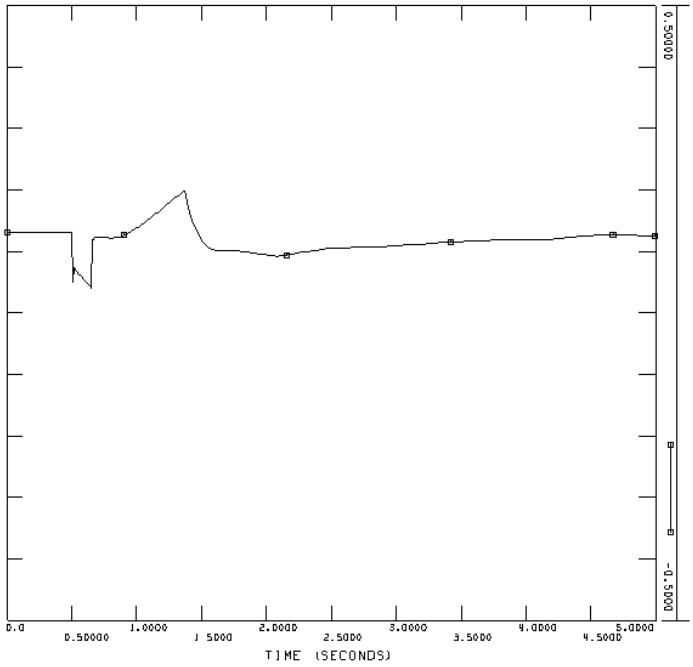

Reactive power from one SVC [pu on system base]

Event 2, line fault and tripping of line

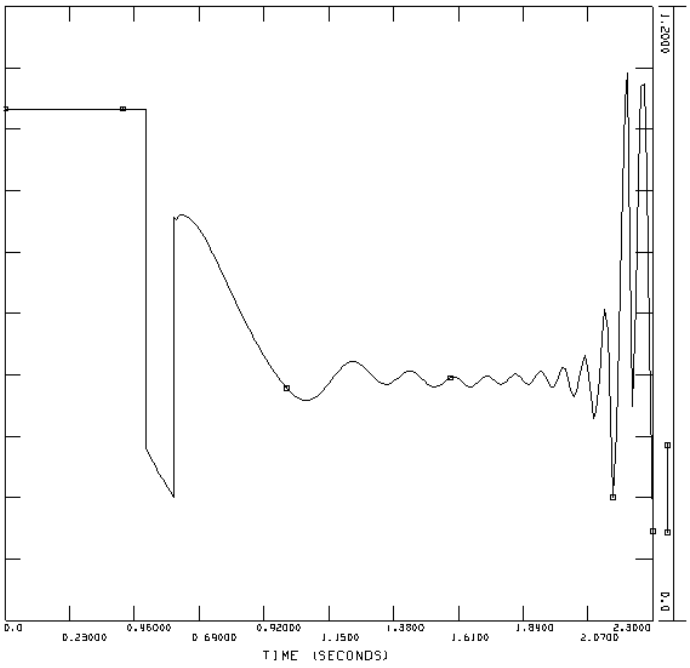

Voltage at Kårstø [pu]

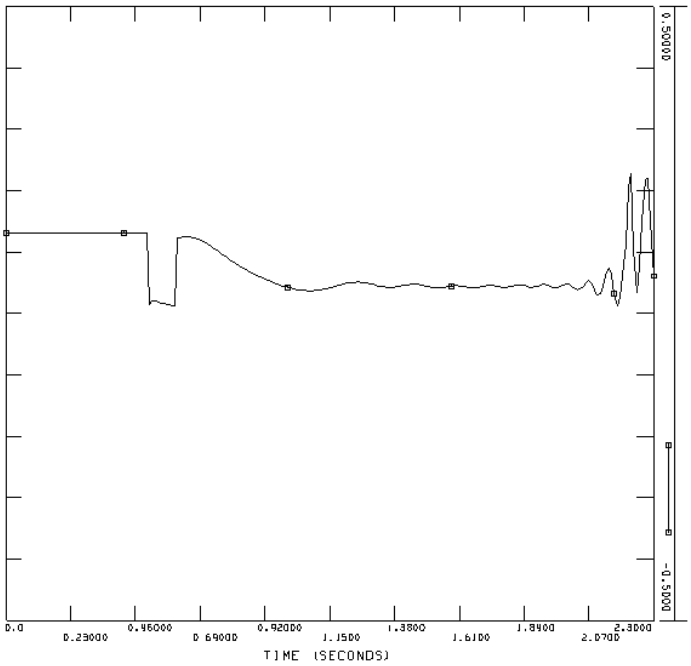

Reactive power from one SVC [pu on system base]

Event 3, three-phase short-circuit at Kårstø

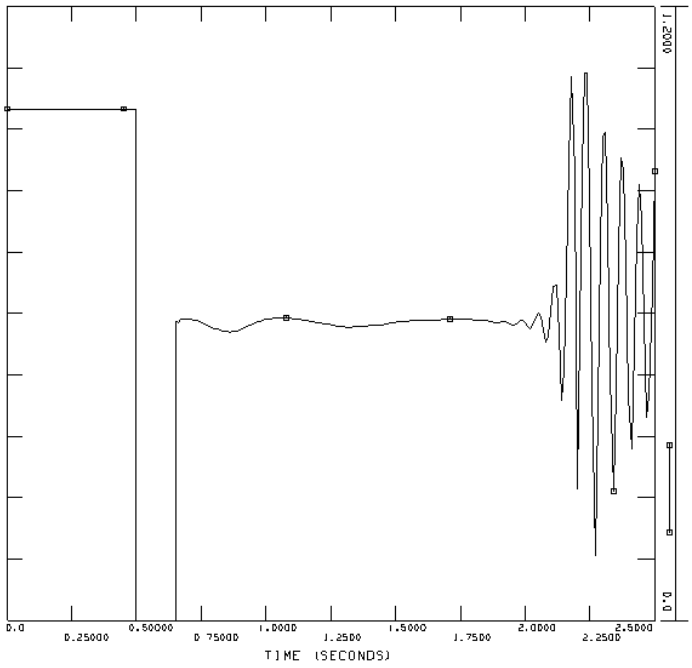

Voltage at Kårstø [pu]

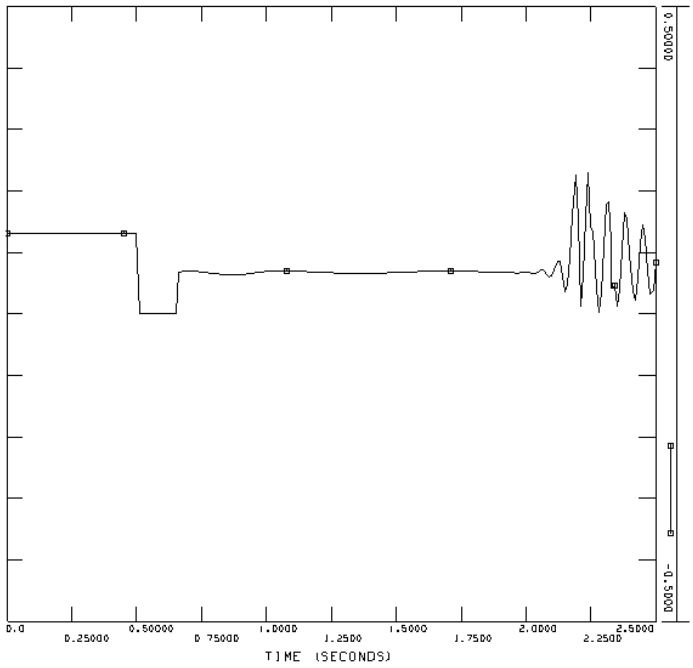

Reactive power from one SVC [pu on system base]

Case 4, HVDC Light

Event 1, bus fault at Sauda

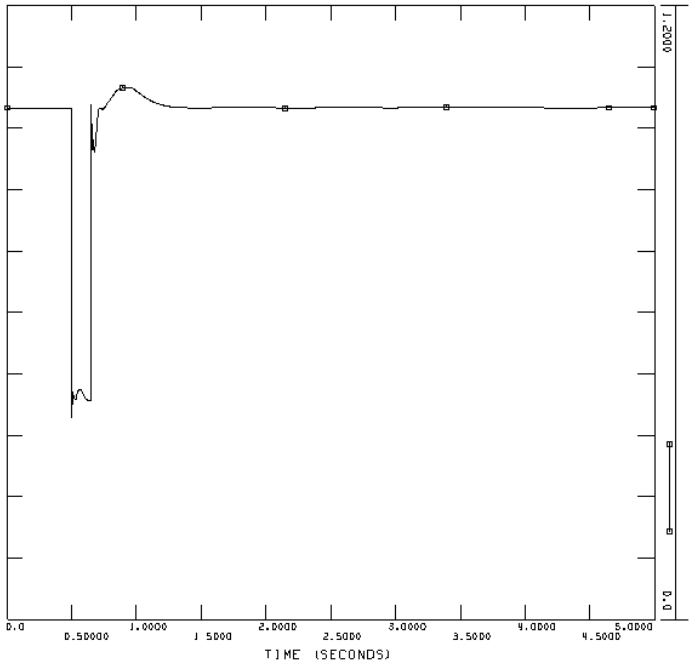

Voltage at Kårstø [pu]

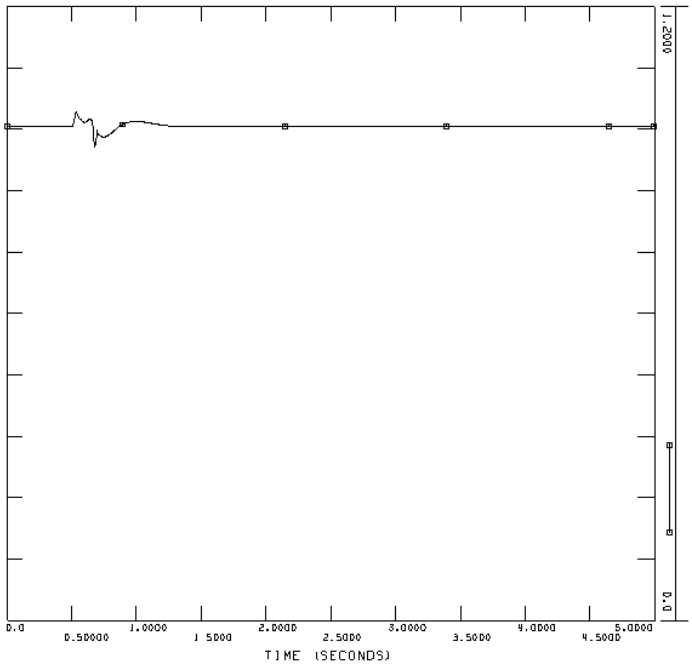

Voltage offshore [pu]

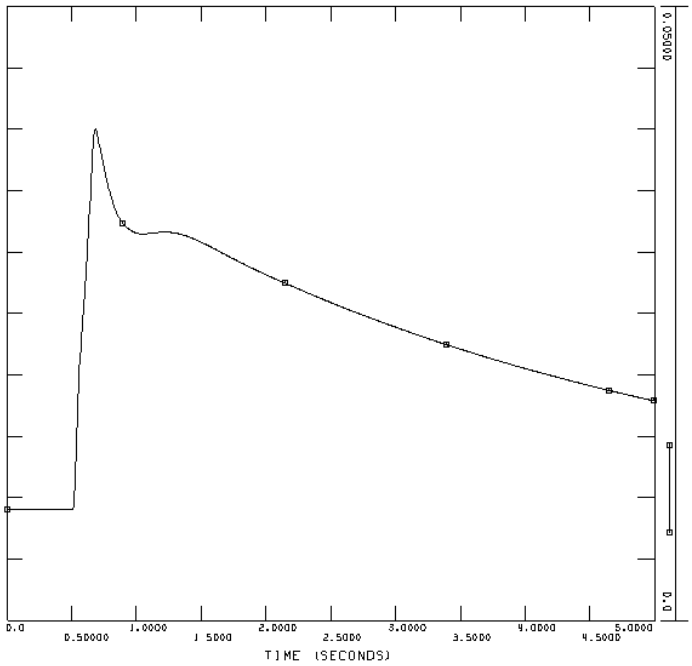

Speed deviation of wind turbine generators [pu]

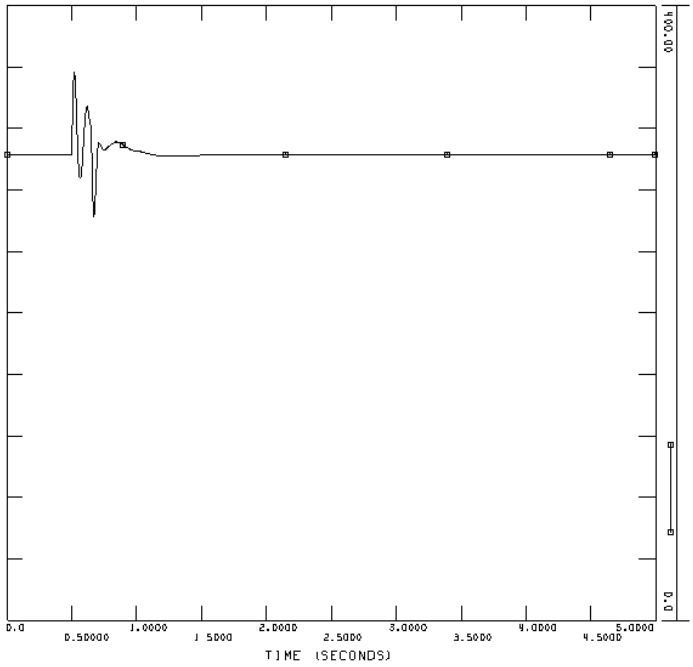

DC voltage at the voltage regulating HVDC Light converter [kV]

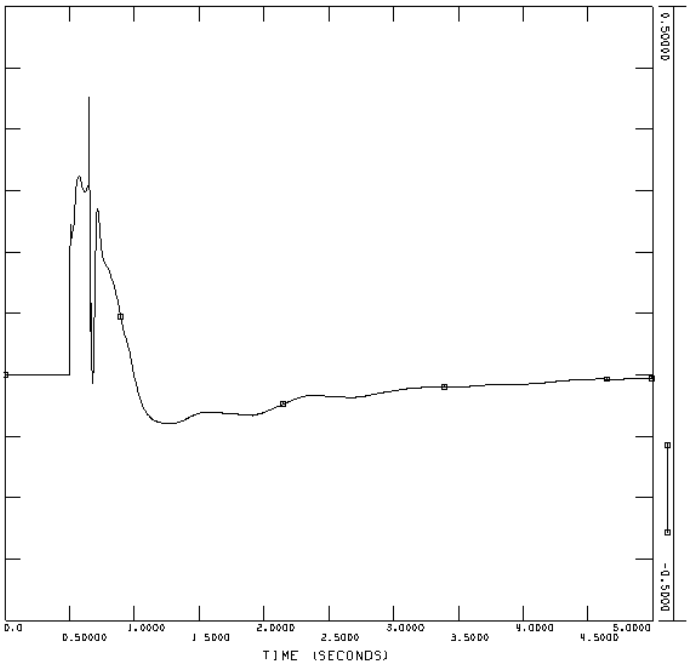

Reactive power from the HVDC Light converter at the connection point [pu on system base]

Event 2, line fault and tripping of line

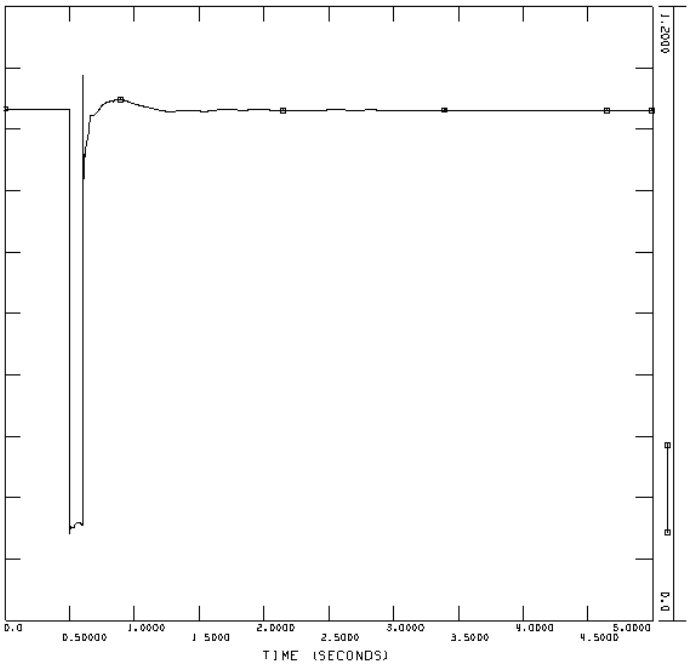

Voltage at Kårstø [pu]

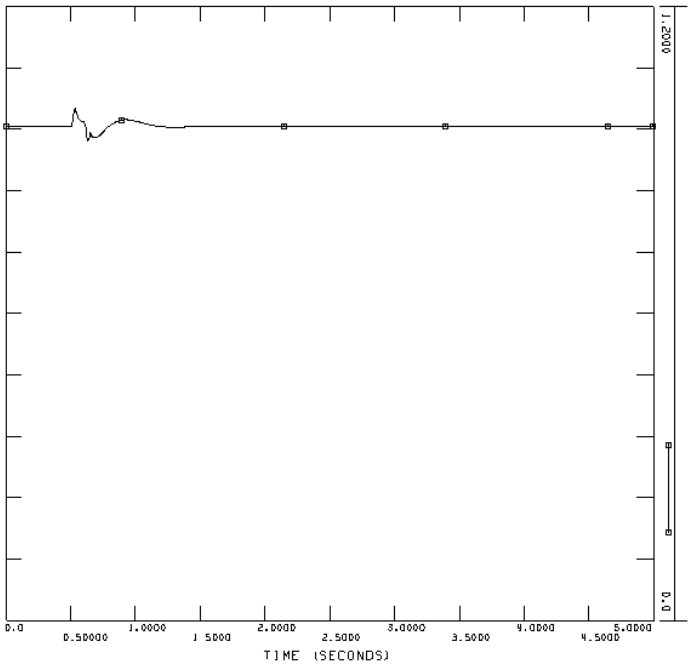

Voltage offshore [pu]

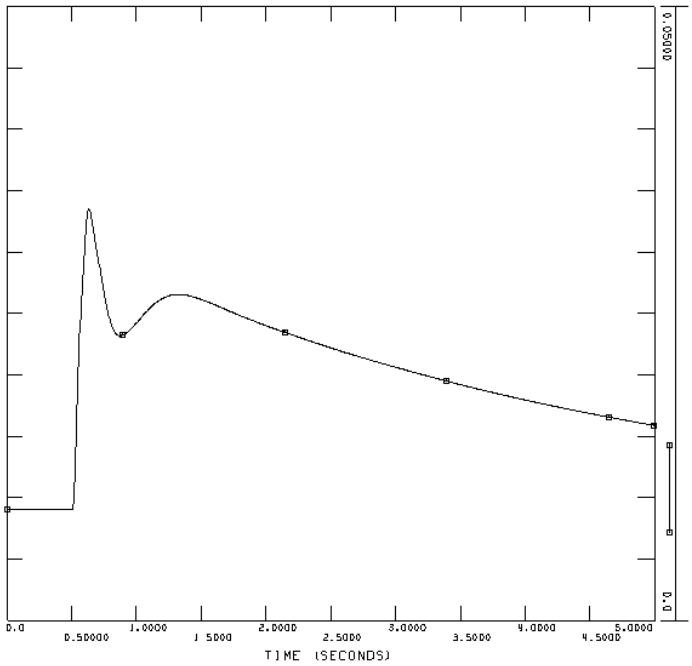

Speed deviation of wind turbine generators [pu]

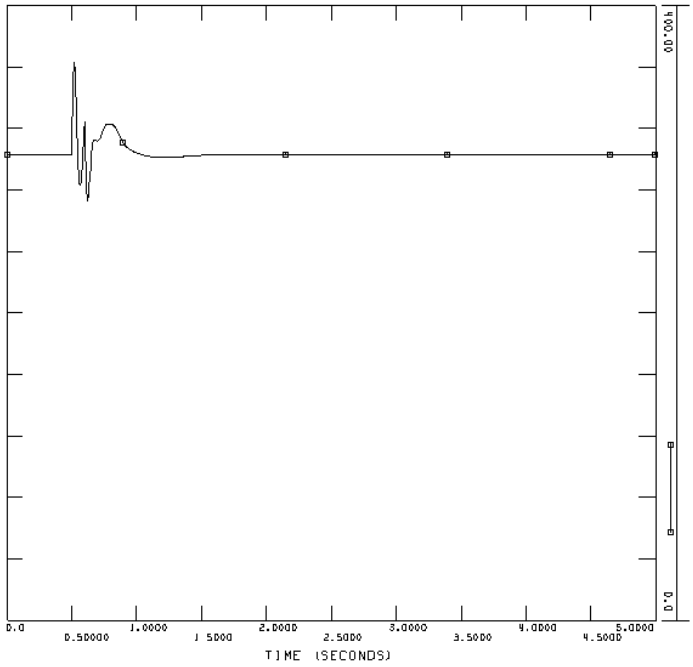

DC voltage at the voltage regulating HVDC Light converter [kV]

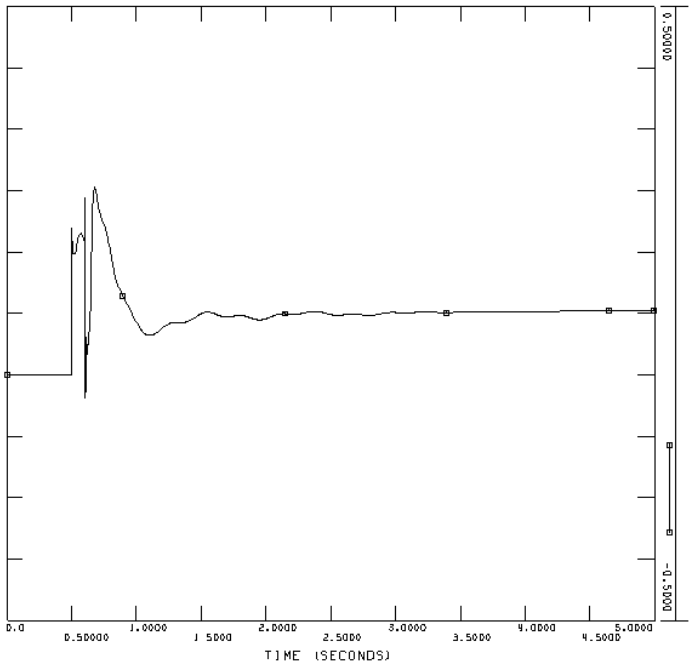

Reactive power from the HVDC Light converter at the connection point [pu on system base]

Event 3, three-phase short-circuit at Kårstø

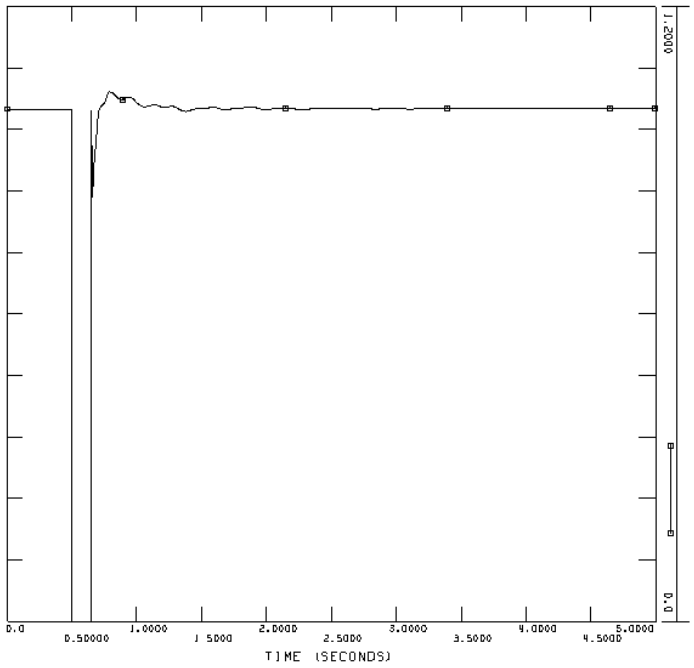

Voltage at Kårstø [pu]

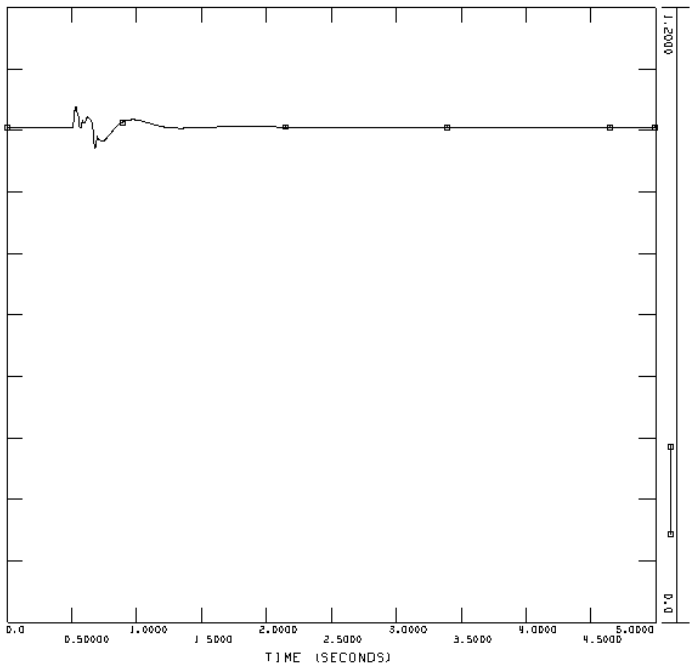

Voltage offshore [pu]

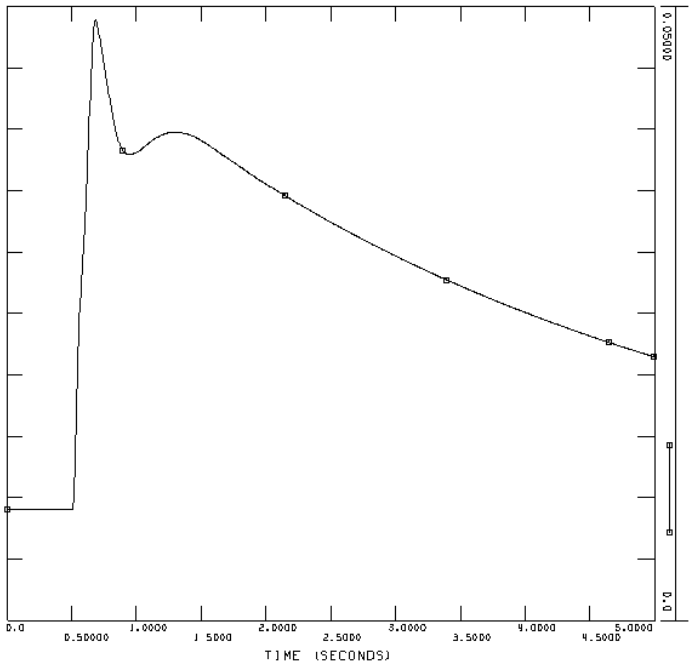

Speed deviation of wind turbine generators [pu]

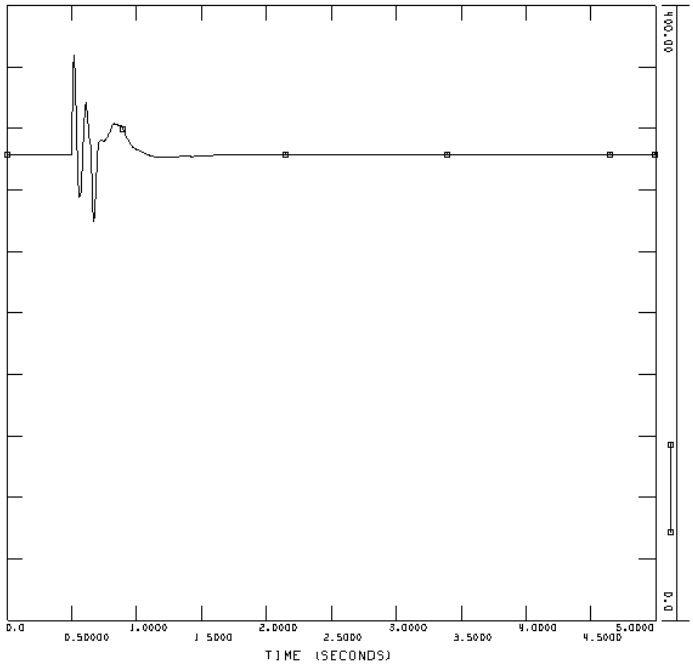

DC voltage at the voltage regulating HVDC Light converter [kV]

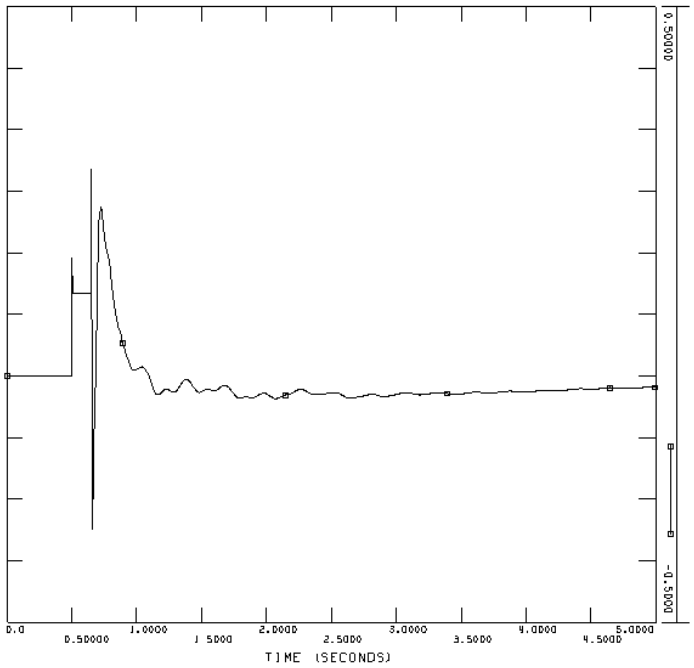

Reactive power from the HVDC Light converter at the connection point [pu on system base]

Case 5, AC cable

Event 1, bus fault at Sauda

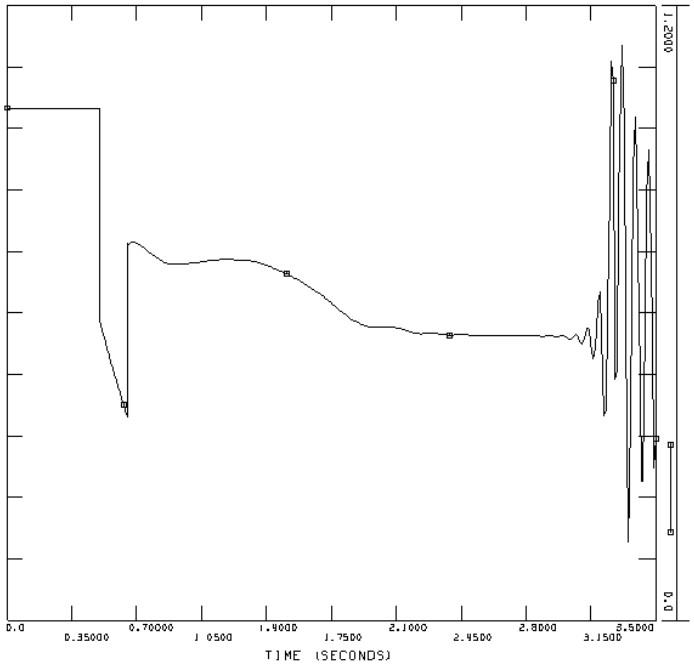

Voltage at Kårstø [pu]

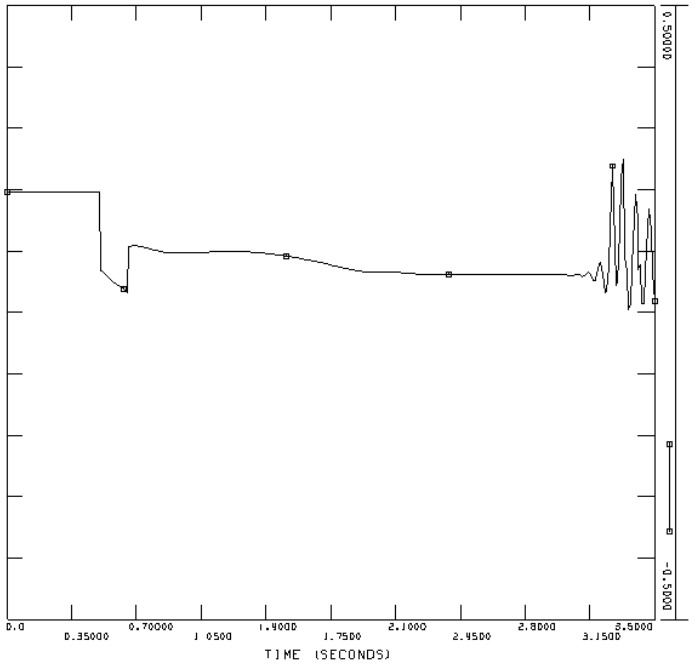

Reactive power from one SVC [pu on system base]

Event 2, line fault and tripping of line

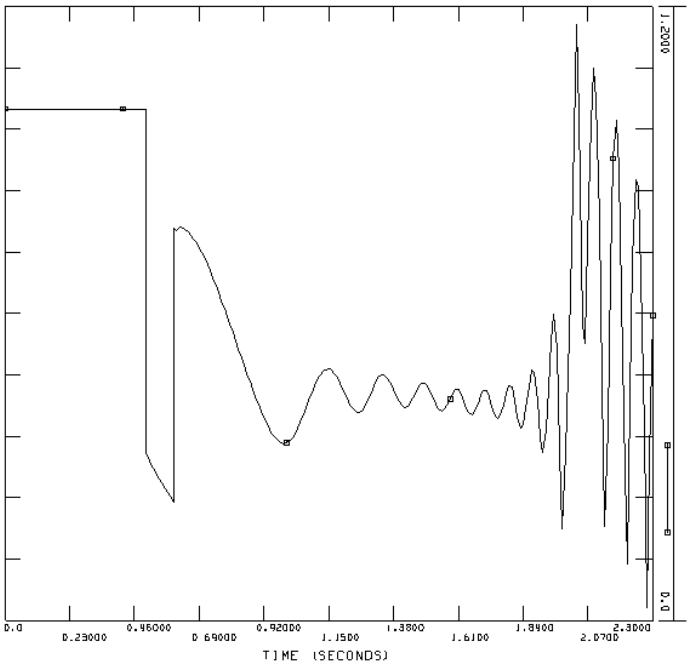

Voltage at Kårstø [pu]

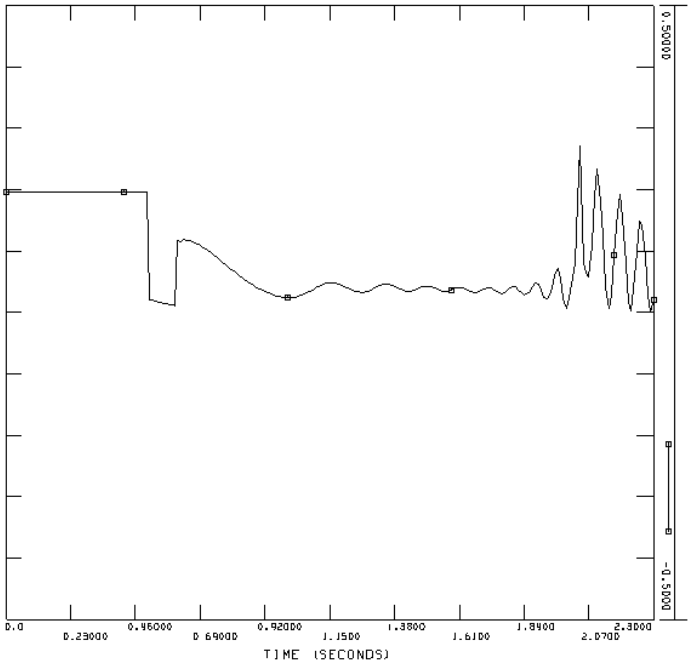

Reactive power from one SVC [pu on system base]

Event 3, three-phase short-circuit at Kårstø

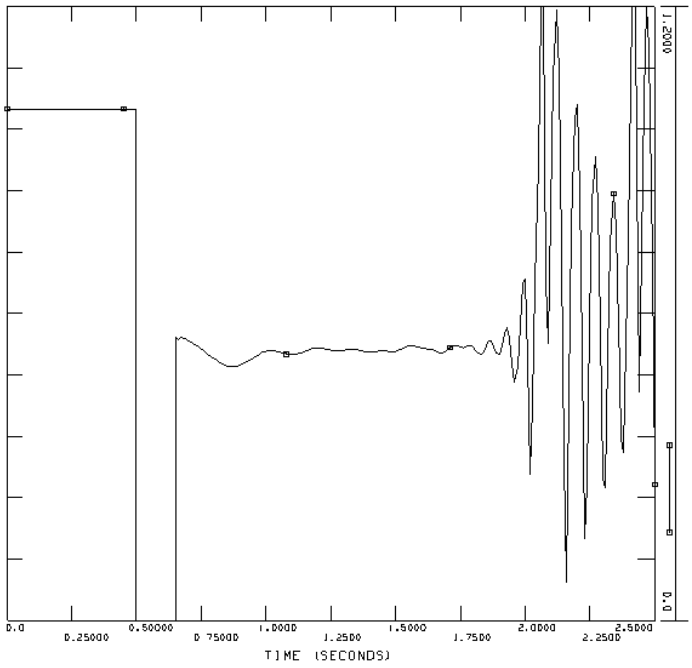

Voltage at Kårstø [pu]

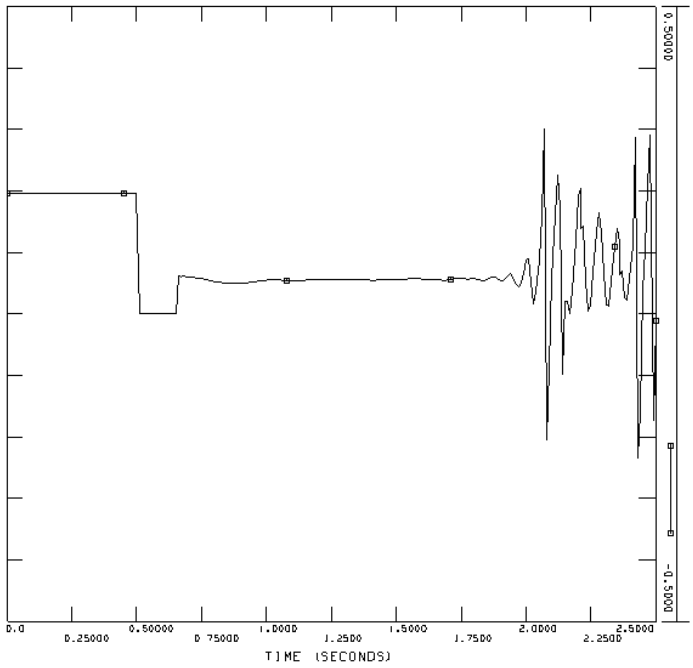

Reactive power from one SVC [pu on system base]

Case 5, HVDC Light

Event 1, bus fault at Sauda

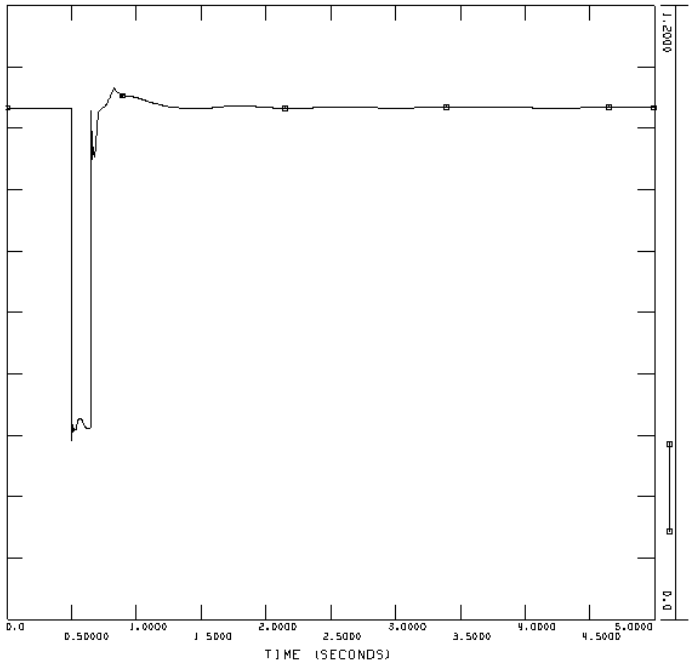

Voltage at Kårstø [pu]

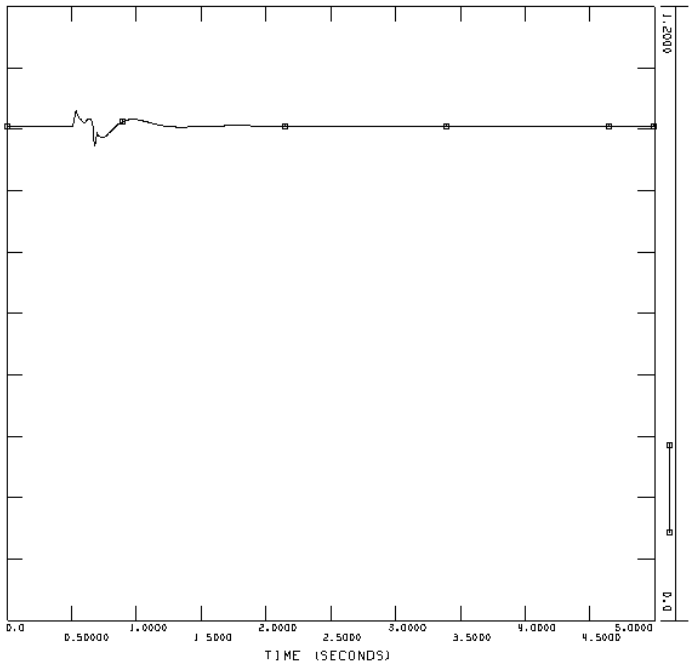

Voltage offshore [pu]

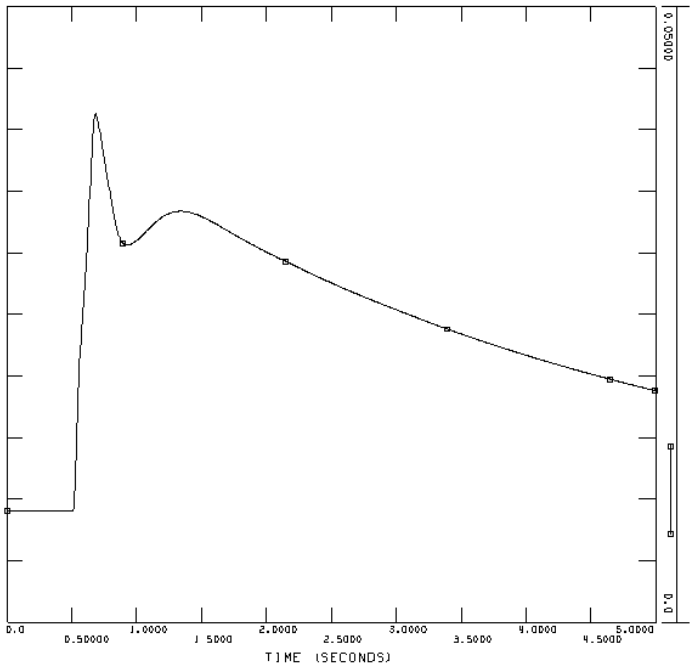

Speed deviation of wind turbine generators [pu]

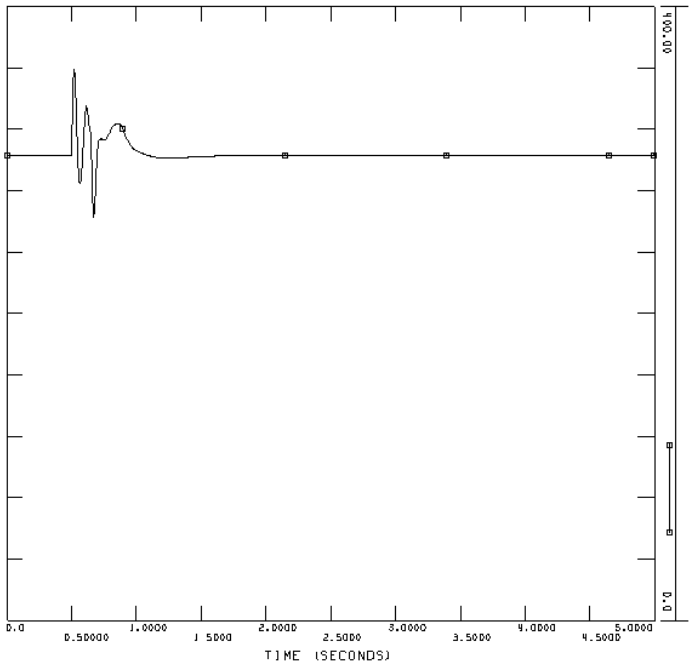

DC voltage at the voltage regulating HVDC Light converter [kV]

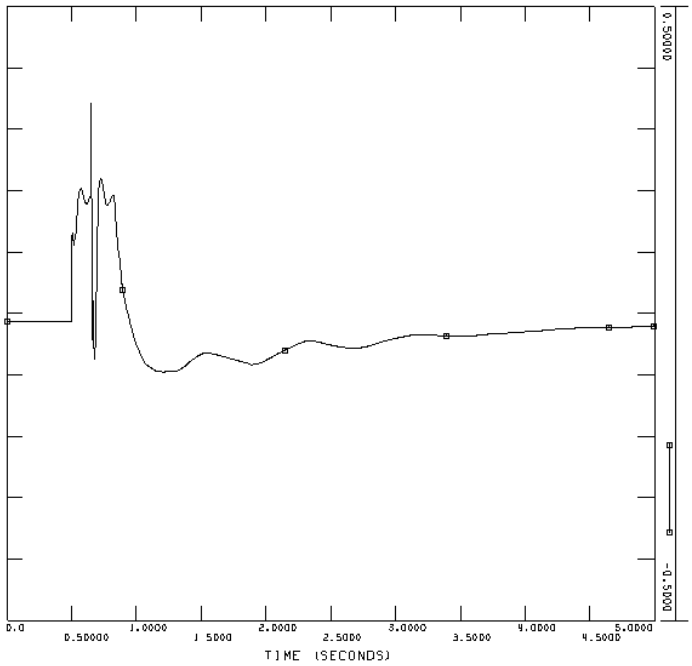

Reactive power from the HVDC Light converter at the connection point [pu on system base]

Event 2, line fault and tripping of line

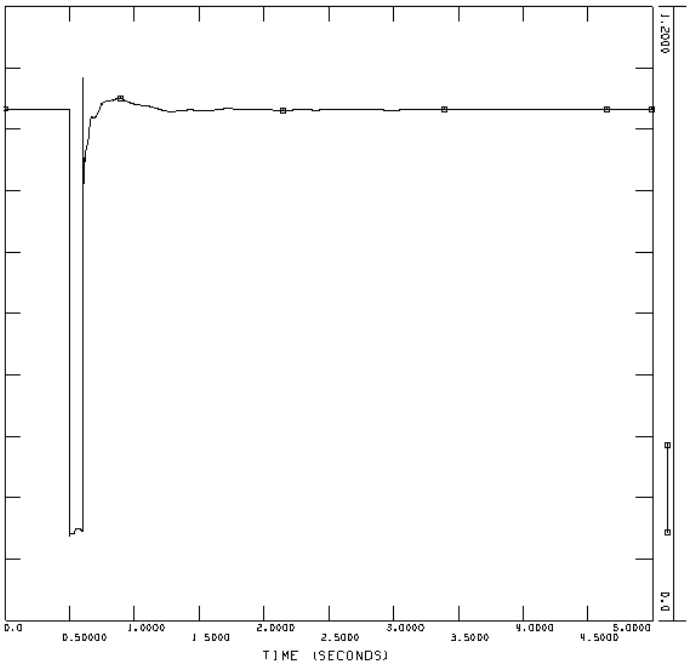

Voltage at Kårstø [pu]

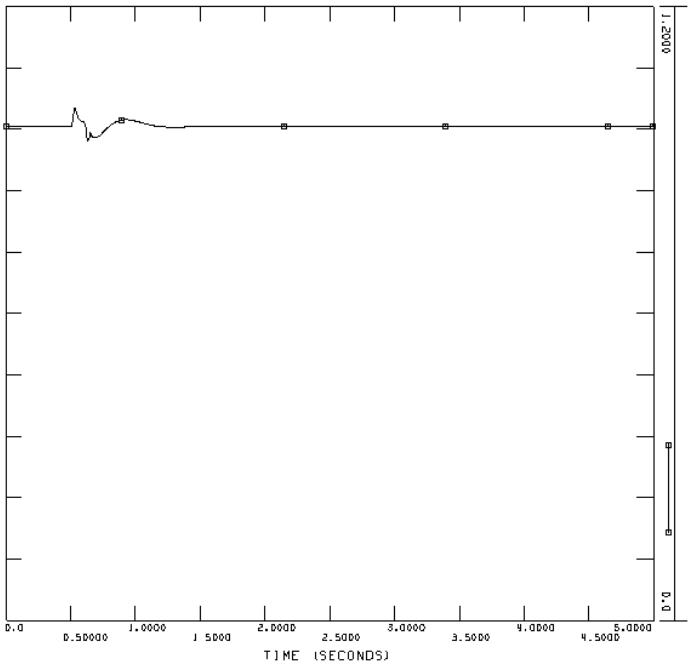

Voltage offshore [pu]

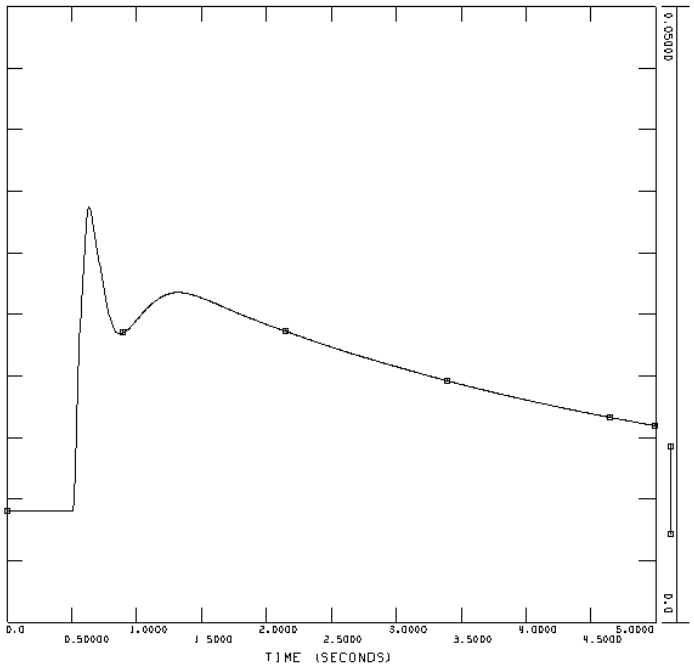

Speed deviation of wind turbine generators [pu]

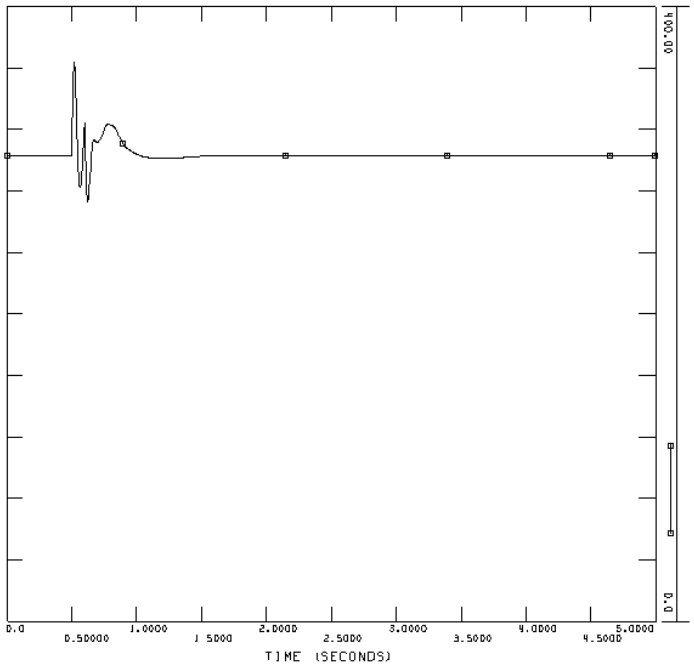

DC voltage at the voltage regulating HVDC Light converter [kV]

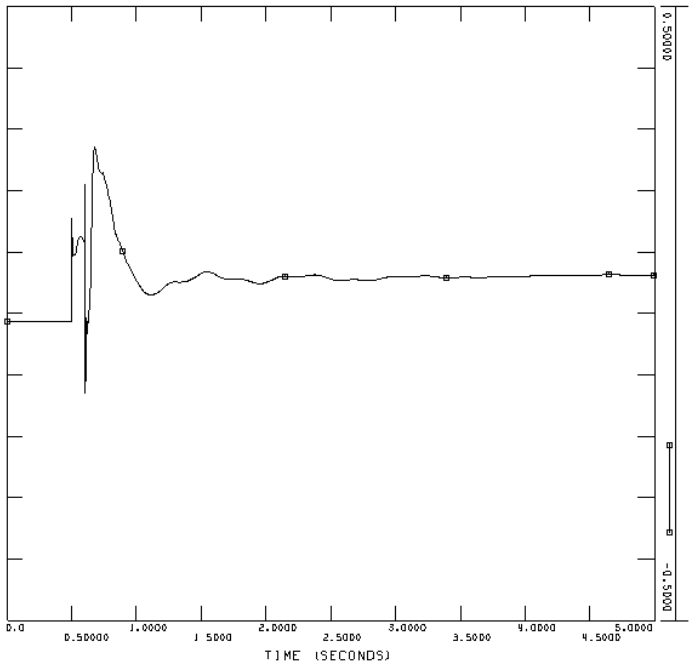

Reactive power from the HVDC Light converter at the connection point [pu on system base]

Event 3, three-phase short-circuit at Kårstø

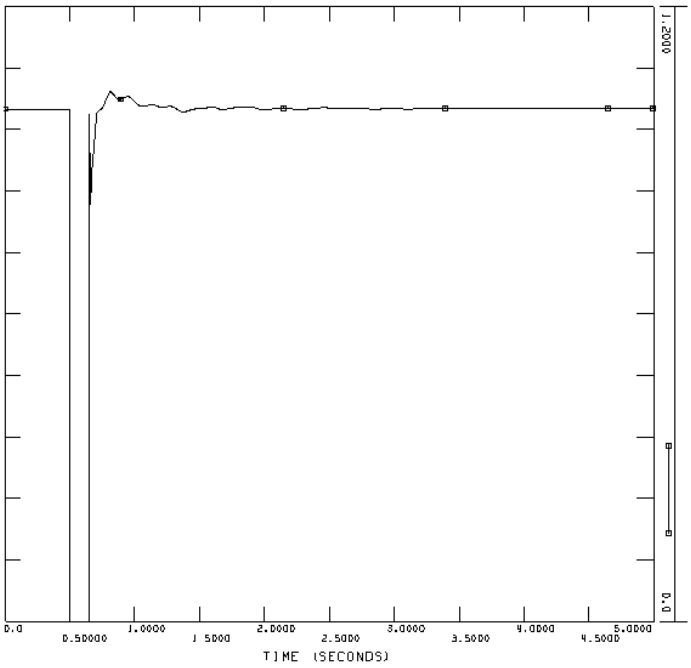

Voltage at Kårstø [pu]

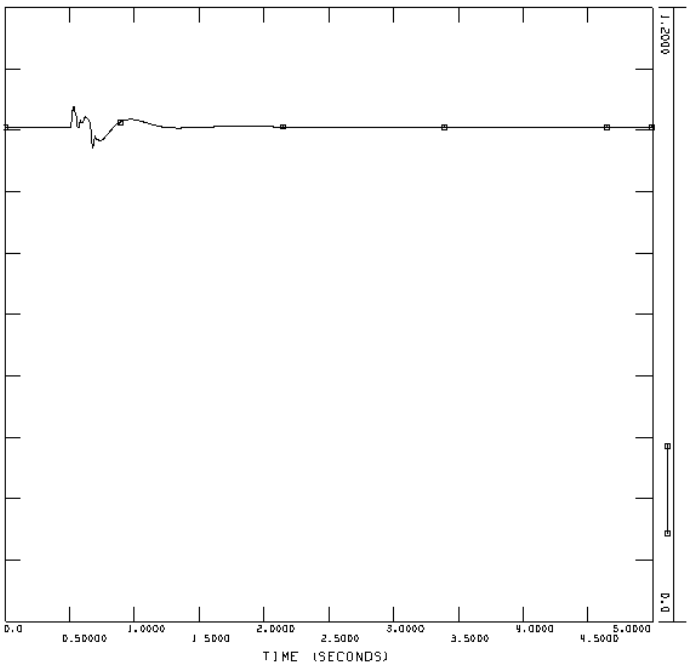

Voltage offshore [pu]

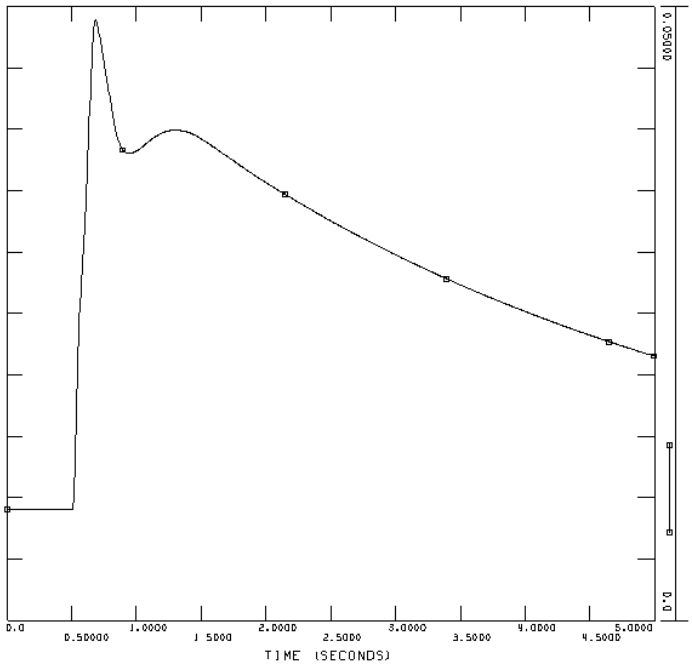

Speed deviation of wind turbine generators [pu]

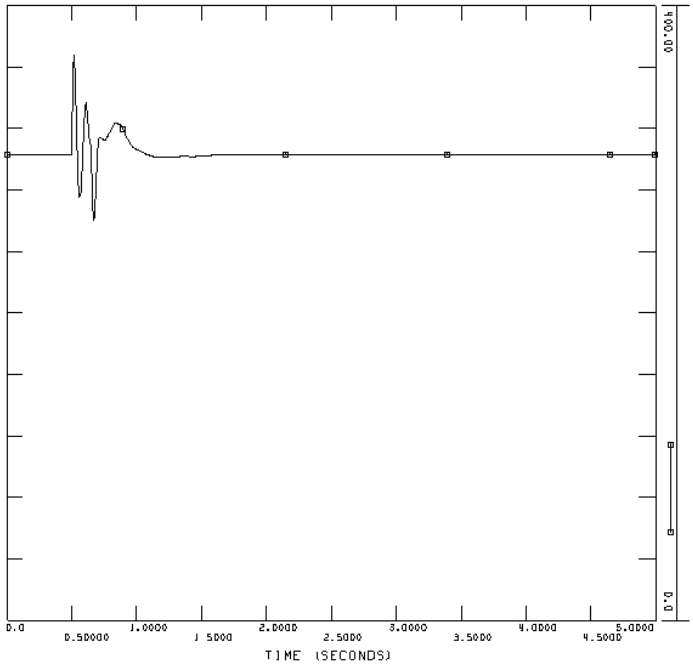

DC voltage at the voltage regulating HVDC Light converter [kV]

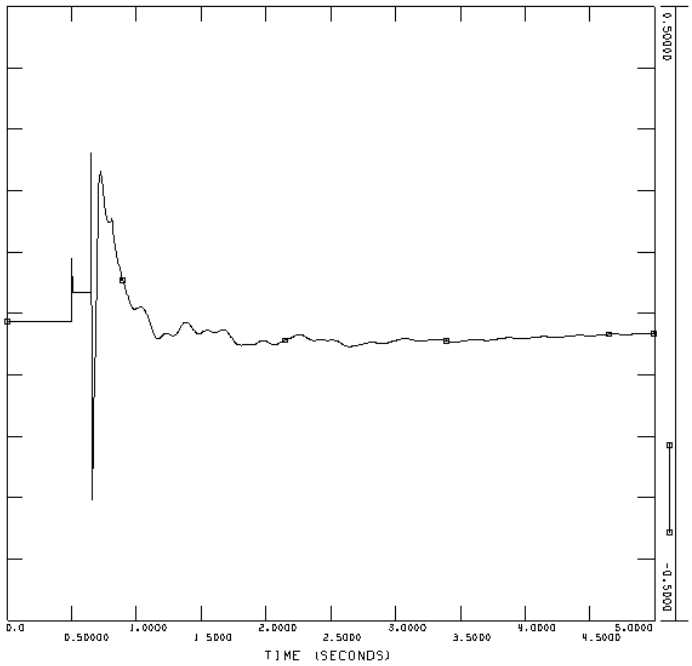

Reactive power from the HVDC Light converter at the connection point [pu on system base]